Targeted Differentiation of Pluripotent Stem Cells to Hepatocytes

A thesis submitted for the degree of

Doctor of Philosophy

University of London

By

Matthew T Shephard

Department of Endocrinology

William Harvey Research Institute

Barts & The London School of Medicine and Dentistry

Queen Mary University of London

Charterhouse Square

London EC1M 6BQ

Statement of Originality

I, Matthew T Shephard, confirm that the research included within this thesis is my own work or that where it has been carried out in collaboration with, or supported by others, that this is duly acknowledged below and my contribution indicated. Previously published material is also acknowledged below.

I attest that I have exercised reasonable care to ensure that the work is original and does not to the best of my knowledge break any UK law, infringe any third party's copyright or other Intellectual Property Right, or contain any confidential material.

I accept that the College has the right to use plagiarism detection software to check the electronic version of the thesis.

I confirm that this thesis has not been previously submitted for the award of a degree by this or any other university.

Signature:

Date:

Acknowledgements

I would first and foremost like to express my gratitude to my supervisor Dr Tristan McKay for giving me the chance to undertake a PhD at Queen Mary, University of London. Thank you for your advice and guidance over the past four years. Thank you to members of the WHRI who have provided support which has helped me in so many ways. This research project was funded through a BBSRC CASE studentship award which allowed me to undertake this study. I would like to thank Plasticell Ltd for allowing me to undertake a collaborative industrial CASE studentship and for providing funding. In particular, Dr Diana Hernandez of Plasticell Ltd has always given me sound guidance for which I am extremely grateful. I must also express my thanks to Dr Peter King who undertook a primary academic supervisory role in the latter half of my PhD.

Thank you to all members of the McKay research group, 'Team McKay', at St George's, University of London for all their help. Juliette Delhove of the McKay research group has been particularly helpful with molecular cloning and all manner of advice.

I express my gratitude and respect to my friend Chris Schultz for his unwavering support over the past twelve years and for joining me on this 'PhD rollercoaster ride'; truly a friend for life. A special thank you to Darren Crowley for all the good times that we've shared and for making the heavy times feel that much lighter and enjoyable. Emma Kay has helped me in more ways than I could possibly mention and has always been there for me in both the good times and the bad. I will always be thankful for the experiences that we've shared together. I would like to express my upmost appreciation to my parents and family for their love and support and never letting me entertain the idea of giving up. To them I dedicate this thesis.

Abstract

Pluripotent stem cells (PSCs) possess the ability to differentiate to virtually any cell type whilst retaining the capacity to self-renew. There is an unmet need for an inexhaustible supply of hepatocytes to perform drug toxicity and metabolism screens on early stage drugs. PSCs therefore hold potential to generate mature hepatocytes for pharmaceutical testing. To realise this potential, there is a requirement to recapitulate hepatocyte specification *in vitro*. There are two main bottlenecks in generating metabolically relevant hepatocytes. The first is the specification of definitive endoderm (DE), where it is known that the TGFβ family member Nodal is the key driver *in vivo*. Currently the closely related TGFβ family member Activin A (AA) is universally used to mimic this process. However, it has been observed that AA results in off-target gene modulation that may be deleterious to the production of DE; from which the hepatic lineage arises. Preliminary data from the McKay group has shown that AA stimulates endogenous Nodal activity when applied to PSCs; leading to the hypothesis that Nodal is the true driver of DE specification *in vitro*. To address this avenue of investigation, tools to modulate Nodal signalling were assessed in different cell culture systems. Findings included the need to use an appropriate viral promotor to efficiently express lentiviral vectors in PSCs. The second major bottleneck concerns hepatic maturation where the signalling pathways and key regulators *in vitro* are not fully understood. Consequently, current derived hepatocyte-like cells (HLCs) show low functionality. Utilising Plasticell's CombiCult® allowed thousands of growth factor and small molecule combinations to be screened to define efficient differentiation protocols. Protocols were derived containing novel differentiation factors that give rise to CYP450 inducible HLCs. Lentiviral reporters were then used to determine optimum concentrations of small molecules and to test ligands for the upregulation of hepatic master regulators. Findings gained from this thesis have contributed new insights into the differentiation of PSCs to hepatocytes.

Table of Contents

Table of Figures

Index of Tables

Chapter 1: General Introduction

1.1 Activin/Nodal Signalling in Pluripotency and Endoderm

1.1.1 Mammalian Development and Pluripotency

The development of a mammalian living organism is initiated by the fertilisation of an egg to form a zygote. The zygote then undergoes cleavage stages to form a four-cell morula [1]. The ability of a cell to produce all the different cell types constituting an organism both somatic and germline, including the extra-embryonic tissue, is termed “totipotent” [2] [3] [4]. These transient unrestricted totipotent cells are found in the early embryo at the four-cell morula stage. As development proceeds to the blastocyst stage, the first cell specialisation events take place with the formation of two distinct cell populations. The first being in the outermost layer of the blastocyst called the trophoblast, from which the extra-embryonic endoderm develops [5]. The extra-embryonic tissue is required for implantation and in the support and maintenance of the developing embryo. As development progresses from the totipotent morula stage, the ability to contribute to extra-embryonic tissue is lost but the ability to differentiate into all cell types of the three embryonic germ layers, that being endoderm, mesoderm, ectoderm and also the germline is retained [6]. This ability to produce all cell types of both the embryo and associated germline cells is termed “pluripotent” [7] [8] [9]. Pluripotent cells are found at the sixteen-cell cleavage stage developing mammalian blastula in a subset of cells called the inner cell mass (ICM) (Figure 1).

Following differentiation of pluripotent stem cells down defined lineages, more restricted “multipotent” adult stem cell populations are found; named for their ability to produce a limited number of lineage specific cells types [10] [11]. Multipotent stem cells are retained in adulthood but are more restricted in their differentiation potential and have the capacity of replenishing cells types constituting defined lineages following injury or replacement of ageing cells.

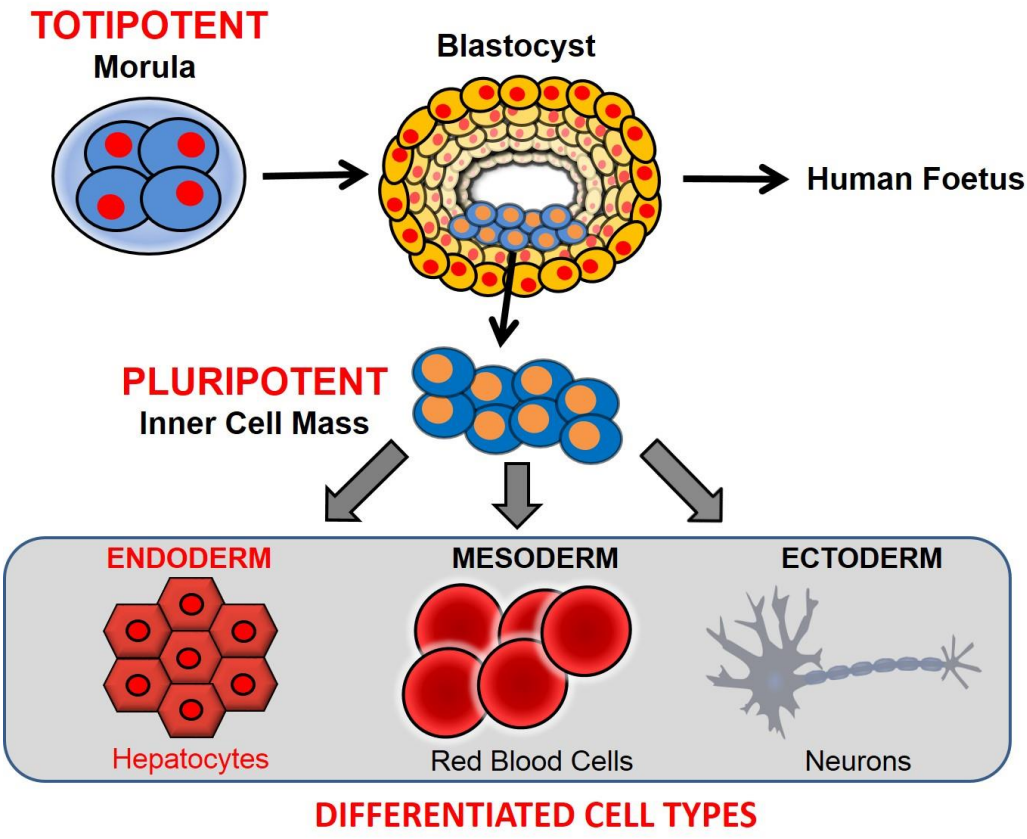

Figure 1: Overview of mammalian development

Developmental progression from fertilised egg to the four-cell totipotent morula and subsequent progression to the blastocyst stage of mammalian development. Pluripotent cells found in the ICM of the cleavage stage blastocyst have the potential to differentiate down cellular lineages to produce all the cell types representing the three germ layers: endoderm, mesoderm and ectoderm. The endodermal lineage is highlighted in red as it is the focus of this thesis giving rise to definitive endoderm and subsequently hepatocytes.

1.1.2 Embryonic Stem Cells

Pluripotent cells found in the ICM of the cleavage stage blastula can be isolated and cultured *in vitro* as embryonic stem cells (ESCs) [12] [13]. This was first achieved with mouse ESCs (mESCs) through the culture of the isolated ICM from pre-implantation blastocysts [12] and subsequently with human ESCs (hESCs) [8]. *In vitro* cultured ESCs possess the ability to differentiate into any cell type constituting the three germ layers, whilst also retaining the capacity to self-renew and are therefore pluripotent [8] [14] [15] [16]. The ICM is separated from the trophectoderm by the process of immunosurgery. The first stage in this process is the acid digestion of the zona pellucida (ZP), the outermost layer of the developing embryo with Acid Tyrode's solution. The isolated ICM can then be plated onto supportive feeder layers from which they expand to form established hESC colonies. Established hESC colonies are characterised by a high nuclear to cytoplasmic ratio and their ability to be cultured for extended periods of time, possibly indefinitely [8].

To support the growth of hESCs *in vitro*, mitotically inactivated mouse embryonic fibroblast (MEF) feeder layers are largely utilised [17]. MEFs secrete an undefined cocktail of growth factors whilst also laying down an extracellular matrix (ECM), supporting cell maintenance and proliferation whilst crucially maintaining pluripotency of hESC colonies (Figure 2A). The secreted MEF cocktail of factors maintain hESC pluripotency through the regulation of pluripotency transcriptional networks. This is in conjunction with exogenously supplemented basic fibroblast growth factor (bFGF/FGF2) to cell culture media to suppress BMP signalling, which promotes the differentiation of hESCs [18]. The co-operation of Activin/Nodal signalling in conjunction with FGF signalling has been shown to be sufficient to maintain pluripotency of hESCs [19].

The culture of mESCs relies on the addition of leukemia inhibitory factor (LIF) to cell culture media. This promotes pluripotency through the activation of the signal transducer and activator of transcription 3 (STAT3) pathway to maintain an undifferentiated state; withdrawal of LIF causes mESC differentiation [20]. However, the culture of hESCs does not require the addition of LIF and STAT3 activation to maintain pluripotency and studies have found these pathways to be inactive in hESCs [21], [22]. Instead hESCs require activation of the Activin/Nodal signalling pathway to promote pluripotency *in vitro* [19] [23] [24].

Xu et al. (2001) amongst others have shown it is possible to grow and maintain pluripotent hESCs without supportive MEF feeder cells [15] [25] [26] [27]. This is termed “feeder-free” culture and is achieved using a defined culture medium with supplemented growth factors accompanied by the use of an appropriate synthetic ECM [15] [28] [29] (Figure 2B). The feeder-free growth of hESCs is advantageous for a number of reasons. Firstly, the use of defined culture conditions removes complicating variables associated with the use of an undefined cocktail of secreted growth factors in MEF conditioned culture media [30]. Secondly, the translational application of hESCs in regenerative medicine would require the absence of contaminating xenogenic components to achieve clinical grade Good Manufacturing Practice (cGMP) [29].

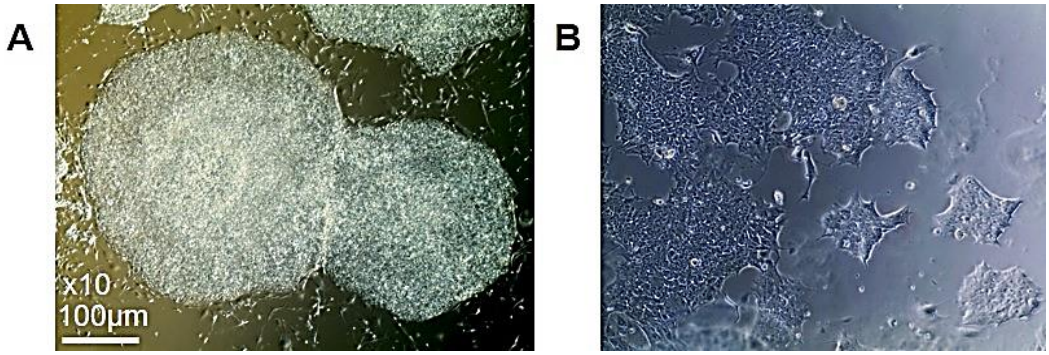

Figure 2: *In vitro* methods for hESC culture

(A) Pluripotent Shef-3 hESC colonies cultured on mitotically inactivated MEF feeder layers to support proliferation and maintenance of pluripotency *in vitro*. Established hESC cultures can be maintained and propagated indefinitely. **(B)** Feeder-free adapted Shef-3 hESCs grown in chemically defined media on fibronectin coated plates. Cell cultures were imaged at x10 magnification.

It is of fundamental importance to confirm pluripotency in newly derived or long-term maintained ES cell lines by showing the capacity to differentiate to cells representative of the three germ layers [8] [16] [31]. There are two common methodologies for confirming the pluripotent capabilities of ES cell lines. Firstly, *in vivo* teratoma formation; a tumor representing cell types of all three germ layers upon transplantation of ESCs, which is used as a test of pluripotency [32] [33] [34]. *In vitro* cultured pluripotent hESCs can be injected into immunocompromised mice which do not reject human cells and can indeed produce teratomas and contribute to cell lineages comprising the three germ layers [35], [12] [36] [37]. Secondly, *in vitro* embryoid body (EB) formation where 3D aggregates have the ability to spontaneously differentiate into the three germ layers in the absence of pluripotency-maintaining culture media [12] [38] [39].

1.1.3 Pluripotency Regulatory Networks

The pluripotent state has been well characterised and the expression of a specific set of pluripotency-associated markers including genes and cell-surface antigens has been defined and mechanistically interrogated [8]. A core transcriptional network involving octamer-binding transcription factor 4 (OCT4), sex determining region Y-box 2 (SOX2) and NANOG have been shown to be key regulators that cooperate in the maintenance of hESC pluripotency [24] [40] [41] [42] [43] [44] [45] [46]. Core pluripotency factors are responsible for supressing genes involved in the differentiation of hESCs whilst also maintaining the expression of other downstream genes involved in the maintenance of pluripotency [47]. This is evident in the OCT4 regulation of REX1 [48], a key regulator of pluripotency found to be expressed at high levels in hESCs then rapidly decreased upon differentiation [49]. OCT4 has been shown to have a regulatory role on the status of the REX1 promoter [48]. When OCT4 is expressed at high levels, the REX1 promoter is repressed by OCT4 and conversely when OCT4 is not actively expressed, REX1 is upregulated through the activation of the REX1 promoter. The interaction of NANOG and REX1 is also evident through the ability of NANOG to activate the REX1 promoter and prevent differentiation [50]. However, high levels of variability are evident amongst the core pluripotency transcriptional network including NANOG and REX1 [51] [52] in pluripotent stem cells. It has been shown that NANOG expression levels fluctuate transiently in sub populations of pluripotent stem cells without losing an undifferentiated state [46]. Purified populations of pluripotent stem cells expressing either high or low levels of NANOG expression were observed to eventually revert to a heterogeneously expressing population despite previous purification.

Extensive mapping of the epigenetic state of CpG promoter regions reveals that genes associated with differentiation are repressed and highly methylated in pluripotent stem cells and subsequently become demethylated upon lineage committed differentiation [47].

Pluripotent hESCs display a unique set of surface antigen markers which can be used to distinguish them from their differentiated progeny. The characterisation of hESCs is also important to ensure that differentiation studies are carried out on high quality, undifferentiated starting populations. The most commonly utilised antigens to identify pluripotent stem cells include the glycolipid stage specific embryonic antigen 3/4 (SSEA3/4) and the keratin sulphates TRA-1-60 and TRA-1-81 [8] [31] [53] [54] .

1.1.4 TGFβ Signalling Pathway

Members of the transforming growth factor beta (TGFβ) superfamily including TGFβ1, TGFβ2, TGFβ3, bone morphogenetic proteins (BMPs), Nodal, Activins and growth and differentiation factors (GDFs) and their corresponding antagonists play a central role in a wide range of biological processes including the regulation of cell growth, stem cell maintenance and cellular differentiation [55], [56] [57]. There are three known classes of TGFβ cell-surface receptors with which TGFβ family member ligands interact, TGFRI (also known as Activin-like kinases (ALKs)), TGFRII and TGFRIII [58]. The difference between the three classes of TGFβ receptors is concerned with their affinity for different TGFβ family ligands. It has been suggested that there is a large degree of overlap between TGFβ family ligand binding to TGFβ receptors due to the large number of ligands compared to prospective receptors [58].

TGFβ family members signal through the binding of ligands to cell surface type I and II serine-threonine kinase receptors [59] [60]. Downstream of the TGFβ receptors, intracellular mothers against decapentaplegic (SMAD) proteins are then involved in the mediation of TGFβ signalling. This involves the targeted phosphorylation of the C-terminal MHII domain of SMAD proteins by corresponding TGFβ serine-threonine kinase receptors [60] [61] [62]. There are eight SMAD proteins encoded by the human genome, however only five function as signalling substrates for the TGFβ family of receptors. SMAD proteins that interact with TGFβ receptors as referred to as receptor-regulated SMADS (R-SMADs). R-SMADS include SMAD1, SMAD2, SMAD3, SMAD5 and SMAD8. TGFβ, Activin and Nodal receptors are associated with signalling through SMAD3 and the less common isoform SMAD2, whilst the BMP signalling pathway is associated with SMAD1, SMAD5 and SMAD8 [63]. The other two SMAD proteins, SMAD6 and SMAD7, serve as inhibitory SMADS (I-SMADs) involved in the interference of SMAD-receptor and SMAD-SMAD dimerization [63].

Upon phosphorylation, R-SMADs are released from SMAD anchor for receptor activation (SARA) which function to regulate the availability of R-SMADs to interact with activated TGFβ receptors [64]. Phosphorylation of the R-SMAD proteins is then followed by the association with the common signal transducer SMAD4 (Co-SMAD) and subsequent translocation to the nucleus, where the SMAD complexes accumulate and bind transcription factors to regulate the transcription of target genes [65]. SMAD proteins undergo a constant process of cytoplasmic to nuclear shuttling in response to TGFβ mediated receptor activation. In this way, SMAD signalling allows cells to respond to external TGFβ signals and mediates transcriptional responses [66].

Co-SMAD4 contains a nuclear export signal (NES), which is typically a cluster of basic residues recognised by nuclear importation factors [67] [68]. The presence of the NES on SMAD4 facilitates the shuttling of SMAD protein complexes between the nucleus and cytoplasm [67]. In this way SMAD mediators localised in the cytoplasm are able to efficiently respond to TGFβ signalling and regulate transcription of target genes [69]. TGFβ signalling elicits very different responses in a cell-type specific manor through the interaction with master regulators of particular cell types [66]. SMAD binding elements (SBEs) have been found in the promoter regions of cell-type specific master regulators [66]. SBEs consist of a CAGACA sequence that directs the binding of SMAD protein complexes to the promoter regions in TGFβ target genes [70].

R-SMADS and Co-SMAD4 share highly conserved N-terminal MHI domains in contrast to the I-SMADs which show diversity in the N-terminal region [71] [72]. The R-SMADs are distinct in their linker region amino acid sequences whereas the C-terminal region is conserved amongst all the SMAD proteins [73]. The linker region of the SMAD protein contains binding sites for SMAD-associated factors including SMAD ubiquitination-related factor (SMURF) as well as sites for phosphorylation through interactions with protein kinases. SMURF functions to selectively regulate the levels of SMAD proteins through proteasomal degradation via ubiquitination [74]. This allows for SMAD protein levels in both unstimulated and activated cells to be tightly controlled [75] [76].

1.1.5 TGFβ Signalling in Pluripotency

TGFβ signalling is known to be active in pluripotent stem cells, cooperating with exogenously supplemented bFGF/FGF2 *in vitro* to exert control on elements of the pluripotency network, although the precise mechanisms remain unclear [18] [19] [24]. It has been shown that NANOG is a direct target of Nodal/Activin signalling with SBEs, responsible for recruitment and binding of SMAD complexes, found in the NANOG promoter [59] [65]. TGFβ signalling has also been shown to cooperate with OCT4 to maintain pluripotency, similarly to NANOG, SBEs have been found in the promotor of the OCT4 gene [66].

SMAD2/3, the effectors of Activin/Nodal signalling, have been shown to control pluripotency-associated factors in hESCs such as OCT4, NANOG, REX1, forkhead box D3 (FOXD3), developmental pluripotency-associated 4 (DPPA4), telomerase reverse transcriptase (TERT), MYC and undifferentiated embryonic UTF1 [66]. The SMAD2/3 regulation of NANOG has been demonstrated to block FGF signalling which would otherwise promote a neuroectodermal fate, the default differentiation pathway of primed hESCs [19] [77] [78] [79] [80]. In pluripotent hESCs, NANOG limits the transcriptional activity of the SMAD2/3 pathway which in turn suppresses endodermal specification and maintains a pluripotent state. BMP signalling promotes differentiation of hESCs; consequently the active inhibition of BMP signalling in hESC cultures has been found to be beneficial for the maintenance of self-renewal and maintenance of pluripotency [23] [81].

Activin/Nodal signalling has also been shown to play a critical role in endodermal development [23] [82] [83]. Endodermal cells are regulated upstream of SMAD2/3 demonstrating the divergent transcriptional networks that are controlled by Activin/Nodal signalling.

The mechanisms by which Activin/Nodal signalling control this divergent range of responses is yet to be fully understood, however, could explained through the interactions of SMAD2/3 with tissue specific binding partners [66].

1.1.6 TGFβ Signalling During *In Vivo* Endoderm Development

During early embryogenesis, a structure known as the Primitive Streak (PS) is formed, into which uncommitted epiblast cells migrate and subsequently leave as either committed mesoderm or definitive endoderm (DE) [55] [84]. The PS has been shown to possess varying developmental potential achieved through differential gene expression and signalling gradients [85] [86]. A tightly regulated interplay of signalling factors controls the development of multipotent precursors, termed mesendoderm [87]. It has been shown that during development, a population of bi-potent mesendoderm precursors arise from the anterior PS possessing the ability to give rise to either mesoderm or endoderm depending on Nodal signalling cues [88] [87].

Nodal has been shown to be critical in DE specification and subsequent lineage fate choice between endoderm and mesoderm [89] [90] [91] [92]. Nodal signalling is controlled extracellularly through its EGF-CFC partner cofactor, Cripto/TDGF-1 (epidermal growth factor-Cripto-1/FRL-1/Cryptic). Nodal signalling is further regulated through the Nodal antagonists Lefty and Cerberus [91] [93] [94]. The co-activator FoxHI is also involved in Nodal signalling through the binding of SMAD2 and regulation of target gene activation [95] [96] [97]. The modulation of Nodal signalling allows for both endoderm and mesoderm specification from mesendoderm precursors [88] [87] [96].

It has been shown that high levels of Nodal signalling specify cells to an endodermal fate, whereas lower levels of Nodal signalling lend to a mesodermal fate [87] (Figure 3). These findings have also been confirmed *in vitro* by the derivation of pancreatic cells, which arise from mesendoderm, through low levels of Nodal-like signalling [98] and hepatocyte-like cells (HLCs) being derived through endodermal precursors utilising high levels of Nodal signalling mimicked through the exogenous addition of Activin A [99] [83].

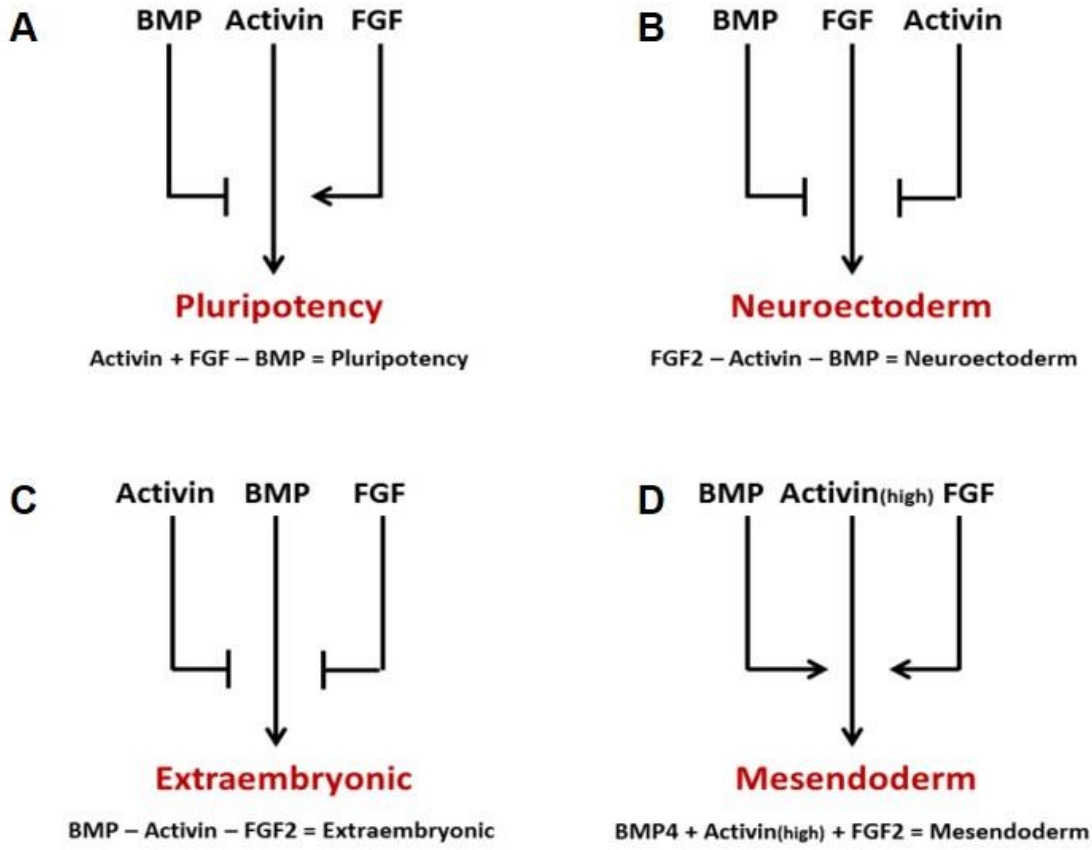

Figure 3: TGFβ signalling in pluripotency and differentiation

(A) Activin signalling in conjunction with exogenously added FGF maintains pluripotency provided BMP signalling is inhibited. **(B)** Sole FGF signalling promotes neuroectoderm differentiation in the absence of BMP and Activin signalling. **(C)** Sole BMP signalling in the absence of Activin and FGF signalling leads to an extraembryonic fate. **(D)** When BMP, FGF signalling are active in a high Activin environment mesodermal differentiation is initiated.

1.1.7 *In Vitro* Definitive Endoderm Specification

The *in vitro* specification of endoderm is of particular interest for regenerative medicine as both the hepatic and pancreatic cell lineages arise from DE [98]. Despite the large interest in endodermal progenitor cells, progress in deriving the cells *in vitro* has been hampered partly due to the lack of distinctive markers that are currently available to identify cell types of interest. Currently, combinations of markers are used to distinguish differentiated cell populations but this is made difficult by the significant overlap of expressed markers in different cell types [100] [101] [102].

Progression to DE is associated with the co-expression of chemokine (C-X-C Motif) receptor 4 (CXCR4), sex determining region Y box 17 (SOX17) and forkhead box protein A2 (FOXA2/HNF3β) [77] [103] [104] [105]. These markers are often used to discriminate DE from visceral endoderm (VE); the latter being distinguished by the lack of GSC expression coupled with robust hepatocyte nuclear factor-α (HNF4α) expression [106] [103]. High levels of HNF4α expression at this stage are characteristic of extra embryonic endoderm, which would indicate that VE had been specified [106]. VE can also be identified from DE by the extra-embryonic endoderm markers sex determining region Y box 7 (SOX7) and caudal type homeobox 2 (CDX2) [107]. Specification to DE from mesendoderm can therefore be monitored *in vitro* by the expression of $FOXA2^{+}$, GSC^{+}, $CXCR4^{+}$ in populations of differentiated cells, [87] [103] [108].

TGF-β Signalling

It is known that the TGFβ family member Nodal is a key regulator for the establishment of DE specification *in vivo* [92] [109]. To this end Activin A, another related TGFβ family member to Nodal, is routinely used *in vitro* to induce DE specification from pluripotent stem cells [87] [110] [111] [84] [106] [83]. Activin A binds to the same Activin type I/II receptors as Nodal and activates similar signalling pathways *in vitro*. There are however distinct differences in the signalling of Activin A and Nodal. Nodal is dependent on its co-factor Cripto to bind Activin type II receptors and initiate SMAD signalling through the recruitment and phosphorylation of SMAD2/3. This is followed by the association with the common signal transducer SMAD4 and subsequent translocation to the nucleus to modulate gene expression; whilst Activin A is not reliant on Cripto to bind Activin type II receptors [91].

Using high levels of exogenous Activin A, typically 100ng/ml for five to six days, specifies DE from pluripotent stem cells through mesendodermal precursors, [87] [99] [110] [84] [106] [112] [107] [83]. Differentiation to a cell-type synonymous with mesendoderm *in vivo* can be identified through the expression of markers such as Brachyury (T) and Goosecoid (Gsc) [87]. It is thought that the specification of endoderm by Activin A is dependent on the inhibition of the phosphoinositide-3-kinase (PI3K) signalling in low concentrations of knock-out serum replacement (KSR) [83]. McLean *et al*. (2007) proposed that factors present in serum drive PI3K signalling and block the differentiation of hESCs [83].

There has been evidence uncovered showing that there are significant off-target effects caused by the utilisation of Activin A to induce DE specification *in vitro* (McKay *et al*., unpublished data). Expression of the visceral endoderm marker OTX2 and mesodermal markers Brachyury (T) and BMP2 were found to be increased upon the exogenous addition of Activin A over the course of six days.

Activin A is hypothesised to stimulate the transcriptional up-regulation of Nodal which then promotes DE specification from this study. The differences in signalling networks between Activin A and Nodal are hypothesised to account for the heterogeneous populations of DE produced through this procedure. Work is therefore required to dissect the underlying mechanisms involved in Nodal signalling during the specification of DE.

WNT Signalling

Wnt signalling has been shown to have a key role during early embryogenesis and in the self-renewal and maintenance of hESCs [87] [113] [114] [115] [116] [117]. The canonical Wnt signalling pathway that involves binding of the Wnt family ligands WNT1, WNT3A and WNT8 to the trans-membrane protein Frizzled (Fzd) and low density receptor-related protein 5/6 (LDRRP5/6) which activates Wnt/β-catenin signalling [118] [119]. Fzd is then involved in the recruitment of the intracellular protein Dishevelled (Dvl) which subsequently localises the axin-glycogen synthase kinase 3 (GSK3) to the cell membrane initiating two rounds of LDRRP5/6 phosphorylation firstly by Axin-GSK3 and finally by casein kinase 1 (CK1). This series of events leads to the inactivation of the β-catenin destruction complex and allows the accumulation and translocation of β-catenin to the nucleus where it binds to TCF/LEF transcription factors [120] (Figure 4). The abolition of WNT3 signalling results in the lack of PS formation during embryogenesis [113]. *In vitro* hepatocyte differentiation has also provided evidence for the importance of canonical WNT3A signalling during early DE specification steps [99] [121].

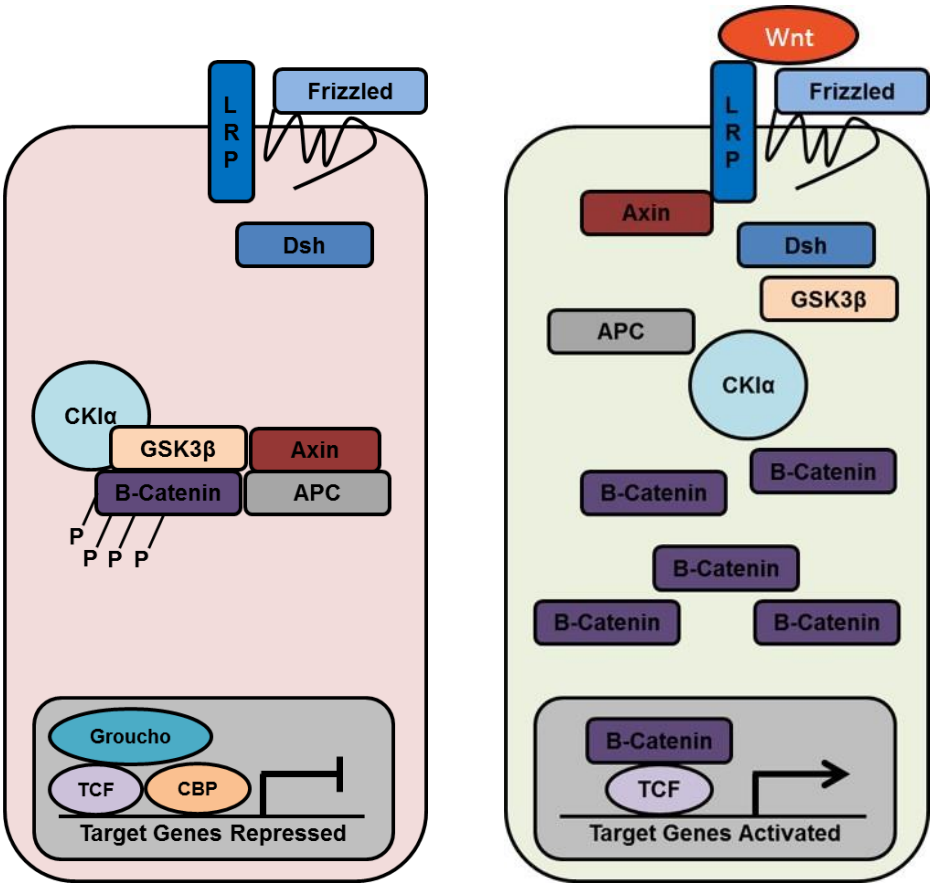

Figure 4: Canonical Wnt signalling pathway

Overview of the canonical Wnt signalling pathway in both the activated or repressed states. During the inactive state, β-catenin is sequentially phosphorylated leading to ubiquitination and subsequent proteasomal degradation; preventing β-catenin from reaching the nucleus. Upon Wnt ligand binding the β-catenin destruction complex disassociates and β-catenin accumulates and subsequently translocate to the nucleus where it binds to TCF/LEF transcription factors and activates downstream targets of Wnt signalling.

Recent studies utilising small molecules to mimic WNT3A signalling through the inhibition of the GSK3 pathway have provided evidence for the requirement in DE specification [121]. Bone et. al (2011) showed that a chemically synthesised selective GSK3 inhibitor, 1M, when used in defined culture conditions efficiently promote the differentiation of hESCs towards DE through mesendoderm precursors [121]. These findings conclude that the inhibition of GSK3 signalling does not support pluripotency, when assayed in hESCs through the loss of the pluripotency-associated surface markers SSEA-4 and TRA-1-60. It was found that 1M mediated differentiation of hESCs resulted in a transient increase in Nodal expression. A further non-structurally related GSK3 inhibitor, BIO, was also used in parallel in the same study and showed a similar trend in promoting the differentiation of hESCs towards an endodermal fate [121]. Further evidence of the importance of WNT signalling has previously been shown by Tahamtini et al. (2013) where the small bioactive molecule CHIR99021, a GSK-3β inhibitor, was used to prime pluripotent stem cells before differentiation to DE using Activin A. Specified DE cells exhibited stronger expression of both SOX17 and FOXA2 with CHIR99021 priming followed by Activin A differentiation than populations of DE produced without initial Wnt signalling priming [122].

Other signalling pathways active during DE differentiation

The role of FGF signalling in the specification of anterior definitive endoderm (ADE) has been examined by studying the expression of the early ADE and mesendodermal marker, homeodomain protein (Hex) [77]. Morrison *et al*. (2008) utilised a fluorescent reporter gene under the control of Hex along with the DE marker, CCXR4 to examine the role of FGF during hESC differentiation to DE [77].

Results from this study showed that FGF signalling promoted the specification of ADE from hESCs. Previous studies showed that if FGF signalling is abolished by the knock-out of the corresponding receptor FGFR1, there is an inability to contribute to endoderm [123].

1.2 Hepatocyte Differentiation *In Vitro*

1.2.1 Application of Embryonic Stem Cells to Drug Discovery

There is a demand from the biotechnology industry for an inexhaustible supply of hepatocytes to be used in regenerative medicine to help to repair, augment or replace damaged tissues and with which to perform drug toxicity screens [124] [125]. As the liver is the primary organ to metabolise drug compounds, it is susceptible to damage through drug toxicity. The pharmaceutical industry has a current unmet need for hepatocytes to carry out drug safety testing and this is further compounded by the fact that isolated primary hepatocytes quickly lose their proliferative potential when cultured *in vitro* and dedifferentiate; losing their functional activity [126]. Phenotypic and genotypic variability is also a significant problem amongst isolated donor primary hepatocyte samples [127]. The use of current *in vitro* HLC models for pre-clinical drug development is also of limited value, as it is not directly translatable to the predictive drug toxicity and metabolism in humans [4]. HepG2 and Huh7 hepatocarcinoma cell lines are widely used as a model for hepatocytes, however they show limited metabolic activity so are unsuitable for drug induction assays [124] [128] [129] [130].

HepaRG cells are a bi-potent progenitor hepatocarcinoma cell line which possesses the potential to differentiate towards either biliary-like cells or hepatocytes-like cells [128] [129] [131] [132]. The differentiation to more differentiated cell type is achieved through the application of DMSO, a HDAC inhibitor, to cell culture media to promote terminal differentiation [133]. HepaRG cells have been shown to possess metabolically significant drug induction levels, albeit at lower levels than seen in primary hepatocytes. It is also of note that HepaRG cells serve as a poor model for hepatotoxicity studies [124] [128].

Pluripotent stem cells therefore hold immense promise to produce an unlimited amount of fully differentiated hepatocytes through the directed step-wise differentiation *in vitro* using chemically defined culture conditions. To realise this potential, there is a need to understand the cell fate specification with a view to efficiently and reproducibly differentiate pluripotent stem cells to hepatocytes. Studies have shown that *in vitro* derived HLCs to date show some degree of hepatic maturation [107] [99] [106] [134] [135]. Functional characteristics of primary hepatocytes include ureagenesis and gluconeogenesis [110] [99], albumin production [110] [111], indocyanine green (ICG) secretion [110] [111] and CYP450 activity [110] [136]. Differentiated HLCs produced so far have been assessed to show some degree of functional capability albeit at significantly lower levels than seen in isolated primary hepatocytes. This leads to the conclusion that the HLCs that have been derived so far in these *in vitro* studies resemble immature, foetal hepatocytes [137] [138] [139].

The CYP450 family play a critical role in metabolism and detoxification of drug compounds and other xenobiotics [140] [141] [142] [143]. Therefore, it is important to elucidate the mechanisms underlying hepatic maturation to produce fully functional and mature HLCs for application in pre-clinical drug toxicity screening.

Proof of principle studies have shown that these derived HLCs can be transplanted *in vivo* and have the potential to contribute to liver function in recipient rat models demonstrating the potential for regeneration of damaged livers through transplantation of differentiated HLCs [106].

1.2.2 Hepatic Specification *In Vitro*

The process of liver specification *in vivo* is complex, relying on a number of factors involving secreted growth factors along with cell-cell interactions and ECM microenvironment [144] [145] [146] [147]. Although the fundamental signalling pathways involved in DE differentiation are well characterised the more complex regulatory networks involved in these processes are still not yet fully understood.

The *in vitro* differentiation of pluripotent stem cells down the hepatic cell lineage to ultimately form mature hepatocytes can be broken down into four distinct stages of mammalian development (Figure 5A). The first step is the specification of DE from pluripotent stem cells, followed by hepatic specification and finally hepatic maturation to produce mature, functional cells. *In vitro* hepatocyte differentiation strategies attempt to mimic the tightly regulated signalling pathways involved in DE formation, hepatic specification and maturation *in vivo* using key stage-specific markers to assess the progression [83, 84, 87, 99, 106, 107, 110, 112] (Figure 5B).

A

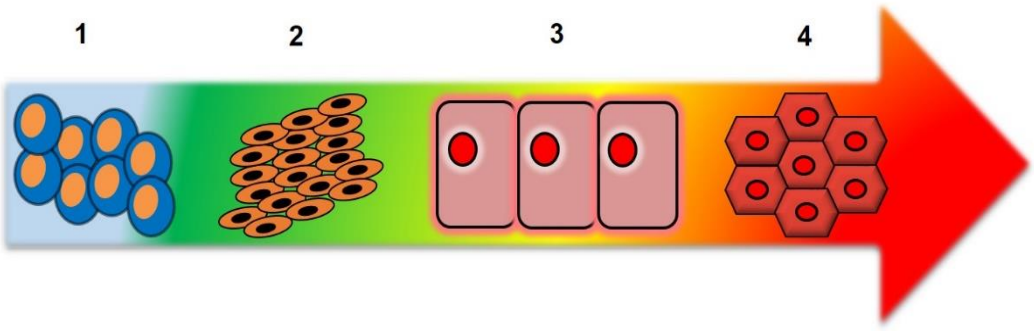

B

Stage Number	Cell Type	Associated Markers
1	Pluripotent Stem Cells	OCT4, NANOG, SSEA-4, TRA-1-60, TRA-1-80
2	Definitive Endoderm	SOX17, FOXA2, CXCR4
3	Hepatic Progenitors	FOXA2, HNF4α, AFP, ALB, α1AT
4	Mature Hepatocytes	CYP450, G6P, ALB

Figure 5: *In vitro* stages of hepatocyte differentiation from pluripotent hESCs

(A) Overview of the four main developmental stages of differentiation from pluripotent stem cells to definitive endoderm, hepatic progenitors and finally mature, functional hepatocytes. **(B)** Table highlighting the Key stage-specific gene and cell surface markers associated with the progression through distinct phases of hepatic lineage development.

HLCs have been induced from populations of pluripotent stem cells *in vitro* firstly through the utilisation of Activin A or prolonged 1M/BIO/GSK3β inhibitor use, mimicking canonical WNT3A signalling [148] [121]. After DE specification hepatic induction is carried out to produce bi-potent liver precursors, termed hepatoblasts. Hepatoblasts have the ability to produce both metabolically active hepatocytes or biliary epithelial cells constituting two of the cell types of the liver [149] [150].

The presence of alpha fetoprotein (AFP) and HNF4α, characteristic of hepatoblast progenitor cells at this stage, can be detected demonstrating the capacity of growth factors and small molecule inhibitors to modulate signalling pathways, allowing the differentiation of hESCs to a DE and a subsequent hepatic fate [151] [152] [153] [111] [106].

A reduction in serum concentration to between 0.5–2% has also been shown to increase the expression of hepatic markers although the precise mechanism is unclear [148] [135]. An increase in Albumin (ALB), AFP, alpha 1-anti trypsin (α1AT), HNF4α and FOXA2 was seen after the reduction of the serum concentration in culture media [135]. FGF4 and BMP2 have been shown to be critical in the specification to the hepatic lineage in studies of mouse embryos [154] [155] [135] and are frequently used during hepatic lineage specification steps. *In vivo* studies have also shown that BMP and FGF signalling are involved in hepatic progenitor proliferation stages upon liver injury [156] [157].

As well as the characterised role of the canonical WNT3A in DE specification, the related non-canonical Wnt family member WNT5A has been implicated in differentiation along the hepatic lineage. It has been proposed that WNT5A could act as an antagonist to repress canonical Wnt signalling dependant on the differentiation status of the hepatic cells [158] [159]. In this way, differential Wnt signalling is active during the different developmental stages from canonical Wnt signalling in early differentiation stages to non-canonical signal activation upon the maturation of hepatic cells.

It has been shown by Cai *et al*. (2007) that the combination of both FGF4 and BMP2 has an increased effect on the expression on ALB, a hepatoblast marker, indicating a role in hepatic specification *in vitro* [110]. The addition of either FGF4 or BMP2 alone in the same study however was shown to have had no effect, demonstrating the cooperative effect. These results were demonstrated using the FGF inhibitor SU5402 and the BMP inhibitor Noggin. In a separate study Song *et al*. (2009) used FGF4 and BMP2 to induce hepatic specification in cultures of DE, differentiated from induced pluripotent stem cells (iPS) lines [107].

After culture with FGF4 and BMP2 for a period of four days, expression of hepatic markers and liver-enriched transcription factors were detected when analysed through qPCR. The hepatic markers AFP, ALB, Cytokeratin-8 (CK-8), CK-18, HNF4α, Hex and GATA binding protein 4 (GATA4) were all found to be expressed in cells treated with FGF4 and BMP2 [107].

Hepatocyte growth factor (HGF) has been used in studies after DE has been specified, to induce differentiation towards the hepatic lineage and expand the population of hepatic-like cells [99], [107], [106]. Addition of HGF was shown to up-regulate AFP and FOXA2 expression levels, whilst immunostaining showed that the cells were double positive for AFP and FOXA2, indicating that the cells had been induced to a hepatoblast fate [106].

There has been support from studies that dimethyl sulfoxide (DMSO), a histone deacetylase (HDAC) inhibitor, provides an inductive effect towards differentiation to the hepatic lineage from primed DE [99]. Because DMSO alters the epigenetic state of cells, it is thought that exposure of cells to DMSO provides inductive effects towards certain cell fates by altering methylation and epigenetic modifications and promoting terminal differentiation [160]. Typically, 2% DMSO is used in specified DE cultures alongside both FGF4 and BMP2 to induce hepatic specification and promote proliferation. The addition of 2% DMSO to Huh7 cells, a liver carcinoma cell line used as an *in vitro* model for studying hepatocytes, resulted in terminal differentiation and consequently elevated levels of late stage hepatic markers [161]. Another HDAC inhibitor, sodium butyrate (NaB), has also been used to induce hepatic specification from hESCs in a similar manner as DMSO [162].

The second stage of *in vitro* hepatocyte differentiation is concerned with the expansion of the specified hepatic progenitor cells. For this reason, FGF4 and HGF are commonly used as they are known to be involved in cell proliferation and expansion of the hepatic progenitor pool. FGF signalling has a number of roles in determining cell fate in embryogenesis and in differentiation [78]. FGF/MAPK signalling is also known to be involved in the regulation of hepatic gene expression whilst HGF has been seen to be highly upregulated upon hepatectomy [163] [164]. As well as the addition of FGF2 to maintain hESCs in a proliferating and pluripotent state, the related family member FGF4 is involved in the proliferation and maintenance of hepatic progenitors [165].

Vascular endothelial growth factor (VEGF) is known to play a role in the proliferation of hepatocytes and has been documented to induce proliferation and function in EBs [166] and also to play a role in liver regeneration in coordination with HGF [167]. Along with VEGF, FGF and HGF the cytokine GDF15, a divergent member of the TGFβ superfamily, has been shown to be upregulated following liver injury. It has been found that the mRNA expression and protein secretion levels of GDF15 were increased after acute Hepatitis C virus (HCV) infection, surgical and chemical liver injury [168], [169].

Upregulation of GDF15 following liver injury was seen to induce the activation of Akt signalling, which is involved in a wide variety of cellular processes including glucose metabolism, cell proliferation and transcriptional modulation. Activation of Akt signalling leads to the downstream target phosphorylation of this pathway which includes GSK3β, E-cadherin and β-catenin. Inhibition of GSK3β through Akt activation could therefore increase glycogen synthesis and lead to Wnt signalling activation which has been shown to be important in hepatic organogenesis [170].

It has been previously reported that the inhibition of TGFβ1/SMAD signalling through the overexpression of the I-SMAD7 improves liver regeneration through suppression of TGFβ1 signalling [171] [172]. SB-431542 selectively inhibits Alk4, Alk5 and Alk7 which are responsible for the transmission of TGFβ1 signalling. Specific inhibitor of SMAD3 (SIS3), a selective inhibitor of the SMAD3 pathway, has been shown to attenuate TGFβ1 mediated transcriptional activity without exhibiting inhibitory action on SMAD2 [173]. Consequently, after DE specification where TGFβ/SMAD signalling is of critical importance, SIS3 and SB-431542 could be utilised to expand the hepatic progenitor cell population.

1.2.3 Hepatic Maturation

The CYP450 family of mono-oxygenases are key players in the removal of xenobiotic compounds from the body; mainly involved in phase I and II of metabolic reactions which includes oxidation, hydrolysis and reduction reactions [140] [141] [142] [143]. The inductive level of CYP450 metabolic activity is therefore of critical importance if the promise of the application of pluripotent stem cell derived HLCs to drug toxicity screens is to be fulfilled. Targeting the regulatory mechanisms that underlie CYP450 expression is used as an approach in the production of more mature hepatocytes [174] [175]. There is a wide diversity on the specificity of interactions of the CYP450 family members; some being very selective in substrate interactions whilst some having a more generalised association with xenobiotic targets [176] [177]. Diversity amongst the CYP450 family members is also seen in the expression of different isoforms that are induced by the presence of xenobiotic compounds [178].

Members of the CYP3A family have been found to be the most abundant CYP450 family member present in the liver and also display the widest range of xenobiotic substrate interaction [179] [180]. CYP3A4 can be induced through the addition of the drug rifampicin [181]. CYP1 is another key member of the CYP450 family involved in phase I metabolic reactions and activated by some polycyclic aromatic hydrocarbons (PAH) [182]. CYP1 can be experimentally induced through the addition of the proton pump inhibitor drug omeprazole [183].

Oncostatin M (OSM) has been identified as a potent extra-cellular inducer of hepatic development *in vivo* [146]. OSM has been shown to up-regulate the expression of the hepatic markers HNF4 and ccaat-enhancer binding proteins (C/EBPα) [184] and promote morphological changes as well as functional characteristics of primary hepatocytes [146]. Consequently, OSM is added to cultures for a period of seven to ten days after hepatic specification to induce the maturation of differentiated HLCs *in vitro* [185] [99] [135] [106] [186]. Dexamethasone (Dex) is routinely added to cultures along with OSM to improve hepatic cell viability, through the ability of Dex to suppress apoptosis through the upregulation of anti-apoptotic factors [187]. In separate studies, Dex has been shown to be sufficient to induce a reprogramming switch from pancreatic cells to a hepatic fate, identified by the upregulation of hepatic markers [188]. Insulin has also been used utilised in the maturation process of differentiated HLCs because of its ability to regulate glycogen synthesis [135] [99].

It is known that HNF4α, a transcription factor of the steroid hormone receptor superfamily and plays a key role in the development of the liver [189] [190] [191] [192] [193] [194] [195]. HNF4α regulates a wide variety of liver specific factors including hepatocyte proliferation [196] and the CYP450 superfamily of metabolic enzymes, which play a central role in drug metabolism [197] [198] [199].

The importance of HNF4α in the regulation of members of the CYP450 family was demonstrated in primary human hepatocytes through the expression of HNF4α antisense RNA resulting in a 50% reduction of CYP3A4 mRNA expression levels [198]. Further evidence was shown by reduction in the mRNA of phase II enzymes and xenobiotic transporters in Hnf4α-null mice [200].

However, the HNF4α ligand has remained elusive despite a number of possible candidates including the essential fatty acid, linoleic acid [201]. HNF4α contains both DNA and ligand binding domains [202] and can regulate discrete targets through the association with coactivators [203] [204]. It is known that nuclear receptor ligand binding domains exist in two forms; the active and inactive bound conformations [205] [206]. Differences between these two states of activity depends on the conformation of the helix α12, also known as AF-2. In the inactive state, the ligand binding pocket is accessible and “open” which prevents the binding of coactivators. In the active state, the ligand binding pocket is in the “closed” conformation and allows the association and binding of coactivators. The process of conformational change to transition between the active and inactive states of other nuclear hormone receptors has led to the theory that ligand binding is required for the activation of HNF4α [205] [206] [207] [202]. This theory is challenged however by the fact that not all fatty acids can bind and induce a conformational change in HNF4α from the inactive to active states; being necessary for HNF4α activation but not sufficient on their own [208]. Previous studies have suggested that HNF4α is constitutively bound to fatty acids [207] and possesses a binding pocket that is different than other nuclear receptors including peroxisome proliferator-activated receptor (PPAR) and retinoid x-receptor (RXR) [209].

The binding pocket of HNF4α has previously been shown through the x-ray crystal structure analysis to contain fatty acids; therefore suggesting that fatty acids are in fact the endogenous ligands [202]. Despite the evidence that fatty acids can indeed bind to the ligand binding pocket of HNF4α, there is limited evidence to show the subsequent modulation and effects on activity [210] [208]. Progress in understanding and identifying potential ligands that modulate HNF4α activity is particularly hampered by the discovery that ligand exchange in the ligand binding pocket is very poor *in vitro*; meaning changes in HNF4α activity upon addition of fatty acids is difficult to study [202] [207]. The lack of definitive answers has raised the question of whether ligands do indeed bind and modulate HNF4 activity or rather ligand binding results in a conformational change [210].

Due to the key role played by HNF4α in the regulation of the CYP450 family members, targeting the upregulation of HNF4α during the hepatic maturation phases of differentiation is critical in producing more metabolically active hepatocytes [211] [212]. *In vitro* studies have further shown that Hnf4α is critical for the maintenance of differentiated hepatocyte functions [213]. Nuclear hormone receptor (NHR) proteins are key regulators of liver metabolism and in the detoxification and removal of xenobiotic compounds from the body [214]. There is a growing body of evidence that another function of the nuclear hormone receptors is the protection of cells from the accumulation of toxic metabolic intermediates [215]. Toxic intermediates activate nuclear hormone sensors which in turn upregulate members of the CYP450 family with a view to eliminate them. Xenobiotic-mediated activation of the nuclear hormone receptors results in the activation of a battery of the phase I and II metabolic enzymes. There are several nuclear receptor families that are involved in these processes and are therefore targeted for manipulation with a view to produce more metabolically relevant HLCs for use in drug toxicity screens [216].

HNF4α has been shown to important in the nuclear hormone receptor-mediated activation of CYP3A4 through binding to the enhancer region of CYP3A4 and allowing subsequent nuclear hormone receptor-mediated transcriptional activation of CYP3A4 [217]. In the same study, it was demonstrated that the deletion of Hnf4α resulted in the abolition of CYP3A in fetal mice and conditional deletion in adult mice resulted in the lack of CYP3A inducibility and a reduction in basal levels [217].

PXR Family

The pregnane X receptor (PXR) family of nuclear hormone receptors are activated by many xenobiotic compounds including steroids and antibiotics as well as hyperforin, a component of St. John's Wort [218] [219]. The PXR family function as generalised sensors of hydrophobic toxins; in contrast to other nuclear receptor family members which act more specifically and recognise a smaller number of ligands [220] [221]. Hyperforin has been shown to have an inductive effect of the CYP450 family members, in particular, CYP3A4 and CYP2C9 through the activation of PXR [222] [174] [220] [175] [223].

Upon sensing of xenobiotic compounds, PXR binds to DNA regulatory elements of CYP3A4 along with other factors involved in the metabolic process, resulting in the removal of the compound from the body. This system of PXR activation of CYP3A has been previously established *in vivo* [224] [225]. Since the CYP3A family is involved in a large proportion of xenobiotic drug metabolism and PXR has been shown to play a regulatory role in all stages of metabolic process, PXR activation would seem to be a key target in trying to induce CYP450 family members to levels of activity seen in primary hepatocytes.

CAR Family

The constitutive androstane receptor (CAR) family of nuclear hormone receptors function as sensors and regulators for the metabolism of endobiotic and xenobiotic compounds in conjunction with PXR [226] [227]. CARs regulate transcription of genes including members of the CYP450 family of enzymes involved in drug metabolism [221]. CITCO, a small biologically active molecule, has been demonstrated to be an agonist of the CAR [228]. In a similar manor clofibrate, an organic compound found to be an activator of lipoprotein lipase, has been shown to have an inductive effect on members of the CYP450 family of enzymes, particularly CYP4A in rat hepatocyte cultures *in vitro* [229]. However, the effects have been seen to be transient and the underlying molecular mechanisms remain largely unknown.

LXR Family

The liver X receptor (LXR) family of transcription factors are closely related to nuclear factors such as peroxisome proliferator activated receptor-α (PPARα) and function to regulate cholesterol, fatty acid and glucose homeostasis and sense the presence of xenobiotics [230]. In addition, LXR has been shown to upregulate the expression of CYP3A [231] and is of interest during hepatocyte maturation.

The small molecule agonist T0901317 has been shown to upregulate LXR and consequently ATP-binding cassette transporter 1 (ABC1) which has been shown to be a major regulator of both cholesterol and phospholipid homeostasis [232]. Whilst LXR functions to regulate the homeostasis of cholesterol, fatty acids and glucose the role of LXR in promoting hepatocyte differentiation was examined as a method of increasing metabolic activity in pluripotent-derived HLCs in this thesis.

In vitro studies using HepaRG cell cultures have shown that the overexpression of LXR corresponds with an increase in hepatic functions associated with mature hepatocytes including CYP450 family member upregulation [233]. Interestingly, it was seen that the overexpression of LXR and the corresponding maturation of hepatocytes was dependant on cooperative HNF4α signalling.

1.3 CombiCult®

The primary challenge of *in vitro* stem cell differentiation is recapitulating the complex set of signalling cues in normal *in vivo* mammalian development. The ability to target key lineage specific signalling pathways with growth factors and small molecules to direct stem cell differentiation toward desired cell lineages is a major challenge in research and threatens to create a bottleneck in an otherwise rapidly advancing field [234] [235] [236]. Trial and error methods for the determination of revised stem cell differentiation protocols and the associated titration optimisation steps are both costly and time-consuming procedures resulting in slow progress. The ability to grow cell lines long-term *in vitro* relies on delineating the precise culture conditions allowing the retention of cell line integrity in terms of cell viability, morphology, and proliferative potential.

Plasticell, a biotechnology company specialising in stem cell differentiation, has developed combinatorial cell culture, (CombiCult®), a powerful multiplexed screening platform, for the establishment of new stem cell differentiation protocols [237] [238] [239]. The CombiCult® platform achieves this through step-wise assessment of the application of growth factors and/or small bioactive molecules to stem cells to direct differentiation towards cell types of interest (Figure 6).

CombiCult® allows for the multiplexing of a large range of variable cell culture media combinations through a process known as split-pooling; currently allowing for up to 20,000 possible culture media permutations to assess differentiation potential [239]. This enables not only for the trial of new growth factors and bioactive small molecules but also the temporal sampling and titration so that the optimal combination of cell culture media variables can be delineated to faithfully recapitulate normal developmental cues.

Advantages of the CombiCult® platform include the ability to carry out vast multiplexed combinatorial cell culture in small scale, greatly reducing the cost associated with discovering new differentiation protocols [239]. The elimination of serum from cell culture and the use of defined culture conditions enables the precise combination of signalling cues involved in cell lineage fate to be identified [240]. Other advantages of CombiCult® include the plasticity of cell lines that can be seeded onto the polymer beads. Different hESC lines are known to be better suited and more capable of differentiating to certain cell lineages than others [241] [242] [243]. It is therefore possible to identify the optimal hESC line to be used in conjunction with the optimal culture conditions for the step-wise differentiation to hepatocytes. The ability to screen small molecule libraries to direct cell differentiation is advantageous as it reduces the costs associated with the use of growth factors in culture media.

The CombiCult® screening platform is therefore a powerful tool to identify critical factors important in the differentiation of hepatocytes from pluripotent stem cells. This will be of great value in identifying new and novel differentiation protocols and overcoming the major bottlenecks associated with the early differentiation and subsequent maturation of hepatocytes.

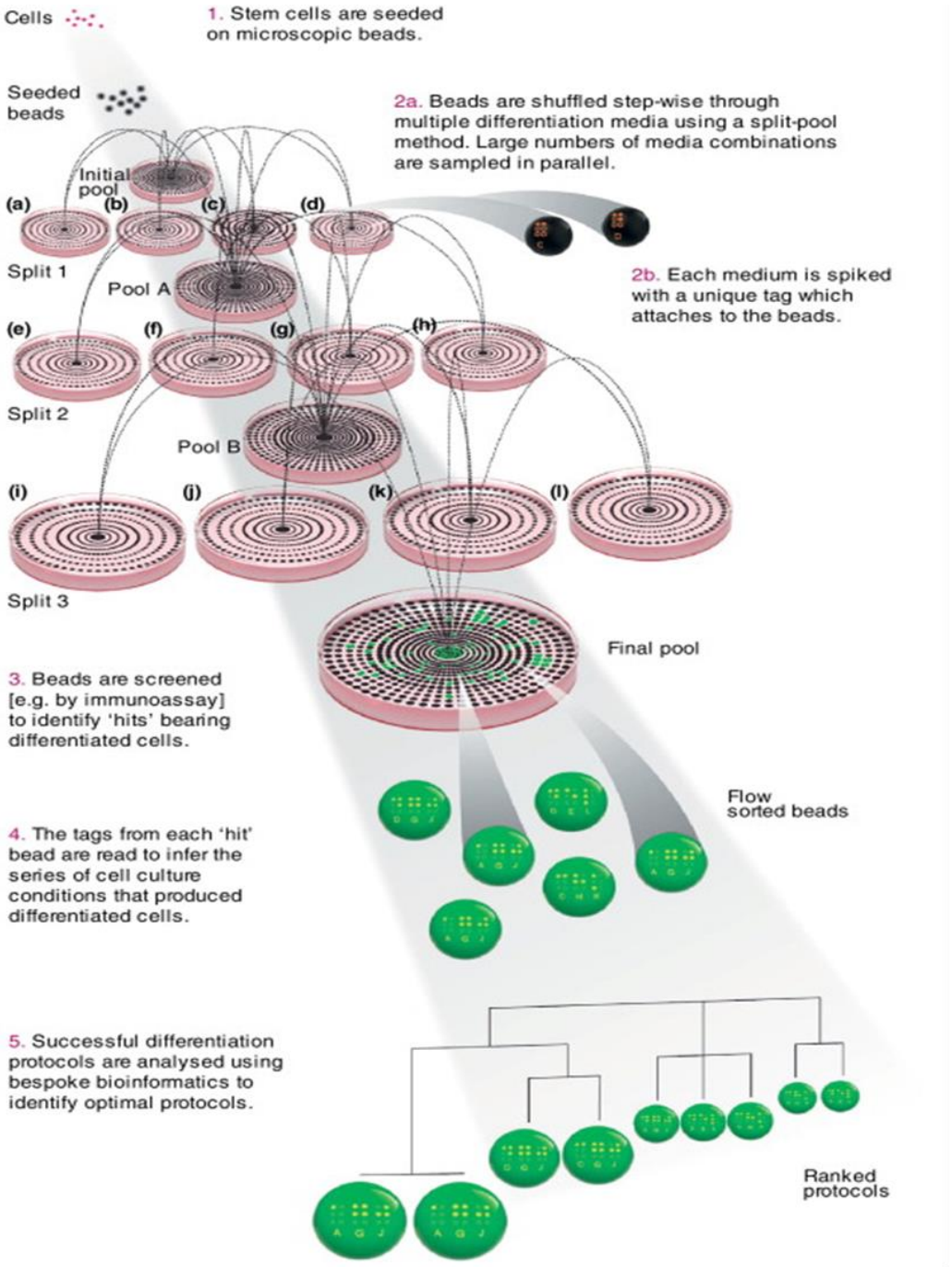

Figure 6: CombiCult® split pooling workflow overview

Overview of the CombiCult® split-pooling procedure for shuffling microcarriers seeded with hESCs through sequential media combinations. Each media condition is spiked with a unique fluorescent tag to allow tracking of cell culture history to identify new and novel differentiation protocols by assessing the cell culture history of "hits". Credit: Plasticell Limited.

1.4 Aims of Thesis

There has been great progress in the understanding of liver development and consequently protocols have been developed for the *in vitro* differentiation of pluripotent stem cells to hepatocyte-like cells (HLCs). However, there remains two major bottlenecks in the efficient differentiation of functional hepatocytes with which to apply to early stage drug toxicity screens. The research questions addressed in this thesis were aimed to contribute to the overall understanding and knowledge of the hepatic differentiation process *in vitro* and shed new light on further avenues of investigation.

The first bottleneck in this process is in the homogenous differentiation of DE from cultures of pluripotent stem cells. To date, hepatic differentiation protocols almost exclusively use Activin A, used as a substitute of Nodal signalling, in the first stage of pluripotent stem cell differentiation to specify DE. Tools to investigate these early developmental steps are therefore required to better assess the populations of DE produced through the manipulation of Nodal/Cripto signalling; with a view to more efficiently and homogenously differentiate pluripotent stem cells as a starting point for subsequent hepatic lineage specification. Consequently, gene modulation tools and cell differentiation systems to investigate these early developmental processes were assessed in this thesis. The working hypothesis would be that Nodal is in fact the driver for DE specification *in vitro* and the absence of Nodal signalling would produce a more heterogeneous population of cells compared to a cell differentiation environment with high levels of Nodal signalling. To investigate this hypothesis, lentiviral vectors to knock down or overexpress Nodal/Critpo signalling were assessed with a view to create tools with which to compare DE homogeneity in future studies.

The second bottleneck concerns the maturation of differentiated hepatic cells to possess the functional capabilities that are characteristic of mature hepatocytes. The incorporation of novel hepatic maturation factors at appropriate concentrations to *in vitro* differentiation protocols is therefore required with a view to induce terminal differentiation to functional hepatocytes. To address this research problem in this thesis, a CombiCult® differentiation screen was conducted to identify combinations of hepatic differentiation factors that promote the most mature HLCs *in vitro*. Growth factors and small molecule inhibitors/agonists which have not previously been applied to hepatic *in vitro* differentiation protocols were incorporated into the CombiCult® differentiation screen to identify and define novel differentiation protocols. Lentiviral reporter vectors were then further used to determine optimum concentrations of small molecule agonists and to validate potential ligands for master hepatic regulators.

To investigate these research problems, this thesis will address the following aims:

- Validate lentiviral vectors to overexpress or knock down Nodal and/or Cripto.
- Compare different Nodal/Cripto conditioned media systems to differentiate pluripotent cells to DE.
- Design and conduct a CombiCult® screen to identify novel factors for the optimal hepatic differentiation of pluripotent stem cells to HLCs.
- Isolate top CombiCult® hepatic differentiation protocols for further analysis of maturation in monolayer culture.
- Optimise *in vitro* hepatic differentiation differentiation procedure using CombiCult®-derived protocols over the 28-day time course.
- Create a hepatic reporter applicable to the CombiCult® platform to replace ICC staining as a readout for mature HLCs.
- Validate hepatic reporters for the *in vitro* titration of hepatic maturation inducing factors identified through CombiCult®.

- Identify optimal concentration ranges for small molecule agonists for *in vitro* studies of HLC maturation.

Chapter 2: Methods

2.1 Cell Culture Techniques

2.1.1 Cell Lines

All cell lines were cultured at 37^0C in humidified incubators supplemented with 5% CO_2. Human Embryonic Kidney (HEK) 293T cells (originally obtained from European Collection of Authenticated Cell Cultures (ECACC): 12022001)) were used at passage 10 (P10) to produce lentivirus. The hepatocarcinoma cell lines Huh7 (originally obtained from ECACC: 01042712), HepG2 at P15 (originally obtained from ECACC: 85011430) and HepaRG at P5 (Invitrogen, Loughborough, UK) were used as *in vitro* hepatocyte models. The human colon adenocarcinoma cell line LS174T (originally obtained from ECACC: 87060401) was used to validate levels of LGR5 knockdown using shRNA clones at P11. HeLa cells (originally obtained from ECACC: 93021013) were used to validate Nodal/Cripto shRNA knockdown clones at P15. The mouse fibroblast cell line NIH-3T3 (originally obtained from ECACC: 93061524) was used as a non-hepatic control to validate hepatic lentiviral reporters at P3. Mouse Embryonic Fibroblasts (MEFs) were obtained from Dr. Simon Waddington at University College London (UCL) and used as feeder cells for human Embryonic Stem Cells (hESC) culture upto P4. Karyotypically normal 46, XY Sheffield (Shef)-3 hESCs were obtained from Dr. Diana Hernandez of Plasticell Ltd. (Stevenage, UK) at P28. Feeder-free conditioned huES1-OCT4-eGFP hESCs were grown at The University of Manchester and obtained from Dr. Tristan McKay at P7 post conditioning to feeder-free conditions. Mycoplasma PCR testing was routinely carried out on cells lines to ensure there was no contamination.

2.1.2 Cell Culture

The cell lines 293T, HepG2, Huh7 and HeLa adherent were plated onto cell culture treated flasks (Greiner Bio-One, Stonehouse, UK) in Dulbecco's Modified Eagles Medium (DMEM) (Sigma-Aldrich, Dorset, UK), 10% heat inactivated (HI) fetal bovine serum (HI-FBS) (Life Technologies, Loughborough, UK), 1% non-essential amino acids (NEAA) (Life Technologies), 1% GlutaMAX (Life Technologies) and 1% penicillin/streptomycin (P/S) (Life Technologies), termed "DMEM-complete media". Cells were cultured to 70% confluence before passaging which consisted of removing DMEM-complete media and washing cells twice with phosphate buffered saline (PBS) (Sigma-Aldrich). Cells were then incubated with 0.25% Trypsin (Sigma-Aldrich) at 37^0C until cells detached from the culture flask surface. Trypsin was neutralised with the addition of DMEM-complete at a 2:1 ratio of serum containing media to trypsin to neutralise enzymatic activity before pelleting cells at 300xg for five minutes. Cells were split at a 1:10 ratio which resulted in cells being passaged twice weekly. Freezing media consisting of 90% HI-FBS supplemented with 10% DMSO (Sigma-Aldrich) to -80^0C in a slow freezing vessel filled with 100% isopropanol (NALGENE, Loughborough, UK) before being transferred to liquid nitrogen for long-term storage.

2.1.3 LS174T Culture

Human colon adenocarcinoma LS174T cells were cultured in RPMI-complete media consisting of RPMI 1640 (Sigma-Aldrich) containing 20% HI-FBS, 1% NEAA, 1% GlutaMAX and 1% P/S. Cells were cultured to 80% confluence before passaging as previously described (see Methods 2.1.2). Cells were replated at a 1:10 seeding density resulting in cell passaging being carried out twice weekly.

Cryopreservation of LS174T cells was carried out using freezing media consisting of 90% HI-FBS supplemented with 10% DMSO. Cell vials were frozen at -80^{0}C in a slow freezing vessel filled with 100% isopropanol before being transferred to liquid nitrogen for long-term cryopreservation.

2.1.4 HepaRG Culture

HepaRG cells were plated onto collagen I (Corning, Flintshire, UK) coated tissue culture surfaces in hepatocyte basal media (HBM) (Lonza, Slough, UK) supplemented with the provided SingleQuots. HepaRG cells were grown to confluence and then passaged by washing the cells with PBS and incubated with Accutase (EMD Millipore, Watford, UK) at 37^{0}C until the cells detached from the plastic culture surface. Cells were replated at a 1:10 seeding density resulting in cell passaging being carried out twice weekly. Cryopreservation of HepaRG cells was carried out by pelleting HepaRG cells pelleting cells at 300xg for five minutes and resuspending in ProFreeze serum free freezing media (Lonza). Cell vials were frozen at -80^{0}C in a slow freezing vessel filled with 100% isopropanol before being transferred to liquid nitrogen for long-term cryopreservation.

2.1.5 DE Basal Differentiation Media

DE basal differentiation media consisted of William's E media (Lonza), 1x B27 (Life Technologies), 1% NEAA, 1% GlutaMAX, 1% Sodium Pyruvate (Life Technologies) and 1% P/S.

To produce conditioned overexpression differentiation media, basal media was applied to overexpression cell lines and allowed to be conditioned for a period of 24 hours by before being filtered using a .22µm syringe. Conditioned media was refreshed every 24 hours unless stated otherwise.

2.1.6 Isolation of MEFs

Wild type CD1 mouse embryos were obtained at E12.5 from pregnant female mice. Embryos were isolated by cutting between individual implantation sites along the uterine wall to isolate individual embryos. Enclosed embryos were dissected out and internal organs and heads were removed using a scalpel and tweezers. Dissected embryos were sequentially washed in PBS until all blood was removed.

Prepared embryos were then incubated in 0.25% Trypsin/EDTA or 1 µg/ml Collagenase I (Sigma-Aldrich) at 37^0C to digest the dissected embryos for approximately fifteen minutes until visible dissociation could be observed. Dissociation enzyme was then neutralised with the addition of complete DMEM-complete media and then cells then were plated at a density of three embryos per 0.1% gelatin (Sigma-Aldrich) coated T175 flask and the adherent fraction of cells amplified. MEFs were expanded in culture and passaged at 70% confluence until they reached P4.

2.1.7 Mitotic Inactivation of MEF Feeder Layers

MEFs were mitotically inactivated through the supplementation of DMEM-complete cell culture media containing Mitomycin C (Sigma-Aldrich) at 10µg/ml for three hours. Inactivation media was then removed, cells washed three times with PBS before being passaged with 0.25% Trypsin at 37^0C until cells detached from the culture flask surface. MEFs were plated at a density of 200,000 cells/6cm diameter tissue culture dish which had previously been pre-coated coated with 0.1% gelatin.

2.1.8 Feeder-Based hESC Culture

Pluripotent hESCs were grown on mitotically inactivated MEF feeder layers supplemented with hESC culture media. Pluripotent hESC media consisted of KnockOut DMEM (Life Technologies), 20% KnockOut Serum Replacement (KSR) (Life Technologies), 1% Non-Essential Amino Acids (NEAA) (Life Technologies), 1% GlutaMAX, 1% P/S, 0.1M 2-Mercaptoethanol (Life Technologies) and 10ng/ml bFGF/FGF2 (R and D Systems, UK).

Every two days differentiated areas of cells were removed by manual scraping and media was refreshed until approximately 70% confluence was reached. At this stage, hESC colonies were manually passaged by cutting into equal sized small colony pieces and replated on to fresh MEF feeder layers. Cryopreservation of feeder-based hESCs was achieved by freezing colonies in mFreSR (Stem Cell Technologies, Cambridge, UK) to -80^0C in a slow freezing vessel (NALGENE) containing 100% isopropanol before being transferred to liquid nitrogen for long-term cryopreservation. Karyotypically normal 46, XY Shef-3 hESCs were used for a maximum of 10 passages from the point of obtaining them at P28.

2.1.9 Feeder-Free hESC Culture

Feeder supported hESC colonies were grown on MEF feeder layers and then enzymatically passaged with TrypLE (Life Technologies) and replated onto 50µg/ml fibronectin coated dishes (EMD Millipore). Initially enzymatically passaged hESCs were cultured in pre-conditioned MEF hESC media supplemented with 10ng/ml bFGF and 10µM ROCK inhibitor (Y27632) (EMD Millipore) immediately following plating to support single cell passaging. After a period of two days, media was replaced with a 50:50 split of MEF conditioned hESC media supplemented with 10ng/ml bFGF and mTeSR (Stem Cell Technologies). The proportion of mTeSR was subsequently increased until hESCs were adapted to grow in fully feeder-free conditions. Subsequent passaging of feeder-free hESCs was carried out by incubation with TrypLE for five minutes at 37^0C before replating on fibronectin coated plates supplemented for two days of 10µM ROCK inhibitor treatment. Cryopreservation of hESCs was achieved by freezing colonies in mFreSR to -80^0C in a slow freezing vessel.

2.1.10 Mammalian Cell Transfection

Cells to be transfected were grown in six well plates and allowed to reach 70% confluence. To produce the cell transfection mix, 2.75µg of plasmid DNA was mixed with 327.25µl of OptiMEM (Life Technologies) and left to incubate for five minutes at room temperature. In parallel, 2.75µl of 0.1mM Polyethylenimine (PEI) (Sigma-Aldrich) was mixed with 327.25µl of OptiMEM and incubated for five minutes at room temperature. After five minutes of incubation the DNA-OptiMEM and PEI-OptiMEM mixtures were mixed in a final volume of 660µl and left to incubate for a further 20 minutes at room temperature.

This was carried out for every well of a six well plate to be transfected and the volume of transfection mix was scaled up accordingly based on lentiviral preparation size. Cells to be transfected were then washed with PBS to remove serum-containing culture media and the transfection mix added for three hours at 37^0C. Transfection mix was then removed and cells washed with PBS before addition of DMEM-complete to transfected cells**.**

2.1.11 Production of Lentivirus

Lentivirus was created by transfecting plasmid DNA along with pCMVR8.74 packaging and pMD2.G envelope plasmids (Plasmid Factory, Bielefeld, Germany) into 293T viral producing cells. The following day, transfection media was removed and refreshed with DMEM-complete media. Lentivirus was collected in media supernatant at 48 and 72 hours post transfection. Viral supernatant was subsequently filtered using a 0.22µM syringe filter and centrifuged at 4500xg overnight at 4^0C to pellet lentivirus particles. The supernatant was aspirated and viral particles re-suspended in OptiMEM containing no serum, aliquoted and cryopreserved at -80^0C.

2.1.12 Lentiviral Titering

Lentiviral titering was carried out using a p24 antigen capture ELISA assay (ZeptoMetrix, New York, US) as per the manufacturer's instructions. The p24 assay allows the detection of the number of lentiviral envelope particles with a view to be able to determine an appropriate multiplicity of infection (MOI) with which to transduce cells. Briefly, 96 well plates were coated with a monoclonal antibody specific for the p24 gag gene product of the HIV-1 virus. Viral antigen in test samples were subsequently applied to wells and captured with the monoclonal antibody specific for the p24 gag gene product. The captured antigen was then reacted with a high titered human anti-HIV-1 antibody conjugated to biotin. The assay then relies on a subsequent incubation with a streptavidin-peroxidase enzyme resulting in a colour change resulting from bound enzyme reacting with the substrate. The colorimetric reaction was then analysed at 595nM wavelength using the GloMax® Multi+ machine (Promega, Southampton, UK).

2.1.13 Mammalian Cell Transduction

For lentiviral transduction, cells were cultured to 70% confluence and lentiviral particles suspended in OptiMEM were added to fresh cell culture media at the desired MOI concentration. Typically, this was done at 20MOI unless stated otherwise along with the addition of polybrene (EMD Millipore) at a concentration of 5µg/ml to increase lentiviral transduction efficiency. Lentiviral transduction was carried out for a period of 48 hours after which transduction media was removed and replaced with the appropriate fresh culture media.

2.2 Molecular Biology

2.2.1 Isolation of Plasmid DNA

To isolate plasmid DNA, 8ml lysogeny broth (LB) was supplemented with appropriate selection antibiotics. Antibiotics used was either ampicillin or kanamycin (Sigma-Aldrich) at 100mg/ml which allowed the selection of plasmid DNA containing antibiotic-resistant bacteria. LB selection media was inoculated with a single bacterial colony and incubated overnight at 37°C on a shaking platform. Bacterial cultures were centrifuged at 300xg for 10 minutes. Plasmid DNA was isolated using the Plasmid Mini Kit (Qiagen, Manchester, UK), which is based on a modified alkaline lysis procedure followed by binding of plasmid DNA to an anion resin under appropriate low salt and pH conditions using the manufacturer's instructions. The isolated DNA was then eluted in 30µl of nuclease-free water.

2.2.2 Gel Extraction

To isolate DNA fragments from agarose gels a commercially obtained Gel Extraction Kit (Qiagen) was used according to the manufacturer's instructions. Isolated DNA captured in the anion resin of the gel extraction column was eluted in 30µl of nuclease-free water. Additional steps in the extraction process using RNase (Qiagen) was used degrade contaminating RNA to further purify DNA samples.

2.2.3 Restriction Digests

Restriction digests of plasmid DNA were carried out using restriction enzymes obtained from NEB (Hitchin, UK). In a reaction volume of 50µl, 500ng of plasmid DNA was digested using the appropriate restriction digest buffer and incubation temperature according to the manufacturer's instructions. Restriction digests were carried out for one hour unless otherwise stated.

2.2.4 Ligation Reactions

Ligation reactions were carried out using 50ng of lentiviral backbone vector using a 1:3 molecular ratio of backbone vector to insert. Reactions were carried out in a total volume of 20µl using the Quick Ligase kit (NEB) and incubated at 25ºC for five minutes as per manufacturer's instructions. Reactions were carried out as follows:

Backbone vector	50ng
Insert	(1:3 molecular ratio)
2x Quick Ligation buffer	10µl
Quick Ligase	1µl
Nuclease-free water	to a total of 20µl

2.2.5 Gateway Cloning

Gateway cloning (Invitrogen) was carried out to shuffle genes of interest from a donor vector, pENTR-1A, into a lentiviral vector. The pENTR-1A donor vector contains aatL sites flanking the gene of interest and the destination vector contains corresponding attR sites. The use of the clonase™ enzyme (Invitrogen) allows recombination of the gene of interest from the donor clone into the destination vector at high efficiency and in a specific orientation. To carry out LR clonase™ recombination the following reaction was carried out: and left to incubate at 25ºC for sixty minutes before 2µl of Proteinase K solution (Invitrogen) was added to stop the reaction:

Entry clone (100-300ng)	1-10µl
Destination vector (150ng/ml)	2µl
5x LR clonase™ reaction buffer	4µl
TE buffer (pH 8.0)	to a total of 16µl

2.2.6 Plasmid DNA Transformation

Plasmid DNA was transformed into stable competent DH5α bacterial cells (NEB) to amplify and extract clones of interest. 50µl aliquots of competent cells were thawed on ice and mixed with 100ng of plasmid DNA by carefully flicking the transformation mix tube. The transformation mix was then incubated on ice for 30 minutes before being heat shocked at 42ºC for 30 seconds. The transformation mix was again incubated on ice for five minutes before 500µl of super optimal broth with catabolite repression (SOC) media was added and incubated for sixty minutes. Transformation mix was then plated onto appropriate antibiotic containing agar petri dishes under sterile conditions and left to incubate overnight at 37ºC.

2.3 Gene Expression Analysis

2.3.1 Agarose Gel Electrophoresis

Agarose gels were prepared depending on the DNA fragment size by dissolving agarose (Sigma-Aldrich) in 1x Tris-acetate-EDTA (TAE) buffer (Thermo Scientific, Loughborough, UK). Agarose gels were mixed with SYBR Safe (Invitrogen) to visualise DNA bands. Sample DNA was mixed with gel loading buffer at a 1:5 ratio before being loaded into cast wells. Appropriate sized DNA HyperLadder™ (Invitrogen) was selected depending on the size of the DNA band in question.

2.3.2 RNA Extraction

Total RNA was isolated from monolayer cell cultures using an RNeasy Kit (Qiagen) as per manufacturer's instructions. Briefly, cells were washed three times with PBS before being subjected to lysis using RLT buffer (containing 1:100 concentration 2-Mercaptoethanol to inhibit RNases). Cell lysate was homogenised to shear high molecular weight DNA and other cellular components by passing samples through a QIAshredder Column (Qiagen) followed by RNA isolation from cell lysate using an RNeasy kit. On column DNase I treatment (NEB) was carried out to remove contaminating genomic DNA from individual samples. RNA integrity was checked by denaturing RNA secondary structure by heating to 70ºC for 5 minutes followed by running the sample on a 1.5% agarose gel to check the relative quantities of 18S and 28S subunits. Quantitative measurements were calculated using a NanoDrop™ spectrophotometer (Thermo Scientific) and a 260/280 ratio assessed. A ratio of ~2.0 is indicative of pure RNA and a cut off was established which excluded RNA from being further assessed if a score of less than 1.9 or greater than 2.1 was achieved.

2.3.3 cDNA Synthesis

First strand cDNA synthesis was subsequently carried out on high purity RNA samples using a cDNA synthesis kit (Agilent, Craven Arms, UK) using 2µg of purified RNA following manufacturer's instructions. Confirmation of successful synthesis of cDNA was carried out through the amplification with housekeeper genes β-Actin and GAPDH by RT-PCR followed by visualisation through agarose gel electrophoresis.

2.3.4 RT-PCR

RT-PCR reactions were carried out on synthesised cDNA using a Taq DNA polymerase kit (NEB) as per manufacturer's instructions. RT-PCR reactions were carried out for 30 cycles using appropriate annealing temperatures for the primer set depending on nucleotide length and composition. PCR reactions for each primer set containing no reverse transcriptase (noRT) controls were carried out to check for genomic DNA contamination in the RNA samples. Further no template controls (NTC) were carried out by omitting template cDNA to check for additional nucleic acid contamination and for primer dimer formation. NoRT and NTC control samples were ran on agarose gels along with test samples to check for the absence of PCR product bands which would be indicative of DNA contamination from RNA samples. The following RT-PCR master mix and PCR cycling parameters was used:

Standard Taq reaction buffer (10x)	5µl
Deoxynucleotide solution mix (10mM)	1µl
Forward primer (10µM)	1µl
Reverse primer (10µM)	1µl
DNA template	1ng
Taq DNA polymerase	0.2µl
Nuclease-free water	to a total of 50µl

1 minutes at 95ºC

30 seconds at 95ºC
45 seconds at 60ºC } 30 cycles
45 seconds at 72ºC

5 minutes at 72ºC

Hold at 4ºC

2.3.5 SYBR Green qPCR

Synthesised cDNA was quantitated as a surrogate for mRNA using SYBR Green qPCR (Applied Biosystems, Warrington, UK). All qPCR primers were ordered from Sigma-Aldrich and were designed to span exon boundaries to eliminate genomic DNA amplicons. Other primer design criteria included being 21-24 nucleotides in length, approximately 50-60% GC content and having a melting temperature (Tm) variation between forward and reverse primers of less than 2ºC. Primer efficiencies were calculated for each set of primers using a dilution curve of the target amplicon. The cycle threshold (Ct) values that were generated for each serial dilution was plotted on a logarithmic scale. A linear regression curve was then calculated using these data points and the slope of the trend line calculated.

Primer sets were only used if they produced an efficiency of between 90-100%. Dissociation curves were analysed following qPCR amplification to check that only a single target amplicon was generated and there was an absence of multiple amplification products.

For absolute quantification of gene expression, product amplification standards for each qPCR target gene were produced. These standards were created by amplifying the target gene of interest using 1µl of wildtype cDNA for 30 cycles of PCR amplification. The PCR reaction was then electrophoresed on an agarose gel, visualised on a UV gel imaging system and the product band extracted using a Gel Extraction Kit (Qiagen) to isolate DNA as per manufacturer's instructions. Serial dilutions of gel purified PCR product ranging from 10^{-3} to 10^{-7} was produced with which to obtain a qPCR standard amplification curve which allowed quantification of test sample gene expression. For gene expression analysis, qPCR primers were first validated using serially diluted wildtype cDNA at a range of 10^{-3} to 10^{-6}. This was done to check for the absence of primer dimers which could distort the gene expression quantification reading.

For all qPCR reactions, GAPDH was used as a housekeeping gene control with which to normalise gene expression to the fold expression change of the gene of interest. GAPDH levels as assessed by the Ct were seen to be unchanged throughout test samples. SYBR Green qPCR was carried out by mixing 5µl of SYBR Green Mastermix (Applied Biosystems) with 1µl of template cDNA. Working stock 10µM solution forward and reverse primers was then added along with 0.2µl of Rox^{low} (Applied Biosystems) to normalise the fluorescent signal and made up to a total reaction volume of 10µl. qPCR reactions were carried out in triplicate in 96 well PCR plates.

PCR reactions for each primer set containing no reverse transcriptase (noRT) controls were carried out to check for DNA contamination in the RNA samples. Further no template controls (NTC) were carried out by omitting template cDNA to check for additional nucleic acid contamination and for primer dimer formation in SYBR Green qPCR reactions. Three biological repeats were carried out for each validation experiment which consisted of assessing experiments using cells from different passage numbers. Three technical replicates of target gene amplification were carried out for each biological repeat. The SYBR Green qPCR reaction programme cycle was as follows:

3 minutes at 95ºC

20 seconds at 95ºC
20 seconds at 57ºC
20 seconds at 72ºC
} 40 cycles

Hold at 4ºC

Gene	Forward Primer 5'-3'	Reverse Primer 5'-3'	Product Size	Efficiency
α1AT	CTCCGTACCCTAAACCAGCC	TTCTTGGCCTCTTCGTGATCC	167bp	90.3%
ALBUMIN	CCCACGCCTTTGGCACAAT	CCCAAATCTTTAAACCGATGAGCA	135bp	99.3%
CRIPTO	CATAGTTGCCTGACTCCCCG	GGCGCGGTATTATCCCGTAT	579bp	98.7%
CYP1A1	CTATCCTGCTGCAACGGGTG	AAGTAAGTTGGGTAAGAGCGCA	135bp	99.7%
CYP1A2	CTGGGCACTTCGACCCTTAC	TCTCATCGCTACTCTCAGGGA	99bp	98.4%
GAPDH	TGATGACATCAAGAAGGTGGTGAAG	TCCTTGGAGGCCATGTGGGCCAT	230bp	98.2%
NODAL	AGAAGCAGATGTCCAGGGTAGC	AGAGGCACCCACATTCTTCC	536bp	99.1%

Table 1: PCR primer sequences

PCR primer sequences used to assess gene expression. Forward and reverse 5'-3' sequences are displayed along with the corresponding PCR product size. PCR primer efficiencies are also displayed which were calculated using a dilution curve of the target amplicon. Primer sets were only used if they produced an efficiency of between 90-100%.

2.4 Protein Expression Analysis

2.4.1 Protein Extraction

Protein was extracted from cell lysates by firstly pelleting cells following incubation with 0.25% Trypsin at 37^0C until cells detached from the culture flask surface. Pelleted cells were washed three times with ice cold PBS. Cell pellets were resuspended with 1x RIPA buffer (1x PBS, 1% NP40, 0.5% sodium deoxycholate, 0.1% SDS) (Cell Signalling, Hitchin, UK) to lyse cell pellets and allow the isolation of cytoplasmic, nuclear and membrane-bound proteins. RIPA buffer was supplemented with a protease inhibitor cocktail (Roche, Welwyn Garden City, UK) to prevent protein degradation. Cell lysate was then pelleted by centrifugation at 4500xg for ten minutes. Protein containing supernatant was removed and stored at -80^0C.

2.4.2 Protein Concentration Quantification

A colorimetric protein assay was used to quantitatively measure the total protein concentration in test samples (Bio-Rad, Watford, UK). The Bio-Rad protein assay is based on the Bradford dye-binding principle and test samples compared to known protein standard [244]. Protein concentration was determined using a 96 well plate microplate protein assay. Protein standards ranging from 0, 0.25, 0.5, 1, 2, 4 and 8µg BSA per well were produced as a reference with which to determine protein levels in samples. One-part Bio-Rad protein assay reagent was then diluted in $_dH_20$ giving a 1:5 dilution and 195µl added to each well. To each well containing the protein assay reagent, 5µl of standard was added along with 5µl of test sample. The plate was then read for absorbance at 595nm wavelength using a spectrophotometer (Promega GloMax® Multi+).

2.4.3 SDS Polyacrylamide Gel Electrophoresis (SDS-PAGE)

Equal concentrations of quantified protein samples were prepared by mixing with 2x Laemmli buffer (4% SDS, 0.1M Tris pH 8.9, 2mM EDTA, 0.1% bromophenol blue and 20% glycerol) and boiled for 10 minutes at 95^0C. Samples were centrifuged at 4500xg for five minutes and 20µl was loaded into individual wells of pre-cast sodium dodecyl sulphate (SDS) polyacrylamide gels (Invitrogen). Novex pre-stained protein standards (Invitrogen) were used to determine protein sample size and relative mobility. Protein gels were usually run at 150V for one hour at 200mA or until appropriate migration through the gel was achieved.

2.4.4 Western Blotting

SDS PAGE gel, PVDF transfer membrane (Thermo Scientific) and filter paper were equilibrated in 1x transfer buffer (for 1L of 10x: 24g Tris base and 90g glycine was dissolved in $_dH_20$). SDS PAGE gel was placed over the PVDF transfer membrane in between two pieces of filter paper to keep the gel and membrane wet in a semi-dry blotter. Proteins were then transferred to the membrane for 40 minutes at 15V. Once proteins have been transferred, the PVDF membrane was blocked with PBS containing 5% skimmed milk powder for one hour. PVDF membrane was then washed in PBS containing 0.1% Tween-20 (PBS-T). Primary antibody incubation was then carried out in PBS-T with 5% skimmed milk powder on a rocking platform overnight at 4^0C using antibody dilutions according to manufacturer's instructions. Antibodies used in western blotting and the appropriate dilutions can be found in the following table:

Antibody	Supplier and Catalogue Number	Dilution
Human Nodal	R and D Systems #MAB1315	1:1000
Human Cripto	R and D Systems #AF145	1:1000
Secondary Alexa Fluor anti-goat 488	Thermo Fisher #A-11055	1:2000
Secondary Alexa Fluor anti-mouse 594	Thermo Fisher #A-11005	1:2000

Table 2: Western blot antibodies

Primary and corresponding secondary antibodies used in Western blot analysis of protein levels. Appropriate dilutions in PBS-T for each primary and secondary antibody are displayed along with supplier and catalogue numbers.

2.4.5 Immunocytochemistry (ICC)

Cells were first washed three times with PBS before being fixed with 4% paraformaldehyde (PFA) (Electron Microscopy Sciences, Hatfield, US) for one hour at room temperature. Samples were then washed three times with PBS and subsequently blocked and permeabilised in PBS containing 1% BSA (Sigma), 0.2% Triton X-100 (Sigma). Primary antibody incubations were then carried out on a rocking platform overnight at 4^0C. Cells were then washed three times with PBS followed by the addition of a corresponding fluorescent Alexa Fluor (Invitrogen) secondary antibody for two hours on a rocking platform at room temperature under aluminium foil to prevent exposure to light. Cells were washed three times with PBS to remove traces of secondary antibody and then stored under foil at 4^0C until visualisation. Secondary only antibody controls were also carried out with no primary antibody to check for background fluorescence. Antibodies used in ICC and the appropriate dilutions can be found in the following table:

Antibody	Supplier and Catalogue Number	Dilution
Primary CYP1A1	Santa Cruz Biotechnology #sc-25304	1:100
Primary CYP1A2	Santa Cruz Biotechnology #sc-53241	1:100
Primary CYP3A4	Santa Cruz Biotechnology #sc-27639	1:100
Primary SOX17	R and D Systems #AF 1924	1:1000
Primary FOXA2	R and D Systems #AF2400	1:1000
Secondary Alexa Fluor anti-goat 488	Thermo Fisher #A-11055	1:2000
Secondary Alexa Fluor anti-mouse 594	Thermo Fisher #A-11005	1:2000

Table 3: Antibodies used in ICC staining

Primary and corresponding secondary antibodies used in ICC staining. Appropriate dilutions in for each primary and secondary antibody are displayed along with supplier and catalogue numbers.

2.4.6 Flow cytometry

Cells undergoing flow cytometry were prepared by removing DMEM-complete media and washing cells twice with PBS. Cells were then incubated with 0.25% Trypsin at 37^0C until cells detached from the culture flask surface. Trypsin was neutralised with the addition of DMEM-complete at a 2:1 ratio of serum containing media to trypsin to neutralise enzymatic activity before pelleting cells at 300xg for five minutes. Cell pellets were then washed three times with PBS before being resuspended in 1ml PBS. Samples were run on LSRFortessa flow cytometer (BD) using FACSDiva software. Live cells were identified from the sample data by forward scatter (FSC) and side scatter (SSC) profile. Background autofluorescence was then calibrated and gated using non-transfected cells. Data was subsequently analysed using FlowJo version 7.6.4 (Treestar, Oregon, US).

2.5 Fluorescent and Luminescent Assays

2.5.1 EROD Assay for CYP1A1/A2 Activity

The fluorescent ethoxyresorufin-O-deethylase (EROD) assay was used to quantify levels of CYP1A1/A2. Cells were first washed with assay medium consisting of William's E media (Lonza) containing 10µg/ml insulin (Invitrogen), 0.1µM Hydrocortisone (Stem Cell Technologies), 2mM L-glutamine and 1% P/S. 20µM of 7-ethoxyresorufin (0.2% final concentration DMSO) diluted in assay media was then added and incubated for two hours at 37ºC. Following incubation with 7-ethoxyresorufin, EROD assay media was removed and transferred to NUC96ft plates (Nunc) and liberated resorufin was analysed for excitation at 560nm and emission at 590nm wavelength on a GloMax 96 well plate reader (Promega).

2.5.2 p450Glo Assay for CYP3A4 Activity

CYP3A4 activity in HLCs was quantified using the luminescent p450Glo assay kit (Promega). Cells were washed with assay media consisting of William's E media containing 10µg/ml insulin (Invitrogen), 0.1µM Hydrocortisone (Stem Cell Technologies), 2mM L-glutamine and 1% P/S before being incubated with luciferin IPA (1:1000) in assay medium. Cells were incubated for sixty minutes at 37ºC. Supernatant was then removed and transferred to white walled NUC96fw plates (Nunc) and 50µl of detection reagent was added and left to incubate for twenty minutes at room temperature. Luminescence readings were then taken with an integration time of 500ms on a GloMax® Multi+ 96 well plate reader.

2.5.3 Luciferase Assay using Luciferin

Cells were washed three times with PBS followed by the addition of 300µl of luciferase lysis buffer ((0.65% NP40, 10mM Tris (pH 8.0), 1mM EDTA (pH 8.0) and 150mM NaCl)). Lysis buffer was left at room temperature for five minutes to lyse cells. To completely lyse cell samples, three freeze/thaw cycles at -80ºC were carried to ensure complete lysis. Samples were then centrifuged for two minutes at 4500xg to precipitate nuclei and cellular debris. Samples were then stored at -80ºC or direct quantitation carried out immediately. In a 96 well white walled plate, 20µl of cell lysate was mixed with 20µl of luciferase buffer B ((50mM Tris Phosphate (pH 7.8), 2mM DTT, 2mM EDTA, 2% Triton X-100, 16mM $MgCl_2$ being added to 3ml glycerol, 80 µl 100mM ATP (Sigma) and 2ml of 10% BSA)). Luciferase reactions were performed in biological triplicate repeats using cells from different passage numbers.

A background reading was taken for ten seconds before the injection of luciferin to test samples, which was then subtracted from actual readings after luciferin administration. This is particularly importance if luciferase levels are low and the gain adjustment, or sensitivity, of the machine is high. 40µl of 3mM luciferin was injected to each test well to give a final concentration of 1.5mM. Bradford assays were carried out to determine protein concentrations (see Methods 2.4.2) as a method to normalise luciferase readings to account for cell numbers between test samples.

2.5.4 NanoLuc Secreted Luciferase Assays

NanoLuc (Nluc) secreted luciferase assays were used to give a real-time readout of reporter activation on a day-on-day basis in living cells. Cells were transduced with the Nluc luciferase constructs at a concentration of 20MOI as described previously. Cells transduced with Nluc luciferase containing lentiviral vectors were allowed to condition culture media for 24 hours before media samples being taken. As a control for cell number between cell samples, secreted Vargula luciferase (Vluc) was utilised as an alternative to lysing cells and normalising to Bradford protein assays.

In a 96 well white bottomed plate, 20µl of cell lysate was mixed with 20µl of luciferase buffer B (containing no ATP) to make luciferase reaction buffer in a final volume of 40µl in each well. A background reading was taken for ten seconds before the injection of coelenterazine and vargulin substrates to test samples, which was then subtracted from actual readings after substrate administration. Luciferase reactions were performed in biological triplicate repeats using cells from different passage numbers.

2.6 CombiCult® Hepatocyte Screen

2.6.1 CombiCult® Growth Factors and Small Bioactive Molecules

Plasticell Ltd. developed a combinatorial cell culture platform, CombiCult®, for the establishment of new stem cell differentiation protocols The CombiCult® platform assesses the step-wise application of growth factors and/or small bioactive molecules to stem cells to direct differentiation towards cell types of interest. Multiplexing of a large range of variable cell culture media combinations can be achieved through split-pooling which allows for up to 20,000 possible culture media permutations.

The CombiCult® hepatocyte screen was carried out to identify key differentiation inducing factors over a four-stage protocol to mimic *in vivo* hepatocyte differentiation incorporating novel factors with a view to produce more metabolically relevant hepatocytes. Each stage of differentiation was designed to mimic DE specification, hepatic specification, hepatic progenitor expansion and finally hepatocyte maturation.

At each stage of the differentiation process cell culture media contained combinations of three factors consisting of small molecules and growth factors. Combinations of growth factors and small molecules at each stage of differentiation were added to a hepatocyte basal differentiation (HBM) media consisting of William's E Media (Sigma-Aldrich), 1x B27 (Life Technologies), 1% Sodium Pyruvate (Life Technologies), 1% NEAA and 1% P/S was used for the first and second stages of the differentiation process. At the third and fourth stage of hepatic differentiation, 10µM dexamethasone (Sigma-Aldich) and 0.1µM hydrocortisone (Stem Cell Technologies) were added to hepatocyte basal media along with combinations of small molecules and growth factors.

Growth factors that were used in hepatic differentiation were reconstituted in appropriate buffers as per manufacturer's instructions to a stock concentration of 100µg/ml and diluted in HBM to appropriate concentrations. Small molecule inhibitor/agonists were reconstituted in DMSO to a stock concentration of 10mM and subsequently diluted in HBM. The following differentiation inducing factors at the concentrations stated were used in the CombiCult® hepatocyte screen:

Hepatocyte differentiation basal media
100ng/ml Activin A (human recombinant, R and D Systems)
20ng/ml HGF (human recombinant, R and D Systems)
10ng/ml FGF4 (human recombinant, R and D Systems)
2µM BIO (Sigma)
100nM CITCO (Calbiochem)
1µM Mysteric Acid (C14-AS) (Calbiochem)
1µM Hyperforin (Calbiochem)
100nM Isoproterenol (Calbiochem)
1µM SR12813 (Calbiochem)
100µg/ml Linoleic Acid (LAC18:2) (Sigma)

Table 4: CombiCult® Stage 1 - DE Specification

Factors added in various combinations in hepatocyte differentiation basal media in the first stage of the CombiCult® hepatocyte differentiation screen concerned with the specification of DE from pluripotent stem cells. Combinations of three differentiation-inducing factors were added in each protocol.

Hepatocyte differentiation basal media
10ng/ml VEGF (human recombinant, R and D Systems)
20ng/ml HGF (human recombinant, R and D Systems)
25ng/ml WNT5A (human recombinant, R and D Systems)
2% DMSO (Sigma)
10µM SB-431542 (Sigma)
10ng/ml FGF4 (human recombinant, R and D Systems)
50ng/ml GDF15 (human recombinant, R and D Systems)
10nM Mysteric Acid (C14-AS) (Sigma)
1µM Clofibrate (Sigma)
10µM SMAD3 Inhibitor (SIS3) (Calbiochem)

Table 5: CombiCult® Stage 2 - Hepatic Specification

Factors added in various combinations in hepatocyte differentiation basal media in the second stage of the CombiCult® hepatocyte differentiation screen concerned with differentiation towards the hepatic lineage. Combinations of three differentiation-inducing factors were added in each protocol.

Hepatocyte differentiation basal media (with dexamethasone and hydrocortisone)
20ng/ml TGFα (human recombinant, R and D Systems))
20ng/ml Il6 (human recombinant, R and D Systems)
10ng/ml BMP7 (human recombinant, Invitrogen)
1µM Glucagon: (Calbiochem)
20ng/ml HGF (human recombinant, R and D Systems)
20ng/ml OSM (human recombinant, R and D Systems)
1µM All-trans retinoic acid (Calbiochem)
10ng/ml Growth Hormone (human recombinant, R and D Systems)
10nM Mysteric Acid (C14-AS) (Sigma)
100ng/ml Progesterone (Calbiochem)

Table 6: CombiCult® Stage 3 - Hepatic Progenitor Expansion

Factors added in various combinations in hepatocyte differentiation basal media in the third stage of the CombiCult® hepatocyte differentiation screen concerned with expanding hepatic progenitor cells. Combinations of three differentiation-inducing factors were added in each protocol.

Hepatocyte differentiation basal media (with dexamethasone and hydrocortisone)
20ng/ml HGF (human recombinant, R and D Systems)
25ng/ml WNT5A (human recombinant, R and D Systems)
100ng/ml Progesterone (Calbiochem)
10μM βEstradiol (Calbiochem)
10ng/ml Insulin (Invitrogen)
10ng/ml FGF4 (human recombinant, R and D Systems)
10ng/ml Growth Hormone (human recombinant, R and D Systems)
20ng/ml Il6 (human recombinant, R and D Systems)
20ng/ml OSM (human recombinant, R and D Systems)
10ng/ml IGF-1 (human recombinant, R and D Systems)
100nM Glucagon (Calbiochem)
100nM CITCO (Calbiochem)
1mg/ml Linoleic Acid (LAC18:2) (Sigma)
1μM SR12813 (Calbiochem)
100nM Isoproterenol (Calbiochem)
1μM TJU103 (Sigma)
1μM T0901317 (Sigma)
1μM GW7647 (Sigma)
1μM Docosahexaenoic Acid (Sigma)

Table 7: CombiCult® Stage 4 - Hepatic Maturation

Factors added in various combinations in hepatocyte differentiation basal media in the fourth and final stage of the CombiCult® hepatocyte differentiation screen concerned with the maturation of hepatic cells. Combinations of three differentiation-inducing factors were added in each protocol.

2.6.2 Four-Stage Hepatocyte Differentiation CombiCult® Screen

2.6.2.1 Microcarrier Seeding

During the CombiCult® split-pooling process cells seeded on microcarrier beads were maintained in a 37ºC humidified incubator with 5% CO_2. At D0, the day before the start of a CombiCult® experiment, 600,000 PTC5000 microcarrier beads (Plasticell, Stevenage, UK) were sterilised by autoclaving and washed twice with PBS before being equilibrated in hESC culture media. Microcarriers were then transferred to suspension culture plates (Greiner Bio One) at a concentration of 4000 beads/well in 2mL of hESC media. Shef-3 hESCs grown in monolayer culture were then dissociated through incubation with 0.1µg/ml collagenase I at 37^0C for five minutes. Shef-3 hESC colonies were then cut by mechanical passaging into small colony pieces and seeded onto microcarrier beads by adding 1ml of media containing $5x10^5$ cells to each well, then left to attach overnight. Viable cells were then visualised under a light microscope by staining microcarriers with 1:100 dilution neutral red solution (Sigma) for 30 minutes.

2.6.2.2 CombiCult® Split Pooling

The following day (D1), Shef-3 seeded microcarrier beads were washed, pooled in serum free media and split equally into ten tubes. Microcarrier beads in each tube were resuspended in the appropriate stage 1 differentiation media and a unique species of fluorescent tag added to each media combination tested. The tags used in the CombiCult® screen comprised of thirty unique populations of inert fluorescent microspheres (Plasticell). Fluorescent tags ranged in size from 1-10 microns with a range of ten fluorescent intensities for each size of tag.

The fluorescent tags bind to the microcarrier surface during the differentiation process. There is very infrequent tag hopping between microcarriers and conditions have previously been made to minimise this.

After five days incubating in stage 1 cell culture media beads were washed with hepatocyte basal media to remove excess tags and detached cells. Beads were then pooled together followed by splitting again into the next set culture conditions as before. This process was subsequently repeated through the desired number of culture condition steps to recapitulate the developmental cues specifying mature hepatocytes *in vivo*. Pooling and splitting occurred in this way on D5 and D10 with the addition of unique sets of fluorescent tags. On D17, stage 4 differentiation protocols were kept in isolation without the addition of fluorescent tags for the last stage of hepatocyte differentiation; protocols were not repooled and mixed at the end of stage 4.

2.6.2.3 CYP1A1/A2 and CYP3A4 Drug induction

At the end of hepatic differentiation split-pooling, HLCs on microcarrier beads were induced with 10µM omeprazole + 50µM dexamethasone (CYP3A4 inducers) and 50µM rifampicin (CYP1A1/A2 inducer) diluted in assay media consisting of William's E media containing 10µg/ml insulin (Invitrogen), 0.1µM Hydrocortisone (Stem Cell Technologies), 2mM L-glutamine and 1% P/S. Induction was carried out for three days with induction media being refreshed every day. As a control, assay media containing 0.2% DMSO vehicle control was used to compare levels of CYP1A1/A2 and CYP3A4 induction to basal levels.

2.6.2.4 Microcarrier Immunocytochemistry Staining

Following end point drug induction or vehicle control treatment, ICC staining was carried out. Microcarriers were then washed three times in PBS before being fixed with 4% paraformaldehyde (PFA) (Electron Microscopy Sciences) for an hour and blocked in 1x PBS containing 1% BSA (Sigma-Aldrich), 0.1% Triton X-100 (Sigma-Aldrich). Primary antibody incubations for CYP1A1, CYP1A2 and CYP3A4 enzymes (Santa Cruz Biotechnology, Dallas, US) was carried out overnight at 4^0C at 1:100 dilutions before washing three times and incubating in Alexa Fluor secondary antibody (Invitrogen) at 1:1000 dilutions. A secondary only control containing no primary antibodies was used to establish levels of background fluorescence.

2.6.2.5 COPAS Sorting

The COPAS PLUS large particle sorter (Union Biometrica, Holliston, US) is capable or sorting large particles, in this case microcarriers seeded with cells, based on size and fluorescent intensity utilising two channels allowing for dual staining of differentiated HLCs to be analysed. The COPAS sorter is equipped with both a 488 nm and 561 solid state lasers and green photomultiplier tubes (PMT) 514/23 nm and red PMT 615/45 nm optical emission filters. COPAS was utilised to isolate individual microcarriers based on fluorescence intensity after ICC staining. Fluorescence intensity gating was established firstly by sorting a secondary antibody only microcarrier control which gave a measure of background fluorescence intensity which was to be omitted. Subsequently, an aliquot of stained microcarrier beads from each of the final twenty conditions was pooled to establish a threshold with which to identify high levels of CYP1A1/A2 (red) and CYP3A4 (green) fluorescence following drug induction across all HLCs.

Once threshold gates were established, microcarrier beads from each of the final twenty pools were processed in the COPAS large particle sorter and beads which exceeded the gated fluorescence intensity threshold were sorted into individual wells of a 96 well plate. The COPAS large particle sorter allows the isolation of individual microcarriers with HLCs that exceed the established fluorescence gating to be isolated in individual wells of a 96 well plate. In this way, the highest expressing CYP1A1/A2 and CYP3A4 HLCs can be isolated for cell culture history processing.

2.6.2.6 FACS Tag Analysis

Bound tags on microcarrier surfaces were removed and transferred to individual FACS tubes for differentiation history analysis in the FACS Canto II flow cytometer (BD) to analyse cell culture history of the most highly expressing HLCs. Three sizes of fluorescent tag were used for the first three split-pool procedures at D1, D5 and D10 with each sized tag having ten fluorescent intensity graduations. Individual tags were assigned to each media condition at each stage of differentiation allowing tracking of unique cell culture history. COPAS isolated beads representing the most highly expressing CYP1A1/A2 and CYP3A4 HLCs isolated into individual wells of a 96 well plate. Prior to fluorescent tag analysis, a reference tag set was used with which to establish side and forward scattering gates on the BD FACS Canto II flow cytometer to calibrate fluorescence intensity of each specific tag set.

2.6.2.7 Ariadne Differentiation Pathway Analysis

Differentiation histories were deconvoluted and analysed in the Plasticell proprietary Ariadne™ bioinformatics software using only microcarriers with three distinct tags from stages 1-3 of differentiation i.e. contained full differentiation histories to identify clusters of media permutations. The clusters are identified based on the probability of any given combination of culture conditions to be present in a positive bead given the total number of positive beads and the total number of possible combinations.

In the CombiCult® hepatocyte screen there were 20,000 possible pathways. From this total number of pathways only some returned CYP1A1/A2 and CYP3A4 positive beads. From the positive beads, common combinations of media conditions were identified, creating differentiation media history clusters. Ranked protocols were produced based on linkages between cell culture stages which resulted in the most highly expressing CYP1A1/A2 and CYP3A4 HLCs. Differentiation culture history clusters were identified when they contain three or more events with near identical scattering and fluorescence values.

2.6.3 Statistics

Quantitative data obtained from gene expression, fluorescent and luminescent assays were analysed using GraphPad Prism 6.03 (GraphPad, San Diego, CA). Graphs are displayed as representative images of “n number” of experiments as detailed per the individual legends. Graphed data are displayed as the arithmetic mean ± standard error of the mean (SEM) unless otherwise stated. Statistical significance was evaluated by unpaired two-tailed Student’s *t*-test, or 1- or 2-way ANOVA followed by Bonferroni’s post-test for multiple comparisons.

A 1-way ANOVA was used if there was a single variable factor between the test groups and a 2-way ANOVA was used if there was more than one variable test factor. ANOVA analysis was used to determine if there was any significant difference between the mean values from two or more test groups compared to the control mean in normally distributed samples; the null hypothesis being that there is no statistical difference between groups. A Bonferroni's post-test for multiple comparisons was subsequently carried out to assess type I error in groups that had been identified as significantly different from an ANOVA statistical test. Data was classed as significant when *p* values were below 0.05. *<0.05, **<0.01, ***<0.001.

Chapter 3: Investigating Definitive Endoderm Specification

3.1 Introduction

The efficient production of homogenous populations of DE is a key starting point in the differentiation of pluripotent stem cells to hepatocytes. Activin A and Nodal are both members of the TGFβ family and share common signalling pathways (Figure 7A). However, Nodal signalling relies on its signalling co-factor Cripto to bind and initiate SMAD signalling whereas Activin A does not and functions independently of Cripto [91]. It has been shown that the addition of exogenous recombinant Nodal to monolayer cultures of pluripotent stem cells did not specify DE or result in the suppression of pluripotency-associated markers [245]. Consequently, Activin A is used in an attempt to mimic the process of Nodal signalling which is known to be crucial *in vivo* in the establishment of DE [87] [110] [111] [84] [106] [83].

There has been evidence uncovered through genome arrays to show that there are significant off-target effects caused by the utilisation of Activin A to induce DE specification *in vitro* (McKay *et al*., unpublished data) (Figure. 4B, 4C and 4D). Expression of the visceral endoderm marker Orthodenticle Homeobox 2 (OTX2) (Figure 7C) and mesodermal markers Brachyury (T) and Bone Morphogenetic Protein 2 (BMP2) (Figure 7D) were found to be increased upon the exogenous day-on-day addition of Activin A to pluripotent hESCs over the course of six days (McKay *et al*., unpublished data). In fact, the working hypothesis from this study is that Activin A stimulates the transcriptional upregulation of Nodal which then in turn promotes DE specification.

The differences in signalling networks between Activin A and Nodal are hypothesised to account for the heterogeneous populations of DE produced through the exogenous application of Activin A. Work is therefore required to dissect the underlying mechanisms involved in Nodal signalling during the specification of DE *in* as a starting point to differentiate towards the hepatic lineage. Studies including that of Takenaga et al. (2007) have investigated the role of Nodal signalling in an attempt to more efficiently differentiate hESCs to DE [246]. Nodal signalling was regulated in transduced hESCs using a tetracycline-on (tet-on) lentiviral system and was found that Nodal-related molecules showed the potential to differentiate genetically unmanipulated hESCs towards DE and mesoderm. To further address this research problem in this thesis, lentiviral vectors to knock down or overexpress Nodal and its extracellular co-factor Cripto were utilised. The working hypothesis is that in an environment lacking Nodal signalling, i.e. in pluripotent stem cells transduced with a Nodal knock down lentiviral vector, there would be a more heterogeneous population of DE produced after the six-day differentiation time course. The converse would be true for pluripotent stem cell cultures transduced with a Nodal overexpression vector.

Building on the overexpression approach to produce more homogenous populations of DE, the ability of Nodal/Cripto proteins to efficiently differentiate hESCs will be investigated in different experimental systems. This will be though either the production of “feeder-cells” which have been genetically manipulated to overexpress secreted Nodal/Cripto proteins or through the production of conditioned media to apply to hESCs with a view to differentiation towards DE. The aim of these studies is to produce tools with which the profile of DE produced to be examined and compared with or without the use of Activin A; using SOX17 and FOXA2 as a readout of specified DE cells in future studies.

3.2 Aims

- Validate lentiviral vectors to overexpress or knock down Nodal and/or Cripto.
- Produce Nodal/Cripto knock down or overexpression transduced cell lines.
- Compare Nodal/Cripto conditioned media differentiated cells to Activin A derived cells for SOX17 and FOXA2.
- Assess conditioned media approaches to differentiate pluripotent cells to DE.

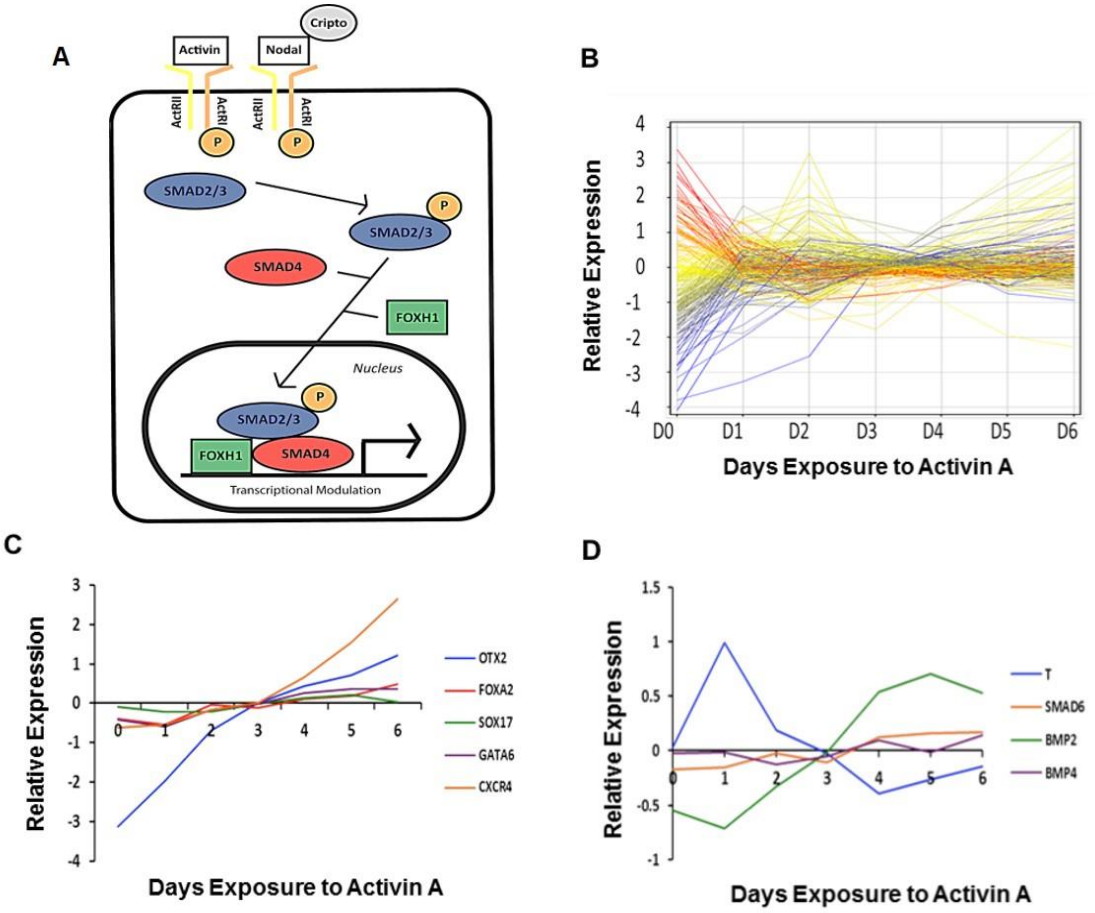

Figure 7: Activin/Nodal signalling in DE specification

(A) Simplified overview of the similarities and differences in the signalling pathways of the TGF- β family members Nodal and Activin A. Nodal signalling relies on Cripto to bind and initiate SMAD signalling whereas Activin A does not. **(B)** Whole transcriptomic analysis of day-on-day gene expression modulation following Activin A treatment on feeder free hESCs to induce DE specification for a period of six days. **(C)** Endodermal marker transcriptomic analysis showing evidence of off-target gene modulation such as, OTX2 (marker of visceral endoderm). **(D**) Mesodermal marker transcriptomic analysis showing the upregulation of Brachyury and BMP2 (mesodermal markers) during Activin A induced DE specification (McKay et al., unpublished data).

3.3 Results

3.3.1 Creation of Lentiviral Constructs

To validate tools with which to investigate the role of Nodal/Cripto signalling during in vitro DE specification, lentiviral shRNA knock down and overexpression vectors were employed. Knock down and overexpression lentiviral vectors were validated in HeLa cells, which have been shown to express both Nodal and Cripto at levels appropriate for the analysis of gene modulation to be quantified.

3.3.1.1 Nodal/Cripto Knock Down Lentiviral Vectors

For gene knock down experiments, eight pGIPZ lentiviral vectors containing different shRNA sequences targeting Nodal and Cripto along with a scrambled targeting control were obtained from Open Biosystems as bacterial stab cultures. Nodal/Cripto shRNA knock down clones included: V2LHS_155453, V2LHS_278899, V2LHS_194508, V2LHS_403216, V2LHS_403219, V2LHS_352858, V2LHS_352856 and V2LHS_403217. Bacterial stab cultures were streaked onto individual ampicillin plates. Individual antibiotic resistant clones were then picked after 37^0C incubation overnight followed by clone amplification before Miniprep DNA extractions were carried out (see Methods 2.2.1) (Figure 8). Clones were then sequenced to confirm correct Nodal/Cripto sequences.

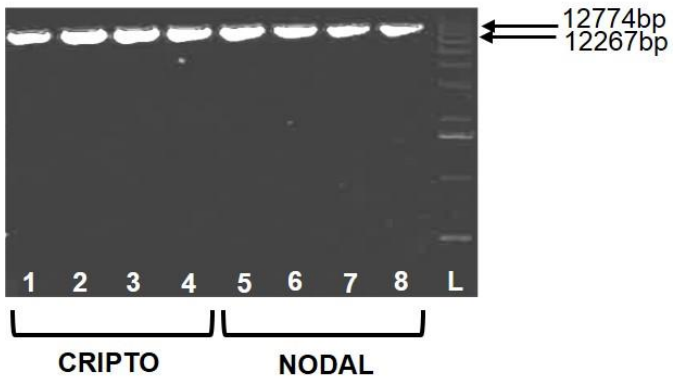

Figure 8: Gel extracted pGIPZ Nodal/Cripto shRNA lentiviral clones (1-8)

Agarose gel image of the individual pGIPZ shRNA 1-8 knock down clones. DNA extraction was carried out on four Cripto (lanes 1-4) and four Nodal (lanes 5-8) shRNA lentiviral clones obtained from Open Biosystems in the form of bacterial stab cultures. DNA extracted clones were electrophoresed on an agarose gel to check for correct band size of 12774bp (NODAL) and 12267bp (CRIPTO). L= 1kb DNA Hyperladder.

3.3.1.2 Nodal/Cripto Overexpression Lentiviral Vectors

Overexpression lentiviral vectors were produced firstly by the excision of Nodal and Cripto cDNA from commercially obtained pBluescript and pCR4-Topo vectors (Clone IDs: 8327493 and 5286020, Open Biosystems). Restriction digests of pBluescript-CRIPTO and pCR4-Topo-NODAL vectors with *BamH*I:*BamH*I and *EcoR*I:*BamH*I (NEB) restriction digests respectively (see Methods 2.2.3). The excised Nodal/Cripto cDNA insert fragment was separated from the vector backbone through agarose gel electrophoresis and subsequent gel extraction and purification using the QIAquick gel extraction kit (Figure 9) (see Methods 2.2.2). The excised cDNA was then ligated into the multiple cloning site (MCS) of the pENTR-1A entry vector (Invitrogen) (Figure 10A-C).

This was achieved using complementary restriction sites; *BamHI:BamHI* and *BamHI:EcoRI* for Nodal and Cripto respectively and gel extraction of digested vectors (Figure 9A and C). Ligation was carried out using quick ligase (NEB) as per manufacturer's instructions (see Methods 2.2.4). The use of the pENTR-1A entry vector allows the Nodal and Cripto cDNA inserts to be cloned into the delivery vector in the correct orientation utilising the LR clonase system (see Methods 2.2.5).

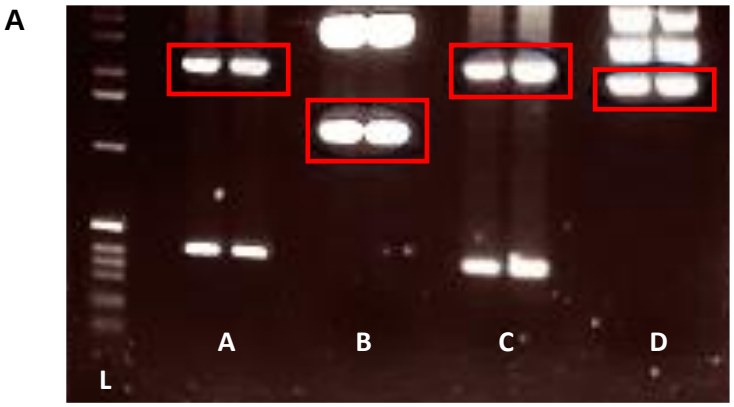

Figure 9: Construction of pLNT-SFFV-Nodal/Cripto overexpression vectors

(A) pENTR-1A entry vector digested with EcoRI restriction enzyme. **(B)** pCR4-Topo-NODAL digested with EcoRI restriction enzyme to release the Nodal cDNA insert. **(C)** pENTR-1A entry vector digested with *EcoRI:BamHI* restriction enzymes. **(D)** pBluescript-CRIPTO digested with *EcoRI:BamHI* restriction enzymes. Red boxes indicate the correct sized DNA bands from each restriction digest which were excised from the agarose gel and carried forward to the next stage of cloning. L= 1kb DNA Hyperladder.

Ligated clones were transformed into competent DH5α *E.coli* cells (NEB) and individual kanamycin resistant clones were picked, DNA extractions carried out followed by restriction enzyme digests to identify correct clones and proper insert orientation (see Methods 2.2.6).

Clonase recombination was then carried out to shuttle Nodal/Cripto cDNA from pENTR-1A entry vector into the pLNT-SFFV-Gateway lentiviral vector (Invitrogen) Figure 10D) before transformation into competent Stabl3 *E.coli* cells (NEB). Individual ampicillin antibiotic resistant clones were then picked and sequenced using cPPT sequencing primers designed for the pLNT-SFFV-Gateway to check for correct insert orientation and Nodal/Cripto cDNA sequence validity.

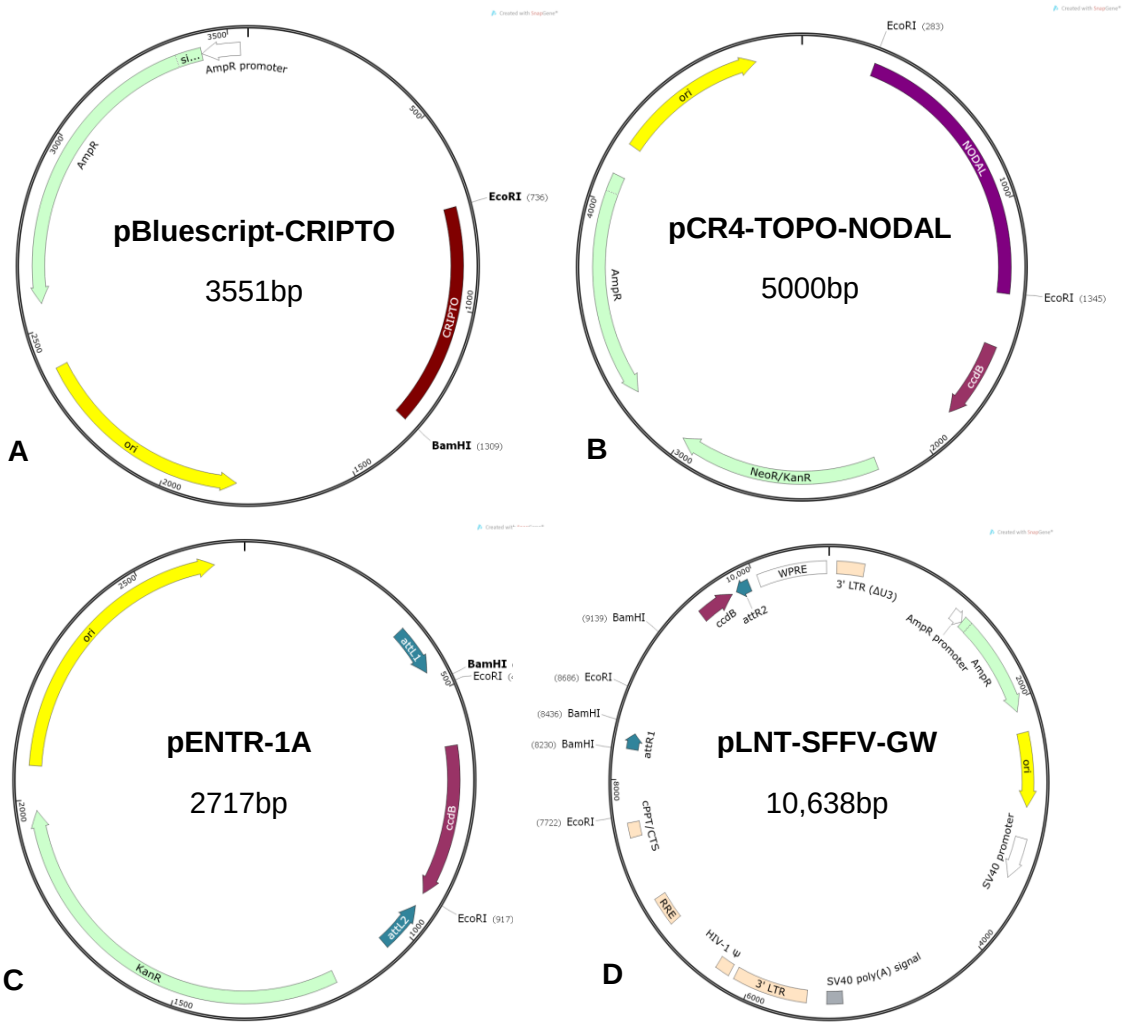

Figure 10: Plasmid maps of Nodal/Cripto overexpression lentiviral vectors

(A) Plasmid map for pBluescript-Cripto (Open Biosystems) with flanking *EcoRI:BamHI* restriction enzyme sites for Cripto excision**. (B)** pCR4-TOPO-Nodal (Open Biosystems) with flanking *EcoRI* restriction enzyme sites. **(C)** pENTR-1A subcloning vector where both Nodal and Cripto cDNA was ligated into complementary *EcoRI* restriction sites. **(D)** Plasmid map of the pLNT-SFFV-Gateway expression vector (Invitrogen) into which the Nodal and Cripto cDNAs were recombined from the pENTR-1A subcloning vectors (Invitrogen).

3.3.2 Validation of Nodal/Cripto Lentiviral Constructs

HeLa cells, shown to express both Nodal and Cripto (Figure 11B), were transduced with pGIPZ knock down lentiviral vectors along with a pGIPZ scrambled target control. Puromycin selection was then carried out at a concentration of 1µg/ml for one week to produce pure populations of shRNA knock down expressing HeLa cells. This was evidenced by eGFP fluorescence merged with phase contrast images of transduced cells (Figure 11A). SYBR Green qPCR analysis was then carried out to assess absolute levels of Nodal and Cripto knock down in transduced cells between the different shRNA clones. SYBR Green qPCR primers were designed to span exon-exon junctions for both Nodal and Cripto to eliminate genomic DNA amplification and erroneous readings of gene expression. SYBR Green qPCR standards with which to compare absolute gene expression values were produced by amplifying pGIPZ scramble control transduced HeLa cell cDNA with Nodal/Cripto qPCR primers followed by gel purification of the obtained PCR product. Serial dilutions from 10^{-3} to 10^{-7} were produced from gel purified standards. GAPDH was used as a housekeeping gene control with which to normalise gene expression values. Standard reactions with which to quantify gene expression values were carried out in triplicate whilst Nodal/Cripto knock down and overexpression samples were analysed through triplicate reactions. Three biological repeats consisting of cells from three different passage numbers were carried out for each validation experiment.

It was determined that the most efficient shRNA Nodal knock down vector was sh4 with a knock down efficiency of 85%-fold change ($p=0.05$) compared to the wildtype control and normalised to GADPH (Figure 11C). Clones sh1, sh5 and sh8 had knock down fold change levels of 80% ($p=0.05$), 70% ($p=0.04$) and 45% ($p=0.12$) compared to the pGIPZ scramble control.

The most efficient shRNA Cripto knock down vector after three biological repeats was determined to be sh2 with a knock down efficiency of 80% (p=0.04) (Figure 11D) compared to pGIPZ scramble control and normalised to GAPDH. Knock down clones sh3, sh6 and sh7 were assessed to be 70% (p=0.05), 55% (p=0.11) and 30% (p=0.04) respectively.

Lentiviral overexpression pLNT-SFFV-Nodal/Cripto vectors were also successfully transduced into HeLa cells alongside a mock SFFV-eGFP vector containing no overexpression cassette to assess transduction efficiency. Through qPCR analysis it was shown that pLNT-SFFV-Nodal/Cripto vectors over-expressed Nodal and Cripto in HeLa cells above twenty-fold compared to SFFV-eGFP control expression levels (p=0.06 and p=0.04 respectively) (Figure 11C-D). The current lack of a selectable marker on the overexpression vector hampers a more accurate quantification of overexpression levels as the efficiency of transduction cannot be assessed. However, as a proof of principle validation of the vectors it can be concluded that the constitutive SFFV viral promoter efficiently drives the overexpression of Nodal and Cripto in HeLa cells.

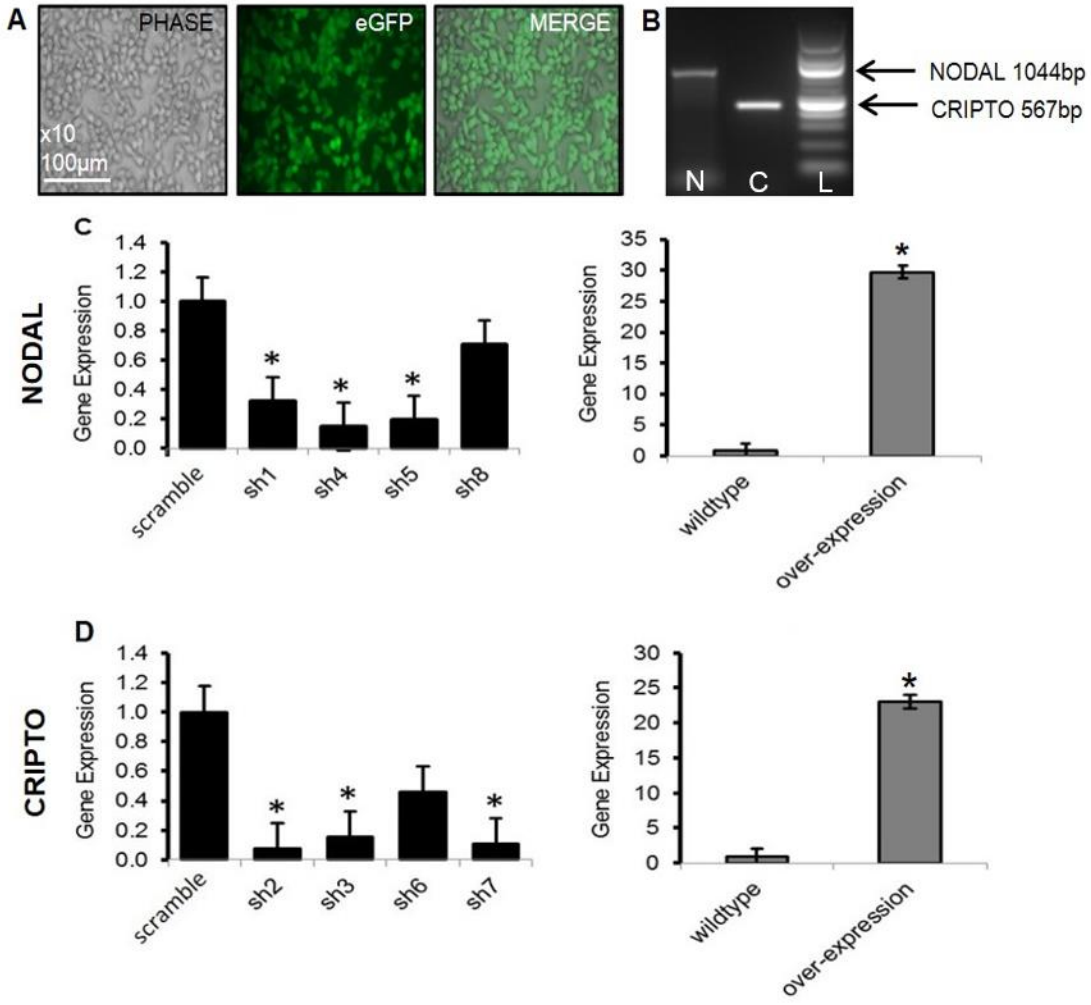

Figure 11: Validation of knock down and overexpression vectors

(A) Representative image of HeLa cell transductions with lentiviral pGIPZ knock down constructs (4 Nodal and 4 Cripto). Imaging of phase contrast (left) eGFP (middle) and merge (right) after one week of puromycin selection to produce pure populations of transduced cells. Three biological repeats consisting of cells from three different passage numbers were carried out validation. **(B)** RT-PCR amplification of pGIPZ scramble control HeLa cell cDNA with primers for Nodal and Cripto to assess expression following 20 cycles. N = Nodal PCR product, C= Cripto PCR product, L = 1kb DNA Hyperladder. **(C, D)** qPCR of HeLa cells transduced with Nodal knock down and overexpression vectors **(C)** and Cripto Nodal knock down and overexpression vectors **(D).** Statistical analysis of gene knock down was evaluated by a 1-way ANOVA with Bonferroni's post-test for multiple comparisons. Data shown as mean ±SEM of three technical replicates of one representative biological repeat. Significance indicated by ***($p<0.001$), **($p<0.01$), *($p<0.05$).

3.3.3 Creation of Nodal/Cripto Knock down hESC Lines

Feeder-free conditioned huES1-OCT4-GFP hESCs were grown on fibronectin coated plates in defined media and enzymatically passaged using trypsin/EDTA to small colony pieces. Colony pieces were transferred onto new fibronectin coated six well cell culture plates and grown to 70% confluence in mTeSR defined pluripotency media (Stem Cell Technologies).

Large scale lentiviral preparations were carried out on the most efficient Nodal and Cripto pGIPZ shRNA knock down clones (sh4 and sh2 respectively) along with a scrambled pGIPZ vector control. Lentiviral titering was carried out and huES1-OCT4-GFP cells were transduced at a concentration of 20MOI. The constitutive knock down huES1 cell lines that were produced were: sole Nodal knock down, sole Cripto knock down, dual Nodal/Cripto knock down and scrambled targeting control. Nodal and Cripto knock down lentivirus was produced and concentrated as described previously (see Methods 2.1.11) and used to transduce huES1-Oct4-GFP cells for 48 hours. The mTeSR culture media was then refreshed every other day for a period of seven days.

After seven days post-transduction, there was no detectable increase in eGFP expression resulting from lentiviral integration of the pGIPZ vectors (Figure 12A). High levels of eGFP should be detected through florescence microscopy at this stage indicating successful incorporation of the lentiviral shRNA knock down constructs.

Even though no increase in eGFP levels was observed following lentiviral transduction, huES1-OCT4-GFP cells were antibiotically selected with 1µg/ml puromycin added to cell culture medium to obtain pure populations of transduced cells. Preliminary studies using an antibiotic kill curve established that a puromycin concentration of 1µg/ml was optimal for hESC selection to allow for quick cell death of non-resistant cells whilst not having a visible effect on resistant cell health. Selection with 1µg/ml puromycin resulted in near total cell death indicating the lack of shRNA lentiviral transduction and expression of the puromycin resistance cassette (Figure 12B).

Transduction of the Nodal/Cripto shRNA lentiviral constructs was also attempted in feeder-free conditioned Shef3 hESCs to ascertain hESC line variation in transduction potential. Lentiviral preparations were carried out as done previously and variable MOI concentrations of shRNA vectors transduced into Shef3 hESCs: 10MOI, 20MOI, and 50MOI. After seven days post-transduction there was no visible eGFP in transduced cells at any of the trialled MOI concentrations and no cells survived 1µg/ml puromycin selection (data not shown). This again indicating the lack of expression of the resistance cassette and corroborates data obtained through the transduction of huES1-OCT4-GFP cells.

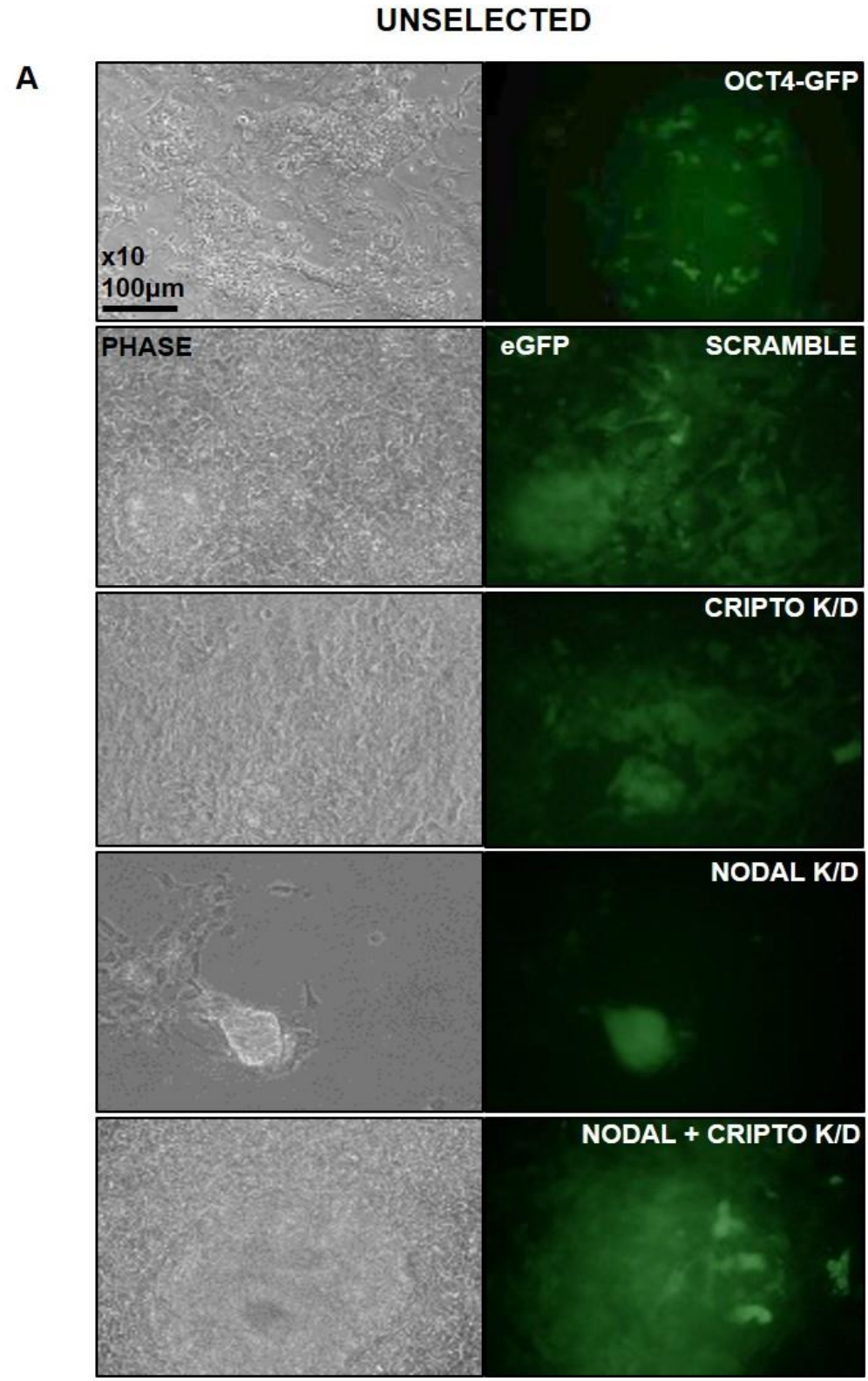
UNSELECTED
A
OCT4-GFP
x10
100µm
PHASE
eGFP
SCRAMBLE
CRIPTO K/D
NODAL K/D
NODAL + CRIPTO K/D

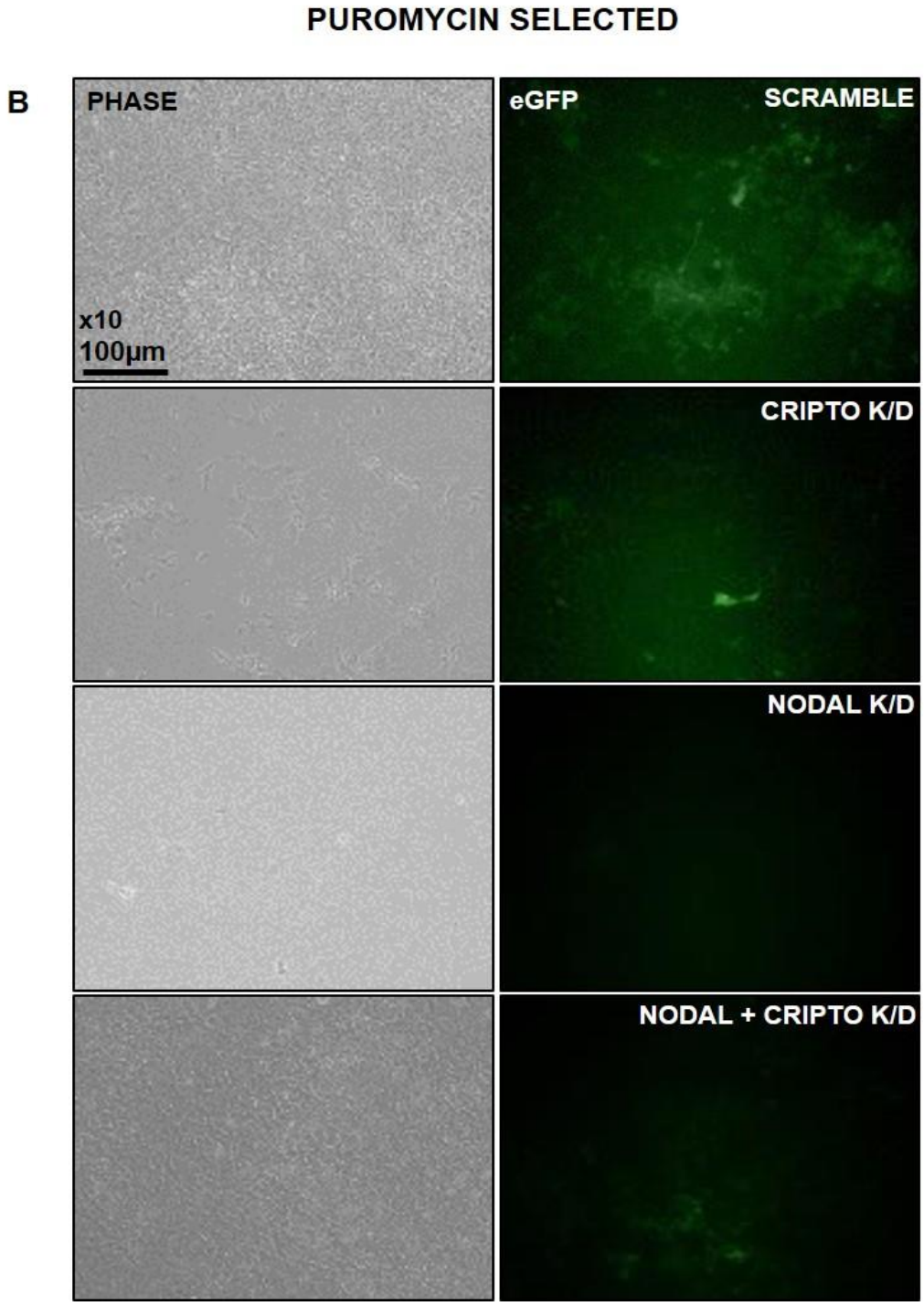

Figure 12: huES1 OCT4-GFP feeder free knock down cell lines

(A) huES1 OCT4-GFP cells seven days post-transduction with Nodal/Cripto knock down and scramble control pGIPZ shRNA vectors. **(B)** pGIPZ shRNA transduced huES1 cells following puromycin selection for four days to select for cells containing Nodal/Cripto knock down constructs. Antibiotic selection of transduced huES1 OCT4-GFP cells with 1µg/ml puromycin resulted in near total cell death indicating the lack of shRNA lentiviral transduction and expression of the puromycin resistance cassette.

3.3.4 Validation of Nodal/Cripto Over-Expression Conditioned Media

Following the data collected from validation of the overexpression and knock down lentiviral vectors, a new approach was used to differentiate pluripotent stem cells efficiently to DE. This was firstly due to the pLNT-SFFV-Nodal/Cripto overexpression lentiviral vectors lacking a selectable marker to facilitate accurate and quantitative levels of transduction efficiency. It would therefore be difficult to assess transduction levels in hESCs and a mock pLNT-SFFV-eGFP transduction would be needed in parallel to ascertain lentivirus production through constitutive eGFP expression. Secondly, lentiviral integration would limit the future application of DE and the ability to differentiate hESCs in a system not requiring lentiviral integration would be advantageous.

To address this research problem, a new system of DE specification from pluripotent stem cells was designed. The pLNT-SFFV-Nodal/Cripto vectors encode for the corresponding secreted proteins meaning over-expression conditioned media containing Nodal and Cripto proteins could be collected, filtered and applied to cultures of pluripotent hESCs to promote the efficient differentiation to DE. To assess the potential of this new approach, pLNT-SFFV-Nodal/Cripto over-expression lentivirus was firstly transduced into 293T cells to create “producer cells”. Producer 293T cells would be employed to secrete Nodal and Cripto protein into DE basal differentiation culture media to produce “conditioned over-expression media” (see Methods 2.1.5). Subsequently, this conditioned media containing Nodal and Cripto proteins would be added to cultures of hESCs to determine the ability of this conditioned media to differentiate the cells efficiently to DE. The ability of the conditioned media to specify DE would be compared to that of exogenously added Activin A and a differentiation control consisting of basal differentiation media without Activin A to evaluate the efficiency and homogeneity (see Methods 2.1.5).

To validate the conditioned media concept, levels of both Nodal and Cripto proteins in the conditioned media needed to be assessed and quantified. This was achieved using a pLNT-SBE-eGFP-luc lentiviral vector created by Juliette Delhove in the McKay lab group at WHRI, QMUL. The pLNT-SBE-eGFP-luc lentiviral vector contains both luciferase and eGFP elements under the control of a SMAD binding element (SBE). Upon the initiation of TGFβ signalling the SBE element will be activated and a quantitative readout of increases in signalling from Nodal/Cripto proteins through both luciferase activity and eGFP florescence would be obtained, allowing assessment of the efficiency of this approach.

The pLNT-SBE-eGFP-luc lentivirus was first transduced into 293T cells to create “reporter cells” that give both a visual indication of the initiation of TGFβ signalling through eGFP florescence and a quantitative readout of activation levels through luciferase activity. To test the responsiveness of the pLNT-SBE-eGFP-luc vector upon the activation of TGFβ signalling, Activin A was exogenously added to the cell culture media of 293T reporter cells. Activin A was used at 0ng/ml (control), 50ng/ml, 100mg/ml and 200ng/ml for a period of six days, with media refreshed every day. Following Activin A treatment the levels of TGFβ signalling activation as determined through the pLNT-SBE-eGFP-luc reporter was assessed by eGFP fluorescence (Figure 13A) and quantitative luciferase assays (Figure 13B).

It was found that the pLNT-SBE-eGFP-luc transduced 293T reporter cells were responsive to the exogenous addition of Activin A in a dose dependant manor. eGFP fluorescence levels were seen to be present at background levels at 0ng/ml (control) indicating basal levels of TGFβ signalling in 293T reporter cells followed by a significant increase in eGFP fluorescence upon the exogenous addition of Activin A (Figure 13A). It was seen that the addition of 50ng/ml, 100ng/ml and 200ng/ml increased reporter activation by 45, 55 and 60-fold over control (0ng/ml) respectively as assessed through luciferase assays ($p<0.001$) (Figure 13B).

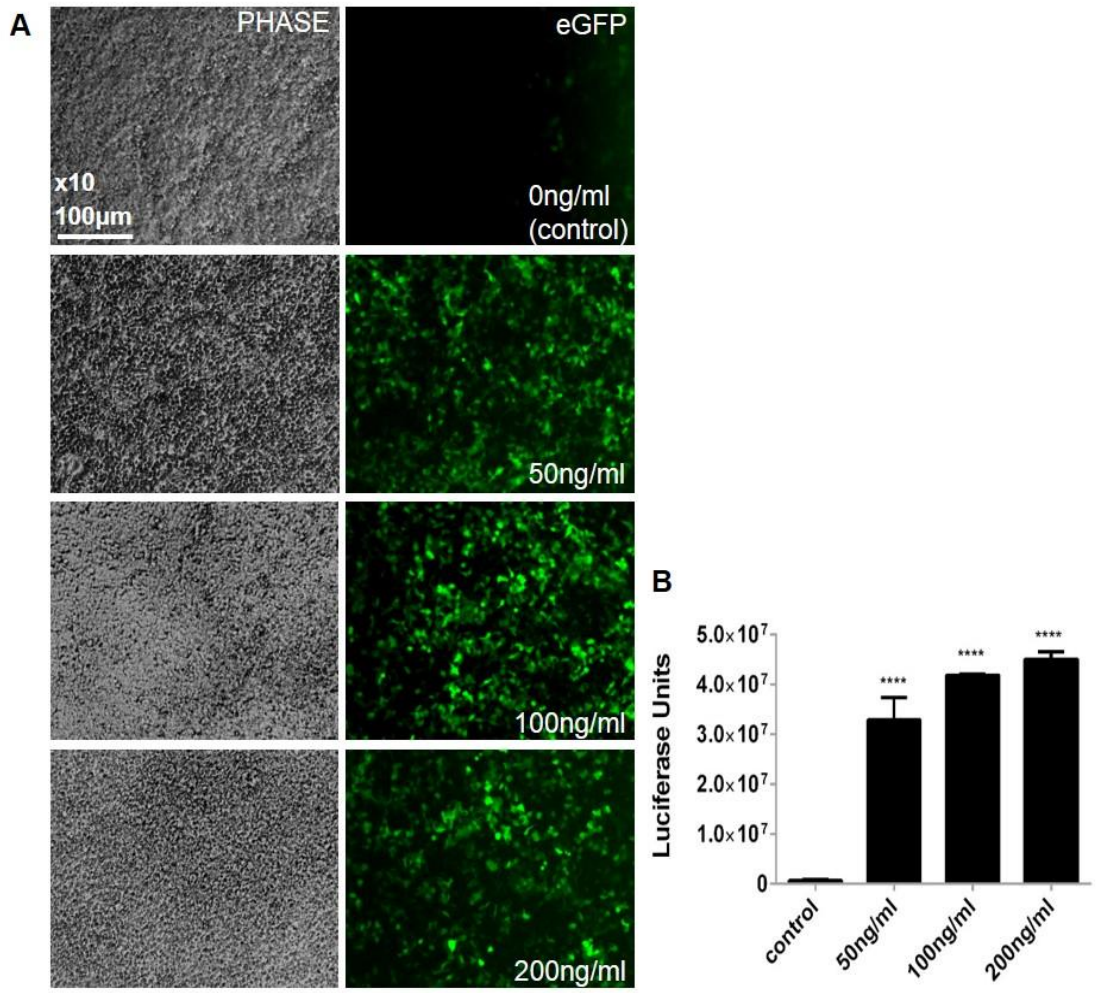

Figure 13: Validation of the pLNT-SBE-eGFP-luc reporter through exogenous Activin A addition to reporter cells

(A) Low levels of background eGFP fluorescence were observed in 293T pLNT-SBE-eGFP-luc reporter cells in control cells (no Activin A addition). A significant increase in fluorescence was observed through the addition of Activin A after five days of treatment. Levels of eGFP fluorescence were observed to be similar in 50ng/ml, 100ng/ml and 200ng/ml. **(B)** Luciferase assays quantitatively showed that there was an increased luciferase reporter activity in a dose dependant manner upon addition of Activin A at 50ng/ml, 100ng/ml and 200ng/ml respectively. Luciferase fold change was measured in comparison to reporter cells without the addition of Activin A. Data are shown at the mean ±SEM from three biological replicates (n=3). Statistical significance was calculated using a 1-way ANOVA with Bonferroni's post-test for multiple comparisons. Significance indicated by *** ($p<0.001$), ** ($p<0.01$), * ($p<0.05$). The pLNT-SBE-eGFP-luc lentiviral vector was created by Juliette Delhove in the McKay lab group at the WHRI, QMUL.

After validation of the pLNT-SBE-eGFP-luc reporter system to assess levels of TGFβ signalling upon the addition of Activin A, it was possible to quantitatively measure inceases in SBE reporter levels from secreted Nodal and Cripto proteins present in conditioned media. To produce Nodal/Cripto overexpression media, 293T cells were transduced with the pLNT-SFFV-Nodal/Cripto lentiviral vectors to create "producer cells". As the pLNT-SFFV-Nodal/Cripto vector doesn't contain a selectable marker to assess levels of transduction, a lentivirus containing an SFFV-eGFP cassette was transduced in parallel into separate populations of 293T cells and found to be ~70% expressed in populations through GFP+ cells. Following successful transduction, conditioned media was produced by adding fresh cell culture media and allowing Nodal and Cripto proteins to be secreted for a period of 24 hours. Subsequently, conditioned media was harvested from the producer cells and filtered followed by the addition to 293T reporter cells measure TGFβ signalling increases. Conditioned media was applied to reporter cells using the same production method for six days with media being refreshed each day. As a control, conditioned media was collected from SFFV-eGFP transduced 293T cells (containing no Nodal/Cripto proteins) and applied to reporter cells in the same manner.

It was found through luciferase assays that sole Cripto conditioned media exhibited SBE-eGFP-luc reporter activation at levels comparable to control conditioned media produced from SFFV-eGFP cells (Figure 14B). However, Nodal conditioned media induced reporter activation six-fold over control ($p<0.05$) as assessed through luciferase activity and exhibited eGFP levels in corroboration with quantitate analysis (Figure 14A). It was not possible to assess the levels of combined Nodal and Cripto conditioned media on SBE reporter activation due to experimental problems and time constraints but would be an avenue of future investigation.

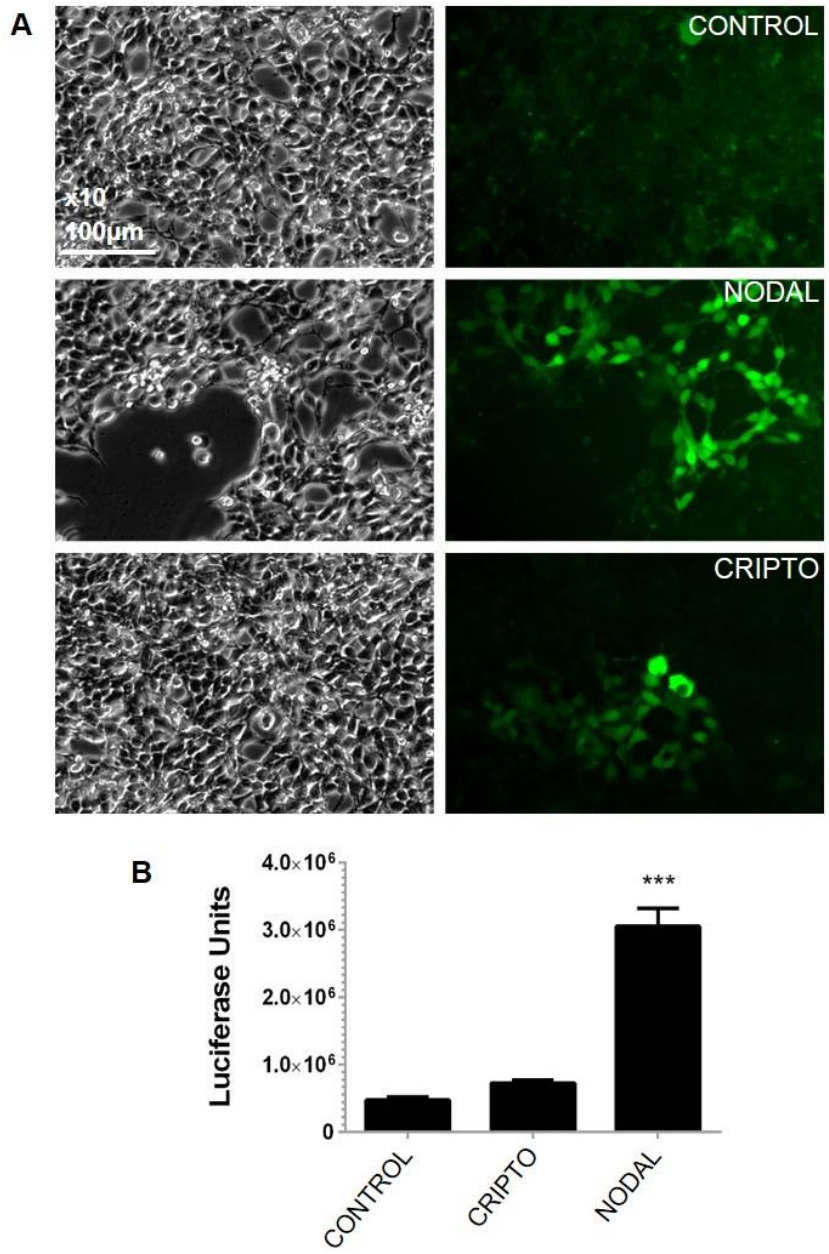

Figure 14: Validation of Nodal/Cripto conditioned media

(A) eGFP fluorescence levels upon TGFβ signalling activation from 293T producer cells following six days of treatment with either control (0ng/ml Activin A), Nodal conditioned media or Cripto conditioned media. **(B)** Quantification of pLNT-SBE-eGFP-luc reporter activation upon the addition of Nodal and Cripto conditioned media after six days of treatment. Data are shown at the mean ±SEM from three biological replicates (n=3). Statistical significance was calculated using a 1-way ANOVA with Bonferroni's post-test for multiple comparisons. Significance indicated by *** ($p<0.001$), ** ($p<0.01$), * ($p<0.05$). The pLNT-SBE-eGFP-luc lentiviral vector was created by Juliette Delhove in the McKay lab group at the WHRI, QMUL.

3.3.5 Differentiation of hESCs with Nodal/Cripto Conditioned Media

Following the validation of the overexpression media system using the pLNT-SBE-eGFP-luc reporter construct, Nodal/Cripto conditioned media was collected from Nodal/Cripto overexpression 293T producer cells and sequentially added day-on-day to feeder free conditioned Shef-3 hESCs for five days. Combinations of conditioned media used to assess DE specification included: sole Nodal overexpression media, sole Cripto overexpression media, combined Nodal and Cripto overexpression media, 100ng/ml Activin A and 0ng/ml Activin A (unconditioned basal media only). Combined Nodal and Cripto conditioned media was used at a 1:1 ratio which resulted in a 50% reduction in concentration when compared to sole application of Nodal or Cripto.

Feeder free conditioned Shef-3 hESCs were transduced with the lentiviral reporter constructs pLNT-SBE-eGFP-Nluc and pLNT-Vluc-eGFP-Nluc at 20MOI. The pLNT-SBE-eGFP-Nluc and pLNT-Vluc-eGFP-Nluc lentiviral vectors were created by Juliette Delhove in the McKay lab group at the WHRI, QMUL. Secreted Nluc lentiviral reporters were used as opposed to the pLNT-SBE-eGFP-luc reporter to better understand the day-on-day TGFβ temporal signalling changes, underlying DE specification from pluripotent stem cells over five days of differentiation (Figure 15A). As the Nluc luciferase is secreted into the culture media, samples can be taken daily and reporter activity can therefore be monitored in addition to eGFP florescence in real time without lysing cells (see Methods 2.5.4).

The secreted Vargula luciferin (Vluc) served as a control to normalise cell numbers between the different wells of the experiment. This was opposed to carrying out Bradford assays which requires the lysing of cells to collect total protein in traditional luciferase assays. Culture media samples of Nluc conditioned media were taken precisely every 24 hours and assessed for secreted luciferase on the GloMax® Multi+ (Promega) machine; allowing for a measure of signalling activity to be quantified (Figure 15B).

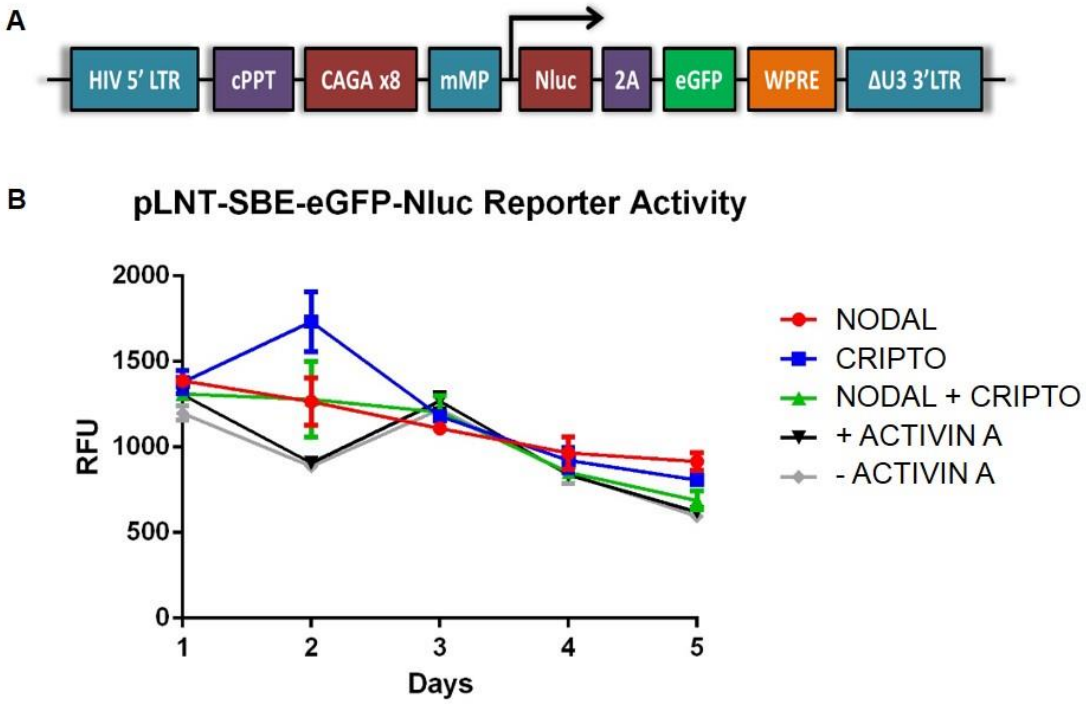

Figure 15: Shef3 differentiation with Nodal/Cripto conditioned media

(A) Schematic diagram of the pLNT-SBE-eGFP-Nluc lentiviral reporter vector used to assess levels of TGFβ signalling during DE specification. The pLNT-SBE-eGFP-Nluc and pLNT-Vluc-eGFP-Nluc (control) lentiviral vectors were created by Juliette Delhove in the McKay lab group at the WHRI, QMUL. **(B)** Nluc secreted luciferase assays showing SBE reporter activity in relative fluorescent units (RFU) over five days of DE differentiation normalised to Vluc. Sole Nodal, sole Cripto and combined Nodal + Cripto conditioned media, 100ng/ml Activin A (+ Activin A) and basal media containing no Activin A (- Activin A) are displayed over the five days of differentiation. Line graphs were created from the average of three biological repeats (n=3) with three technical repeats carried out for each biological repeat. Error bars were calculated for each time point using the ±SEM. Statistical analysis using a 1-way ANOVA gave a significance value of p=0.632 indicating no significant difference between control and conditioned media reporter activity.

Upon transduction of Shef3 hESCs with the pLNT-SBE-eGFP-Nluc reporter, very low levels of eGFP were visualised at 20MOI. Over the course of the differentiation experiment, it was found that there was no significant change in the levels of Nluc lentiviral reporter activity compared to the control over the five days of treatment following normalisation to account for cell numbers with Vluc ($p=0.632$).

Differentiated cells at the day five-time point were subsequently fixed with 4% PFA and stained by ICC for SOX17, a robust marker of DE, which is widely used to assess the populations of DE cells produced (Figure 16). Primary antibody incubations were carried out at 1:1000 dilution using a SOX17 primary antibody and secondary antibody incubation at 1:2000 dilution using Alexa Fluor anti-mouse 594 (see Methods 2.4.5). It was seen that there were exclusively SOX17+ cells in the 0ng/ml Activin A (basal media only) condition group however, the number of positive cells was seen to be at very low numbers. It was also observed that cells produced through the withdrawal of Activin A displayed different cell morphology to those of cells differentiated with either overexpression conditioned media or through the addition of Activin A at 100ng/ml. Overexpression conditioned media differentiated cells were seen to stain strongly for SOX17, indicating DE cells were specified through this approach. Comparative SOX17+ levels were seen between sole Nodal, sole Cripto and combined Nodal/Cripto conditioned media. Cell morphology in conditioned media and +100ng/ml Activin A groups closely resembled that of DE; possessing “cobble stone-like” cell morphology.

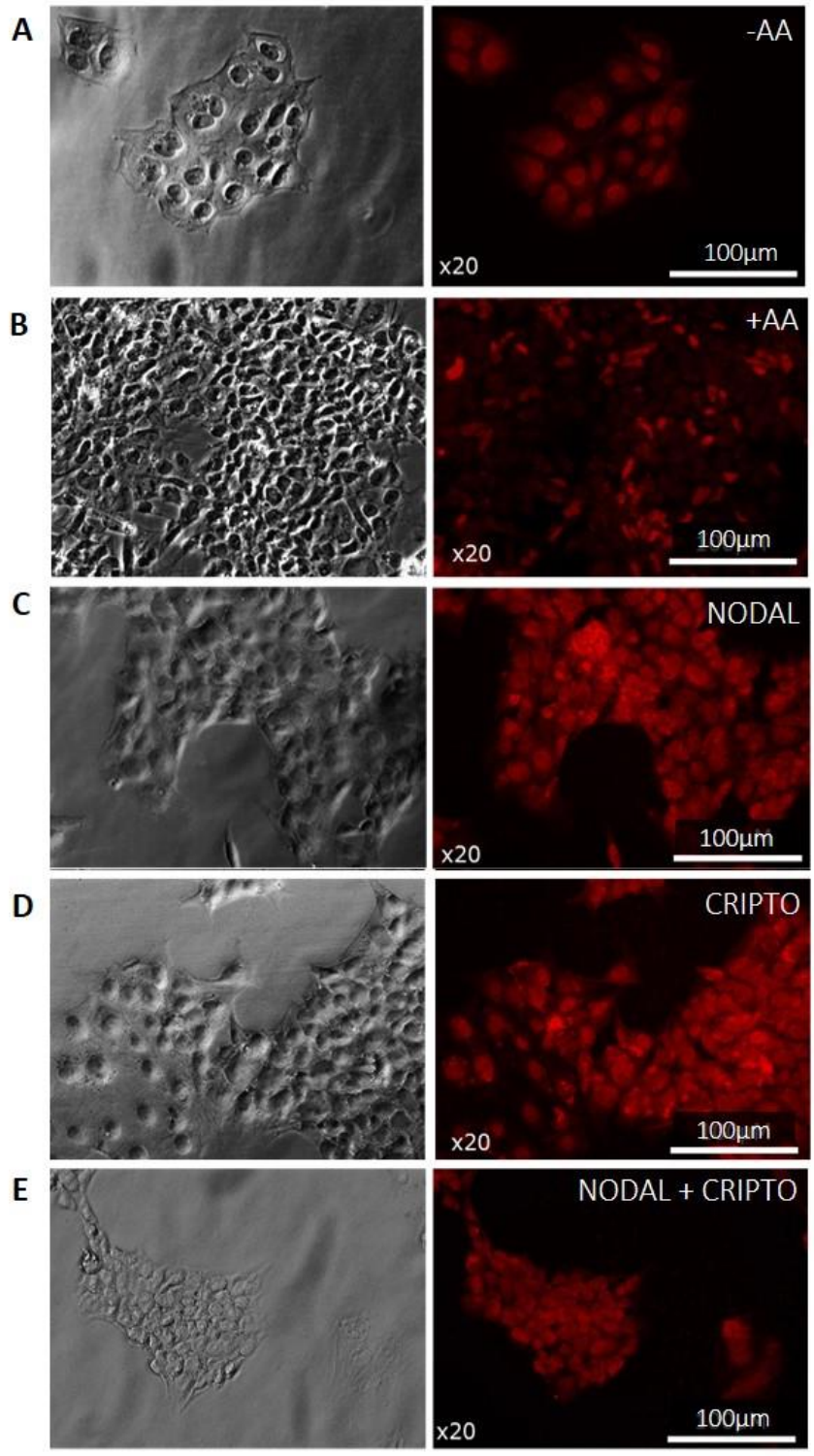

Figure 16: ICC staining of conditioned media differentiated cells

SOX17+ ICC staining of cells differentiated through the addition of conditioned media to feeder free Shef-3 hESCs for five days. **(A)** 0ng/ml Activin A (basal media only), **(B)** 100ng/ml Activin A, **(C)** sole Nodal conditioned media, **(D)** sole Cripto conditioned media and **(E)** combined Nodal and Cripto conditioned media. ICC staining images are from one biological replicate at x20 magnification.

3.3.6 Differentiation of hESCs with Nodal/Cripto Overexpression MEFs

Following the differentiation of hESCs to SOX17+ cells utilising overexpression conditioned media, the possibility of using Nodal/Cripto transgenic overexpression MEF feeder lines to efficiently specify cells expressing DE markers was explored. To create the MEF overexpression lines, pLNT-SFFV-Nodal/Cripto vectors was transduced into CD1 MEFs at passage 1 post-isolation at 20MOI. As a measure of transduction efficiency, a mock pLNT-SFFV-eGFP lentivirus was transduced side-by-side with overexpression constructs into separate populations of MEFs. This was done as the pLNT-SFFV-Nodal/Cripto overexpression vectors lack a marker to assess transduction (Figure 17A). It was assessed through the mock pLNT-SFFV-eGFP transduction that eGFP+ cell expression was approximately 50%. Overexpression MEFs were subsequently expanded to passage 3 to create stocks and inactivated with 100µg/ml mitomycin C to create Nodal/Cripto overexpression feeder cells.

To validate the ability of the overexpression MEFs to induce TGFβ signalling through the secretion of Nodal/Cripto protein into the culture media, the pLNT-SBE-eGFP-luc reporter was used to quantify increases in reporter activity. Overexpression MEF cell lines that were created included sole Nodal, sole Cripto and combined Nodal/Cripto. Nodal/Cripto overexpression MEFs conditioned culture media for a period of 24 hours before being added to reporter 293T cells transduced with the pLNT-SBE-eGFP-luc reporter to assess levels of TGFβ signalling activation. Nodal/Cripto conditioned media was replaced day-on-day for a period of five days before the reporter cells were lysed for luciferase assays (Figure 17B).

As a control for this experiment, conditioned media was collected from MEF feeders transduced with the pLNT-SFFV-eGFP mock lentivirus and applied to reporter cells (no AA). Validation experiments for transgenic overexpression MEFs was carried out in biological triplicate with three technical replicates for each sample being carried out.

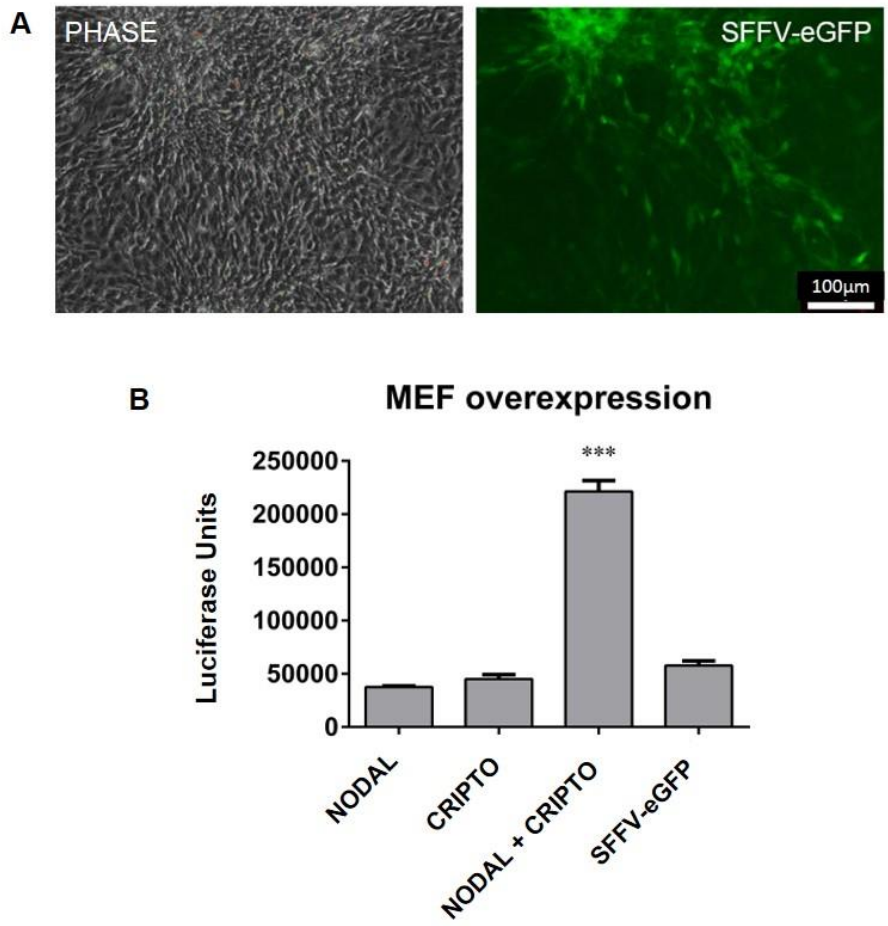

Figure 17: Quantification of Nodal/Cripto overexpression MEF feeders

(A) Phase contrast (left) and eGFP (right) imaging of MEFs transduced in parallel with a mock SFFV-eGFP lentiviral vector as a measure of transduction efficiency of the pLNT-SFFV-Nodal/Cripto overexpression constructs which lack a selectable eGFP marker. **(B)** Levels of Nodal/Cripto overexpression in transgenic MEF feeder cell lines were assessed using the pLNT-SBE-eGFP-luc reporter 293T system. Conditioned media produced from overexpression MEFs was added day-on-day to reporter cells for a period of five days and compared to conditioned media from MEF feeders transduced with the pLNT-SFFV-eGFP. Reporter cells were then lysed for quantitative luciferase assays. Statistical analysis of reporter activation was evaluated by a 1-way ANOVA with Bonferroni's post-test for multiple comparisons. Data is shown as mean ±SEM of three biological repeats. Significance indicated by *** ($p<0.001$), ** ($p<0.01$), * ($p<0.05$). RFU = raw fluorescent units.

It was found that there was no significant difference in SBE reporter levels between control conditioned media produced from SFFV-eGFP MEFs and reporter cells treated with conditioned media produced from sole Nodal and sole Cripto MEFs. However, there was found to be a significant increase in TGFβ reporter activity, through the activation of the SBE reporter element, with combined Nodal and Cripto conditioned media ($p<0.001$). An increase of approximately four-fold was quantified through luciferase assays above control conditioned media treated reporter cells. This result contrasted the inductive potential of sole Nodal activation of the SBE response element seen in conditioned media collected from 293T producer cells (Figure 14). This could be in part due to the cocktail of secreted factors produced from MEF feeder cells which masked a DE inducing effect of secreted Nodal/Cripto proteins.

Following assessment of Nodal/Cripto overexpression levels in transgenic MEF feeders, inactivated MEFs were plated onto 0.1% gelatin coated 12 well plates at 70,000 cells/well 24 hours prior to Shef3 hESC seeding. Feeder free conditioned Shef3 hESCs cultured in mTeSR were dissociated into single cells using Accutase® and replated onto transgenic overexpression MEFs at 70,000 cells/well in mTeSR pluripotency media. Feeder free conditioned Shef3 hESCs were used in this experiment due to problems with contamination in feeder-conditioned Shef3 hESCs and time constraints. The following day, cell culture media was changed to basal differentiation media (see Methods 2.1.5). In addition to using Nodal/Cripto overexpression MEFs to differentiate Shef3 hESCs to DE, inactivated MEFs transduced with SFFV-eGFP were used as control feeder cells. Shef3 hESCs were plated onto either inactivated SFFV-eGFP MEFs in basal media or basal media with the addition of 100ng/ml Activin A. Basal culture media was refreshed every 48 hours in all cell lines to allow for transgenic overexpression MEFs to condition the media for a total of five days.

Following five days of differentiation, cells were fixed with 4% PFA and stained by ICC for SOX17. In addition, FOXA2 ICC staining was also carried out on replicate wells as the presence of SOX17+ and FOXA2+ cells are used in combination as robust markers of DE (Figure 18). Primary antibody incubations were carried out at 1:1000 dilution using SOX17 and FOXA2 primary antibodies and secondary antibody incubations at 1:2000 dilution using Alexa Fluor anti-mouse 594 (see Methods 2.4.5).

Strong FOXA2+ ICC staining was found in all treatment conditions at comparable levels except for Cripto overexpression MEF feeders which were found to exhibit lower levels of FOXA2+ cells (Figure 18A). Cell morphology was also seen to be consistent in all treatment protocols including that of SFFV-eGFP conditioned culture media (containing no added DE inducing factors). In addition, the confluency of the differentiated cells was seen to be at comparative levels across treatments and replicate wells for each condition.

Levels of ICC staining for SOX17+ cells was seen to be at lower levels in both the 100ng/ml Activin A and SFFV-eGFP conditioned media (no AA) than was seen in FOXA2 ICC staining. Levels of SOX17+ cells were seen to be higher in the 100ng/ml Activin A treatment compared to SFFV-eGFP conditioned culture media containing no added DE inducing factors (Figure 18B). This result was expected however, there was predicted to be a larger difference in levels of both SOX17+ and FOXA2+ cells between these treatments as Activin A is routinely used to specify DE from pluripotent hESCs. One explanation for this result in both the SOX17 and FOXA2 staining of control cells could be that the MEF feeder cells secrete a cocktail of growth factors which could be masking the inductive effects of the conditioned media and the 100ng/ml Activin A treatment, through the secretion of TGFβ into culture media.

Cell morphology in SOX17+ cells was seen to be consistent in both SFFV-eGFP conditioned media, 100ng/ml Activin A and dual Nodal/Cripto overexpression conditions and maintained consistent with cell morphology seen in FOXA2+ cells. However, differences in cell morphology were seen in both sole Nodal and sole Cripto treatments. In sole Cripto overexpression cells, there was large amounts of SOX17+ cells however, the cell morphology was seen to be particularly distinct from other treatments; SOX17+ cells were seen to be “cobble-like” in appearance. It is of note that the differentiated cell morphology in the sole Cripto overexpression MEFs largely resembled the that of cells produced in the basal media only (0ng/ml Activin A) of the 293T producer cell conditioned media experiment (Figure 16). Differentiated cells produced through sole Nodal overexpression conditioned media were seen to be found in defined tightly-packed cell clusters with distinct gaps between SOX17+ cell clusters.

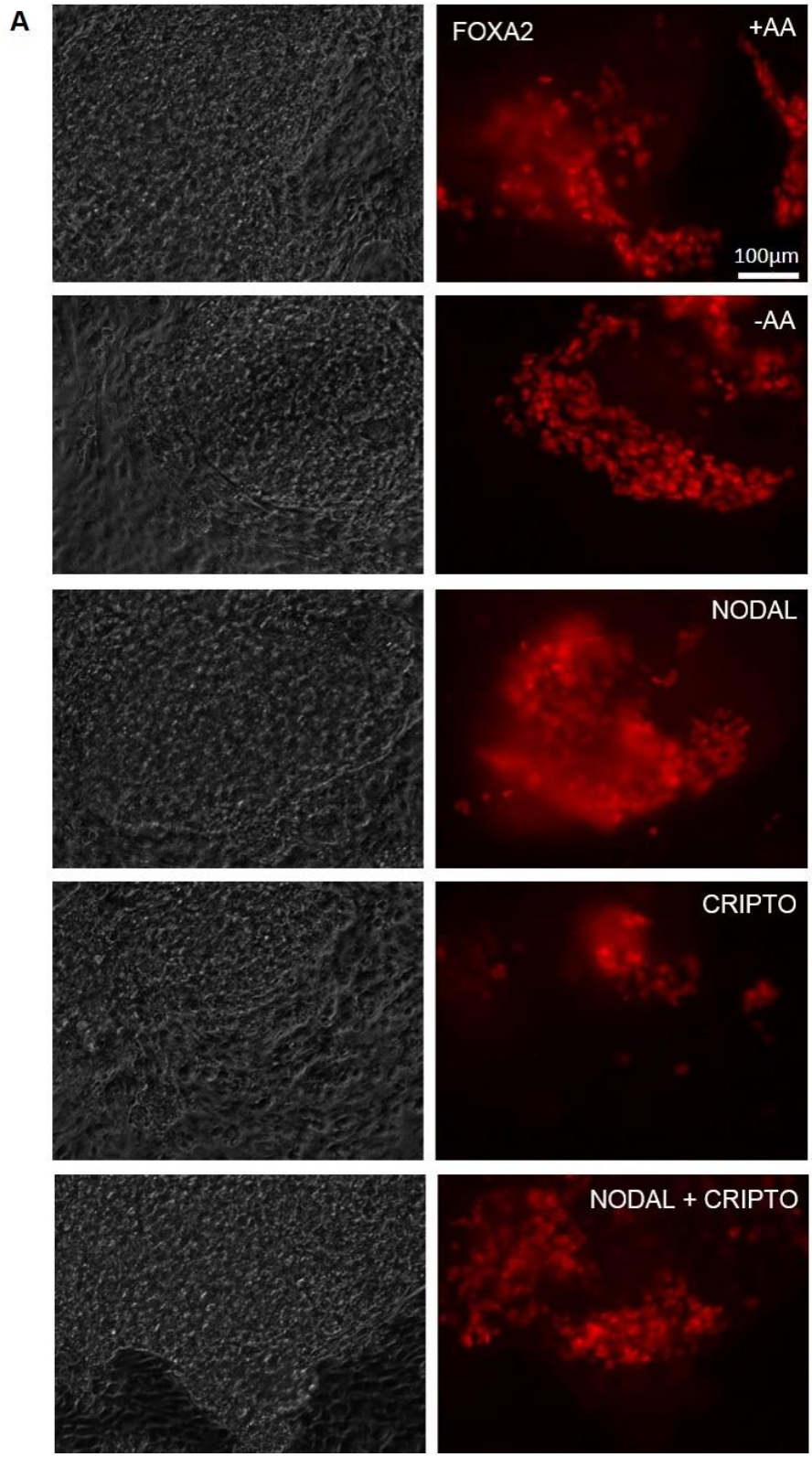
A
FOXA2
+AA
100µm
-AA
NODAL
CRIPTO
NODAL + CRIPTO

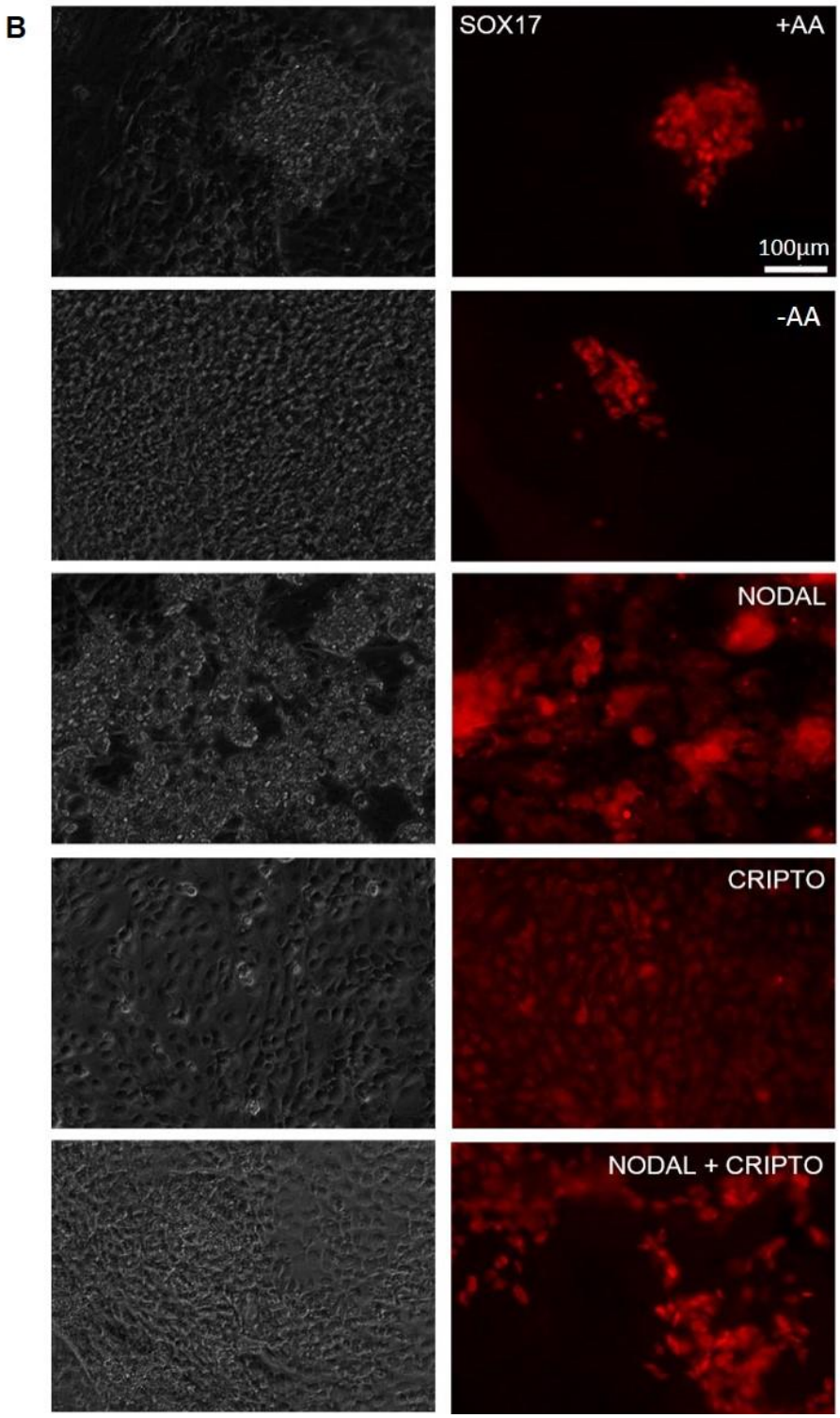

Figure 18: DE cells produced utilising transgenic overexpression MEF feeders

(A) ICC staining for FOXA2+ cells on transgenic MEFs in the different treatment groups at day five of differentiation. **(B)** ICC staining of SOX17+ cells on transgenic overexpression MEFs of the different treatment groups at day five of differentiation. ICC staining images are from one biological repeat at x20 magnification.

3.4 Discussion

As DE cells give rise to the hepatic lineage as well as other cell lineages of therapeutic interest including pancreatic cells, the ability to efficiently specify DE cells from human pluripotent stem cells is an attractive approach that has yet to be realised [87] [247]. Using different methodologies including the use of shRNA knockdown and lentiviral overexpression in both a MEF feeder and feeder-free differentiation systems, human pluripotent stem cells were subjected to DE differentiation methods in comparison to Activin A.

3.4.1 Investigating DE Specification with shRNA Lentiviral Knock Down

The validation of lentiviral shRNA knock down vectors were trialled to validate tools with a view to dissect DE specification and in particular the role of Nodal and its extra-cellular signalling co-factor Cripto. Previous studies have shown that the addition of exogenous recombinant Nodal to monolayer cultures of pluripotent stem cells resulted in a lack of differentiation and continued maintenance of pluripotency markers as assessed through qPCR and undifferentiated colony morphology [245]. Activin A is routinely used to mimic Nodal signalling specify DE *in vitro* [248] [148] [83] [249]. The use of Activin A in place of recombinant Nodal in DE differentiation protocols is therefore due to Activin A exhibiting greater activity than currently available recombinant human Nodal proteins. However, the off-target gene activation caused by the addition of exogenous Activin A maybe deleterious to producing homogenous populations of DE (McKay et al. unpublished data).

There has been evidence provided by Chen et al. (2013) that the use of recombinant Nodal protein at much increased concentrations promotes mES cells to differentiate to more mature and functional insulin-producing cells [250]. Levels of Nodal protein added to mES cells to elicit this response were twenty-fold increased over levels of Activin A that is typically used to specify DE *in vitro*. Therefore, analysis of DE populations in different Nodal/Cripto expression environments would provide a valuable insight into the underlying signalling mechanisms.

Gene expression knock down was validated in HeLa cells, a cell line that was shown to have an intact TGFβ signalling pathway and was shown express both Nodal and Cripto at levels that permitted the assessment of shRNA knockdown. Through this validation, a range of knockdown efficiencies was obtained across the eight Nodal/Cripto clones. However, the use of pGIPZ lentiviral shRNA vectors to carry out gene knock down studies in pluripotent stem cells was not successful in this project. Efficient lentiviral transduction in both huES1-OCT4-GFP and Shef3 hESCs could not be obtained over a variety of MOI concentrations and over multiple biological replicates using different batches of titred shRNA lentivirus; including the use of both freshly produced lentiviral particles and cryopreserved samples. Lentiviral vectors utilising the CMV promoter driving shRNA knock down of Nodal/Cripto could not be expressed in Shef3 hESCs. The lack of expression in both the pGIPZ Nodal and Cripto shRNA lentiviral vectors suggests the problem is with the CMV promoter driving knock down expression.

A previous study by Norrman et al. (2010) compared a number of viral promoters and showed that that the CMV viral promoter is rapidly silenced in transduced hESCs [251]. Other studies have also shown that the CMV promoter was down regulated in transduced hESCs when compared to other viral promoters including EF1α and PGK [252] [253].

Expression levels between the promoters in these studies as assessed through eGFP florescence was seen to be the lowest in hESCs transduced with CMV-containing lentiviral vectors. Liew et al. (2007) were unable to obtain successfully transduced hESCs when a CMV promoter containing vector was used to transfect hESCs [254]. Transfection of hESCs with four different viral promoter containing vectors corroborated other studies and further showed that the CMV promoter is not the most appropriate choice for gene expression studies in hESCs. Taken together, these studies show the variation in strength of expression and in transduction efficiency between different viral promoters and highlight the need for appropriate promoters to be used when transducing particular cell types. This idea is further strengthened by findings in this thesis that very high levels of lentiviral transduction was obtained in the validation phase where HeLa cells were transduced successfully with the knock down constructs and efficient gene expression knockdown was achieved.

3.4.2 Differentiation to DE with Nodal/Cripto Conditioned Media

After the unsuccessful transduction of Shef3 hESCs with the pGIPZ lentiviral Nodal/Cripto shRNA knockdown constructs, a new approach was undertaken with which to differentiate pluripotent stem cells to DE. The pLNT-SFFV-NODAL-luc and pLNT-SFFV-CRIPTO-luc lentiviral vectors encode secreted Nodal/Cripto proteins which were utilised as a method of DE specification using Nodal/Cripto conditioned media. This approach was first validated with the use of the pLNT-SBE-eGFP-luc 293T reporter system. The reporter system validated the proof of principle of using the conditioned media approach to increase signal levels of the TGFβ pathway and consequently was applied to specify DE from pluripotent hESCs.

The Nodal/Cripto conditioned media approach was trialled alongside the use of 100ng/ml Activin A, typically used to specify DE from pluripotent stem cells [87], [110] [111] [84] [106] [83] as well as a pluripotent stem cells exposed to basal media without the addition of DE differentiation inducing factors.

Shef3 hESCs were transduced with the pLNT-SBE-eGFP-Nluc reporter to allow changes in TGFβ signalling to be quantitatively assessed at day-on-day intervals. Following transduction of the pLNT-SBE-eGFP-Nluc lentiviral reporter very low levels of eGFP were visualised at 20MOI. Over the course of the differentiation experiment, it was found that there was no significant change in the levels of Nluc lentiviral reporter activity over the five days of treatment. This either indicates that there were very low levels of lentiviral transduction, possibly accounted for by an erroneous p24 assay detecting non-viable lentiviral particles. The second possibility is that the Nluc lentiviral reporter is not sensitive to changing TGFβ levels. It was seen from the quantitative Nluc analysis that there were no distinct changes in pLNT-SBE-eGFP-Nluc reporter activity between the +100ng/ml Activin A and 0ng/ml Activin A (basal media only) groups. The addition of Activin A should have increased the Nluc reporter activity as seen in the pLNT-SBE-eGFP-luc reporter validation. pLNT-SBE-eGFP-Nluc reporter was not previously tested in 293T reporter cells like the pLNT-SBE-eGFP-luc secreted luciferase reporter which was shown to be responsive and provide a quantitative measure of change. Further investigation is therefore needed to validate the pLNT-SBE-eGFP-Nluc and assess the suitability of this reporter to be applied in the investigation of TGFβ signalling analysis.

After five days of differentiation, with conditioned Nodal/Cripto media combinations being applied day-on-day, it was found that cells stained positive for the DE marker SOX17. Comparisons between the SOX17+ levels seen between sole Nodal, sole Cripto and combined Nodal/Cripto were seen to be comparative between media combinations. This was unexpected as sole Nodal conditioned media was seen to significantly upregulate SBE-JDG-luc reporter activity compared to sole Cripto conditioned media when the approach was first validated. However, it was found in this experiment that pluripotent stem cells differentiated without the application of DE inducing factors (basal differentiation media only) to SOX17+ cells. Differentiated cells from this treatment were present at very low numbers but were almost exclusively SOX17+. It was further observed that cells produced through the withdrawal of Activin A displayed different cell morphology to those of cells differentiated with either overexpression conditioned media or through the addition of Activin A at 100ng/ml. This could be due to batches of Nodal/Cripto conditioned media containing low levels of the proteins and further investigation would include batch testing conditioned media using the pLNT-SBE-eGFP-luc reporter before the application to pluripotent stem cell cultures for DE differentiation.

The use of conditioned media to differentiate human stem cells has been investigated previously using conditioned media from chondrocytes which showed the ability to successfully differentiate Mesenchymal Stem Cells (MSCs) to chondrocytes [255]. Further studies have shown the potential of specific conditioned medias to drive the differentiation of stem cells to osteogenic lineages utilising MSC conditioned media [256]. The application of conditioned media to differentiate pluripotent stem cells to cell types of interest is therefore an interesting proposition to induce lineage specification in a feeder-free environment.

The use of quantitative methods of analysis such as qPCR would better assess the levels of DE specification through the gene expression analysis of markers including SOX17, FOXA2 and CXCR4 amongst others. This could be compared to gene expression analysis of DE cells produced using 100ng/ml Activin A. A further optimisation of the current system that could be applied to future experiments would be to concentrate the Nodal/Cripto conditioned media. Currently, Nodal and Cripto conditioned media is combined at a 1:1 ratio which reduces the concentration of Nodal and Cripto in the overall media by 50% when compared to sole conditioned media. This would make comparisons of the DE differentiation potential of conditioned media test groups to Activin A more consistent between treatment groups.

3.4.3 Differentiation to DE with Nodal/Cripto Overexpression MEFs

The use of Nodal/Cripto transgenic overexpression MEFs was investigated as a potential feeder-based method to efficiently differentiate hESCs to DE through the secretion of combinations of Nodal/Cripto proteins into culture media. This was investigated as an alternative strategy to specify DE cells as opposed to utilising conditioned media from 293T Nodal/Cripto producer cells which was carried out in a feeder-free environment. The ability of transgenic Nodal/Cripto overexpression MEF feeder cells to specify DE was assessed against the use of mock transduced MEFs containing a selectable marker with or without the addition of 100ng/ml Activin A.

From initial validation of the ability of Nodal/Cripto transgenic MEF overexpression media, it was found that levels of SBE-eGFP-luc activity in 293T reporter cells was less pronounced than those achieved in Nodal/Cripto 293T producer cells (Figure 17 and Figure 14). This result could account for the differences in results obtained through both approaches in terms of SOX17+ cells. As 293T cells are more readily transduced than MEFs, it could be that a near pure population of 293T producers was obtained compared to the MEF feeder cells which would exhibit a lower transduction efficiency (assessed to be ~50%). This would enable higher concentrations of Nodal/Cripto DE inducing proteins to be secreted into the conditioned culture media from the 293T producer cells.

The lack of a selectable marker, either eGFP or an antibiotic resistance cassette, in the pLNT-SFFV-NODAL-luc and pLNT-SFFV-CRIPTO-luc lentiviral overexpression constructs prevents an accurate quantification of transduction efficiency, which would need to be incorporated in future validation and DE specification experiments. The incorporation of an antibiotic resistance cassette, for example puromycin, would allow a pure population of both 293T and MEF feeder producer cells to be established with which to carry out DE specification experiments more accurately as opposed to relying on mock parallel transductions with a lentivirus containing a eGFP element. In this way, effects of overexpression MEFs could be more tightly controlled between experiments and the levels of Nodal/Cripto proteins in the conditioned media to be standardised. This approach would address the potential problem of the loss of transgene expression during passaging of the MEF overexpression feeder cells to P3 to obtain sufficient cells to conduct the conditioned media experiments. Further advantages include allowing transduced MEFs to be distinguished from ICC stained SOX17+/FOXA2+ cells for dual colour imaging. This could also have a use in assessing the levels of transgenic MEFs remaining in culture wells over the process of DE specification.

As the hESCs proliferate and differentiate MEF feeders are pushed outwards of the expanding colonies of hESCs; resulting in MEFs undergoing apoptosis and detaching from the surface of the cell culture wells. Consequently, there would be lower numbers of transgenic overexpression MEFs secreting variable concentrations of Nodal and Cripto proteins into cell culture media. This could be a possible reason for the disparity in previous literature and the assumed experimental outcome in contrast to the levels of SOX17+ and FOXA2+ staining following DE differentiation using Nodal/Cripto transgenic MEF feeder cells in this thesis. It was expected that the hESCs treated with basal differentiation media collected from SFFV-eGFP MEFs with no added DE inducing factors would produce much reduced levels of SOX17+ and FOXA2+ cells in comparison to the use of 100ng/ml Activin A, which is routinely used to specify DE. The lack of a significant increase in SOX17+ and FOXA2+ DE cells was particularly surprising between differentiated cells on SFFV-eGFP MEFs supplemented with 100ng/ml Activin A and cells differentiated cells that had been exposed to basal media only without DE inducing factors. Possible explanations for this outcome could be due to MEF feeder cells secreting and undefined cocktail of growth factors into the cell culture media. This allows for the possibility that some of these secreted growth factors, including TGFβ family members, could compensate for the lack of Activin A and promote the specification of DE.

Before the seeding of hESCs in the feeder-based DE differentiation system, mitomycin c was added to inactivate the Nodal/Cripto overexpression MEFs to prevent feeder cell overgrowth. Mitomycin C is routinely used as a method to arrest feeder cell growth in the culture of different cell types including hESCs [257] [258] [259] [260]. Potential effects of mitomycin c on the levels of Nodal/Cripto proteins secreted into conditioned media was not studied in this thesis.

It has however been previously shown that mitomycin c can increase GFP transgene expression in human glioma cells which have been infected with Adeno-Associated Virus Type II (AAV) [261]. This observation was further validated *in vivo* and showed that mitomycin c increases AAV transgene expression in mice. Consequently, mitomycin c treatment wasn't thought to decrease lentiviral transgene expression in the MEF overexpression experimental system and consequently the amount of Nodal/Cripto protein secreted. Future experiments using the feeder-based DE differentiation system could assess possible effects of both active and inactivated Nodal/Cripto secreting MEFs on SBE reporter activation to verify there are no negative impacts through the utilisation of mitomycin c in this experimental system.

Chapter 4: CombiCult® Hepatic Differentiation Screen

4.1 Introduction

4.1.1 CombiCult® Differentiation Matrix Design

Directed differentiation of pluripotent stem cells to cell types of interest has been traditionally a process of trial and error which is both time consuming and expensive. CombiCult® is a combinatorial cell culture platform that allows the multiplexing of a large range of differentiation protocols to be carried out simultaneously – greatly reducing the time taken to identify key factors that can be utilized in defined protocols [237]. The CombiCult® platform has previously been used to successfully identify and optimise protocols to differentiate a number of cell types including osteoblasts [238] and haematopoietic progenitor cells [239].

There is an outstanding requirement in the biotechnology industry for an inexhaustible supply of hepatocyte-like cells (HLCs) to be used in regenerative medicine to help to repair, augment or replace damaged tissues and with which to perform early-stage drug toxicity screens [124] [125]. There is a need for hepatocytes to carry out drug safety testing and this is compounded by the fact that isolated primary hepatocytes quickly lose their proliferative potential when cultured *in vitro* and dedifferentiate; losing their functional activity [126]. Liver hepatocarcinoma cell lines such as HepG2, Huh7 and HepaRG have been used previously as hepatocyte models with which to study drug metabolism and conduct toxicological assays however, the results have varied in reproducibility and are not directly translational to humans [124] [128] [129] [130].

To date, *in vitro* hepatic differentiation protocols have produced HLCs assessed to show some degree of functional capability albeit at significantly lower levels than seen in isolated primary hepatocytes. [111] [99] [107] [106]. These results taken together suggest that the HLCs derived so far resemble immature, foetal hepatocytes. As the process of hepatic differentiation and subsequent maturation has yet to be fully recapitulated *in vitro* to produce metabolically relevant HLCs, combinations of differentiation-inducing factors need to be assessed and compared to the current best models.

A CombiCult® split-pool screen was designed to identify novel protocols for the efficient differentiation of hESCs to mature, metabolically relevant hepatocytes that outperform current hepatocyte *in vitro* models. CombiCult® maturation screens carried out on hepatic progenitor cells by Dr Jey Jeyakumar of Plasticell Ltd. gave insights into candidates involved in the maturation stages of hepatocyte differentiation. Taking previous studies and CombiCult® screen candidates, a new hepatocyte differentiation CombiCult® matrix was designed. I conducted a literature review to identify components that have been shown to play an important role during the different stages of hepatogenesis; that is, DE specification, hepatic specification, hepatoblast expansion and hepatic maturation. Previous knowledge of *in vivo* liver development and the growth factors and signalling mechanisms involved was utilized and applied to *in vitro* hepatocyte differentiation (Figure 19). The new screen further incorporated small bioactive molecules wherever possible to replace growth factors along the key developmental stages of hepatocyte differentiation from pluripotent hESCs (see Methods 2.6.1). The use of small bioactive molecules has many advantages over the use of growth factors and is important for the future industrial application to differentiate pluripotent stem cells to HLCs to reduce costs and increase reproducibility [136].

4.2 Aims

- Validate a CYP450 ICC assay for hepatic maturation in derived HLCs.
- Design and conduct a CombiCult® screen to identify novel factors for the optimal hepatic differentiation of pluripotent stem cells to HLCs.
- Isolate top CombiCult® hepatic differentiation protocols for further analysis.

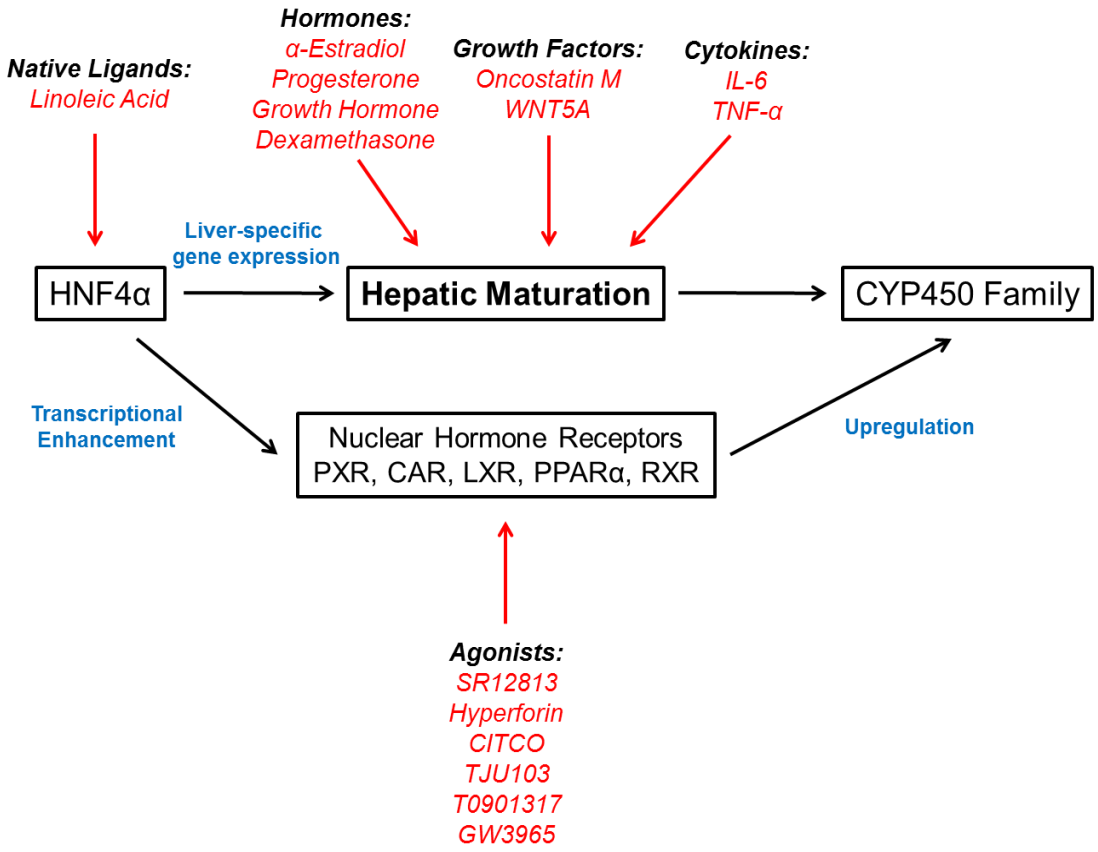

Figure 19: Targetting of regulatory mechanisms to produce more mature HLCs

The mechanisms involved in hepatic specification and maturation were targeted with small bioactive molecules and growth factors. The factors used had either previously been identified as being important *in vivo* or were predicted to have a potential inductive effect *in vitro* with a view to more efficiently differentiate HLCs from pluripotent stem cells.

4.3 Results

4.3.1 Validation of End Point Readout for Hepatocyte Differentiation

For identification and isolation of differentiated HLCs cultured on microcarriers an endpoint readout assay for their maturity and metabolic induction potential was developed by Dr Jey Jeyakumaer of Plasticell Ltd. Immunocytochemistry (ICC) was used to stain for two key members of the CYP450 family of metabolic enzymes, CYP1A1/A2 and CYP3A4, which are key players in xenobiotic drug metabolism and therefore a robust marker of the levels of hepatocyte maturity in differentiated HLCs. ICC staining for mature hepatic markers would be used in conjunction with the COPAS large particle sorter to separate out 'hits', differentiated HLCs present on the microcarrier surface expressing both CYP1A1/A2 and CYP3A4, from non-hepatic cells lacking the expression of these markers. CYP1A1/A2 and CYP3A4 enzymes in differentiated HLCs were induced through the addition of drug cocktails. CYP1A1/A2 was induced with the addition of 10μM omeprazole and 50μM dexamethasone whilst CYP3A4 was induced with the addition of 50μM rifampicin. Microcarriers can therefore be induced solely or dual induced. The levels of CYP1A1/A2 and CYP3A4 induction upon drug addition was compared to uninduced HLCs.

CYP1A1/A2 and CYP3A4 induction assays to detect mature HLCs were first validated on two cell lines. Firstly, on HepaRG cells, a hepatocarcinoma cell line serving as an *in vitro* hepatocyte model [129] [262] [129]. HepaRG cells exhibit some characteristics of primary hepatocytes, such as, metabolic induction; albeit at levels that are vastly lower than in primary hepatocytes. Validation was also carried out on HepG2 cells, another *in vitro* hepatocarcinoma model cell line which lacks the capacity to be significantly induced with omeprazole and rifampicin (Figure 20).

HepaRG cells were maintained on collagen I coated plates in Lonza HBM basal media supplemented with Lonza SingleQuots whilst HepG2 cells were maintained in DMEM-complete media (See Methods 2.1.2 and 2.1.4). HepG2 and HepaRG cells were grown in monolayer culture before being enzymatically dissociated to single cells were counted on a haemocytometer before seeding at a density of 100 cells per microcarrier bead. HepG2 and HepaRG cells and microcarrier beads were then mixed and cell attachment was achieved through overnight incubation at 37^0C. Viable attached cells were then visualised under a light microscope by staining microcarriers with neutral red solution (Figure 20A and Figure 21A). It was determined that 100 cells per bead was the optimal seeding density for the validation assay to allow for sufficient cell attachment without microcarriers becoming over confluent.

After cell attachment to microcarrier surfaces the basal culture media was changed to Wiliam's E Media containing 1% sodium pyruvate, 1% P/S, 0.1µM hydrocortisone and 10ng/ml insulin. Cells were treated with assay media containing 10µM omeprazole + 50µM dexamethasone to induce CYP1A1/A2 or 50µM rifampicin to induce CYP3A4. Combined drug treatment to induce both CYP1A1/A2 and CYP3A4 enzymes was carried out through the addition of 10µM omeprazole, 50µM dexamethasone and 50µM rifampicin to assay media. Drug induction was carried out for a period of three days, with induction media being refreshed every day. As a control, assay media was added containing no CYP1A1/A2 and CYP3A4 inducers but containing a 0.2% DMSO vehicle control (uninduced). The hepatic induction assay used to test the drug inducibility of CYP450 enzymes in differentiated HLCs was designed and previously validated by Dr Jey Jeyakumar of Plasticell Ltd.

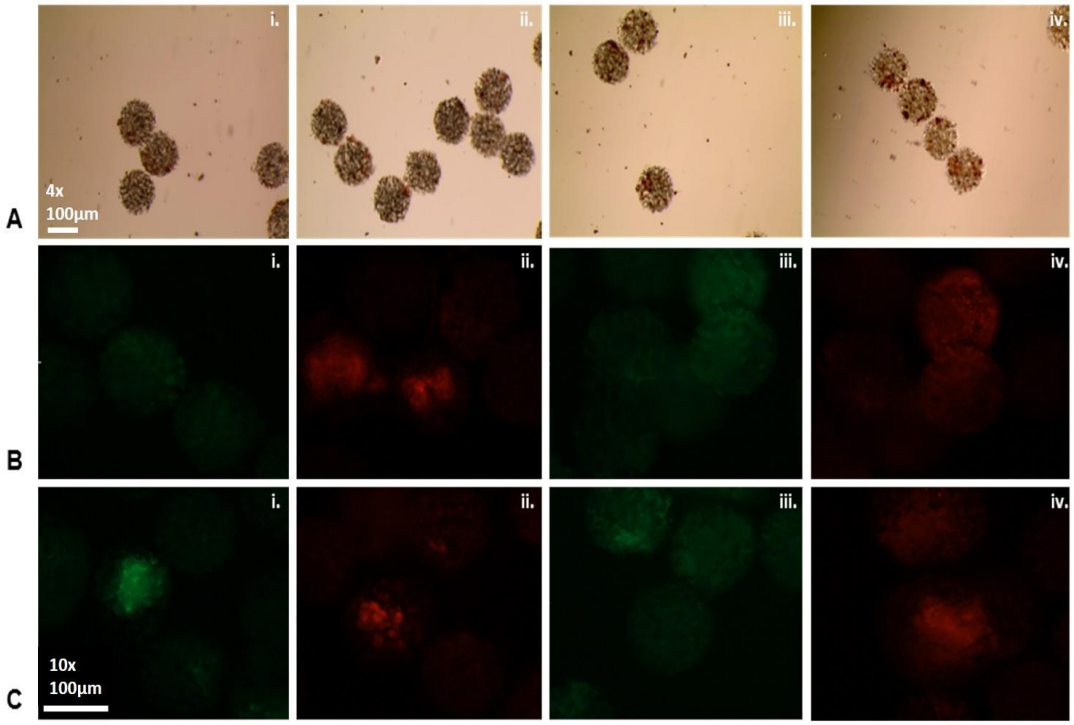

Figure 20: Validation of CYP1A1/A2 and CYP3A4 induction assays on HepG2 cell seeded microcarriers

(A) HepG2 cells seeded onto microcarriers at 70 cells per bead (i-ii) and at 100 cells per bead (iii-iv) stained with neutral red to visualise viable cells on the bead surface (x4 magnification). **(B)** Uninduced HepG2 cells seeded microcarriers treated with 0.2% DMSO vehicle control stained for CYP3A4 (i: green), CYP1A1/A2 (ii: red) and dual CYP3A4 and CYP1A1/A2 (iii-iv: green and red). **(C)** Induced HepG2 cells following three days of drug induction stained for CYP3A4 (i: green), CYP1A1/A2 (ii: red) and dual CYP3A4 and CYP1A1/A2 (iii-iv: green and red).

For ICC staining to assess levels of HLC maturity, microcarriers were washed, fixed and stained (see Methods 2.6.2.4). Primary antibody incubations for CYP1A1, CYP1A2 and CYP3A4 enzymes were carried out overnight at 4^0C at 1:100 dilutions. Microcarriers were subsequently washed three times with PBS and incubated in Alexa Fluor 488 anti-goat (CYP3A4, green) and anti-mouse 594 (CYP1A1/A2, red) secondary antibodies at 1:1000 dilutions. A secondary antibody only control was used to establish levels of background florescence with which to exclude in subsequent analysis of fluorescence intensity. The ICC staining protocol for hepatic induction was initially designed and validated by Dr Jey Jeyakumar of Plasticell Ltd.

As expected, HepG2 cells seeded onto microcarriers showed no visual induction of the CYP1A1/A2 or CYP3A4 enzymes upon drug administration for a period of three days compared to uninduced 0.2% DMSO vehicle control (Figure 20B and C). In contrast, HepaRG cells seeded onto microcarriers showed increased levels of CYP1A1/A2 or CYP3A4 enzymes after drug induction compared to uninduced 0.2% DMSO vehicle control (Figure 21C and E). This increase in CYP1A1/A2 or CYP3A4 levels was observed for both individual and combined drug induction but was particularly evident during the single induction of CYP3A4 with 50µM rifampicin. It was seen that in the dual induced HepaRG seeded microcarriers that there was co-localisation of staining for CYP1A1/A2 or CYP3A4 (Figure 21E iii.-iv).

The ability to isolate cells exhibiting high levels of CYP1A1/A2 and CYP3A4 enzymes is of great importance in identifying the differentiated HLCs with the widest spectrum of metabolic activity. This result demonstrates the ability of the CYP1A1/A2 and CYP3A4 ICC assay to distinguish between cells exhibiting hepatic markers but low levels of metabolic activity from metabolically active HLCs capable of being induced upon appropriate drug cocktail treatment.

As a result, the validated ICC assay is suitable to use as an end point maturation readout to screen for microcarriers containing HLCs at the end of the CombiCult® differentiation process.

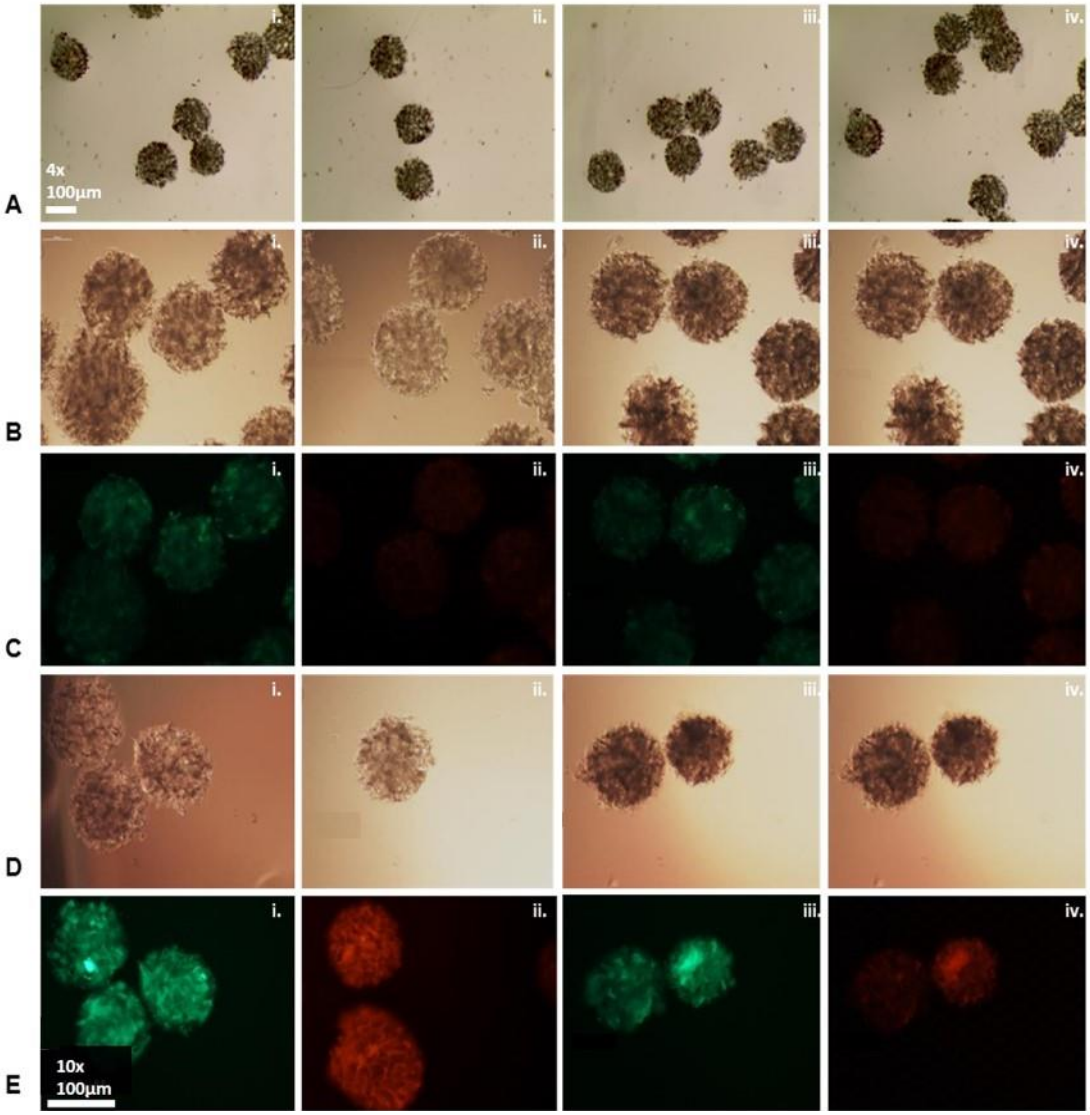

Figure 21: Validation of CYP1A1/A2 and CYP3A4 induction assay on HepaRG cell seeded microcarriers

(A) HepaRG cells seeded onto microcarriers at 100 cells per bead stained with neutral red to visualise viable seeded cells on bead surface (x4 magnification). **(B)** Phase contrast image of uninduced 0.2% DMSO vehicle control treated HepaRG cell seeded onto microcarriers (x10 magnification). **(C)** Corresponding uninduced HepaRG seeded microcarriers treated with 0.2% DMSO vehicle control stained for CYP3A4 (i: green), CYP1A1/A2 (ii: red) and dual CYP3A4 and CYP1A1/A2 (iii and iv: green and red) (x10 magnification). **(D)** Phase contrast image of three days post drug induction HepaRG seeded beads (x10 magnification). **(E)** Corresponding three days post drug induction HepaRG seeded beads stained for CYP3A4 (i: green), CYP1A1/A2 (ii: red) and dual CYP3A4 and CYP1A1/A2 (iii.-iv: green and red) (x10 magnification).

4.3.2 CombiCult® Hepatocyte Differentiation Screen

A four-stage split-pool CombiCult® screen was designed with 10x10x10x20 culture media permutations at each of the four split stages respectively, allowing for a 20,000-multiplexed screen to be carried out. The increased number of media permutations in the final fourth step allows for the testing of an increased number of possible maturation inducing reagents in the most undefined stage of hepatic differentiation. Small bioactive agonists of nuclear hormone receptors as well as CYP450 family members were used in an effort to produce more metabolically active HLCs.

4.3.3 CombiCult® Matrix Design

Hepatocyte basal media (HBM) was formulated as a serum free differentiation media containing of William's E Media, B27, Sodium Pyruvate, NEAA and the antibiotic P/S (see Methods 2.6.2.1). This basal differentiation media was used for the first DE specification stages and in the second stage of hepatic specification. During the process of hepatic progenitor expansion and hepatic maturation 10μM dexamethasone and 0.1μM hydrocortisone were added to the HBM. The differentiation inducing factors at the concentrations stated that were used in the CombiCult® hepatocyte screen is detailed in Table 4-7 (See Methods 2.6.1).

4.3.4 CombiCult® Hepatocyte Split Pooling

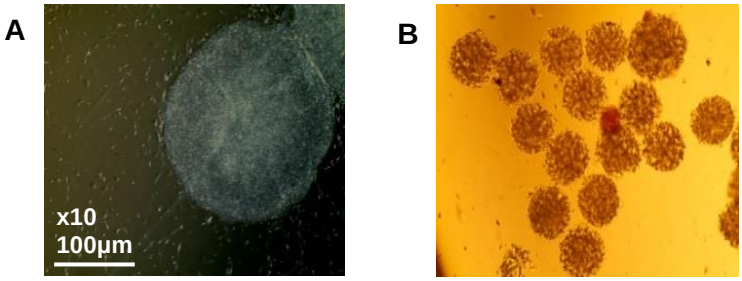

Figure 22: Shef-3 hESC seeding onto microcarrier beads

Representative images of Shef-3 hESCs seeding onto microcarriers **(A)** Shef-3 hESCs grown on MEF feeder layers in monolayer culture followed by manual passaging into small colony pieces and seeding at around 100 cells per microcarrier bead. **(B)** Shef-3 hESCs were subsequently stained with neutral red to visualise viable cells on microcarrier beads. Images were taken at x4 magnification.

Following validation of the CYP1A1/A2 or CYP3A4 end point induction assays on HepaRG seeded microcarriers, Shef-3 cells were grown in monolayer culture on MEF feeder layers (Figure 22A) followed by seeding onto 600,000 microcarriers at 100 cells per bead in small colony pieces (D0) so that each of the 20,000 possible conditions is sampled by at least 30 beads (see Methods 2.6.2.1). MEF feeder cultured Shef-3 cells were used as opposed to feeder-free conditioned cells for consistency with previous hepatic differentiation studies carried out by Dr Jey Jeyakumar of Plasticell Ltd. Viable hESC colony pieces were visualised 24 hours after seeding using neutral red staining (Figure 22B). Shef-3 seeded microcarriers were then pooled together and split through the designed CombiCult® matrix with each media condition spiked with unique fluorescent tag. Three sizes of tag were used for the first three split-pools: small, medium and large, with each size having ten variations for each individual media condition in each stage.

At each split stage, an aliquot of seeded microcarriers was removed from the CombiCult® experiment to assess efficiency of microcarrier tagging (see Methods 2.6.2.2).

Following differentiation in the final split stage, beads were either treated with a combined drug cocktail of 10µM omeprazole, 50µM dexamethasone and 50µM rifampicin to induce CYP1A1/A2 and CYP3A4 or a 0.2% vehicle control for a period of three days as described previously (see Methods 2.6.2.3). Microcarriers were then analysed using the validated CYP1A1/A2 and CYP3A4 ICC assay to assess the presence of HLCs expressing high levels of CYP1A1/A2 and CYP3A4. Stained microcarriers were then sorted using the COPAS large particle sorter for beads possessing HLCs expressing both CYP1A1/A2 and CYP3A4 enzymes (Figure 23). A gated fluorescence threshold was established through analysis of a population of microcarriers representative of all microcarriers across the four stages of differentiation so only the microcarrier beads carrying the most highly expressing HLCs would be selected through COPAS sorting (Figure 24). This was done by collecting a small aliquot of microcarrier beads (termed “all pools”) from all the final twenty pools and analysing the CYP1A1/A2 and CYP3A4 intensity profiles in COPAS. The fluorescent intensity profiles of the pooled microcarriers stained with CYP1A1/A2 and CYP3A4 antibodies, above the background levels of the secondary only antibody controls, served to define the gates for sorting positive microcarrier beads; those carrying HLCs expressing high levels of both CYP1A1/A2 and CYP3A4 from negative ones. Through this method it was seen that distinct populations of microcarrier beads could be separated by their fluorescence intensity profiles (Figure 23).

COPAS sorted 1161 dual-positive microcarriers based on the gating strategy described above, these were then taken forward for FACS deconvolution tag analysis. CYP1A1/A2 and CYP3A4 fluorescence intensity profiles were seen to vary drastically amongst COPAS sorted beads from the twenty final pools owing to varying levels of maturation of the HLCs and the ability of sole and combinations of factors to induce CYP450 family member activity; shifts in CYP1A1/A2 expression were particularly evident amongst microcarriers from different pools.

FACS analysis showed that around 80% of microcarriers were successfully tagged after the first two split pools and displayed defined fluorescent peaks, indicating the presence of only one tag present per split stage and therefore provided the ability to deconvolute the tag cell culture history (Figure 25). Of the 1161 beads sorted by COPAS, complete tagging data was obtained for 512 (40%). These 512 beads were further analysed using Ariadne™ (Figure 25).

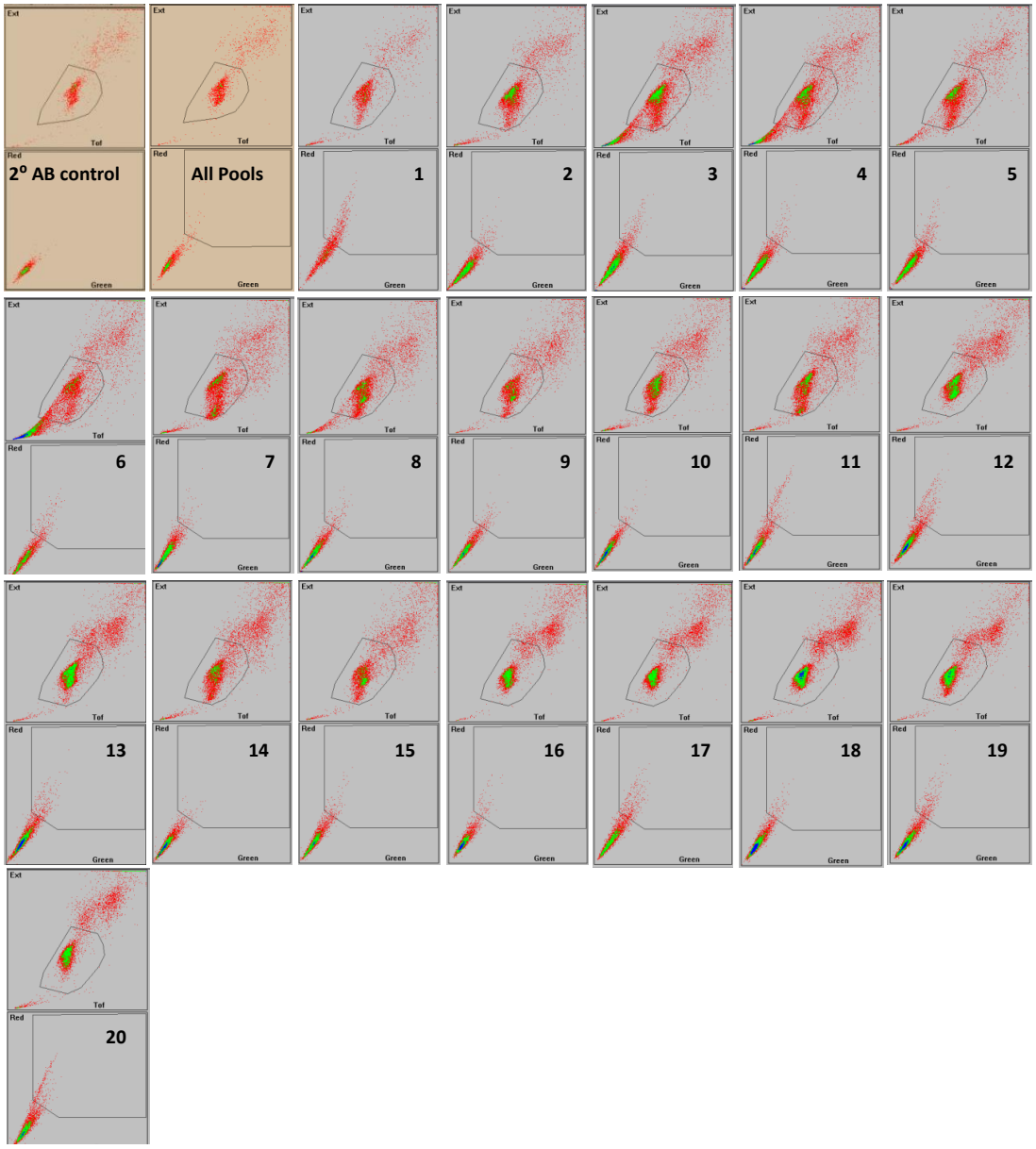

Figure 23: COPAS sorting of beads expressing CYP1A1/A2 and CYP3A4

Final twenty pools (1-20) isolated from the final stage 4 of differentiation. **Top panel**: Scatted profiling for size gating to exclude doublets and microcarrier bead aggregates so only single beads are selected and isolated by COPAS. **Bottom panel:** CYP1A1/A2 (Y axis) and CYP3A4 (X axis) fluorescence intensity profiles of the final 20 culture conditions. Secondary antibody (2º Ab control) only controls were used to exclude any background fluorescence to setup appropriate gates to capture dual-positive beads. An “all pools” sample from all the final 20 differentiation protocols was taken to establish a baseline of fluorescence intensity across all the protocols with which to establish a cut off gate. In this way, only the highest expressing CYP1A1/A2 CYP3A4 microcarriers were selected from the total population.

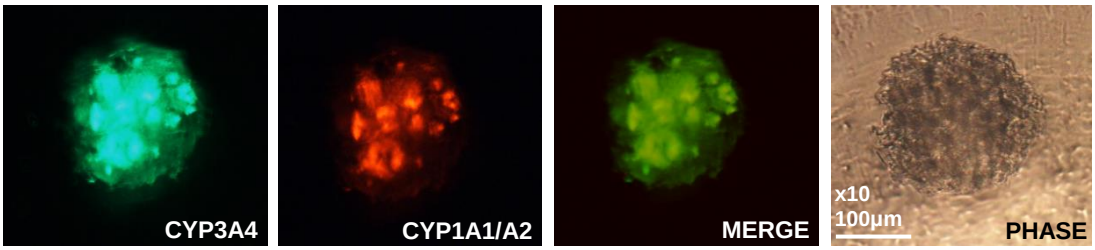

Figure 24: ICC staining for CYP1A1/A2 and CYP3A4 induced HLCs.

Representative images of dual drug induced microcarriers from the final stages of the CombiCult® differentiation screen. Microcarriers were stained for CYP1A1/A2 (Green) and CYP3A4 (Red). Merged overlay images show the dual expression of both CYP1A1/A2 and CYP3A4 in HLCs (Yellow) in differentiated HLCs. A pooled sample from all the final differentiation protocols was taken to establish a gated fluorescence threshold. This was done so only the microcarrier beads carrying the most highly expressing HLCs would be selected through COPAS sorting

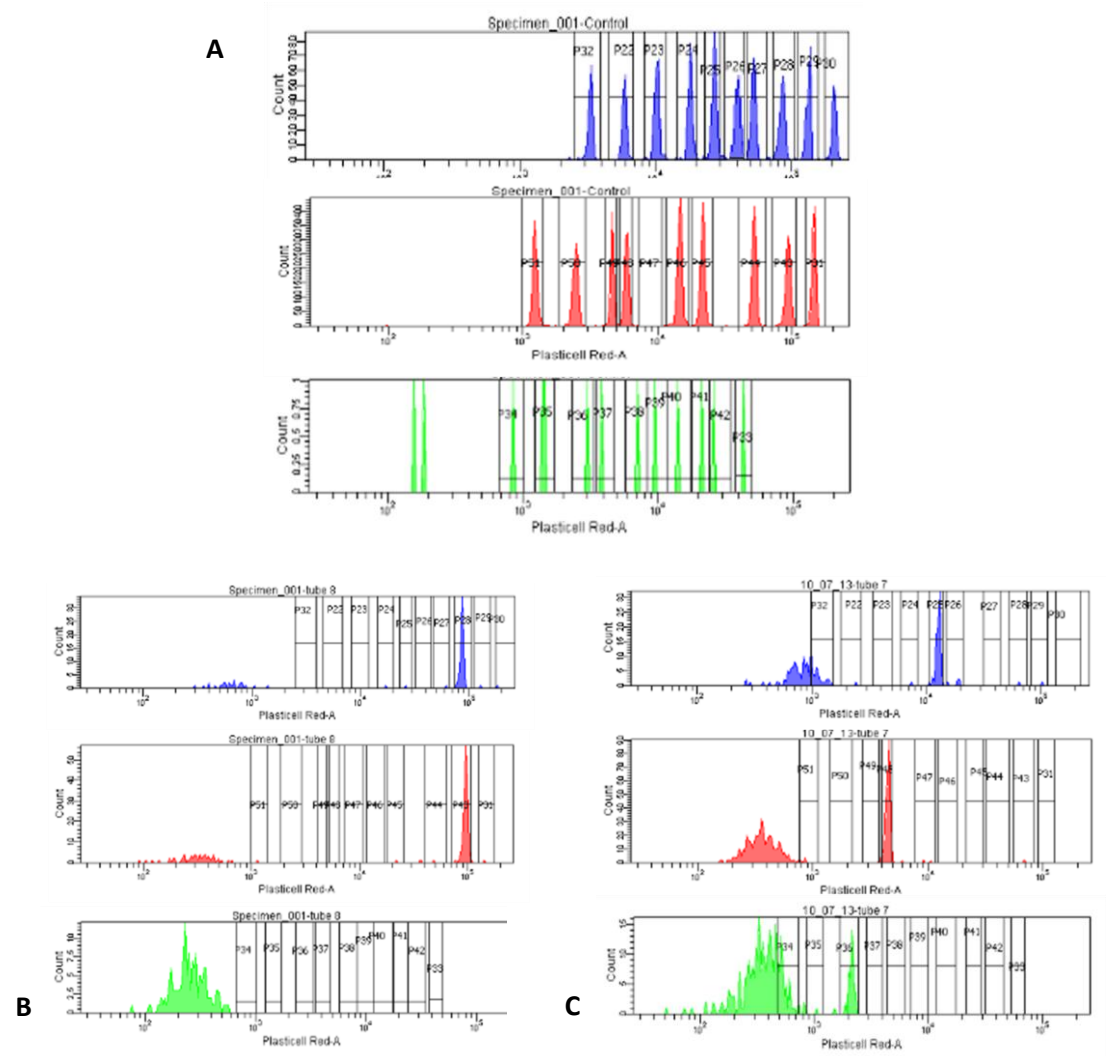

Figure 25: FACS CombiCult® hepatic differentiation screen tag analysis

After the first two split pooling procedures bead aliquots were taken to check for successful tagging. Controls were used consisting of a mixture of all tags to setup voltage gates for small tags (top blue), medium tags (middle red) and small tags (bottom green) used in the different split-pools **(A)**. The ten different variations for each particular sized tag, each emitting at different fluorescence intensity, displaying defined peaks allowing for bead cell culture history to be deconvoluted. **(B)** Example of a microcarrier bead which has successfully been tagged in the first two split stages but has no identifying tag present for the third stage of differentiation. **(C)** Example of a microcarrier which has been tagged successfully in the first three stages of differentiation showing a single defined peak at each stage allowing deconvolution of the complete cell culture history.

4.3.5 Ariadne™ Differentiation Pathway Analysis

CombiCult® Ariadne™ bioinformatics software was used to identify differentiation protocols that most commonly produced dual positive CYP1A1/A2 and CYP3A4 HLCs following dual drug induction. Several strong cell culture linkages were established leading to both whole and partial pathways being identified (Figure 26). Differentiation history analysis resulted in the identification of 23 top differentiation protocols (Table 8). The top 23 protocols were distinguished above the other differentiation protocols in the CombiCult® screen as they were in a distinct group above the highest set gated threshold from the “all pools” baseline. This threshold was chosen as to pick out only the highest expressing CYP1A1/A2 and CYP3A4 microcarriers with which to carry out further investigation. Due to company confidentiality concerning the Ariadne™ software, my FACS tag analysis data was inputted into Ariadne™ by Dr Diana Hernandez of Plasticell Ltd. to produce the differentiation pathway analysis results.

In the first split pool stage, the combination of Activin A, FGF4 and HGF was found to be the most common starting condition for producing HLCs expressing the highest levels of CYP1A1/A2 and CYP3A4. In addition, combinations of Activin A, linoleic acid (LAC18:2) and SR12813 as well as Activin A, hyperforin and linoleic acid were seen to be associated with the most highly expressing levels of CYP1A1/A2 and CYP3A4 as assessed by the ICC readout. Further component analysis was then used to account for the frequency of use of the individual factors in the first stage of the differentiation. This showed that the use of Activin A in the first stage of differentiation was crucial. The majority of beads expressing both CYP1A1/A2 and CYP3A4 enzymes were exposed to Activin A initially to induce DE from pluripotent hESCs.

WNT3A signalling mimicked through the addition of the GSK inhibitor BIO and the CAR agonist CITCO were found to be strongly correlated with the use of Activin A in the preliminary steps. This analysis further indicates that the combination of Activin A, BIO and CITCO was effective in producing HLCs which were dual positive for CYP1A1/A2 and CYP3A4 enzymes.

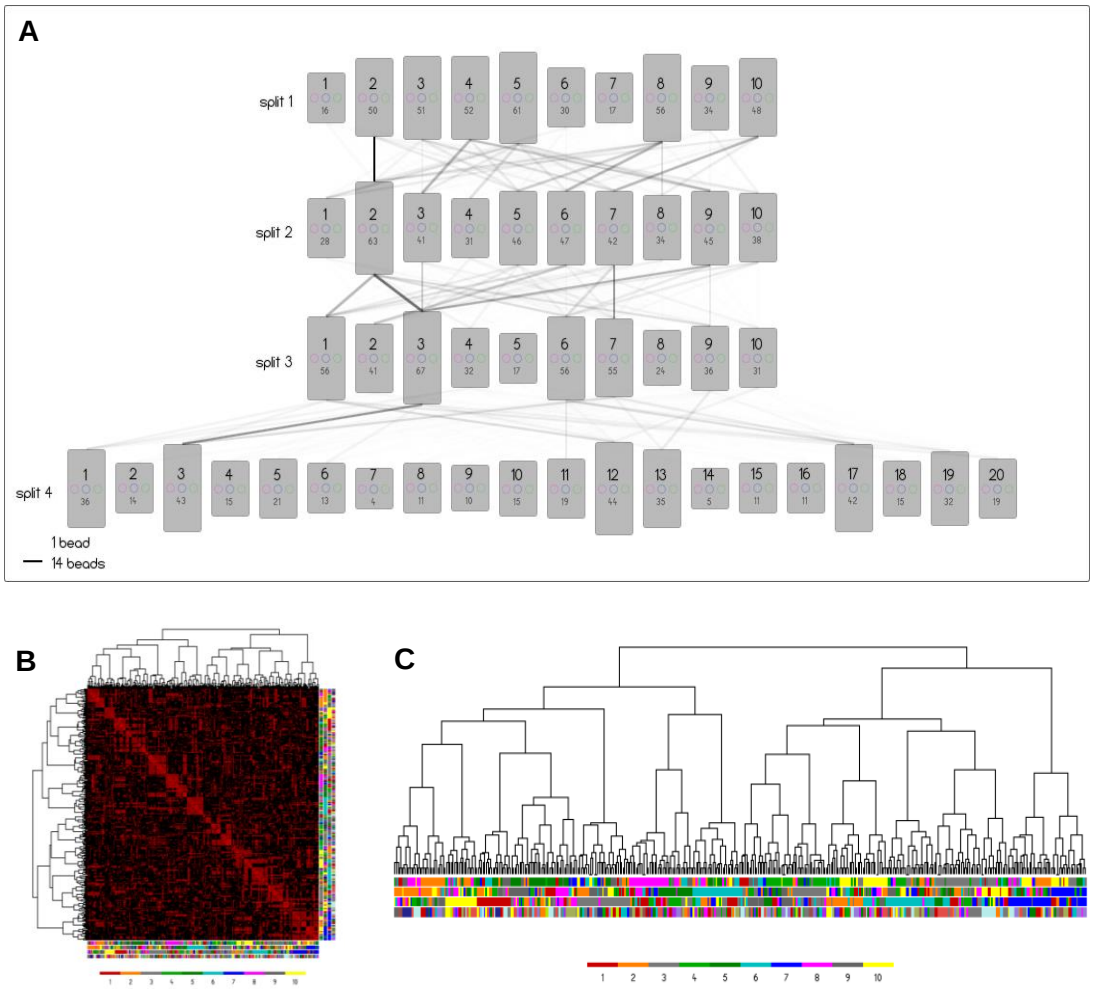

Figure 26: Ariadne™ differentiation pathway cluster analysis

(A) Strongest pathway linkages identified between the four stages of hepatocyte differentiation through tagging analysis. The thickest lines correlate to the strongest significant linkages between beads travelling through conditions in each step resulting in the highest levels of dual CYP1A1/A2 and CYP3A4 activity. **(B)** Heat map and **(C)** dendrogram showing cluster analysis indicating grouping of the most efficient media components between the four stages of differentiation. Due to company confidentiality concerning the Ariadne™ software, my generated FACS tag analysis was inputted into Ariadne™ by Dr Diana Hernandez of Plasticell Ltd. to produce the differentiation pathway analysis results.

An interesting trend was observed in the second split pool phase of differentiation in that SMAD signalling inhibitors were found to be highly associated with producing the most dual-positive CYP1A1/A2 and CYP3A4 HLCs. SB-431542, a TGFβ1/Alk7 inhibitor along with the SMAD3 signal inhibitor SIS3 were found to be present in the majority of top differentiation protocols, indicating that TGFβ signalling inhibition during this stage is important. Growth factors including HGF, GDF-15, WNT5A and VEGF, which are associated with hepatoblast proliferation and expansion upon liver injury *in vivo*, were also found at high frequency. The SR12813, hyperforin and CITCO small molecule agonists of CAR nuclear hormone sensor also featured in the top differentiation protocols along with the potential ligand of HNF4α, linoleic acid.

TGFβ signalling, through the addition of the growth factor TGFα, in contrast was found to be important in the third phase of hepatocyte differentiation; consistent with knowledge that TGFα is upregulated upon liver injury to promote hepatoblast proliferation. HGF and the hormone progesterone also featured highly in the top differentiation protocols during this stage.

The final stages of differentiation the CombiCult® differentiation screen was dominated by the presence of the hormones progesterone and βestradiol as well as the CAR/LXR/PXR nuclear hormone receptor agonists CITCO, SR12813, GW7647, T0901317 and docosahexaenoic acid. The combinations of these factors were found in the majority of top-ranking protocols during the maturation stages of hepatocyte differentiation.

Component analysis allowed for clusters of differentiation inducing factors to be identified in “synthetic pathways”, that is, combining the best media linkages from different stages of the differentiation process. Using this process, it was found that there was a strong linkage between beads passing through condition two in the first stage and condition two in the second stage.

This consisted of hESCs firstly being exposed to Activin A, FGF4 and HGF followed by HGF, 2% DMSO and the TGFβ inhibitor SB-431542. Significant linkages were also found for beads passing firstly through both conditions 8 and 10 in the first split-pool moving to conditions 5 and 7 in the second differentiation step respectively. This corresponded to beads being exposed to Activin A, FGF4 and CITCO followed by WNT5a, 2% DMSO and SB-431542 and secondly beads being exposed to a GSK3β inhibitor (BIO), isoproterenol and HGF followed by GDF-15, SB-431542 and HGF. Between the third and fourth stages of differentiation, there was a strong linkage between condition 3 in third differentiation stage and condition 3 in fourth stage. This differentiation history corresponded to beads being exposed to HGF, OSM and TGFα followed by progesterone, OSM and α βestradiol.

PROTOCOL	STAGE 1	STAGE 2	STAGE 3	STAGE 4
1	Activin A	HGF	HGF	HGF
	FGF4	2% DMSO	OSM	Insulin
	HGF	SB-431542	TGFα	OSM
2	Activin A	HGF	HGF	Insulin
	FGF4	2% DMSO	OSM	#3722
	HGF	SB-431542	TGFα	GH
3	Activin A	HGF	HGF	Progesterone
	FGF4	2% DMSO	OSM	SR12813
	HGF	SB-431542	TGFα	CITCO
4	Activin A	HGF	HGF	#8379
	FGF4	2% DMSO	OSM	#2028
	HGF	SB-431542	TGFα	#5722
5	Activin A	HGF	TGFα	Insulin
	FGF4	2% DMSO	BMP7	#3722
	HGF	SB-431542	HGF	GH
6	Activin A	HGF	TGFα	HGF
	FGF4	2% DMSO	BMP7	Wnt5A
	HGF	SB-431542	HGF	#2028
7	Activin A	HGF	HGF	Progesterone
	Hyperforin	2% DMSO	RA	OSM
	Linoleic Acid	SB-431542	GH	βestradiol
8	Activin A	SIS3	HGF	Progesterone
	Linoleic Acid	GDF-15	OSM	OSM
	SR12813	C14-AS	TGFα	βestradiol
9	Activin A	SIS3	HGF	Progesterone
	Hyperforin	GDF-15	OSM	OSM
	Linoleic Acid	C14-AS	TGFα	βestradiol

10	Activin A	FGF4	Progesterone	Progesterone
	Hyperforin	GDF-15	IL6	#5722
	Linoleic Acid	C14-AS	TGFα	CITCO
11	Activin A	Wnt5A	Progesterone	Progesterone
	FGF4	2% DMSO	IL6	#5722
	CITCO	SB-431542	TGFα	CITCO
12	BIO	GDF-15	Progesterone	Progesterone
	Isoproterenol	SB-431542	IL6	OSM
	HGF	HGF	TGFα	βestradiol
13	Activin A	HGF	HGF	Progesterone
	Linoleic Acid	FGF4	OSM	OSM
	SR12813	SIS3	TGFα	βestradiol
14	Activin A	FGF4	HGF	HGF
	Hyperforin	GDF-15	RA	Insulin
	Linoleic Acid	C14-AS	GH	OSM
15	Activin A	HGF	HGF	Progesterone
	Hyperforin	FGF4	RA	SR12813
	Linoleic Acid	SIS3	GH	CITCO
16	Activin A	HGF	HGF	HGF
	FGF4	VEGF	RA	Insulin
	HGF	Wnt5A	GH	OSM
17	Activin A	2% DMSO	Glucagon	Wnt5A
	Linoleic Acid	SB-431542	HGF	Glucagon
	SR12813	HGF	Progesterone	Progesterone
18	Activin A	HGF	Glucagon	Linoleic Acid
	Hyperforin	VEGF	HGF	SR12813
	Linoleic Acid	Wnt5A	Progesterone	CITCO

19	Activin A	HGF	Progesterone	HGF
	BIO	VEGF	IL6	#2028
	CITCO	Wnt5A	TGFα	OSM
20	Activin A	HGF	Progesterone	Progesterone
	FGF4	VEGF	IL6	#5722
	HGF	Wnt5A	TGFα	CITCO
21	Activin A	FGF4	Progesterone	#8379
	Hyperforin	GDF-15	IL6	#2028
	Linoleic Acid	C14-AS	TGFα	#5722
22	Activin A	Wnt5A	TGFα	HGF
	FGF4	2% DMSO	BMP7	Insulin
	CITCO	SB-431542	HGF	OSM
23	Activin A	GDF-15	HGF	Progesterone
	BIO	SB-431542	RA	CITCO
	Isoproterenol	HGF	GH	βestradiol

Table 8: Top ranking 23 hepatocyte differentiation protocols

The 23-top ranking hepatic differentiation protocols identified through Plasticell's Ariadne™ software. The best *in vitro* hepatocyte differentiation protocols were based on the strongest pathway linkages between the four stages which produced the highest CYP1A1/A2 and CYP3A4 expressing HLCs. Three factor conditions highlighted in red at each stage of the differentiation process identify the most commonly present combinations of growth factors and small molecules across the final 23 hepatocyte differentiation protocols.

4.4 Discussion

An *in vitro* end-point assay previously designed by Dr Jey Jeyakumar to detect levels of hepatic maturation was successful in the isolation of high CYP1A1/A2 and CYP3A4 expressing HLCs in my CombiCult® hepatic screen which utilised novel differentiation inducing factors. Through CombiCult® screening of 20,000 culture media permutations, 23 new differentiation protocols were identified to be taken further for validation in monolayer culture. These protocols featured novel bioactive molecules that have not previously been applied to *in vitro* hepatic differentiation protocols.

These top protocols resulted from 1,161 dual-positive HLCs containing microcarriers expressing high levels of both CYP1A1/A2 and CYP3A4 by ICC staining. Of these high CYP1A1/A2 and CYP3A4 expressing HLC microcarrier beads, 512 could be successfully deconvoluted through FACS tagging analysis and Plasticell's proprietary Ariadne™ bioinformatics software. Through this analysis several candidate factors have been identified as being important at crucial stages of hepatic differentiation. Novel and previously identified stimulation/inhibition of signalling pathways through the addition of small molecules were found to be involved in the most effective differentiation protocols. Small bioactive molecules were trialled with a view to replace currently used growth factors wherever possible to decrease costs and improve reproducibility; this is also important in the future industrial application to differentiate pluripotent stem cells to hepatocytes. In addition, it was found that some of the observations concerning stimulation/inhibition of signalling pathways were consistent with known and previously published *in vivo* signalling mechanisms in mammalian development, but which are not currently being applied to *in vitro* differentiation strategies; future validation is needed to identify the best protocols.

It is known that TGF-β signalling is critical for the establishment of DE both *in vitro* and *in vivo*. High levels of Nodal signalling specify DE at the anterior of the primitive streak *in vivo* [246] [87]. The related TGFβ family member Activin A is routinely used *in vitro* as it signals through similar pathways to Nodal [87] [110] [111] [84] [106] [83]. As expected, Activin A was present in the first stage of all the top-ranking differentiation protocols, commonly in conjunction with WNT/βcatenin signalling in the form of GSK-3β inhibitors. GSK3β inhibitors including BIO, 1M and CHIR99021 have been used previously in combination with Activin A to differentiate pluripotent stem cells to DE [121] [99] [83] [263]. This demonstrates that the specification of pluripotent cells firstly to DE following *in vivo* development is crucial to producing HLCs with high metabolic activity. Following component analysis, it was found that the initial exposure of hESCs to Activin A in the first differentiation stage of the CombiCult® screen was required to produce highly expressing duel positive HLCs.

During the first stage of differentiation, combinations of small molecules and NHR agonists were trialled to ascertain if the classical differentiation process from hESCs to specify DE and subsequently to the hepatic lineage could be enhanced. One factor identified through media component analysis as being important in the early stages of differentiation was hyperforin. It is known that hyperforin is a CYP450 family agonist, specifically CYP3A4 and CYP2C9 [175], as well as being involved in the binding and activation of the nuclear hormone sensor PXR which in turn regulates CYP450 member activity [264]. Its potential role in the maturation and upregulation of CYP450 enzymes is therefore of great interest in producing more metabolically functional hepatocytes *in vitro*.

However, the trial of these novel factors which are not typically utilised in the early stages of differentiation in culture conditions that lacked Activin A were not involved in the production of high expressing CYP1A1/A2 and CYP3A4 HLCs following the four-stage differentiation process. This finding highlights the need to firstly specify DE as opposed to circumventing the classical four stages of hepatic differentiation.

In contrast to the key role played by TGFβ signalling in DE specification, during early hepatic specification stages, TGFβ signalling has been found to be deleterious to hepatocyte proliferation and acts to promote fibrosis upon liver injury *in vivo* [265] [266] [267] a trend also observed in the CombiCult® screen. Component analysis of the most common differentiation pathways revealed the presence of the TGFβ1/Alk7 inhibitor SB431542 along with the SMAD3 signal inhibitor SIS3 as being present at high frequencies in the second phase of differentiation. This temporal change in TGFβ signalling levels could be important for the efficient differentiation of pluripotent stem cells to hepatocytes and has not previously been addressed through *in vitro* differentiation protocols.

The CombiCult® platform allows the identification of critical factors involved in the manipulation of key signalling pathways during the process of obtaining differentiated cell types from pluripotent stem cells. Previous studies into differentiated cell types of interest have relied on the trial and error of growth factors resulting in increased time and cost in the advancement of understanding in the underlying signalling mechanisms. The CombiCult® platform allows for the incorporation of small molecule inhibitors/agonists with a view to replace previously used growth factors to increase reproducibility and reduce costs.

Previous research into the derivation of efficient populations of DE cells with which to differentiate mature hepatocytes has been hampered with optimisation of cell differentiation protocols, which could have been more efficiently determined using the CombiCult® platform. Progress has been made in growth factor derived protocols which are increasingly moving towards the replacement with small bioactive molecules [234] [235] [236]. Previously published growth factors including HGF, FGF4, OSM and IL6 were utilised in the CombiCult® hepatocyte screen and found to be present in top differentiation protocols [110] [106] [107] [136] [99]. In addition to these growth factors GDF-15, WNT5A, BMP7 and VEGF which are associated with hepatoblast proliferation and expansion upon liver injury *in vivo* were found to be present at high frequency in the top differentiation protocols identified through CombiCult®; demonstrating the power of the platform to augment current knowledge and advance understanding of cellular differentiation. The translation of *in vivo* knowledge to the *in vitro* differentiation setting has therefore been shown to be an important avenue of investigation.

In conclusion, analysis of the CombiCult® hepatocyte differentiation screen resulted in the isolation of 23 top ranking protocols after establishing a threshold to select only the most highly expressing dual positive CYP1A1/A2 and CYP3A4 HLCs which are now in the process of being further validated. However, the ICC assay is purely a qualitative means of assessing levels of CYP450 family activity and quantitative means need to be employed alongside ICC readout assays to get an accurate readout of hepatocyte maturity which will be addressed through using p450Glo (CYP3A4) and EROD (CYP1A1/A2) assays.

Chapter 5: CombiCult® Monolayer Validation

5.1 Introduction

Following the completion of the four-stage CombiCult® hepatocyte screen the top 23 differentiation pathways were taken forward to be validated in 2D monolayer culture. Combinations of small bioactive inhibitors and agonists were assessed for their ability to induce hepatocyte differentiation and promote maturation over the four-stages of differentiation. The transition from the 3D bead culture system used in CombiCult® platform through to 2D monolayer culture was investigated to identify potential challenges involved in the adaptation of cell culture systems including cell seeding, passaging of differentiated cells and optimal concentrations of differentiation inducing factors. Initial seeding density was investigated as previous studies has shown a difference in levels of DE markers present following a differentiation time course from pluripotent hESCs [268] [269]. As many of the small bioactive molecules and growth factors have not previously been applied in the context of pluripotent stem cell differentiation to hepatocytes, it is important to trial reagents for adverse effects that could be detrimental to efficient differentiation. It is also important to assess whether the top protocols identified through the CombiCult® screen also differentiate to produce the most efficient HLCs in 2D monolayer culture; a system which lacks some of the cell-cell interactions of 3D culture systems [270].

Imaging analysis was carried out to assess changes in the top 23 protocols as differentiation proceeded with which to identify transition points along the four-stage process. As a measure of the levels of maturity in derived HLCs produced from the top 23 differentiation protocols, ICC staining for CYP1A1, CYP1A2 and CYP3A4 was used as well as quantitative analysis.

Increases in levels of CYP450 family members upon drug induction will give a better indication of functional HLC activity and give a better comparison to the current best hepatocyte models. HepaRG cells have been shown to possess the ability to be induced upon the addition of inducing drugs and the levels of CYP450 family upregulation in 2D monolayer differentiated HLCs will be compared [129] [124] [129].

5.2 Aims:

- Transition the top hepatic differentiation protocols from CombiCult® bead-based platform to 2D monolayer culture.
- Optimise *in vitro* differentiation procedure over the 28-day time course.
- Further assess quantitative levels of hepatic maturity through CYP450 family member activity and hepatic marker expression in differentiated HLCs.

5.3 Results

5.3.1 CombiCult® 2D Monolayer Validation

Shef-3 hESC Seeding (Day 0)

To be able to more accurately measure initial cell seeding density with which to assess the top differentiation protocols, feeder-free cultures of Shef-3 were used as opposed to seeding colony pieces from MEF feeder-conditioned cultures. Feeder free growth conditioned Shef-3 hESCs were cultured on fibronectin coated tissue culture plates in mTeSR pluripotency maintaining culture media. Shef-3 hESCs were subsequently dissociated with Accutase® and seeded in mTeSR at a density of 80,000 cells per well on 24 well plates which were pre-coated with collagen I (D0) (Figure 27). The following day, the Shef-3 hESCs were washed three times with hepatocyte basal media (HBM) (see Methods 2.6.1) before being subjected to the first stage of the differentiation process. Differentiation protocols consisted of HBM supplemented with combinations of three growth factors or small molecules identified through the CombiCult® hepatocyte differentiation screen.

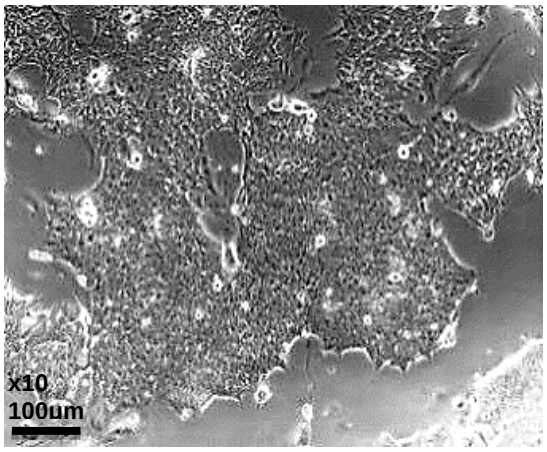

Figure 27: Monolayer differentiation Shef-3 hESC seeding (D1)

Feeder free conditioned Shef-3 hESCs were grown in mTeSR on fibronectin coated dishes and then dissociated with Accutase®. Cells were then counted using a haemocytometer and seeded at a density of 80,000 cells per well of a 24 well collagen I coated plates (D0).

Differentiation Stage 1 (Day 1)

Following washing Shef-3 hESCs with HBM differentiation media to remove traces of pluripotency maintaining mTeSR media, cells were moved into stage 1 of differentiation (D1). Stage 1 largely consisted of the addition of Activin A in combination with other endoderm inducing factors and small molecule agonists of the canonical WNT pathway including BIO which were identified from the CombiCult® hepatocyte screen (Table 8). Small molecule agonists of NHRs were trialled in an attempt to circumvent the classical four-stage differentiation process from pluripotent stem cells to hepatocytes. This was done to more quickly and efficiently generate hepatocytes *in vitro*. Linoleic acid was also included in the first stage of differentiation because of its hypothesised role as a ligand for HNF4α and the high frequency of differentiation protocols containing linoleic acid exhibiting the highest levels of CYP1A1/A2 and CYP3A4 activity.

Exposure to stage 1 differentiation media caused a change in cell morphology across all protocols exhibiting a loss of distinctive tightly packed, rounded hESC colonies with defined edges to cells with a flattened morphology. After five days in the first stage of differentiation it was found that there were ten protocols which had produced viable cells which then proliferated to confluency (Figure 28). These protocols were numbers 1, 2, 3, 4, 5, 6, 7, 11, 16, 20 and 22. It was found that Shef-3 hESCs exposed to protocols containing linoleic acid, did not survive past two days in culture. It was concluded that the type of unconjugated linoleic acid used (Sigma, L1376-10MG) was not suitable to be used in monolayer experiments due to high cell toxicity. This was surprising as the same unconjugated linoleic acid was used in the CombiCult® hepatocyte screen at the same concentration and was involved in producing some of the highest expressing HLCs showing variations between 2D and 3D culture systems. A titration of linoleic acid was conducted to identify a concentration that was compatible with maintaining cell viability. However, it was found to be highly toxic even at concentrations that were twenty-fold decreased than those used in the 3D microcarrier-based CombiCult® hepatocyte differentiation screen.

Protocols consisting mainly of growth factors without the addition of small molecules in the first stage of differentiation were seen to produce the most viable differentiated cells. The combination of Activin A, HGF and FGF4 was seen to be the most effective condition at this stage as the majority of surviving protocols (six out of ten) were produced with this media component combination (Figure 28).

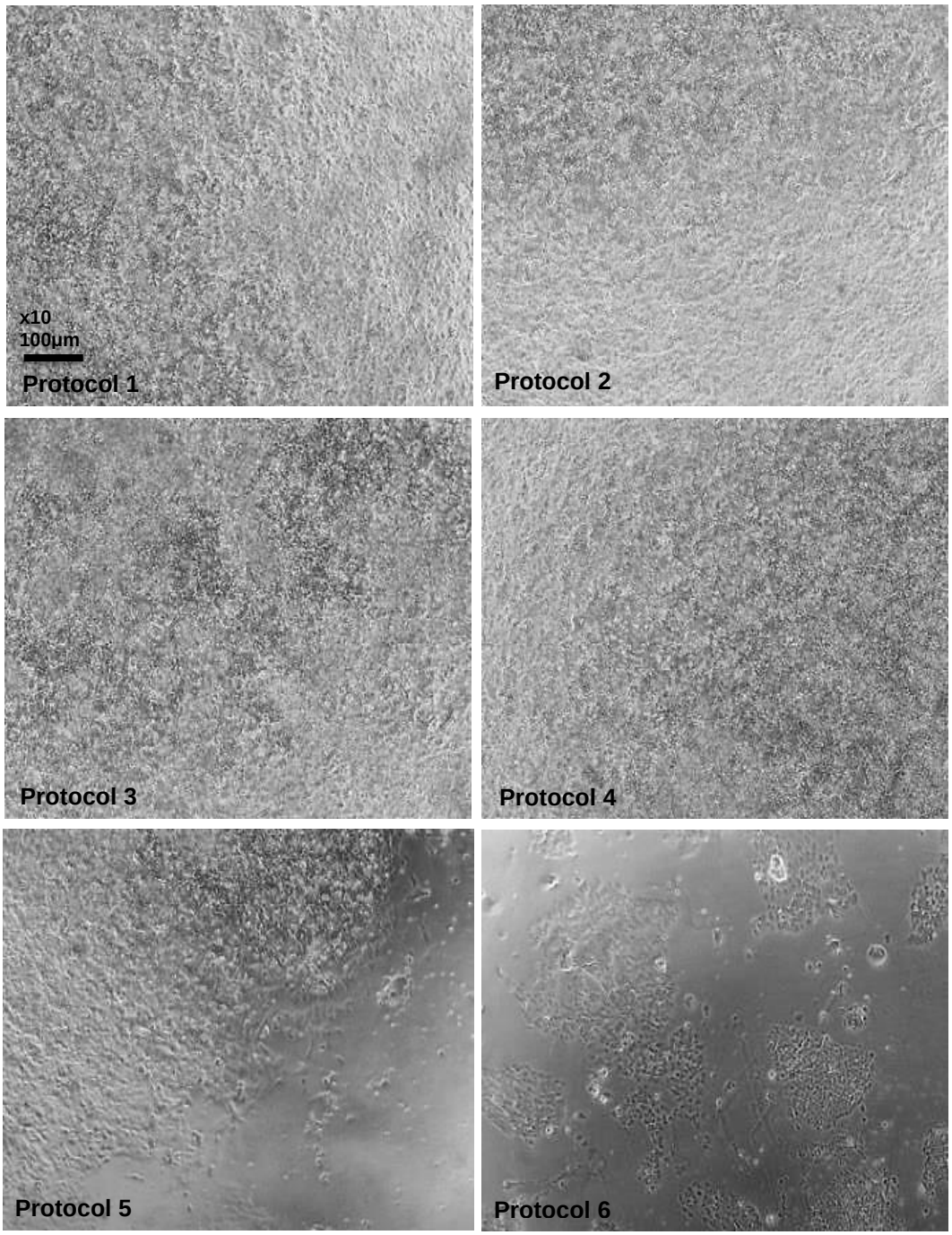
x10
100µm
Protocol 1
Protocol 2
Protocol 3
Protocol 4
Protocol 5
Protocol 6

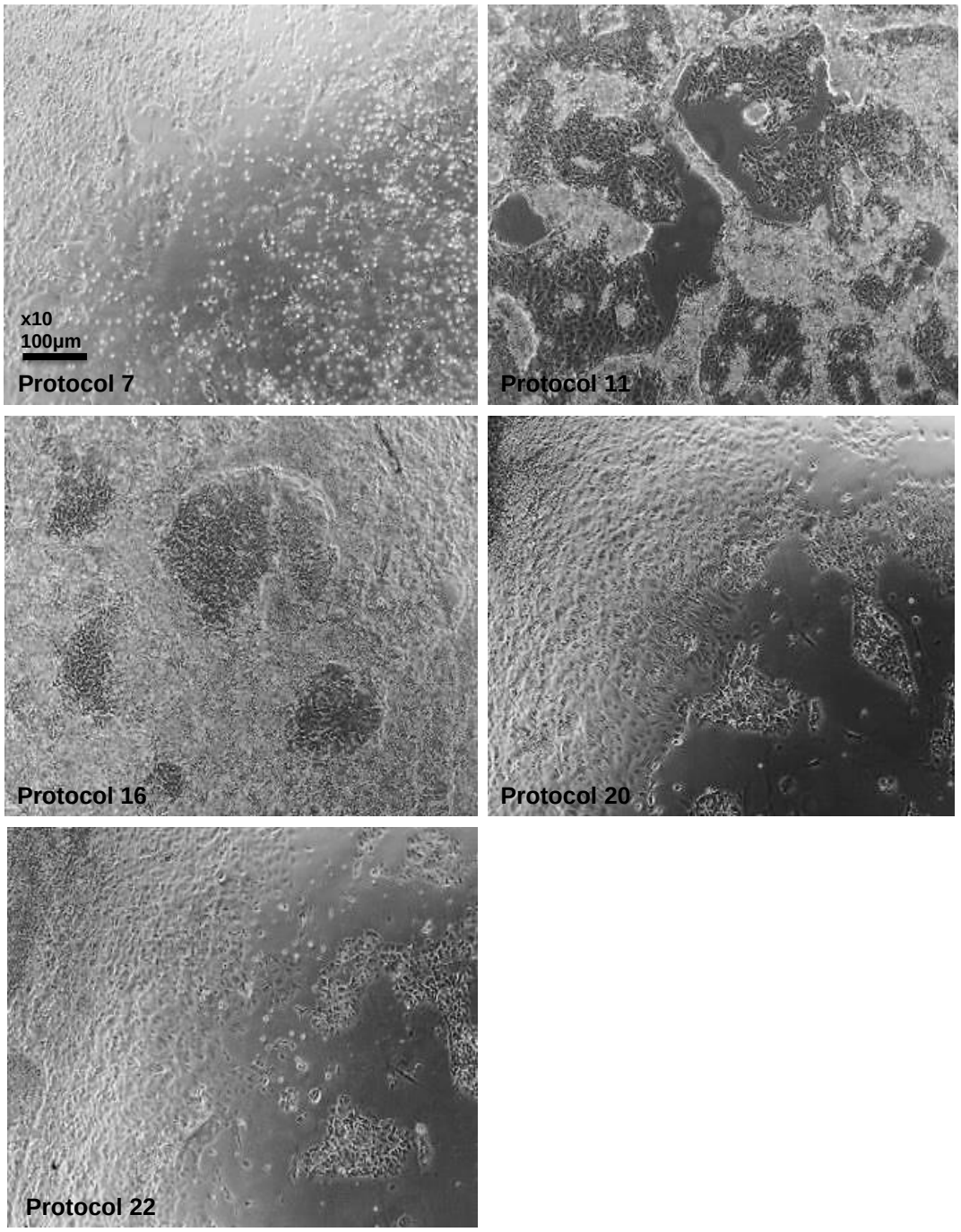

Figure 28: Monolayer Differentiation Stage 1: Day 5

Cell culture images of the remaining 11 differentiation protocols at day 5 in stage 1 conditions (x10 magnification). Exposure to stage 1 differentiation media caused a change in cell morphology across all protocols exhibiting a loss of distinctive tightly packed, rounded hESC colonies with defined edges to cells with a flattened morphology.

Differentiation Stage 2 (Day 6)

Cells exposed to protocols 1, 2, 3, 4, 5, 6, 11, 16, 20 and 22 reached 80-100% confluency after five days of differentiation in stage 1. At the end of stage 1, cells were dissociated to a single cell suspension using Accutase dissociation enzyme and replated on new collagen I coated wells at a 1:3 split ratio. Differentiation media was then changed to that of stage 2 which is classically associated with the expansion of DE. It was found that very low numbers of differentiated cells attached following replating suggesting that splitting cells at this stage or replating straight into stage 2 media is deleterious to cell survival (Figure 29). A better alternative for future experiments would be to split cells later into the differentiation process or to split cells into stage 1 differentiation media and change to stage 2 media the following day.

During stage 2 of differentiation it was found that the cells in protocols 1, 2, 3, 4, 5, 6, and 22 attached following replating and subsequently proliferated more readily than cells undergoing protocols 11, 16 and 20. These protocols contained HGF, 2% DMSO and SB-431542 (Alk4/5/7 inhibitor). Protocols 1-6 and 22 produced differentiated cell types that morphologically resembled endodermal precursors exhibiting a “pebble-like” morphology.

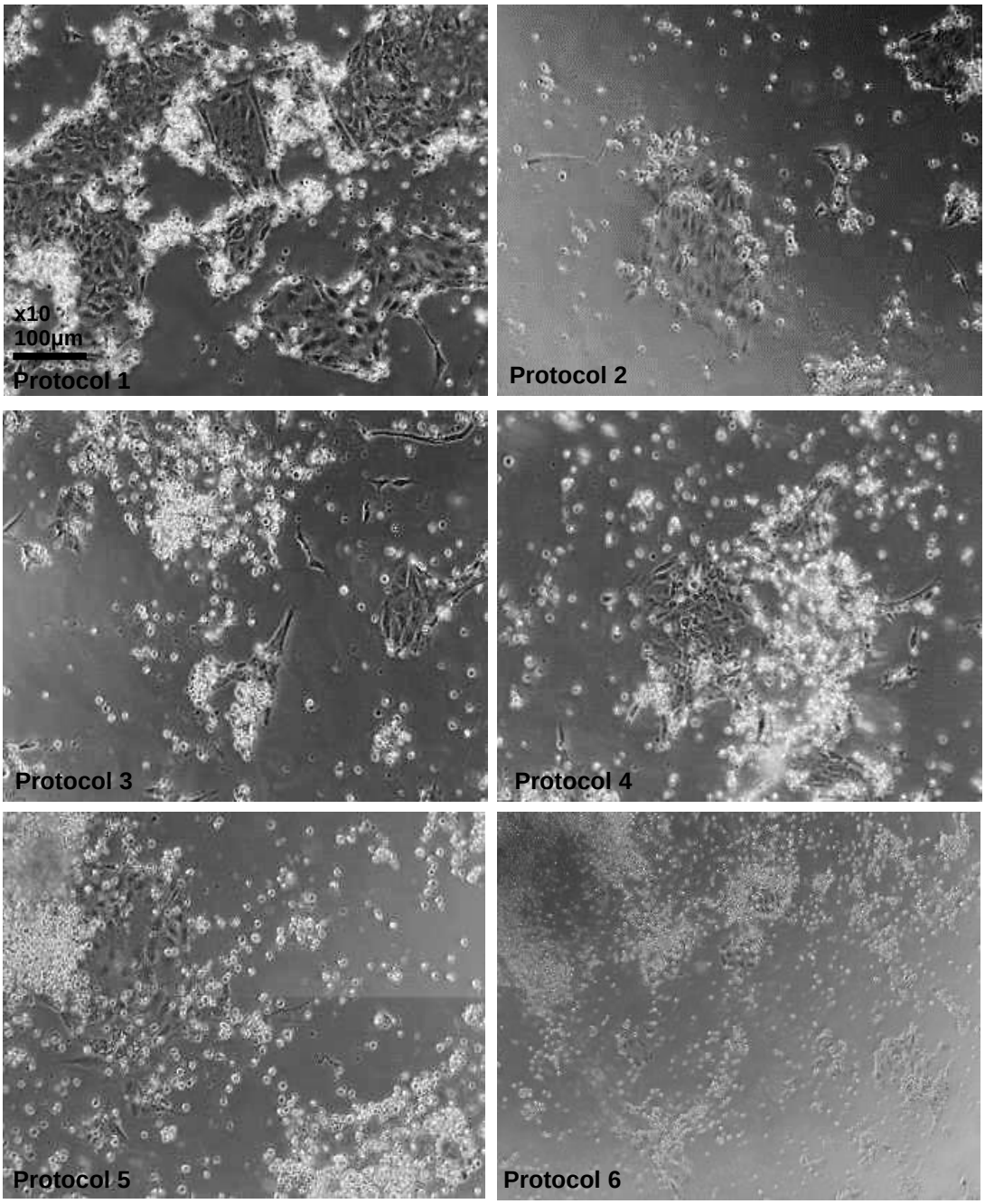
x10
100µm
Protocol 1
Protocol 2
Protocol 3
Protocol 4
Protocol 5
Protocol 6

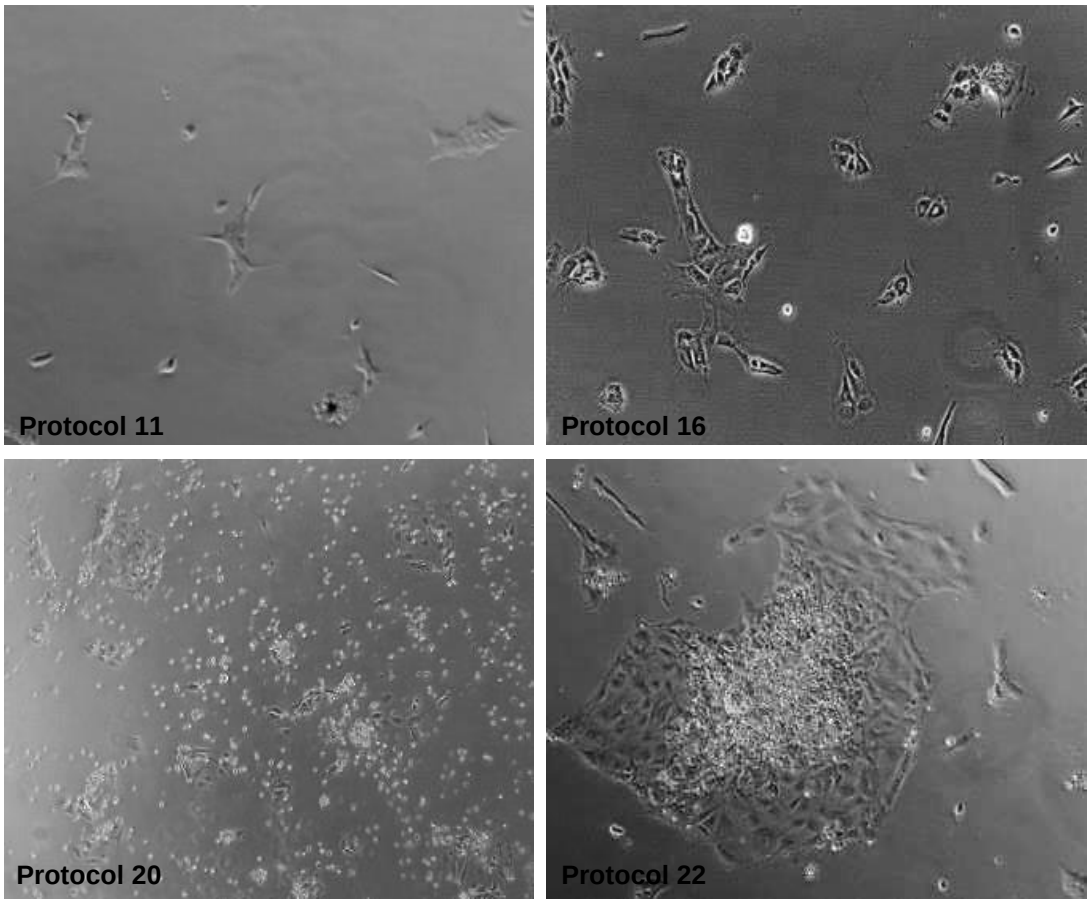

Figure 29: Monolayer Differentiation stage 2: day 6

Cell culture images of the remaining 10 differentiation protocols at day 6 in stage 2 conditions (x10 magnification). Cell cultures exposed to protocols 1, 2, 3, 4, 5, 6, 11, 16, 20 and 22 reached 80-100% confluency after five days of differentiation and were subsequently passaged into stage 2 differentiation medias. Low levels of cell attachment were achieved following passaging of cells.

Differentiation Stage 2 (Day 9)

Attached cells continued to proliferate and It was also seen that cell morphology was consistent and homogenous between replicate wells of the different differentiation protocols (Figure 30). Protocols 1-6, 16, 20 and 22 which survived the replating expanded under media conditions containing HGF, 2% DMSO and SB-431542. Protocol 11 consisting of WNT5A, 2% DMSO and SB-431542 showed a rapid decline in cell number at this point and only small, sparse populations of cells remained. Protocols 16 and 20 containing the growth factors HGF, VEGF and WNT5A produced sparse clusters of differentiated cells which expanded at a slower rate to that of cells produced from protocols 1-6.

As there were low levels of differentiated cells that attached following passaging the confluent cells at the end of the first stage of differentiation, it was decided to continue expanding the cell populations across the remaining protocols at the beginning of the second stage of differentiation. This was undertaken to obtain a usable number of differentiated cells with which to progress to stage 3 as it has been observed that proliferation rates decrease towards the end of *in vitro* hepatocyte differentiation protocols.

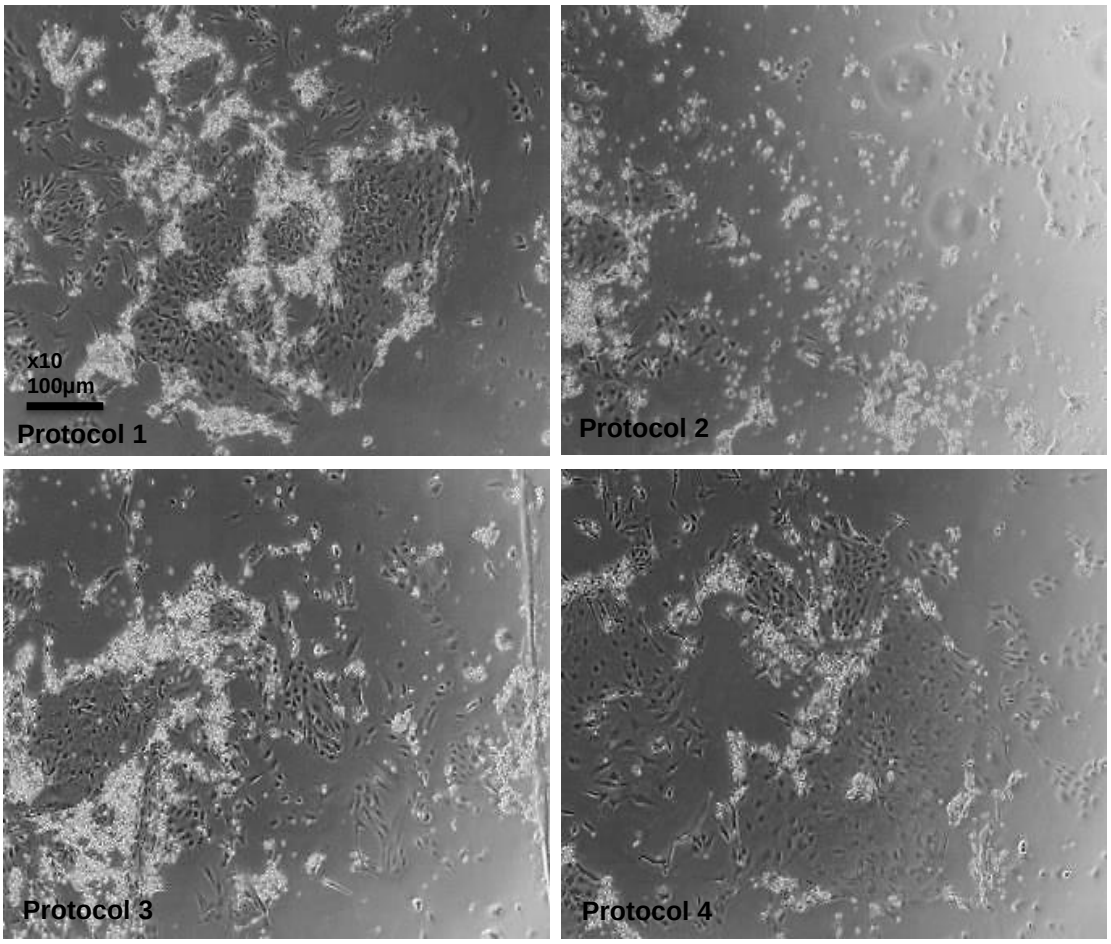
x10
100µm
Protocol 1
Protocol 2
Protocol 3
Protocol 4

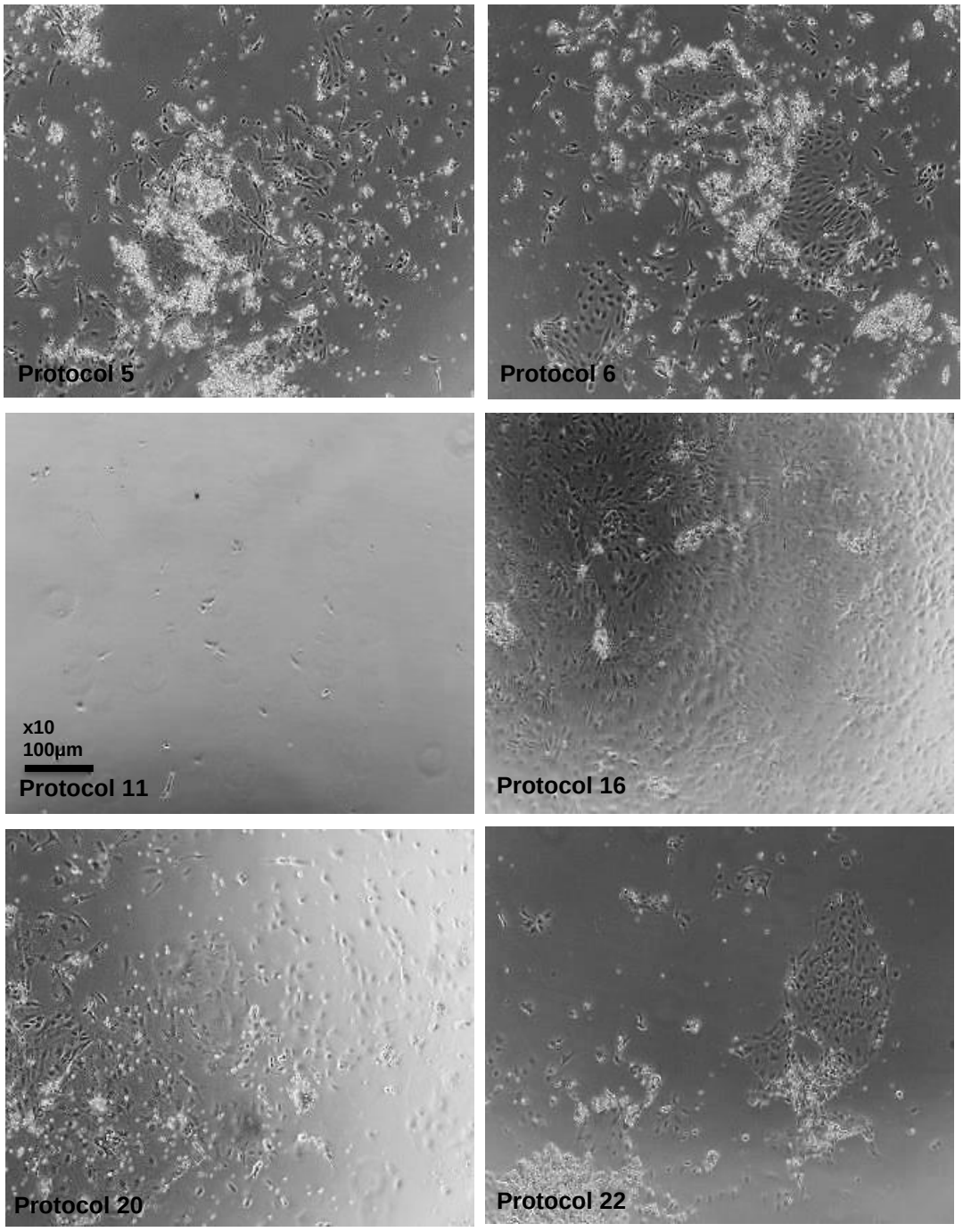

Figure 30: Monolayer differentiation stage 2: day 9

Cell culture images of the remaining 10 differentiation protocols at day 9 in stage 2 conditions (x10 magnification). Following passaging at the start of stage 2 of differentiation, attached cells continued to proliferate and It was also seen that cell morphology was consistent and homogenous between differentiation protocols.

Differentiation Stage 2 (Day 11)

Cells continued to proliferate in stage 2 differentiation media maintaining an endodermal-like morphology (Figure 31). Cell number continued to decline rapidly in protocol 11 and this was also accompanied by a sharp decrease in cells numbers in protocol 16. This represented cells which were exposed to 2% DMSO, SB-431542 and WNT5A in protocol 11 and VEGF, HGF and WNT5A in protocol 16. Protocols 1-6, 20 and 22 continued to proliferate with uniform cell morphology that was consistent between replicate wells of each protocol.

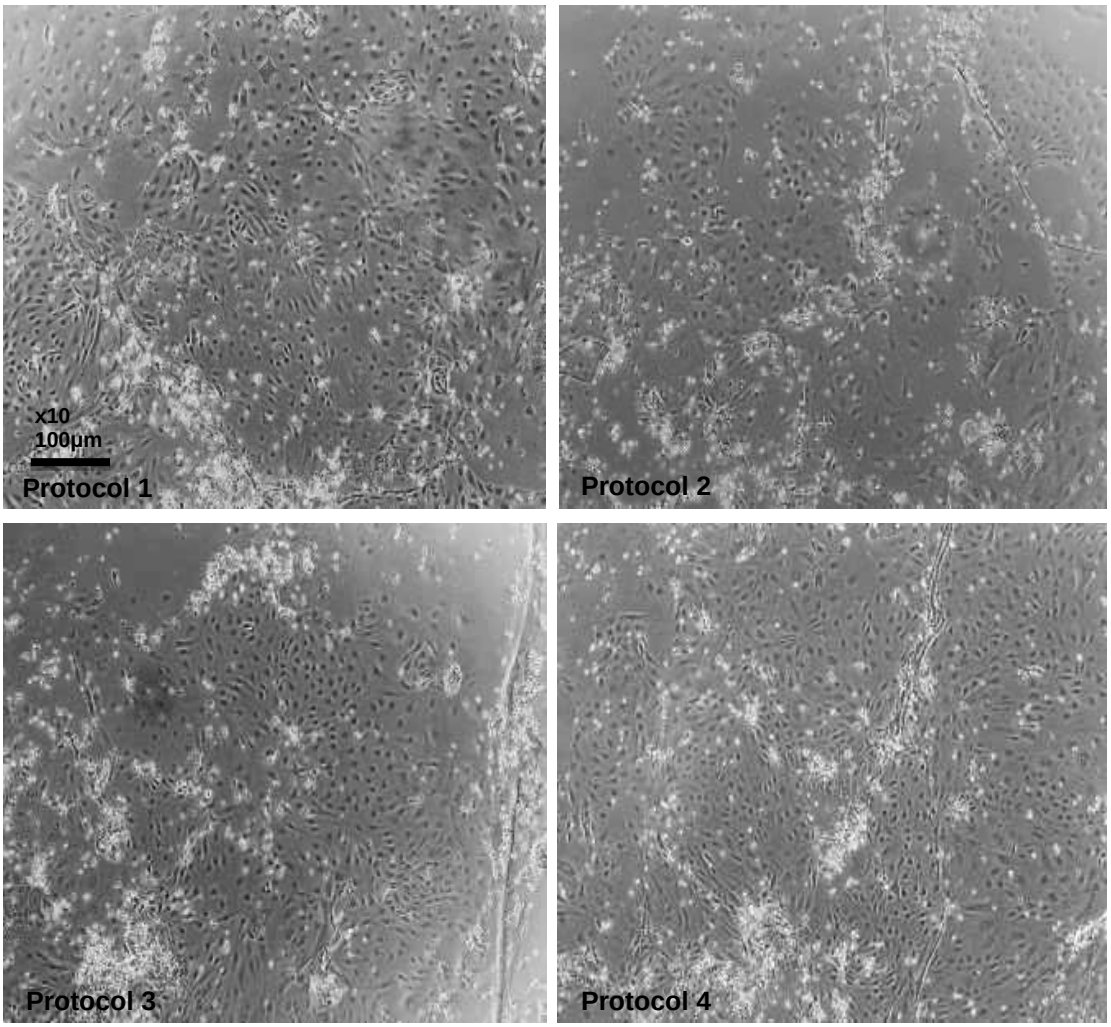

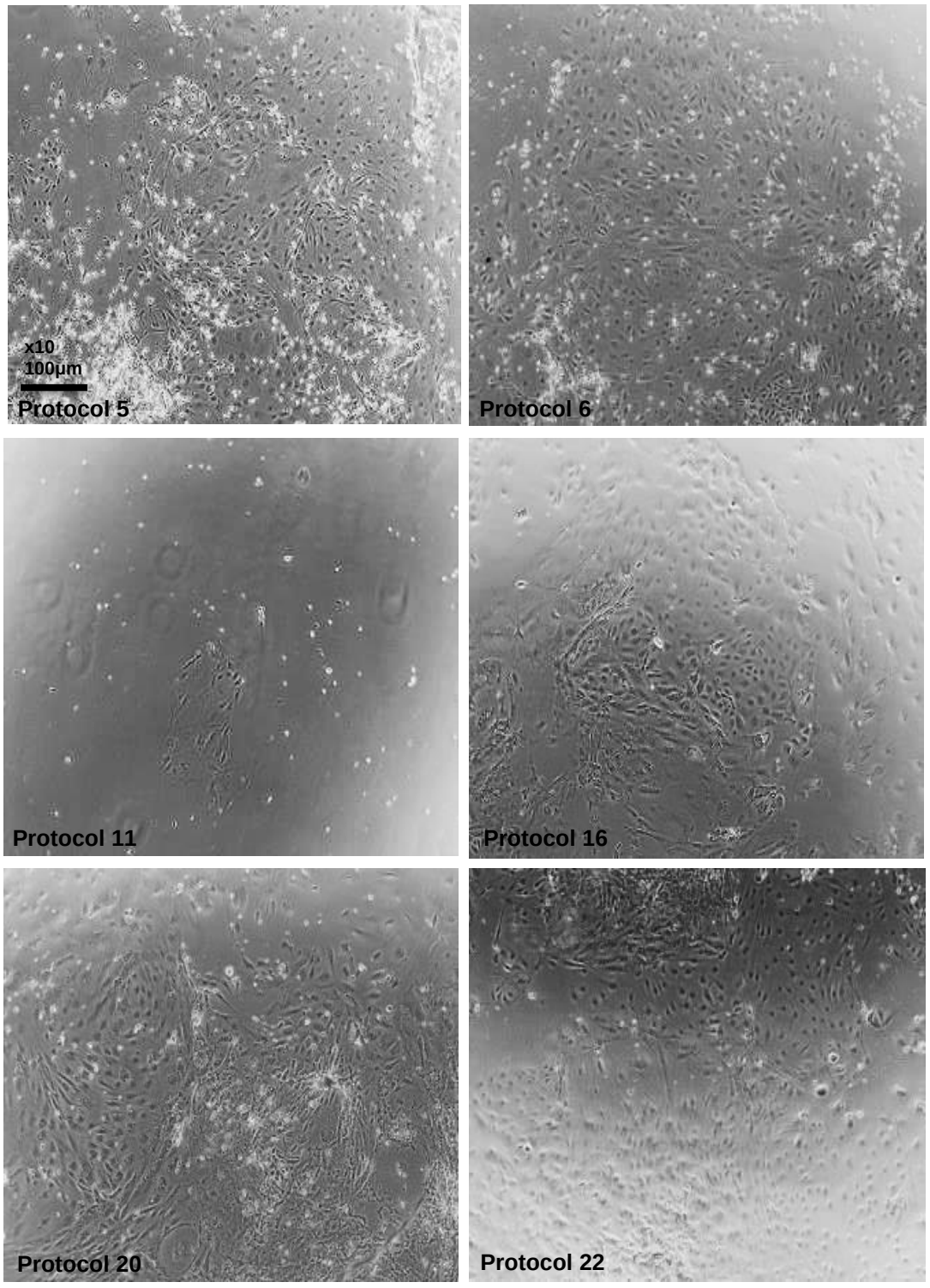

Figure 31: Monolayer differentiation stage 2: day 11

Cell culture images of the remaining 10 differentiation protocols at day 11 in stage 2 conditions (x10 magnification). Protocols 1-6, 20 and 22 continued to proliferate with uniform cell morphology however protocols 11 and 16 showed a sharp decline in cell numbers.

Differentiation Stage 2 (Day 13)

Through previously published research articles regarding hepatocyte differentiation and taking into account knowledge of *in vitro* primary hepatocyte culture, it is known that upon maturation stages that proliferation rates sharply decline. With low levels of cell attachment following stage 1 of differentiation, it was decided that the best approach was to continue to expand DE populations in stage 2 differentiation media that had been designed from the CombiCult® screen to promote proliferation of DE and hepatic progenitors. Stage 2 of differentiation was initially planned for five days however, this was extended by an extra three days to increase the population of differentiated cells. Cells reached sufficient numbers to start stage 3 of hepatic differentiation at day 13.

At this stage of the differentiation process there was two morphologically distinct populations of cells which were present in all protocols (Figure 32). The first type was observed to be rounded and display pebble-like in morphology. It was further seen that this cell type was clustered together in distinct regions of the culture wells. The second distinct population were found to be elongated and typically surrounded the outside of the clusters of pebble-like cells.

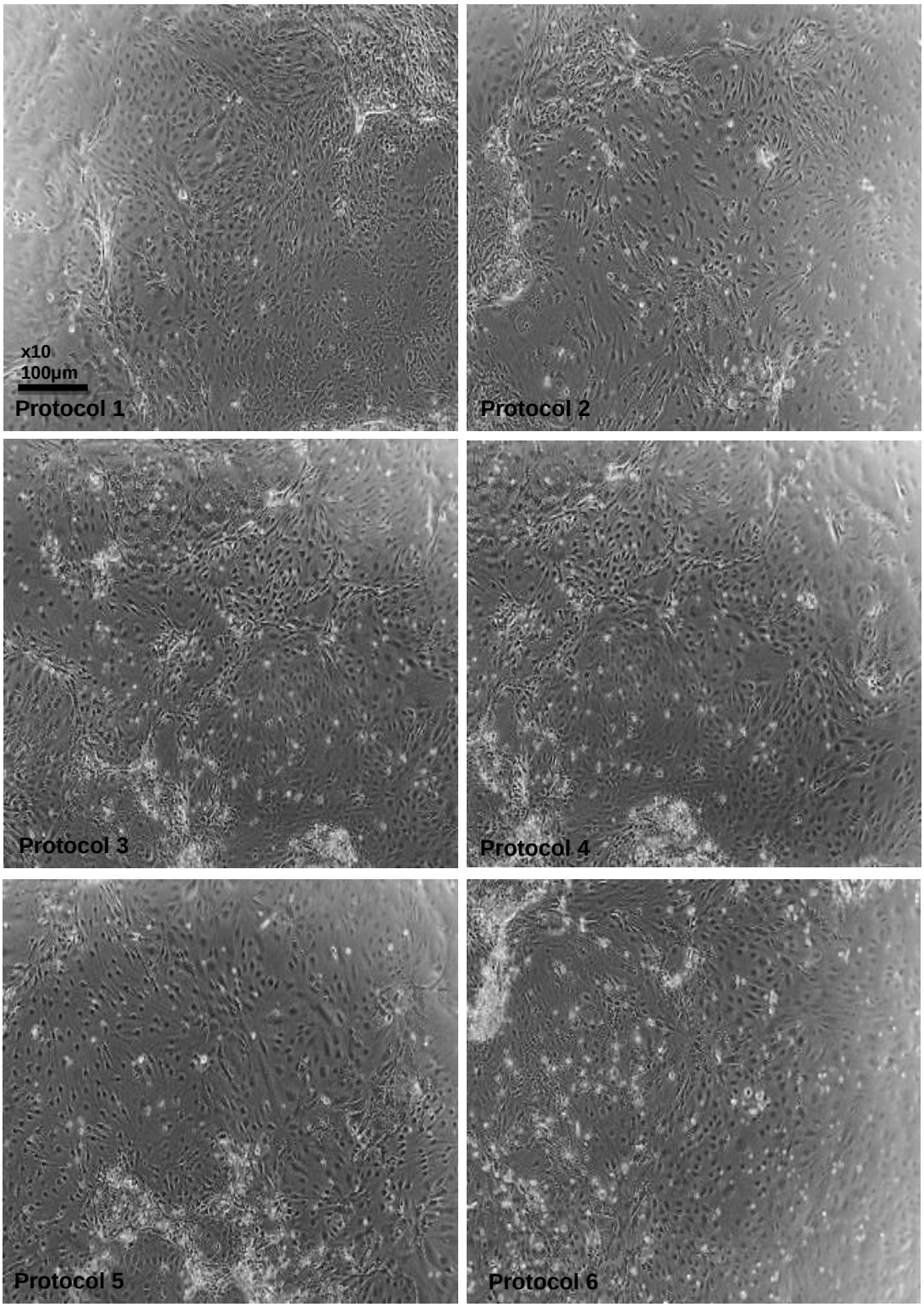
x10
100µm
Protocol 1
Protocol 2
Protocol 3
Protocol 4
Protocol 5
Protocol 6

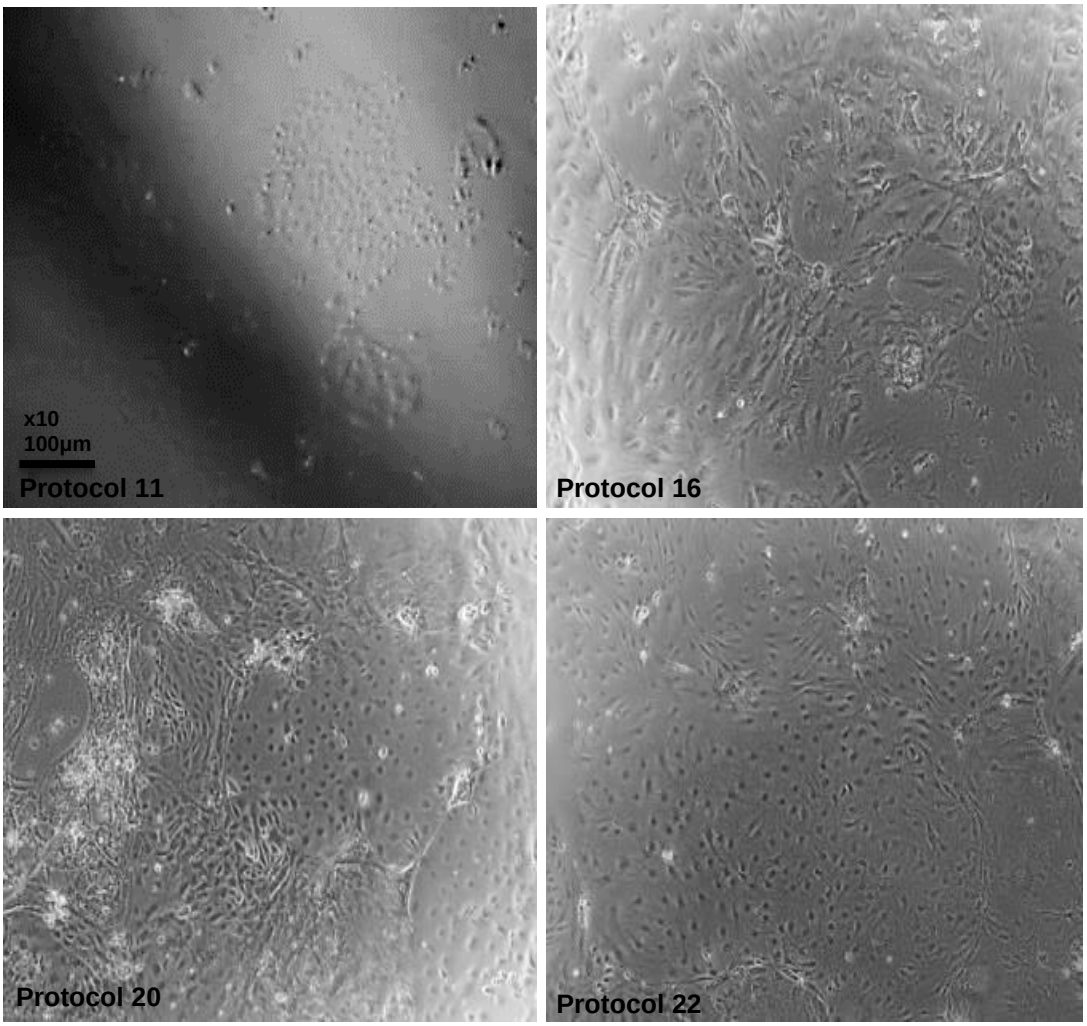

Figure 32: Monolayer Differentiation stage 2: day 13

Cell culture images of the remaining 10 differentiation protocols at day 13 in stage 2 conditions (x10 magnification). Due to low levels of cell attachment at the onset of stage 2 of differentiation it was decided to continue to expand DE populations at this stage to increase cell numbers. The planned time in stage 2 of differentiation media was therefore increased from five to eight days.

Differentiation Stage 3 (Day 14)

Stage 3 of differentiation was designed with a view to commit DE cells to a hepatic fate. Consequently, factors including TGFα and BMP7 were used as it has been seen *in vivo* to promote the expansion of hepatic progenitors upon hepatectomy. Cells exposed to stage 3 differentiation media were seen to undergo further changes in cell morphology (Figure 33). Cells were seen to cluster together whereas previously cells were more dispersed throughout the tissue culture wells. Cell numbers were seen to be decreased across all differentiation protocols after one day in stage 3 differentiation media. This could correspond to cells either committing to a hepatic fate or undergoing apoptosis due to not being able to be supported in stage 3 differentiation media. Protocols 16 and 20 suffered the most cell death and numbers of cells were seen to be very low after only two days in stage 3 differentiation media containing HGF, RA and GH and Progesterone, IL6 and TGFα respectively.

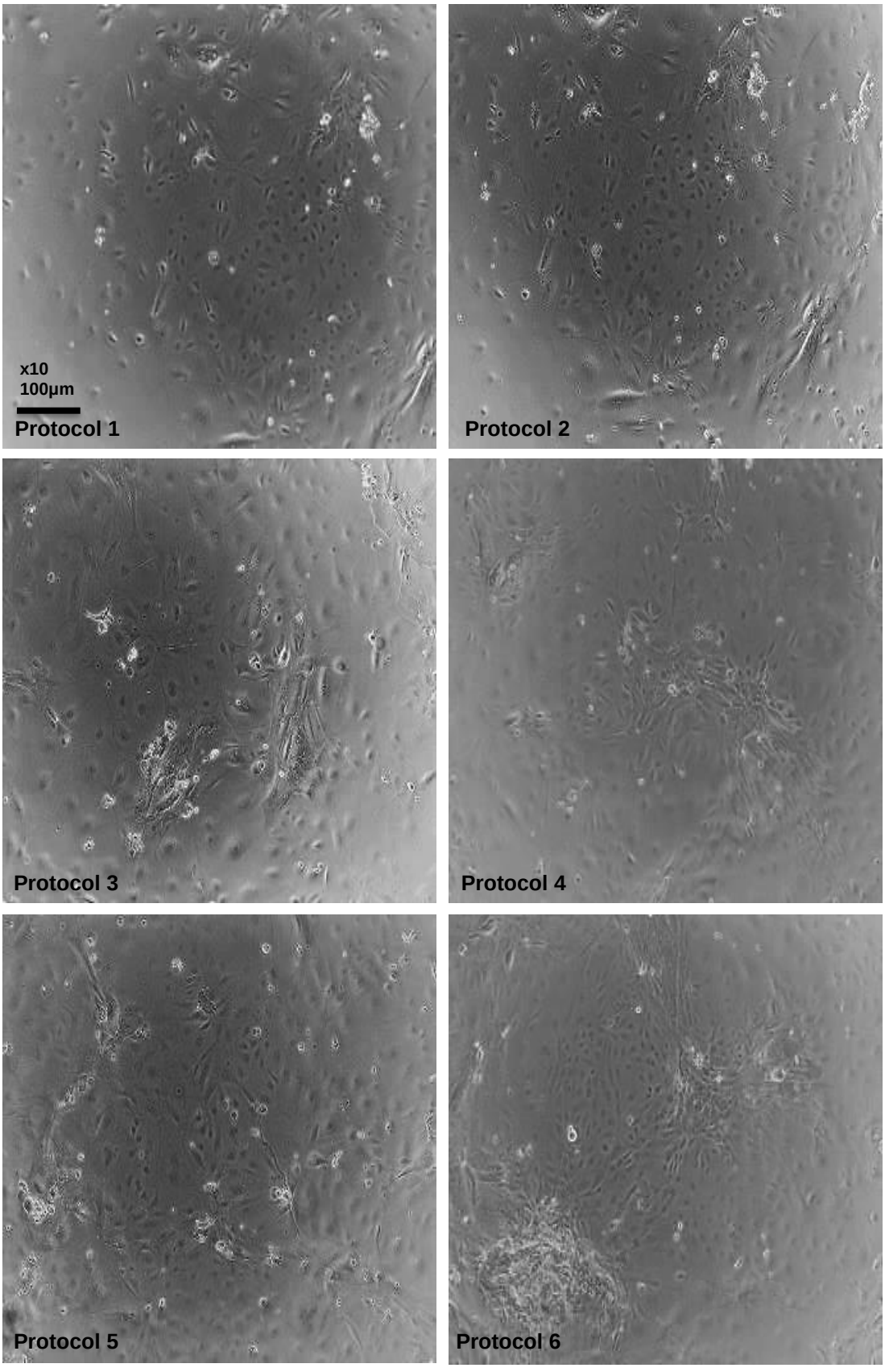
x10
100µm
Protocol 1
Protocol 2
Protocol 3
Protocol 4
Protocol 5
Protocol 6

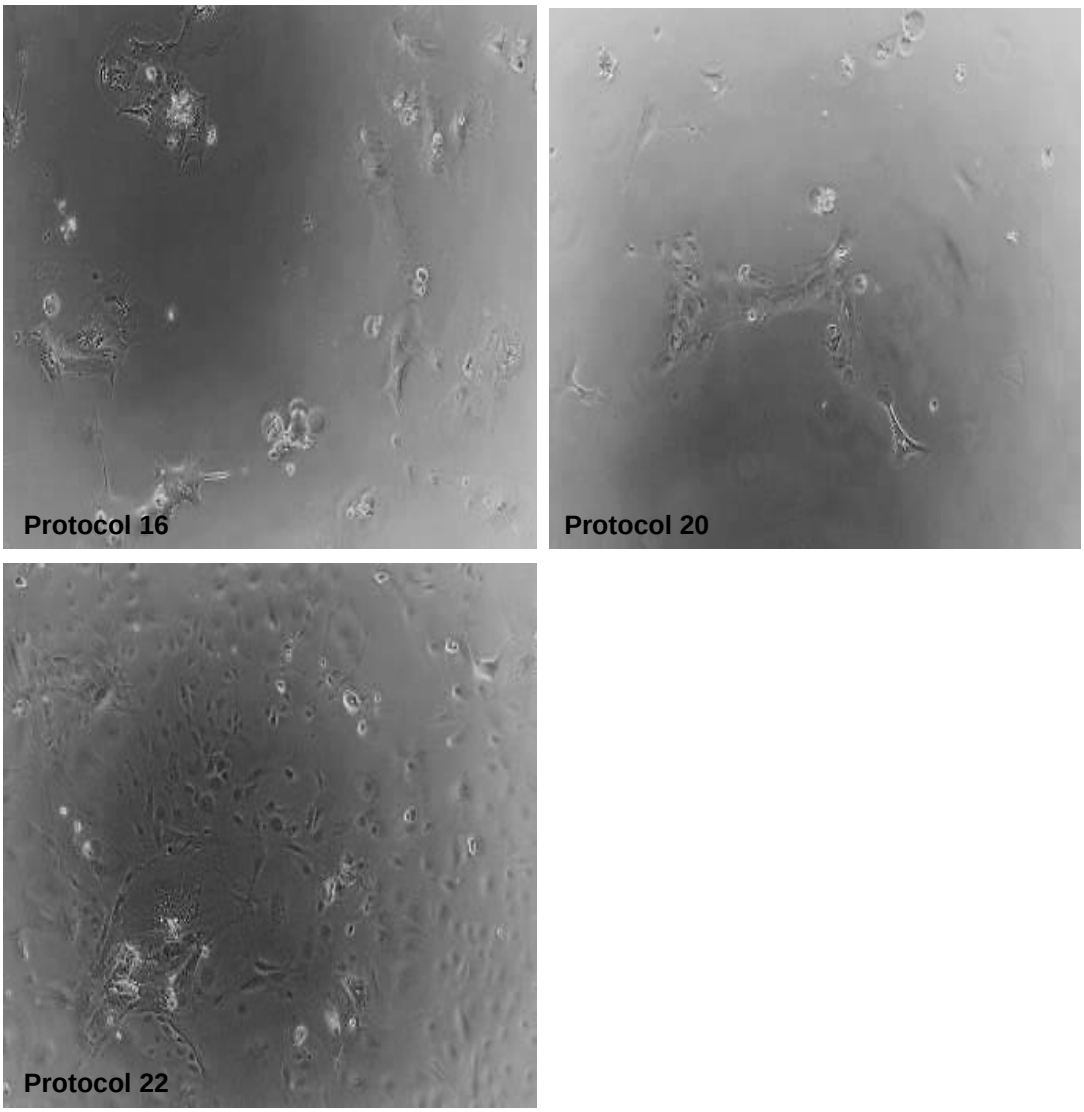

Figure 33: Monolayer differentiation stage 3: day 14

Cell culture images of the remaining 9 differentiation protocols at day 14 in stage 3 conditions (x10 magnification). After increasing the time spent in stage 2 of differentiation to expand cell populations, stage 3 of differentiation was initiated with a view to commit DE cells to a hepatic fate.

Differentiation Stage 3 (Day 20)

Protocols 1-6 and 22 continued to survive in stage 3 differentiation media after twenty days of differentiation. Levels of cell proliferation were seen to be further decreased upon progression through stage 3 of differentiation in accordance with expectations. Protocols 16 and 20 continued to decline in cell numbers and proliferation of existing attached cells until only a very few viable cells remained at day 24 of differentiation. As cells progressed through stage 3 of differentiation, cell morphology was seen to noticeably change in that cobble-like cells which emerged during the DE specification/expansion stages were replaced with elongated cells across all remaining protocols (1-6 and 22) (Figure 34).

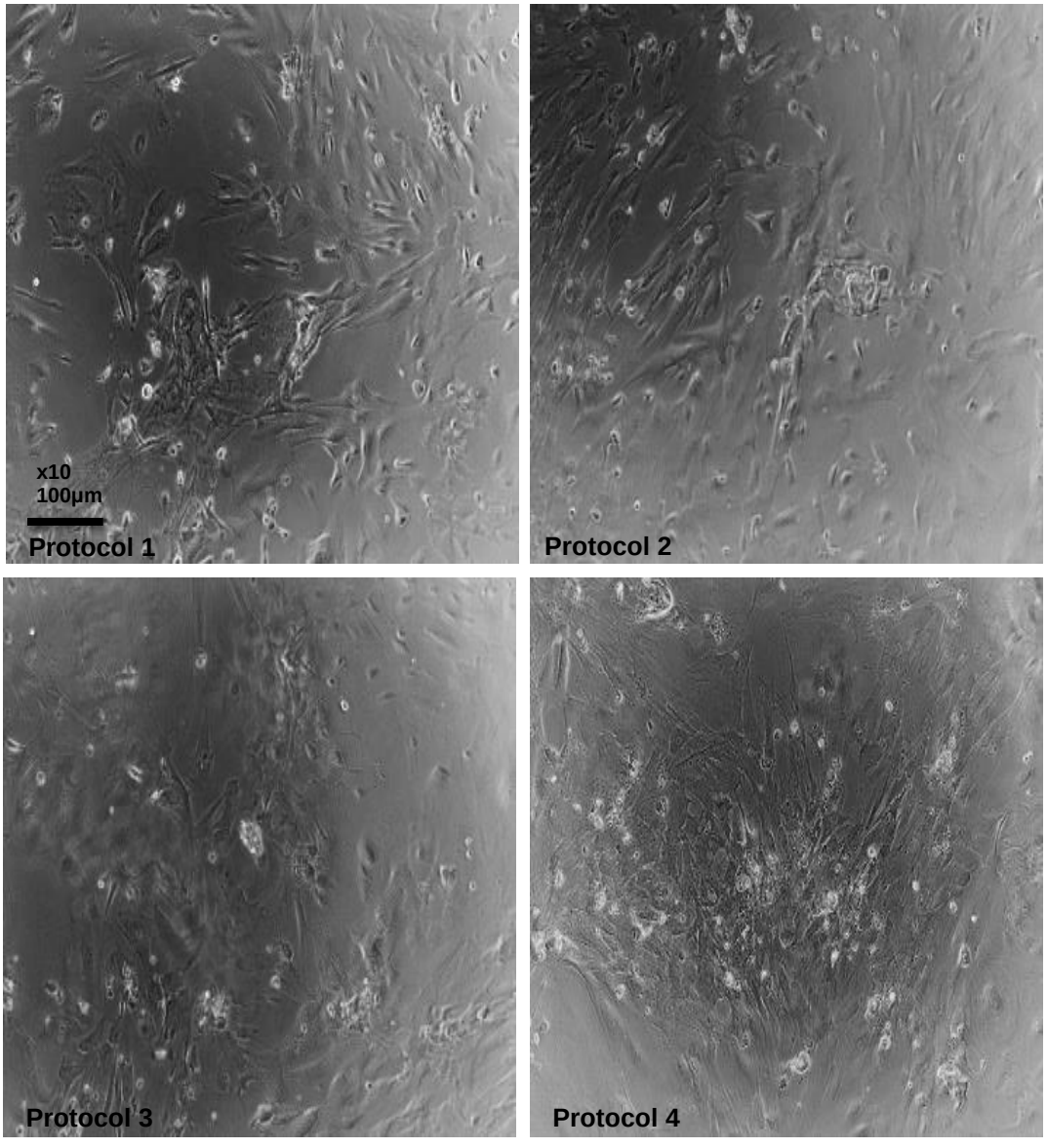

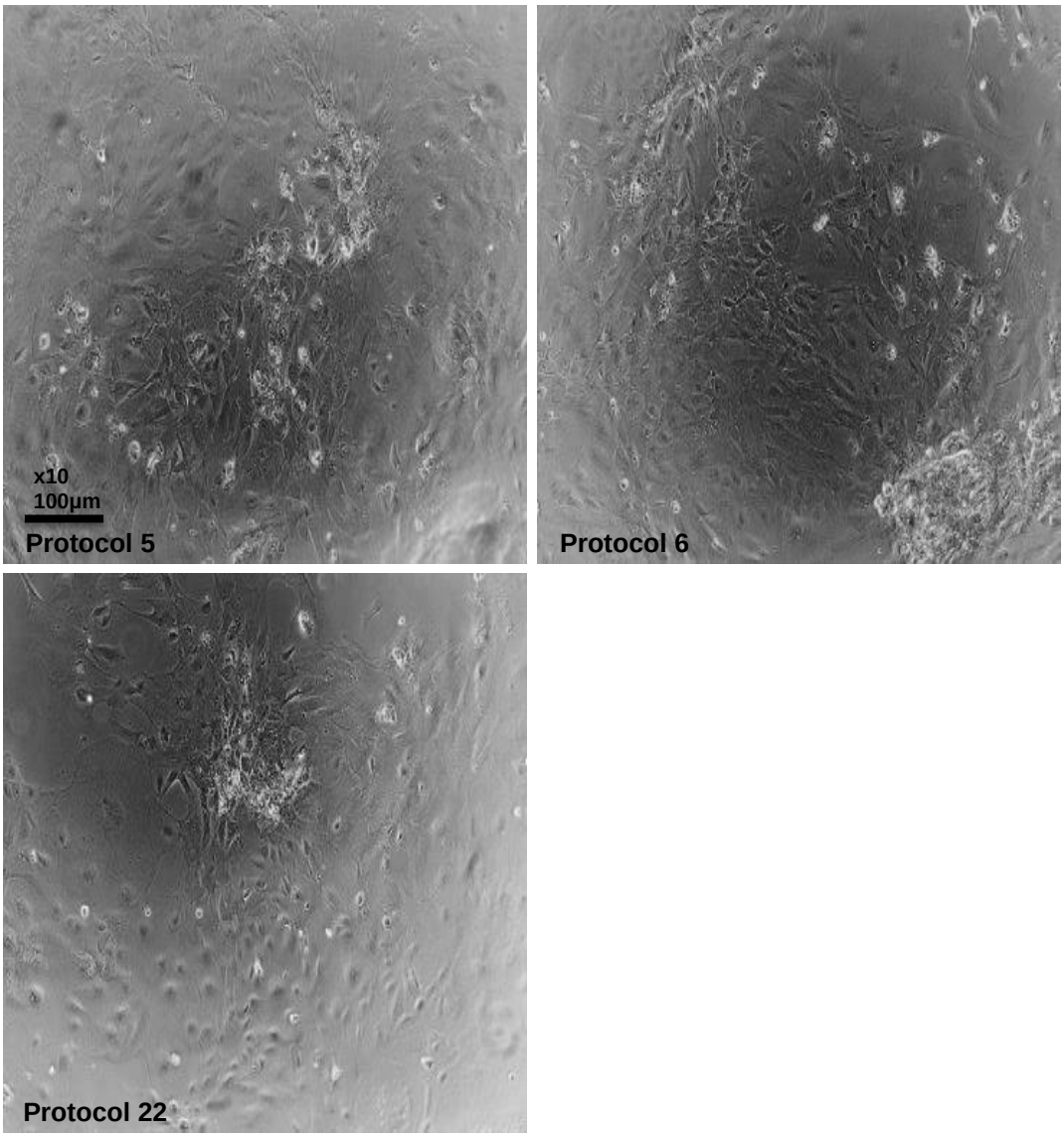

Figure 34: Monolayer differentiation stage 3: day 20

Cell culture images of the remaining 7 differentiation protocols at day 20 in stage 3 conditions (x10 magnification). Levels of cell proliferation in the surviving seven protocols were seen to be decreased in stage 3; typically concerned with hepatic specification.

Differentiation Stage 4 (Day 23)

Stage 4 of differentiation was concerned with the onset of hepatic maturation and combinations of small molecule agonists and anti-apoptotic factors including dexamethasone were added to hepatic basal media. Cell morphology remained consistent in most protocols trough the transition from stage 3 into stage 4 with the exception of protocols 4 and 22 (Figure 35). Protocol 4 contained combinations of small bioactive agonists targeting members of the NHR family as well as agonists of particular CYP450 family members. Protocol 22 consisted of a combination of HGF, insulin and OSM. As predicted, levels of cell proliferation were decreased following the onset of stage 4 and there was no visible level of cell expansion. As stage 4 progressed there was increased amounts of apoptosis and cell numbers continued to decline day-on-day until there were very few amounts of cells remaining at day 4 of stage 4 which formed isolated clusters.

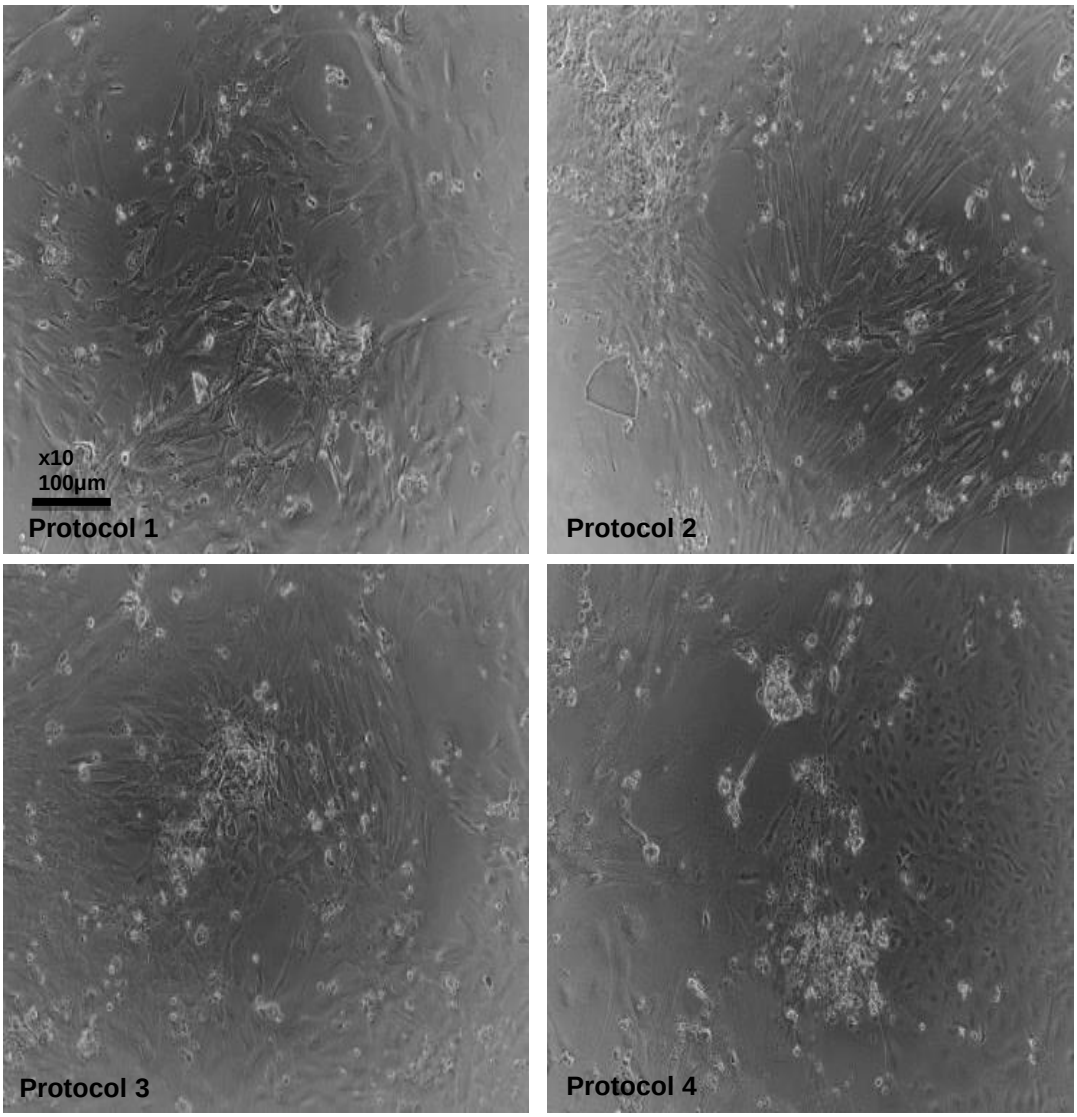
x10
100µm
Protocol 1
Protocol 2
Protocol 3
Protocol 4

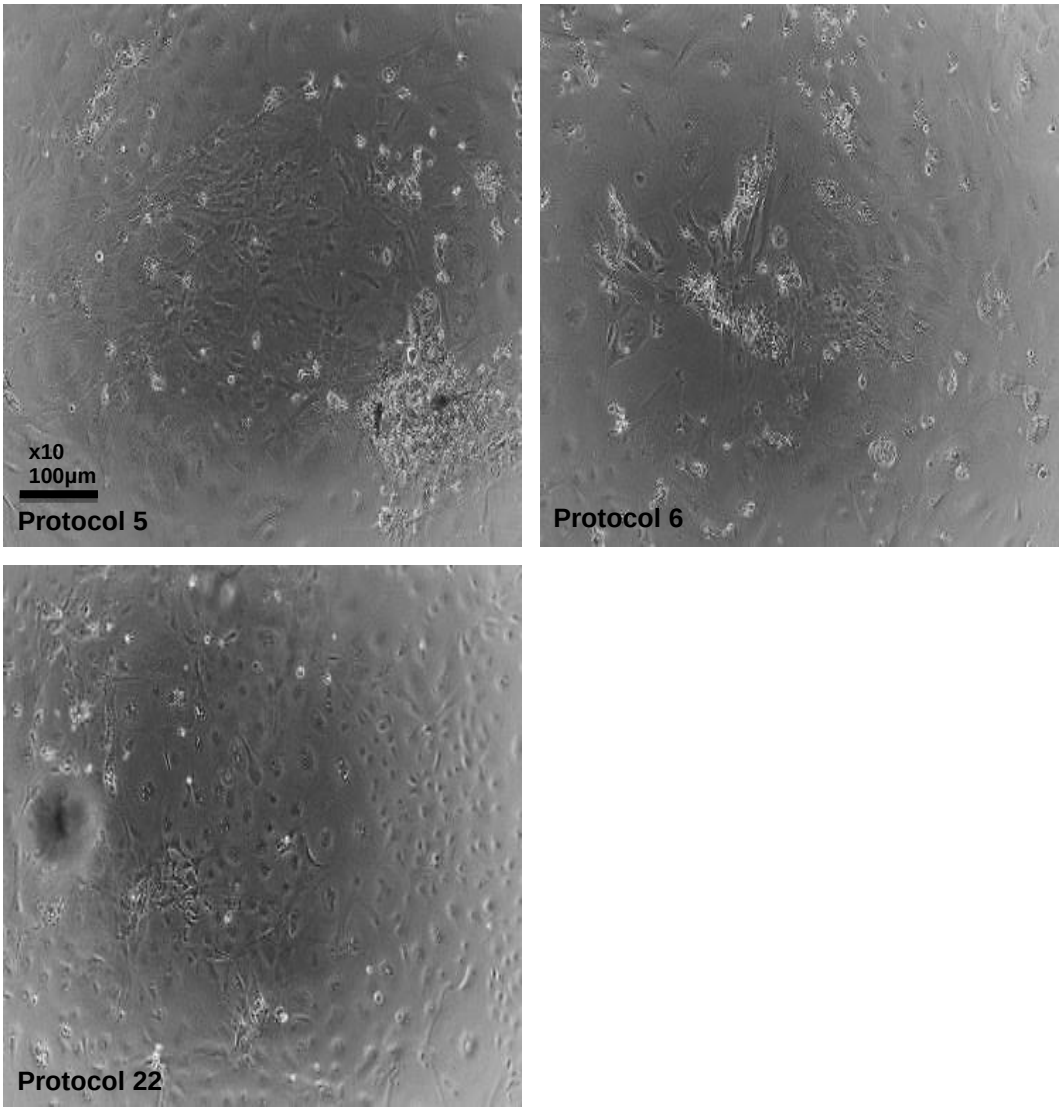

Figure 35: Monolayer differentiation stage 4: day 23

Cell culture images of the remaining 7 differentiation protocols at day 23 in stage 4 conditions (x10 magnification). The transition to stage 4 of the differentiation process concerned the onset of hepatic maturation and accordingly included small bioactive molecules identified through the CombiCult® screen. Cell proliferation was seen to cease during stage 4 in line with expectations and cell morphology remained largely similar across the surviving protocols except for protocols 4 and 22.

Differentiation Stage 4 (Day 28)

Cells in protocols 4 and 22 continued to show a flattened appearance and at day 28 of stage 4 this was also seen in protocols 3 and 5 containing progesterone, SR12813 (PXR agonist) and CITCO (CAR agonist) and Insulin, Docosahexaenoic Acid (DHA) and GH respectively (Figure 36). Cell numbers continued to decline day-on-day until day 30 when there was a significant event resulting in cells in all protocols undergoing apoptosis. Consequently, hepatic maturation analysis through ICC staining for CYP3A4 and CYP1A1/A2 and PCR for key hepatic markers was not possible at the end of the hepatic differentiation process.

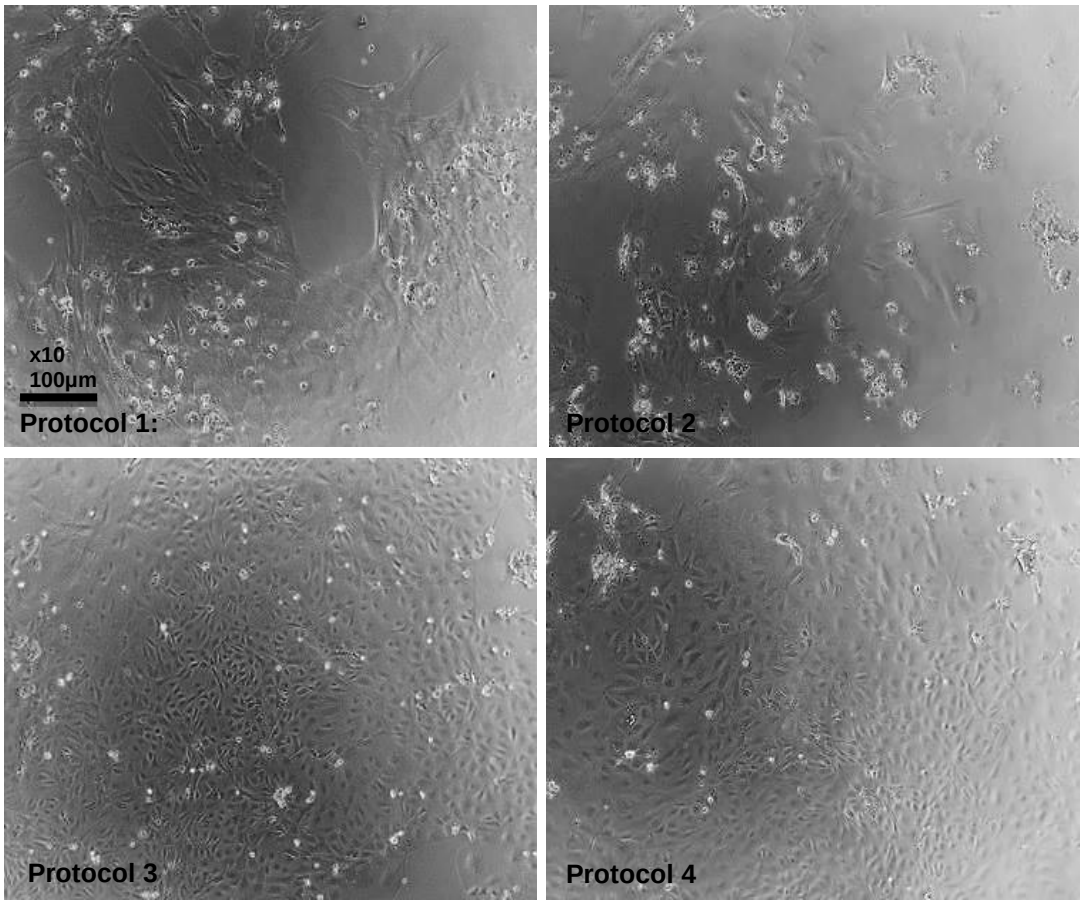

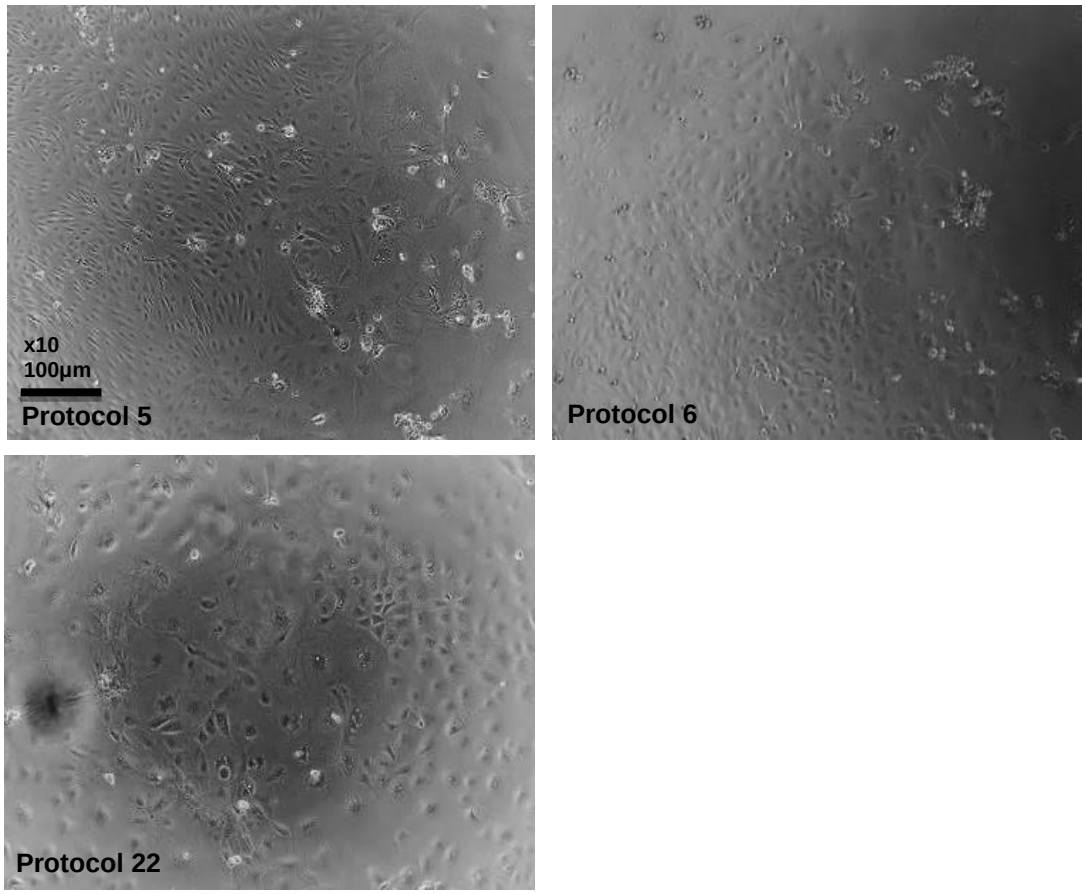

Figure 36: Monolayer differentiation stage 4: day 28

Cell culture images of the remaining 7 differentiation protocols at day 28 in stage 4 conditions (x10 magnification). Cells produced through protocols 4 and 22 continued to show a flattened appearance at day 28 and this was also seen in protocols 3 and 5. Cell numbers in all protocols continued to decline day-on-day until day 30 of stage 4 when there was a significant event resulting in cells in all protocols undergoing apoptosis.

5.3.2 Optimised 2D CombiCult® Monolayer Validation

Shef-3 hESC Seeding (Day 0)

Following completion of the initial monolayer validation experiment the six protocols with particularly interesting combinations of growth factors and small molecules were studied further under optimised conditions; that being protocols 1, 6, 7, 10, 21 and 22. The three major obstacles that were identified in the initial monolayer validation study was firstly passaging of the differentiated cells on day 6 following the completion of stage 1, the toxicity of linoleic acid in the first stage of differentiation and the mass apoptosis of differentiated cells at the end of the fourth stage of differentiation. To address these issues feeder free conditioned Shef-3 hESCs were seeded on collagen I coated plates at a density of $0.3x10^6$ cells per well of a 12 well plate. This density was determined to be the optimal cell number through carrying out titrations of Shef-3 hESC seeding densities followed by differentiation to assess confluency levels after set time intervals. Using the determined $0.3x10^6$ optimal well seeding density allows for the four-stage differentiation process to be completed without the need to passage the cells and associated risk of low levels of cell attachment, as was seen in the first monolayer validation experiment. The optimal density was also determined to seed sufficient cells for analysis following the decrease in cell proliferation in the final stages of hepatic differentiation. On day 0, Shef-3 hESCs were dissociated with accutase and seeded 16 hours before the start of the first stage of differentiation at $0.3x10^6$ cells per well of a 12 well plate (Figure 37).

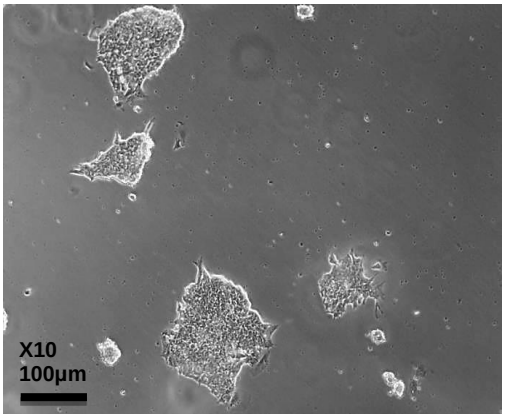

Figure 37: Optimised monolayer differentiation seeding (D1)

Shef-3 hESCs seeded at a density of $0.3x10^6$ cells/well on collagen I coated 12-well plates (D0). Hepatic differentiation in stage 1 media was started 24 hours later (D1).

The second optimisation step from the first monolayer validation experiment was to use a new BSA-conjugated linoleic acid (Sigma #L9530-5ML) which was found to be far less toxic to cells. Titration experiments were carried out over a range of concentrations and it was found that BSA-conjugated linoleic acid had no discernible increase in levels of cell death or stress.

Differentiation Stage 1 (Day 3)

Exposure of Shef-3 hESCs to stage 1 media combinations induced the differentiation of pluripotent stem cell colonies. Differentiated cell morphology across differentiation protocols was seen to be similar at day three, likely due to Activin A being present in all differentiation protocols inducing DE specification (Figure 38). At day 3, differentiation of hESC was initially observed from the periphery of the colonies whilst the centre of the colony maintained a more pluripotent-like morphology. Differentiated cells were seen to proliferate rapidly at equivalent levels across all six protocols at day 3.

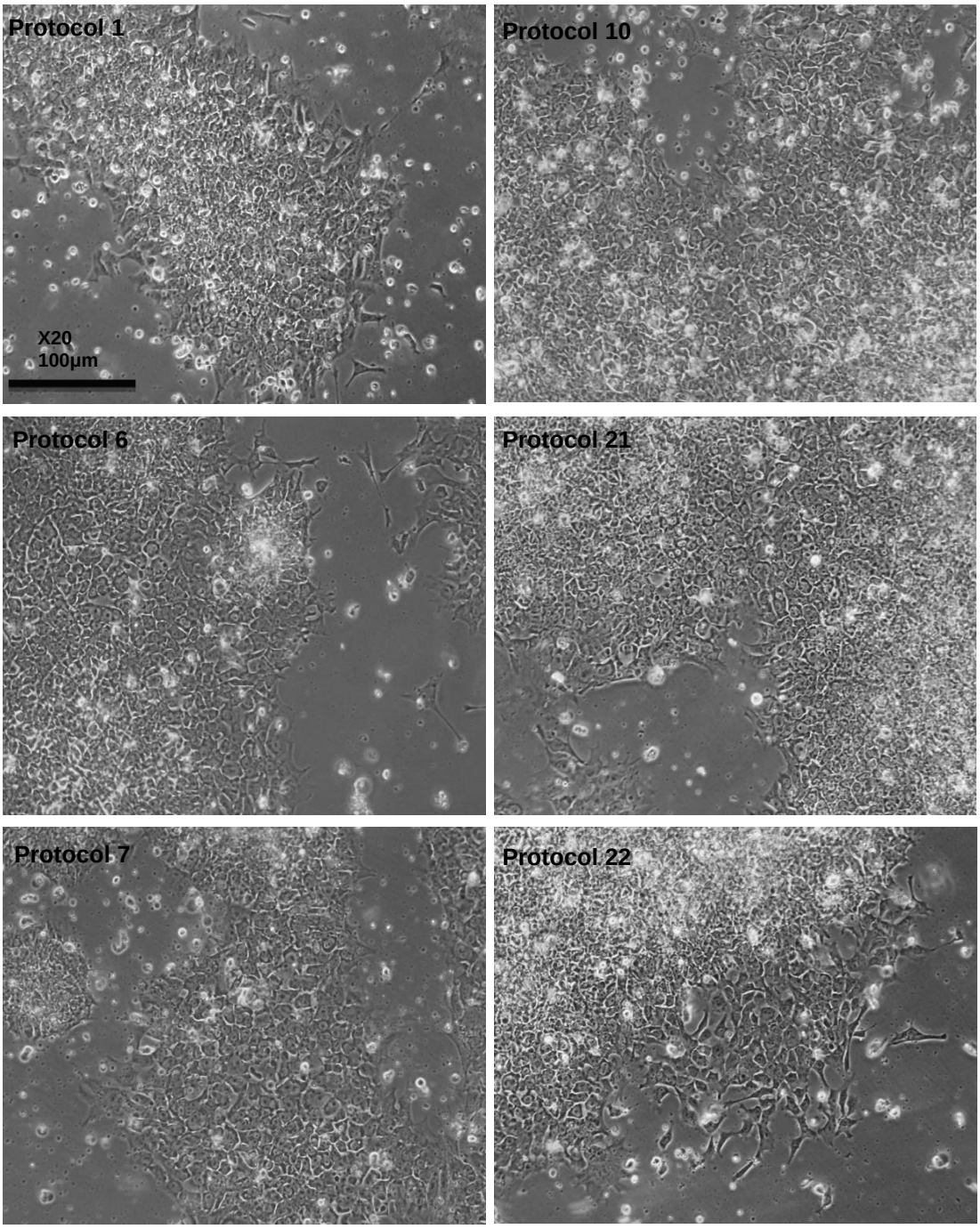

Figure 38: Optimised monolayer differentiation stage 1: day 3

Cell culture images of the top six selected differentiation protocols at day 3 in stage 1 conditions (x20 magnification). Upon differentiation cell morphology was seen to be changed at the edges of stem cell colonies. The morphology of differentiated cells was observed to be consistent across all the six CombiCult®-derived protocols.

Differentiation Stage 1 (Day 5)

Differentiated cells continued to proliferate at equivalent levels between the different protocols to the end of stage 1 of hepatic differentiation upon reaching the last day in stage 1 differentiation media (Figure 39). Cell morphology at this stage was also seen to be consistent across the six differentiation protocols. The majority of differentiated cells displayed flattened endodermal-like cell morphology after DE specification from pluripotent hESCs. Differentiated cells reached a confluency level of approximately 50-60% at the end of the first stage of differentiation across all six differentiation protocols. This level of confluence was determined to be ideal for hepatic differentiation as cells from the previous monolayer validation protocols were seen to proliferate at a lower level at the end of the second stage of the differentiation process and then display very low levels of proliferation upon hepatic maturation steps.

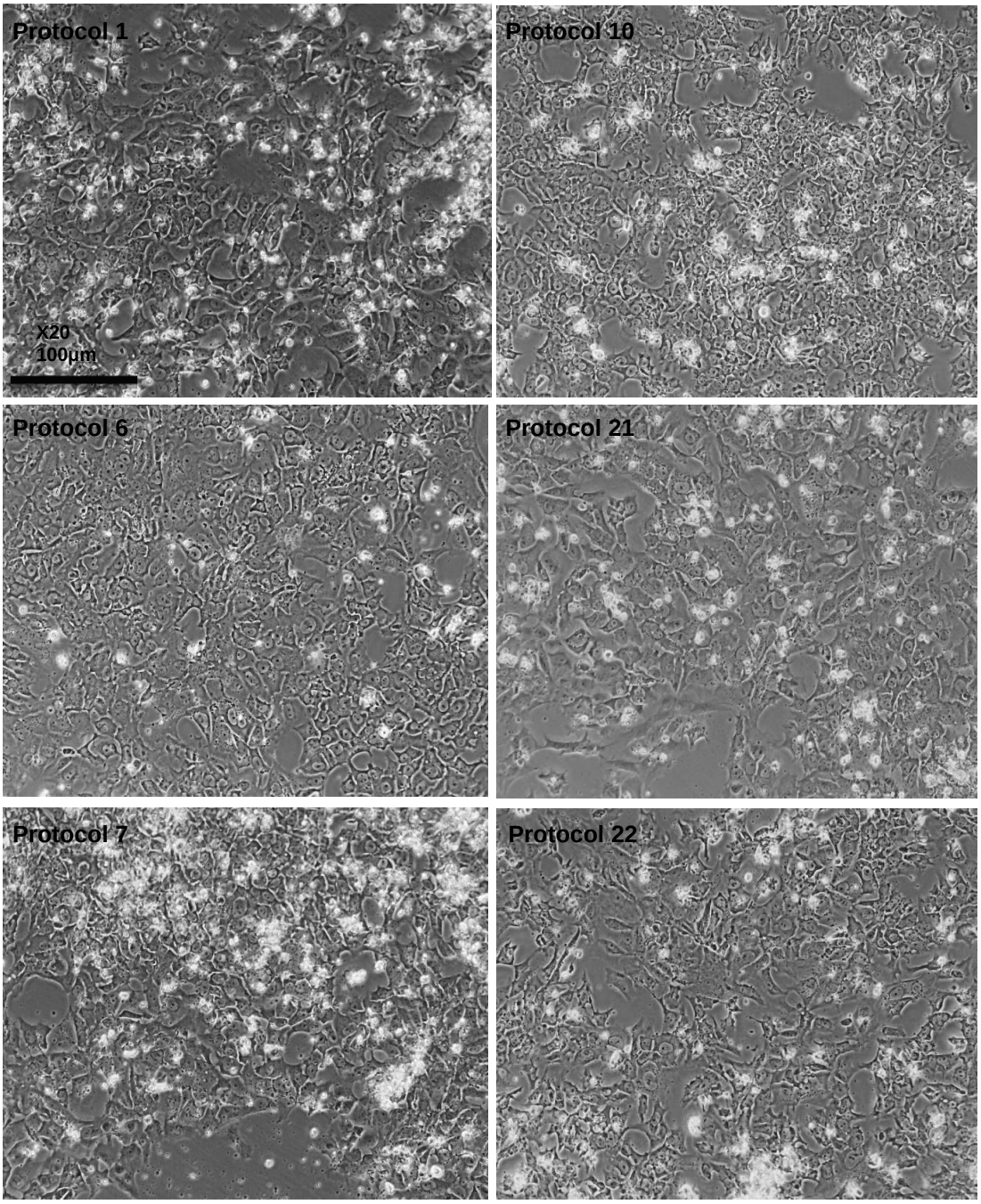

Figure 39: Optimised monolayer differentiation stage 1: day 5

Cell culture images of the top six selected differentiation protocols at day 5 in stage 1 conditions (x20 magnification). Levels of cell proliferation was seen to be consistent across all six CombiCult®-derived protocols displaying similar cell morphology at the end of the first stage of differentiation from pluripotent stem cells.

Differentiation Stage 2 (Day 7)

Stage 2 of differentiation was largely concerned with TGF-β signal inhibition after it was seen that the small molecules SB-431542 (Alk 4/5/7 inhibitor) and SIS3 (specific SMAD3 inhibitor) featured highly in the most efficient protocols identified through the initial CombiCult® screen. TGF-β signal inhibition is known to be important for DE proliferation and hepatoblast formation *in vivo* but has not yet been applied to the *in vitro* differentiation of HLCs. To further push hepatic differentiation, HGF and FGF4 were added in conjunction with WNT5A and GDF-15 which are elevated *in vivo* upon liver injury to proliferate hepatic progenitor populations. After two days in stage 2 differentiation media, cell morphology remained largely similar to that of cells seen at the end of stage 1 although round, flat and compacted cells started to emerge in protocol 1 (highlighted in Figure 40). Levels of cell proliferation was also seen to be consistant between all protocols.

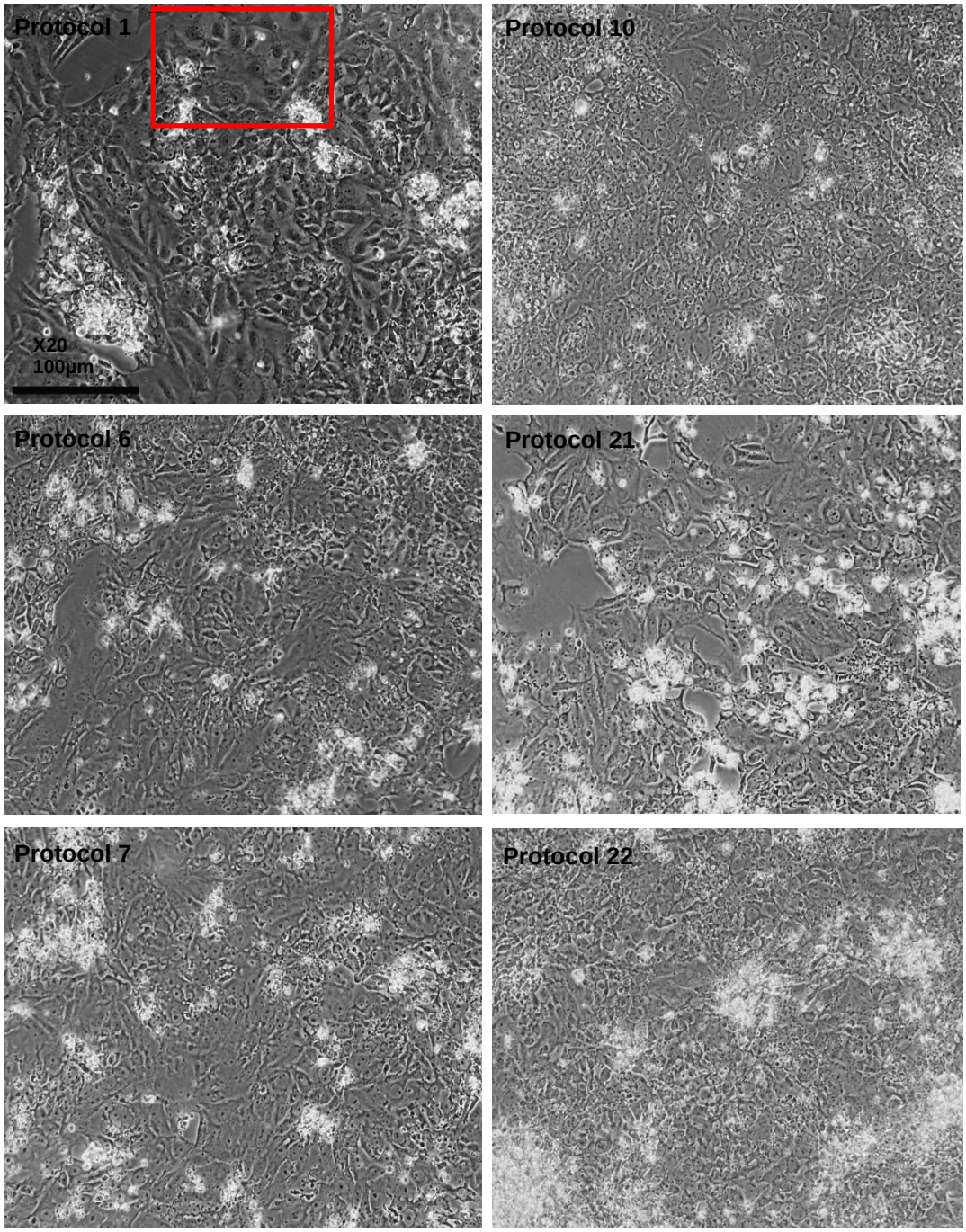

Figure 40: Optimised monolayer differentiation stage 2: day 7

Cell culture images of the top six selected differentiation protocols at day 7 in stage 2 conditions (x20 magnification). Levels of cell proliferation was seen to be similar across all six CombiCult®-derived protocols. Differentiated cell morphology was also seen to be consistent across protocols although round, flat and compacted cells started to emerge in protocol 1 (highlighted in red).

Differentiation Stage 3 (Day 11)

Stage 3 of differentiation consisted of growth factors that have been seen *in vivo* to expand the pool of hepatic progenitors through promoting proliferation upon liver injury. These included HGF, TGFα, BMP7 and Il6. At this stage of differentiation, there was a notable change in cell morphology particularly in protocol 1 (highlighted in Figure 41). Alongside the addition of growth factors promoting proliferation, progesterone was added to protocol 10 and 21 in an attempt to promote hepatic maturation as it had been found to be present at high frequency in the CombiCult® screen in stages 3 and 4 (Figure 41).

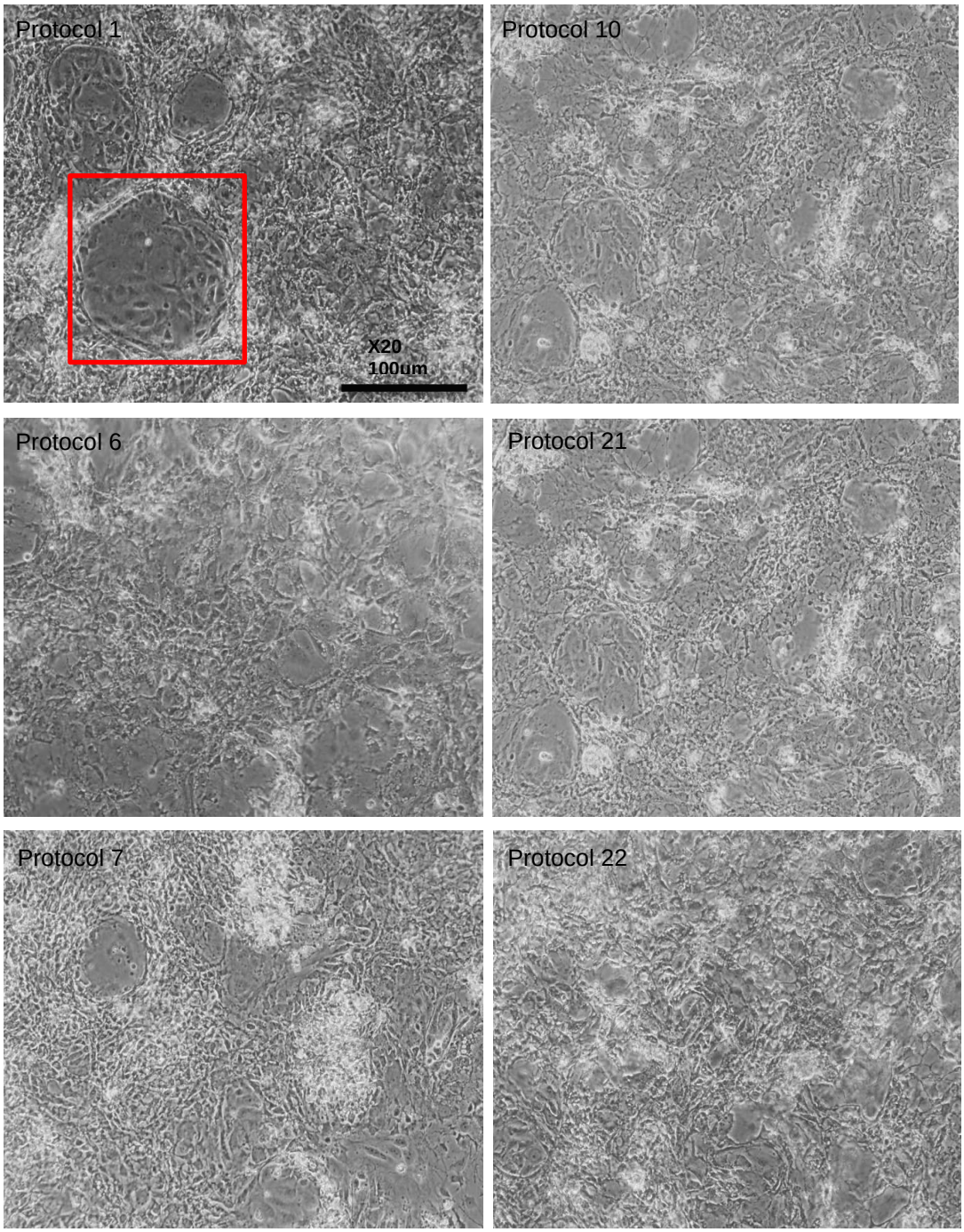

Figure 41: Optimised monolayer differentiation stage 3: day 13

Cell culture images of the top six selected differentiation protocols at day 13 in stage 3 conditions (x20 magnification). At this stage of differentiation process the most notable change in differentiated cell morphology was observed in protocol 1 (highlighted in red).

Differentiation Stage 4 (Day 24)

Levels of proliferation were seen to be drastically reduced in all protocols upon the transition to stage 4 of differentiation following the withdrawal of hepatic proliferation factors to an emphasis of pushing terminal differentiation. This was consistant with findings from the initial monolayer differentiation study and further conforms to published literature. Cell morphology in all CombiCult® derived protocols remained largely similar after the transition from stage 3 to stage 4 of differentiation (Figure 42).

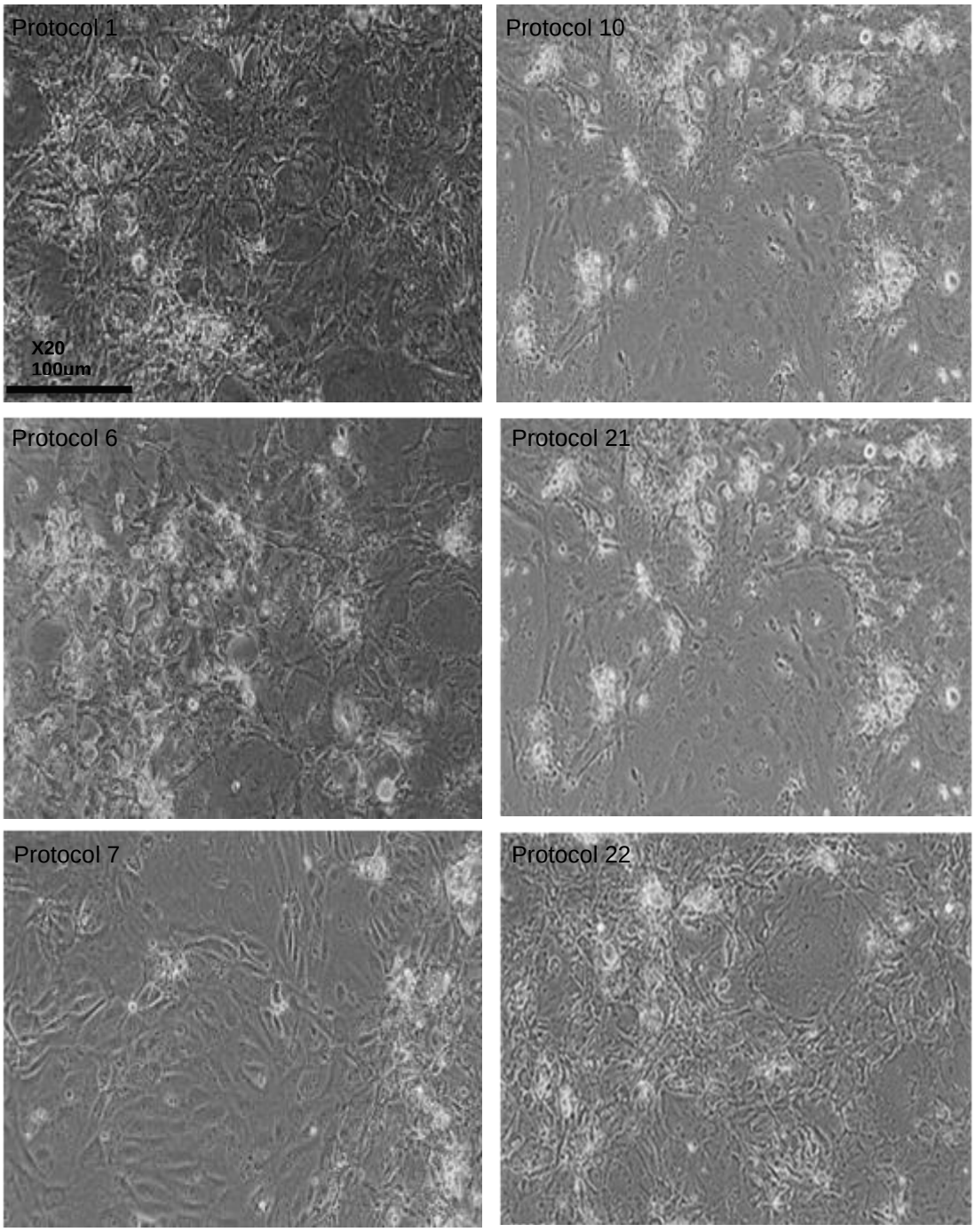

Figure 42: Optimised monolayer differentiation stage 4: day 24

Cell culture images of the top six selected differentiation protocols at day 24 in stage 4 conditions (x20 magnification). In the final stage of differentiation cell proliferation was seen to be greatly reduced in all six tested protocols. Cell morphology was also seen to be largely similar throughout the protocols.

5.3.3 RT-PCR Analysis of Hepatic Differentiation

After completion of the four-stage monolayer differentiation process on D28 cell samples were treated in triplicate with both omeprazole and rifampicin. Cell samples were also treated with 0.1% DMSO vehicle control (uninduced) (see Methods 2.6.2.3). Induction was carried out for a period of three days, with media refreshed every day. Cells were lysed and RNA was isolated for gene expression analysis using PCR. HepaRG cells were also plated in monolayer culture and samples were treated in the same way as the differentiated HLCs. Following induction drug treatment or 0.1% vehicle control, RNA was collected for RT-PCR for both induced and uninduced HLCs (see Methods 2.3.4). However, there were problems with the RNA extraction of the induced drug treated wells of differentiated HLCs which resulted in very low yields of RNA being obtained. Because of this differentiated HLCs treated with inducer drugs were not able to be analysed for gene expression. Uninduced samples were compared to HepaRG cells through RT-PCR to measure basal levels of CYP1A1/A2 as an assessment of hepatic maturation. RT-PCR was carried out for 30 cycles and PCR products analysed on a 2% agarose gel GAPDH was used as a housekeeping gene to normalise gene expression (see Methods 2.3.4).

It was found that all HLCs produced through the differentiation protocols and HepaRG cells expressed Albumin, the highest levels been seen in uninduced HepaRG cells (Figure 43). Albumin expression levels between the HLCs differentiated from the CombiCult® derived protocols was seen to be comparable. Albumin is expressed in hepatic cells at an early stage at low levels and then subsequently increased to maximum levels in mature adult hepatocytes.

The presence of albumin is an indicator that the differentiated cells produced through the CombiCult® derived protocols are in fact hepatocyte-like. CYP1A1 was shown to be upregulated through the addition of inducer drugs in the HepaRG cells compared to uninduced HepaRG cells. This confirms that the inducer drugs do indeed upregulate CYP1A1 in monolayer cultures and can be used as a readout assay for hepatic maturity in both gene expression analysis and ICC staining in the CombiCult® platform. CYP1A1 levels in the CombiCult® derived protocols were seen to be at the comparable levels to those seen in the uninduced HepaRG cells indicating a base level of expression between differentiated HLCs and uninduced HepaRG cells. CYP1A2 was seen to be most strongly expressed in protocol 1 and was shown to be at higher levels than in HepaRG cells. Protocols 6, 21 and 22 were seen to display comparable levels of CYP1A2 expression compared to HepaRG cells. In addition, α1AT was found to be strongly expressed in protocol 1 and to a lesser extent in protocols 6, 7,10 and 22 along with induced HepaRG cells.

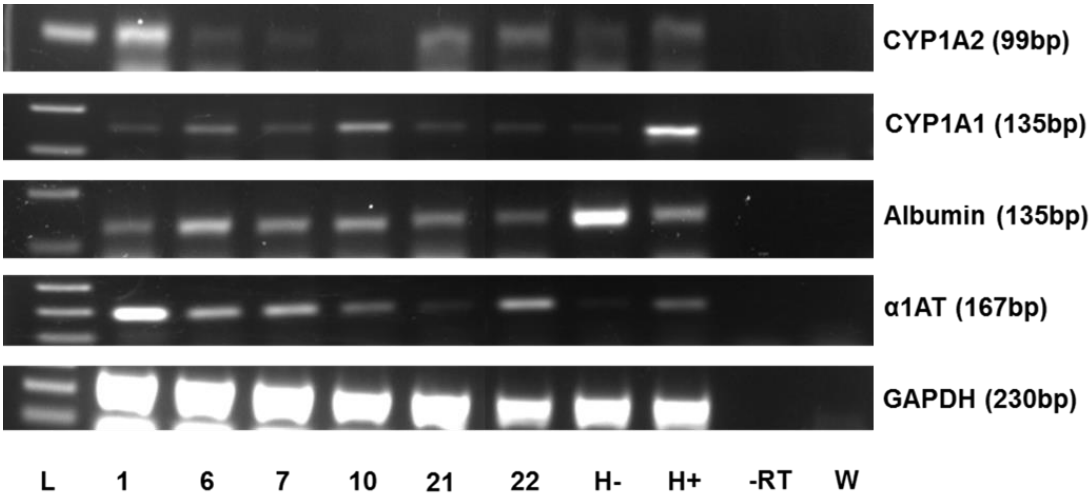

Figure 43: RT-PCR analysis of hepatic markers in differentiated HLCs

RT-PCR reactions were carried out on RNA extracted from differentiated HLCs that were treated with 0.1% DMSO vehicle control (uninduced) for three days. Differentiated HLCs were compared to HepaRG cells that had either been induced of treated with 0.1% DMSO vehicle control. RT-PCR reactions were carried out for 30 cycles and visualised on a 2% agarose gel. L = 100bp DNA ladder, 1-22 = CombiCult®-derived protocol number, H- = uninduced HepaRG, H+ = induced HepaRG, -RT = no reverse transcriptase control, W = water control. Results are representative of n=3 biological repeats.

5.3.4 ICC Analysis of Drug Induced HLCs

After completion of the four-stage monolayer differentiation process on day 24 differentiated HLCs were dual stained with primary antibodies for the CYP450 family members CYP1A1, CYP1A2 and CYP3A4. Secondary antibody incubations were carried out using Alexa Fluor 488 anti-goat (CYP3A4, green) and anti-mouse 594 (CYP1A1/A2, red) antibodies (Invitrogen) at 1:1000 dilutions (see Methods 2.4.5). Cells were also stained with DAPI for nuclear visualisation (Figure 44). This ICC assay had previously been utilised as a measurement of hepatocyte maturity in the CombiCult® platform.

Image J (National Institutes of Health, Maryland, US) was used to count DAPI positive staining in uninduced differentiated HLCs to give total cell numbers present at the end of monolayer differentiation. This was further carried out for cells staining positive for CYP1A1/A2 and CYP3A4 in the six protocols tested. CYP1A1/A2 and CYP3A4 positive cells were found in all hepatocyte monolayer differentiation protocols at similar numbers and florescence intensities apart from protocol 22 which displayed lower numbers of CYP1A1/A2 and CYP3A4 positive cells. It was calculated that approximate numbers of CYP1A1/A2 positive cells in protocol 1 was 20%, 17% in protocol 6, 30% in protocol 7, 21% in protocol 10, 30% in protocol 21 and 3% in protocol 22. CYP3A4 positive staining was calculated to be 27% of cells in protocol 1, 20% in protocol 6, 27% in protocol 7, 17% in protocol 10, 30% in protocol 21 and 3% in protocol 22. It was seen that CYP3A4 and CYP1A1/A2 staining mostly co-localised in the differentiated HLCs analysed through ICC.

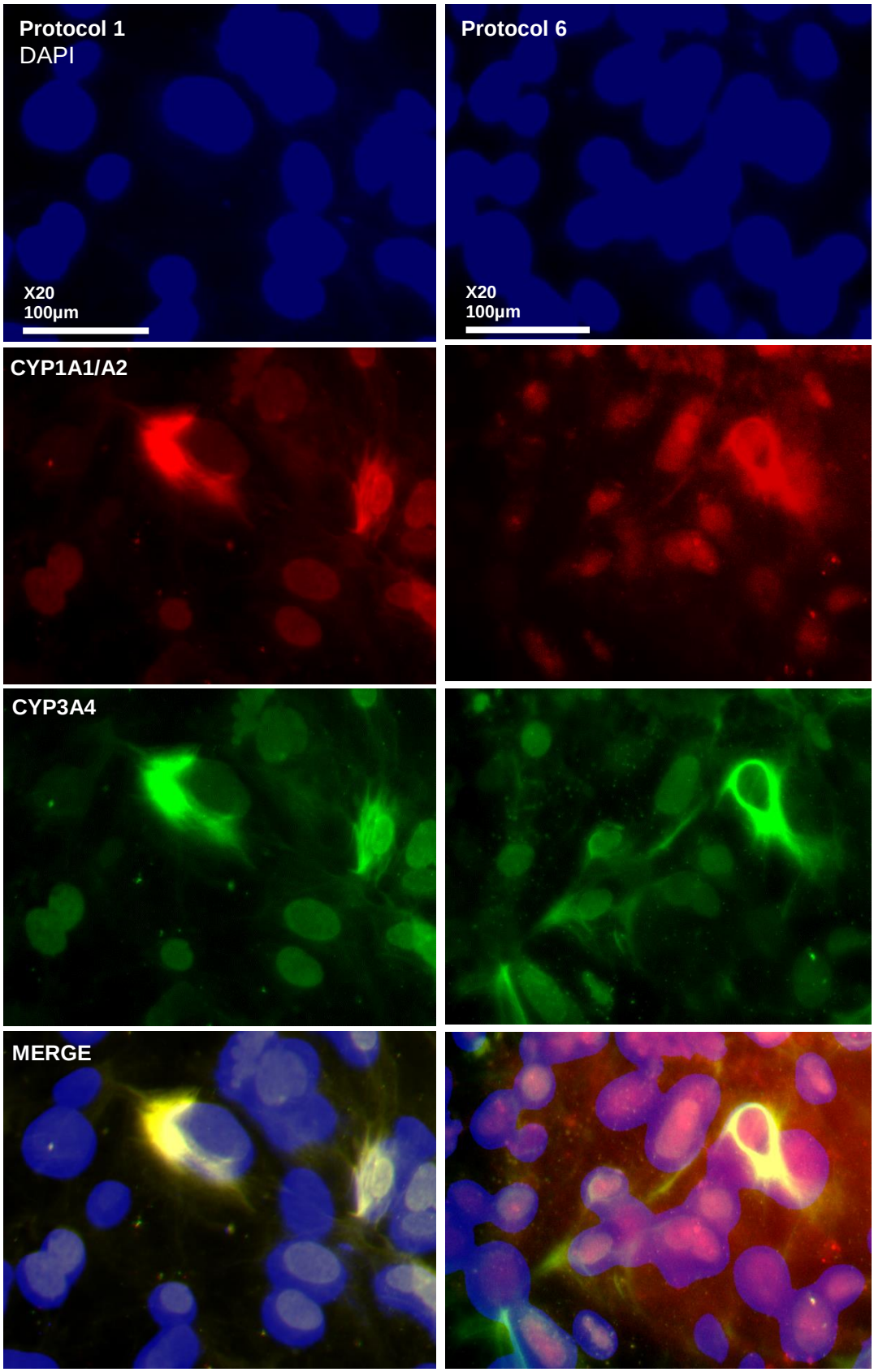
Protocol 1
DAPI
X20
100µm
Protocol 6
X20
100µm
CYP1A1/A2
CYP3A4
MERGE

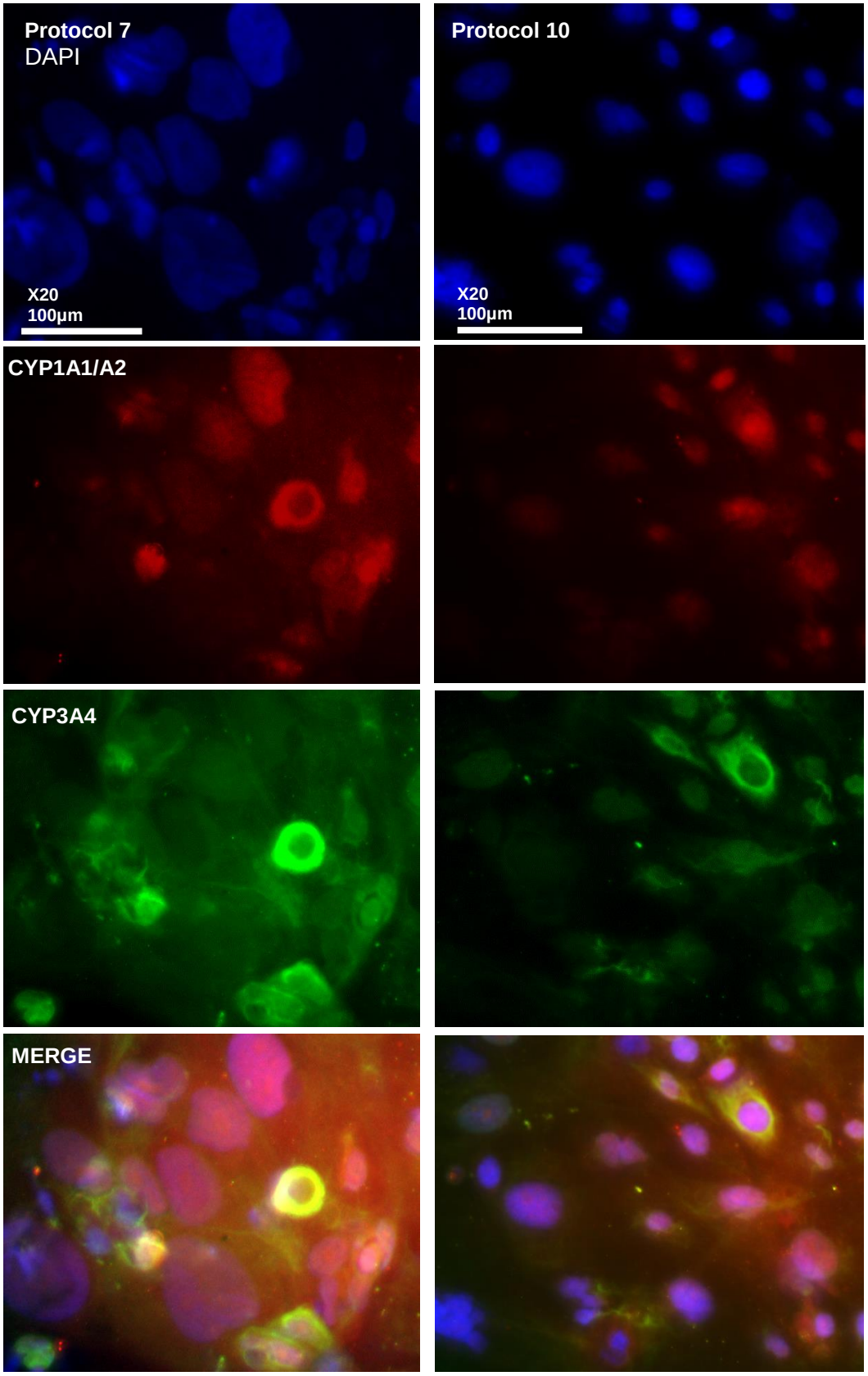
Protocol 7
DAPI
X20
100µm
Protocol 10
X20
100µm
CYP1A1/A2
CYP3A4
MERGE

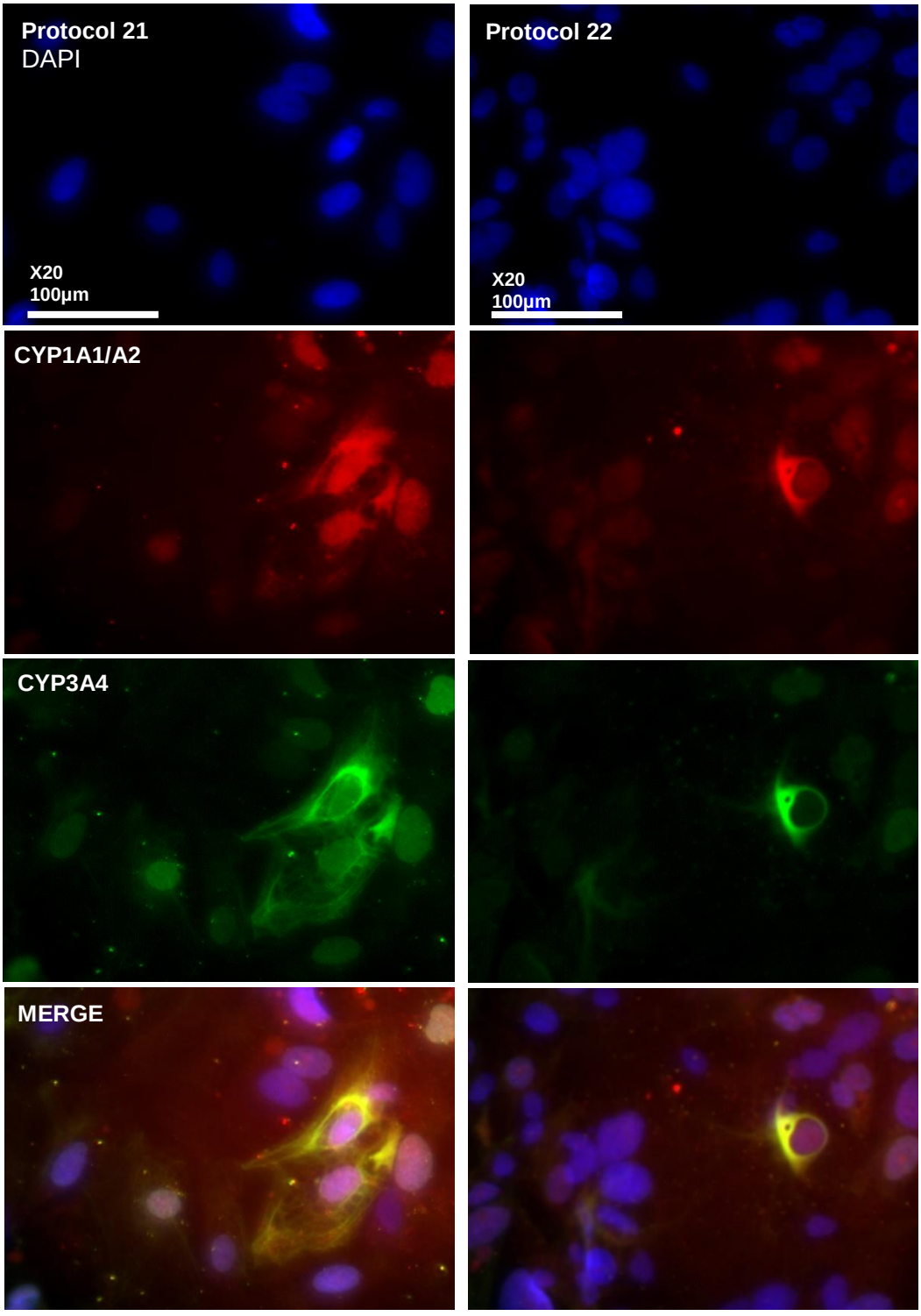

Figure 44: ICC Staining for CYP1A1/A2 and CYP3A4 in Differentiated HLCs

Differentiated HLCs were stained for the CYP450 family members CYP1A1, CYP1A2 and CYP3A4. Corresponding secondary antibody incubations were carried out using Alexa Fluor anti-goat 488 (CYP3A4, green) and Alexa Fluor anti-mouse 594 (CYP1A1/A2, red) antibodies (Invitrogen). Cells were further stained with DAPI for nuclear visualisation (blue).

5.3.5 Quantitative Analysis of CYP450 Functional Levels

Along with gene expression and ICC analysis, differentiated HLCs were assessed for hepatic maturation using both the quantitative luminescent p450Glo (Promega) and fluorescent EROD quantitative assays for CYP3A4 and CYP1A1/A2 activity respectively. These assays were utilised to assess levels of CYP1A1/A2 and CYP3A4 activity upon drug induction.

Following completion of the differentiation protocols, cells were either treated with combined omeprazole and rifampicin/dexamethasone to induce CYP1A1/A2 and CYP3A4 expression respectively or with assay media containing 0.1% DMSO as a vehicle control. Induction was carried out for a period of three days with media being refreshed every day. Induction assays were conducted in biological triplicate repeats with three technical replicates carried out for each test sample (see Methods 2.5.2 and 2.5.1).

5.3.5.1 CYP3A4 Induction Analysis in Monolayer Differentiated HLCs

CYP3A4 activity as assessed by the p450Glo assay was found to be increased upon drug addition in comparison to 0.1% DMSO treated control cells (Figure 45). Induction levels of 1.52 ($p<0.05$), 1.32 ($p<0.05$), 1.54 ($p<0.01$), 1.85 ($p<0.001$), 1.94 ($p<0.001$) and 1.74 ($p<0.001$) were obtained for protocols 1, 6, 7, 10, 21 and 22 respectively. The biggest relative fold increase in CYP3A4 activity between control and drug treated samples was found to be in protocol 21 which contained a combination of two small molecule agonists and a fatty acid precursor in the final stage of hepatic maturation. These factors were GW7647 (PPARα agonist), T0901317 (LXR agonist) and docosahexaenoic acid (fatty acid precursor).

Protocol 21 also contained novel *in vitro* hepatic differentiation factors in early stages including linoleic acid which is a proposed HNF4α ligand and hyperforin which has been shown to upregulate CYP3A4. In stage 3 of differentiation progesterone and TGFα were also incorporated because of the *in vivo* role in hepatoblast expansion upon liver injury.

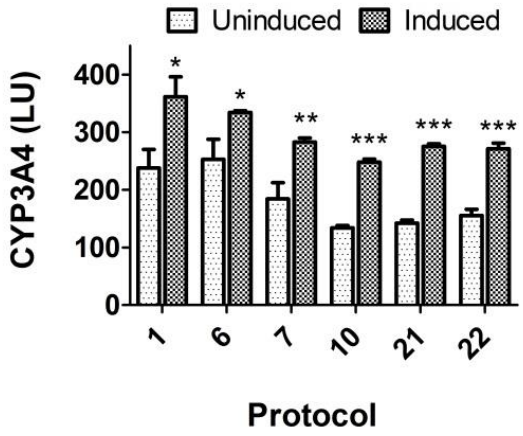

Figure 45: CYP3A4 induction in monolayer differentiated HLCs

The difference between induced versus uninduced CYP34A levels in monolayer differentiated HLCs was quantified using a p450Glo assay. Luciferase units (LU) per protocol were measured and statistical analysis calculated by a Student's t-test. Significance is indicated by *** ($p<0.001$), ** ($p<0.01$), * ($p<0.05$). Data are shown as mean ± SD of n=3 biological repeats.

5.3.5.2 CYP1A1/A2 Induction Analysis

CYP1A1/A2 levels were seen to be consistent in HLCs produced from CombiCult® derived protocols (Figure 46). At the end of hepatic differentiation, HLCs were treated with rifampicin to induce CYP1A1/A2 and an EROD assay carried out to quantify differences between protocols.

Unfortunately, due to cell culture infection, uninduced HLCs were lost and could not be compared to induced HLCs that had been treated with rifampicin for a measure of CYP1A1/A2 levels. Levels of CYP1A1/A2 in induced HLCs were compared to assess differences between the six CombiCult®-derived protocols.

It was found that there was a small but significant difference between CYP1A1/A2 levels in protocol 1 compared to those present in HLCs derived from the other protocols ($p<0.05$). There was also a small but significant difference between increased levels of CYP1A1/A2 in protocol 21 compared to those quantified in protocol 6 ($p<0.05$).

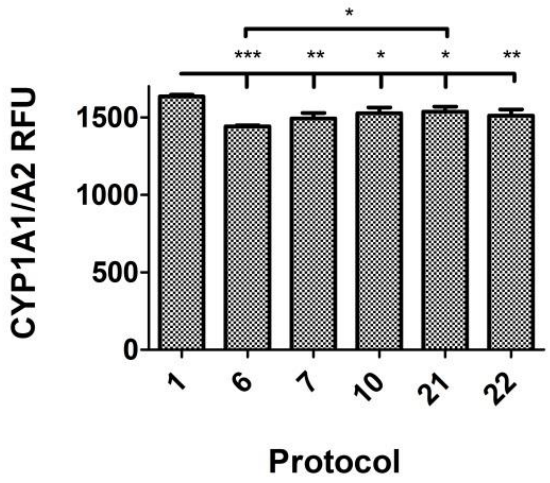

Figure 46: CYP1A1/A2 levels in CombiCult® derived HLCs

CYP1A1/A2 activity measured in raw fluorescence units (RFU) following omeprazole drug induction was assessed by an EROD assay. Differences between CYP1A1/A2 activity in the HLCs produced from the CombiCult® derived protocols were evaluated by a 1-way ANOVA with Bonferroni's post-test for multiple comparisons. Data is shown as mean ±SEM of n=3 biological repeats. Significance indicated by *** ($p<0.001$), ** ($p<0.01$), * ($p<0.05$).

5.4 Discussion

The promise to differentiate unlimited amounts of hepatocytes from pluripotent stem cells with which to carry out *in vitro* drug toxicity screens and metabolic assays has yet to be realised with currently derived HLCs displaying low levels of metabolic activity compared to primary hepatocytes [111] [106] [136]. The aim of the monolayer validation experiments was to translate protocols containing novel factors identified through the CombiCult® hepatocyte screen from a 3D system to monolayer culture. Factors that have been shown to play an important role in hepatocyte differentiation and maturation *in vivo* were incorporated into the CombiCult® screen and some of these factors were indeed found to be highly involved in producing HLCs with the highest levels of CYP450 family activity as assessed through ICC staining.

Previous studies to direct pluripotent stem cells towards the hepatic lineage have relied on the addition of recombinant growth factors including Activin A and WNT3A during the initial stages, FGF4, BMP4 and HGF during the early hepatic specification and OSM and during the latter stages of differentiation [185] [99] [106] [112] [148] [136]. Studies into targeted differentiation have increasingly focused on the replacement of recombinant growth factors with small molecule inhibitors/agonists to specifically target signalling pathways to direct differentiation to cell types of interest. Siller et al. (2015) incorporated the use of small molecules in the absence of recombinant growth factors to differentiate pluripotent stem cells to hepatocytes through the targeting of key hepatic regulators [235]. During the initial stages of differentiation the small molecule agonist CHIR99021 was used to mimic WNT/βcatenin signalling was used to specify DE as previous studies have highlighted the importance of WNT signalling during DE specification [121] [122].

Importantly for the hypothesis that Nodal is the driver of DE specification, Nodal expression was seen in this study to be upregulated after four hours using CHIR99021 [121]. Another study by Lickert et al. (2013) showed the regulation of SOX17 expression through the use of small molecule GSK3β inhibitors, mimicking WNT3A signalling, demonstrating important avenues of investigation to differentiate efficient populations of DE [271].

There is a need for a better understanding of different culture combinations at each stage of differentiation, therefore future screens could be carried out in larger scale. This would be accompanied with the incorporation of time point analysis through qPCR and ICC staining to gain a more in-depth knowledge as to the effect of culture permutations on key hepatic regulators. This is particularly important as factors incorporated into the hepatic differentiation screen could potentially have negative regulatory effects and negate the hepatic maturation properties of factors used in combination.

A key finding from the monolayer validation studies was that specific linoleic acids have toxicities and are not applicable for use during *in vitro* differentiation protocols. Form the first monolayer validation experiment it was found that linoleic acid, which was previously used in the CombiCult® screen (Sigma #L1376), was toxic to hESCs in monolayer culture. Investigation into addressing this problem led to the use of a BSA-conjugated linoleic acid (Sigma #L9530) which was shown to have no visible levels of cell toxicity or stress when applied to cells in the first stage of differentiation. The toxicity of linoleic acid has previously been investigated on different cell types including *in vitro* cell lines derived from the haematopoietic lineage. Cury-Boaventura et al. (2004) showed that the addition of linoleic acid to haematopoietic-derived cells promoted both apoptosis and cell stress [272].

Therefore, the selection of appropriate conjugated forms of linoleic acid and other differentiation promoting factors must be carefully investigated as the transition from 3D to 2D monolayer culture systems could yield different results.

Another important consideration identified through conducting the initial monolayer validation was appropriate initial seeding densities of pluripotent stem cells. Seeding densities were shown to be a critical factor in the survival of differentiated cells at the end of the first stage of differentiation. Enzymatic passaging at these early stages was seen to be deleterious to cell survival and continuation of the protocols. It was necessary to expand cell populations in stage 2 of differentiation to obtain sufficient cell numbers to proceed with differentiation and this extended cell culture could lead to the senescence and apoptosis seen in later stages of hepatic differentiation. It was seen that the rates of cell proliferation decreased as the differentiation protocols entered the third stage of differentiation and further declined during the hepatic maturation stage. The longer that the differentiating cells were in culture the bigger the decline in cell numbers was observed. Therefore, more quickly and efficiently differentiating hepatic progenitor cells to mature HLCs would be very advantageous. It has been shown by Huh et al. (2004) that decreased rates of hepatic proliferation corresponded with a decrease in HGF concentrations [273] [274] [275]. Observations of reduced rates of proliferation could be addressed using proliferation promoting factors at later stages of differentiation, such as HGF, before finally changing culture conditions to switch towards terminal differentiation of HLCs. Activators of the constitutive androstane receptor (CAR) have been shown to be transient inducers of hepatocyte proliferation [276]. In this study the small bioactive molecule CITCO was used as previous studies had identified the ability of CITCO to upregulate CAR [228].

This could be further investigated in future studies for its potential to induce hepatic proliferation at the later stages of the monolayer protocols.

A possibility in the future application of *in vitro* derived HLCs to drug toxicity/metabolic screens could be the identification of targetable proliferation inducing regulators with small bioactive molecules [228]. This would allow progenitor cell populations to be expanded without the senescence and apoptosis that is seen with transition to the final stages of differentiation for extended periods. Hepatic progenitor cells could be identified and isolated through the expression of key markers and then taken forward to hepatic maturation stages through the addition of small molecule agonists of the NHR and CYP450 family. It has been shown that HepaRG cell cultures can maintain levels of metabolic enzymes in culture for a period of 14 days and future investigation would apply the same tests to CombiCult® derived HLCs [133]. Another avenue of investigation that could be used to circumvent the senescence of hepatic cells in the third stages of differentiation could be to shorten the differentiation time course. In addition, the matrix used to differentiate cells plays an important role in recapitulating conditions *in vivo*. Collagen I was used as a basement matrix for monolayer hepatic differentiation studies but Cameron et al. (2015) has shown that Laminin promotes the proliferation of hepatic cells *in vitro* and therefore could be investigated along with the incorporation of proliferation-inducing small bioactive molecules [277].

HepaRG and hepatocellular carcinoma (HCC) cells have been previously used as a model for functional hepatocytes including the induction of CYP1A1/A2 and CYP3A4 and are currently used to study the effects of drugs *in vitro* [133] [124] [129] [278]. There is however batch-to-batch variability of HepaRG cells which have been shown to produce differing levels of inducibility upon the addition of drugs [121].

In this study, batch-to-batch variability of CYP3A4 was seen to vary amongst HepaRG cell lines however, reproducibility within cell lines was seen to be consistent [279]. Members of the CYP450 family have been successfully induced through the use of drugs including rifampicin to induce CYP3A4 [129] [280] [281]. However, it was found that the expression fold-increases of induction in the CYP450 family members was greatly increased using 3D culture systems compared to monolayer cultures.

In the study carried out by Guillouzo et al. (2007) it was found that there was an approximate two-fold induction in CYP3A4 mRNA levels in monolayer culture upon the addition of rifampicin compared to HCC cells without the addition of the inducing drug [129]. This however was much reduced than the effect seen when the HCC cells were cultured in a 3D culture system which displayed much higher basal levels of CYP3A4 mRNA and significantly greater levels of fold-induction in response to rifampicin treatment. In the RT-PCR carried out to assess hepatic maturity in the CombiCult®-derived HLCs, it was found that similar basal levels of CYP1A1/A2 were present in HLCs compared to uninduced HepaRG cells. In fact, protocol 1 was seen to display the highest levels of basal CYP1A2 compared to other protocols and HepaRG cells. Unfortunately, it was not possible to assess the levels of CYP1A1/A2 upon drug induction in this assay and future experiments would be concerned with addressing this to determine comparative levels to HepaRG cells. To better understand and assess the potential of the CombiCult® differentiated HLCs to be induced upon drug addition, future studies would incorporate the use of quantitative qPCR as opposed to the semi-quantitative RT-PCR to examine mature hepatic markers that are characteristic of hepatocytes.

In addition, further expansion of the number of hepatic markers including other members of the CYP450 family that are expressed early in development and lost during the transition to mature hepatocytes, such as CYP3A7 and conversely in the case of CYP2C9 would be a good indication of CombiCult®-derived HLC potential [282].

Comparisons between drug induction levels in control and treated cells revealed low but significant levels of CYP3A4 induction (approximately 1.5-2-fold) across the six differentiation protocols ($p<0.05$) in the p450Glo assay. As novel factors were involved during the process of hepatic differentiation, optimal concentrations have yet to be determined for some small bioactive molecules which could have a significant effect on hepatic maturation. The comparative levels of HepaRG CYP3A4 rifampicin inducibility have been quantified at differing levels in previous studies. Approximate levels from 2-40-fold increase in CYP3A4 levels have been seen in studies assessing the addition of rifampicin to HepaRG cultures [281] [124]. Therefore, it is important to optimise the culture conditions and titrations of differentiation and maturation inducing factors so the true potential of the CombiCult®-derived HLCs can be compared to the HepaRG model. CombiCult® is a powerful tool for identifying key factors in the differentiation process but their transition to monolayer culture needs to be optimised.

Even though relatively low but significant levels of CYP3A4 drug induction were quantified in the CombiCult® derived HLCs, the incorporation of the differentiated HLCs into drug toxicity assays would be a useful study to determine if they could serve as a better model than the current *in vitro* model cell line, HepaRG cells. HepaRG cells have been shown to be able to predict drug toxicity in previous studies alongside human hepatocytes but have been seem to express much lower levels of drug transporters [283].

The hepatocarcinoma cell line Huh-7 has also been assessed for a role in drug toxicity assays and was seen to be more suitable in this application than HepaRG cells [281]. Future work would incorporate HepaRG, primary hepatocytes and other *in vitro* cell lines into metabolic/toxicity assays to better assess the CombiCult® derived HLCs in comparison with the current best models for drug toxicity and metabolism. CYP1A1/A2 levels were seen to be consistent in HLCs produced from CombiCult®-derived protocols at the end of hepatic differentiation following drug induction with rifampicin and assessment in the EROD assay. A small but significant difference between CYP1A1/A2 levels in protocol 1 was observed compared to those present in HLCs derived from the other protocols ($p<0.05$). There was also a small but significant difference between increased levels of CYP1A1/A2 in protocol 21 compared to those quantified in protocol 6 ($p<0.05$). Previous studies have shown that HepaRG cells can be treated with omeprazole or other appropriate drugs to induce CYP1A1/A2 [124]. Gerets et al. (2012) quantified the increase in CYP1A1 levels of approximately two-fold [124] whilst Garcia-Canton et al. (2013) found CYP1A1 and CYP1A2 were significantly increased following drug induction [284]. To fully examine the CYP1A1/A2 fold-increases upon drug induction in future work, the CombiCult®-derived HLCs would be compared alongside HepaRG cells. This would expand upon the quantified basal levels of CYP1A1/A2 in the CombiCult-derived HLCs assessed in this study.

Siller et al. (2015) investigated a small molecule approach to the differentiation of pluripotent stem cells to functional HLCs [235]. Growth factors were replaced in this study with small molecule alternatives to increase reproducibility. Quantitative assays to assess basal CYP1A1/A2 and CYP3A4 levels and further increases upon drug induction with omeprazole (CYP1A1/A2) and rifampicin (CYP3A4) was carried out and compared between growth factor-derived HLCs and small molecule-derived HLCs.

It was shown in growth factor derived HLCs that a two-fold increase in CYP1A2 levels was achieved following drug induction in conjunction with a three-fold increase in CYP3A4. In comparison, small molecule-derived HLCs exhibited a two-fold increase in CYP1A2 levels and a two-fold increase in CYP3A4. Levels of CYP3A4 induction following drug treatment compares to similar levels of induction obtained from CombiCult®-derived HLCs in this thesis. Hay et al. (2008) differentiated hESCs to HLCs using a growth factor approach and showed that the differentiated HLCs expressed Albumin in the latter stages of differentiation however, CYP3A4 levels were seen to be comparable to those quantified in fetal liver and below levels seen in adult hepatocytes [285]. Further assessment of CYP3A4 induction levels following rifampicin drug treatment resulted in a two-fold increase in CYP3A4. Song et al. (2009) demonstrated an approximate two-fold increase in CYP450 family member activity upon drug treatment in three iPSC-derived HLC lines [107]. This was compared to significantly higher basal and drug induced levels of P450 family members present in adult primary hepatocytes. Taken together these results suggest similar levels of maturation as assessed through CYP1A1/A2 and CYP3A4 levels were achieved in CombiCult®-derived HLCs as seen in currently published *in vitro* differentiation protocols.

Following the correction and optimisation of issues arising from the two monolayer validation studies, including cell seeding density and toxicity of differentiation factors, assessment of the other top differentiation protocols identified through the CombiCult® hepatic screen need to be carried out. This will give a better understanding of the levels of hepatic maturity that can be obtained through the differentiation protocols. As many of the differentiation protocols contain factors of interest that have yet to be utilised during *in vitro* hepatic differentiation, it is important to fully determine their application to producing metabolically relevant HLCs.

Chapter 6: Hepatic Reporter Constructs

6.1 Introduction

To aid the identification and development of novel hepatic differentiation protocols through the utilisation of Plasticell's CombiCult® platform, a higher throughput method of assessing hepatic differentiation is needed. This was aimed to improve upon the current ICC maturation readout assay of staining for members of the CYP450 family to move the workflow towards a higher throughput platform. To address this current need, fluorescent lentiviral reporters were designed to allow monitoring of hepatic differentiation in real-time and allow for analysis of populations of differentiated cells throughout the CombiCult® split-pooling process. Utilising fluorescent lentiviral reporters is also advantageous as it doesn't require HLCs to be sacrificed for ICC analysis and opens the possibility for further analysis of maturation on living cells. Differentiated HLCs obtained after the split-pooling process could be put through hepatocyte maturation screens using combinations of small bioactive molecules with an aim to produce more metabolically relevant hepatocytes.

To assess the targeted effects of small bioactive molecules on signalling pathways, lentiviral vectors were created. Designed lentiviral vectors contained liver-specific fluorescence for CombiCult® real-time readouts of maturation and a luciferase reporter for accurate titration of small bioactive molecules in 2D monolayer validation studies. This was firstly investigated to identify ligands for potential hepatic master regulators and secondly to determine optimum differentiation factor concentrations with which to manipulate specific signalling pathways.

Small molecule concentrations were derived for the CombiCult® screen from previously published protocols or through informed assessment of levels during *in vivo* differentiation. However, as many of these molecules have not previously been utilised in the *in vitro* differentiation of pluripotent stem cells, translation of efficacious concentrations was made difficult and a balance between desired activity and toxicity had to be made. To effectively differentiate pluripotent stem cells to hepatocytes, optimum concentrations of small bioactive molecules that have an important role during the *in vitro* hepatic differentiation need to be determined *in vitro*. To this end optimum concentrations of small bioactive molecules to activate key signalling pathways in hepatic maturation luciferase reporter constructs were utilised. Luciferase enzymes catalyse their specific substrates in a reaction that produces light as a by-product which has previously been utilised an alternative means for the quantification of relative protein expression during *in vivo* studies [286]. This makes luciferase reporters a powerful tool and thus the application of luciferase as a reporter gene has been widely exploited in the study of promoter activity during *in vitro studies* [287].

6.2 Aims

- To create a hepatic reporter applicable to the CombiCult® platform to replace ICC staining as a readout for mature HLCs.
- To validate hepatic reporters for the *in vitro* titration of hepatic maturation inducing factors identified through CombiCult®.
- Identify optimal concentration ranges for small molecule agonists for *in vitro* studies of HLC maturation.

6.3 Results

6.3.1 Development of Liver-Specific Fluorescent Reporters

6.3.1.1 CombiCult® Hepatic Reporter Construct

A truncated version of the alpha-1-antitrypsin (α1AT) promoter was used as a liver-specific reporter in the context of hESC differentiation to hepatocytes as α1AT has been shown to be mainly synthesised in hepatocytes [288]. The serum trypsin inhibitor α1AT is expressed outside of the liver, such as in lung where it is involved in protecting tissues from enzymes of inflammatory cells, but is considered to be specifically expressed in hepatocytes in the context of hESC differentiation to the hepatic lineage [288]. The truncated promoter is designed to maintain the core transcriptional activity of the endogenous promoter but it is significantly shorter to aid lentiviral integration [289]. The α1AT promoter has been characterised previously in both *in vitro* and *in vivo* studies and shown to direct stable gene expression in liver cells [290] [291] [292] [293]. A constitutively active spleen focus forming virus (SFFV) viral promoter was used to drive the expression of eGFP to allow for a visible selection marker of successfully transduced cells (Figure 47A). The α1AT truncated promoter was placed upstream of DsRed to drive expression upon hepatic lineage differentiation from pluripotent stem cells (Figure 47B).

The lentiviral pLNT-SFFV-eGFP backbone was first linearised through digestion of a unique *Eco*RI restriction. The α1AT-DsRed insert was removed from the pcDNA3.1-α1AT-DsRed plasmid through digestion with a *PmeI* restriction enzyme to produce a blunt ended fragment.

Before being ligated into the lentiviral backbone the *Eco*RI site was blunt ended through Klenow DNA polymerase to remove the sticky end overhangs left behind through *EcoRI* digestion. Blunt ended ligation was then carried out to produce the pLNT-SFFV-eGFP- α1AT-DsRed lentiviral reporter (Figure 47C) followed by restriction digests of obtained clones to check for correct insert incorporation and orientation (Figure 47D).

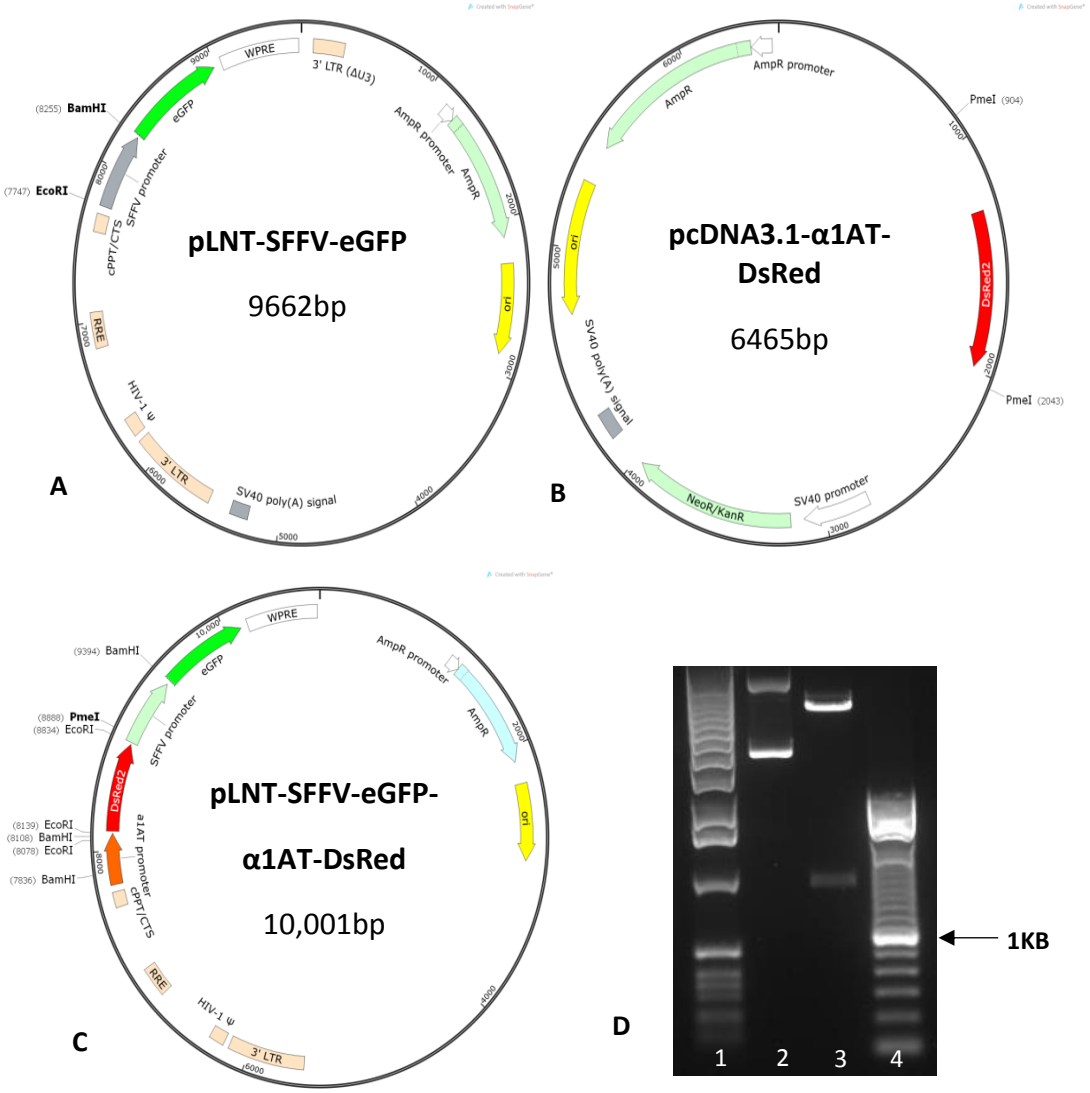

Figure 47: Creation of pLNT-SFFV-eGFP-α1AT CombiCult® hepatic reporter

(A) Plasmid map of pLNT-SFFV-eGFP lentiviral backbone. **(B)** Plasmid map of pcDNA3.1-α1AT-DsRed. **(C)** Plasmid map of completed pLNT-SFFV-eGFP-α1AT-DsRed liver reporter construct following ligatin of α1AT-DsRed into the lentiviral backbone. **(D)** Restriction digest of pLNT-SFFV-eGFP-α1AT-DsRed to check for correct clones containing the α1AT-DsRed insert. Lane 1 = 1kb DNA Hyperladder (Invitrogen). Lane 2 = Restriction digested of pLNT-SFFV-eGFP lentiviral backbone with EcoRI before blunt ending. Lane 3 = Restriction digest of pLNT-SFFV-eGFP-α1AT-DsRed with correct orientation insert α1AT-DsRed following blunt end ligation. Lane 4 = 100bp DNA ladder (Invitrogen).

To validate the liver-specific reporter construct, the *in vitro* hepatocarcinoma cell lines Huh7 and HepG2 were used. The Huh7 and HepG2 cell lines are commonly used as *in vitro* hepatocyte models although both exhibit low levels of metabolic activity and inductive potential upon drug treatment whilst also serving as inferior models for hepatotoxicity compared to primary hepatocytes. The transformed fibroblast cell line NIH-3T3 was used as a non-hepatic control to test the specificity of the liver-specific α1AT promoter. Transfection of the pLNT-SFFV-eGFP-α1AT-DsRed plasmid into hepatic and NIH-3T3 fibroblast cell lines was carried out using PEI (see Methods 2.1.10). pLNT-SFFV-eGFP-α1AT-DsRed lentivirus was produced in 293T cells and titred using a p24 assay (see Methods 2.1.11 and 2.1.12). Titred lentivirus was transduced into cell lines in three biological repeats at a concentration of 20 MOI for a period of two days in fresh DMEM-complete culture media before being refreshed with standard media every two days. Assessment of fluorescence intensity levels for both transfected and transduced cells was carried out on day five post lentiviral application.

It was found that upon transfection of the pLNT-SFFV-eGFP-α1AT-DsRed reporter construct, successfully transfected cells expressed both eGFP and DsRed, owing to HepG2 and Huh7 cells expressing α1AT (Figure 48A). In the fibroblast NIH-3T3 cell line, successful transfection was observed through eGFP fluorescence coupled with the lack of DsRed expression, owing to the integrity of the α1AT promoter and lack of α1AT expression in non-hepatic cells. However, upon lentiviral production and transduction of the hepatic reporter construct into Huh7 and HepG2 cells, there were much lower levels of DsRed expression visible compared to levels seen in transfected cells (Figure 48B). This was observed despite comparable levels of eGFP fluorescence between the transfected and transduced cells.

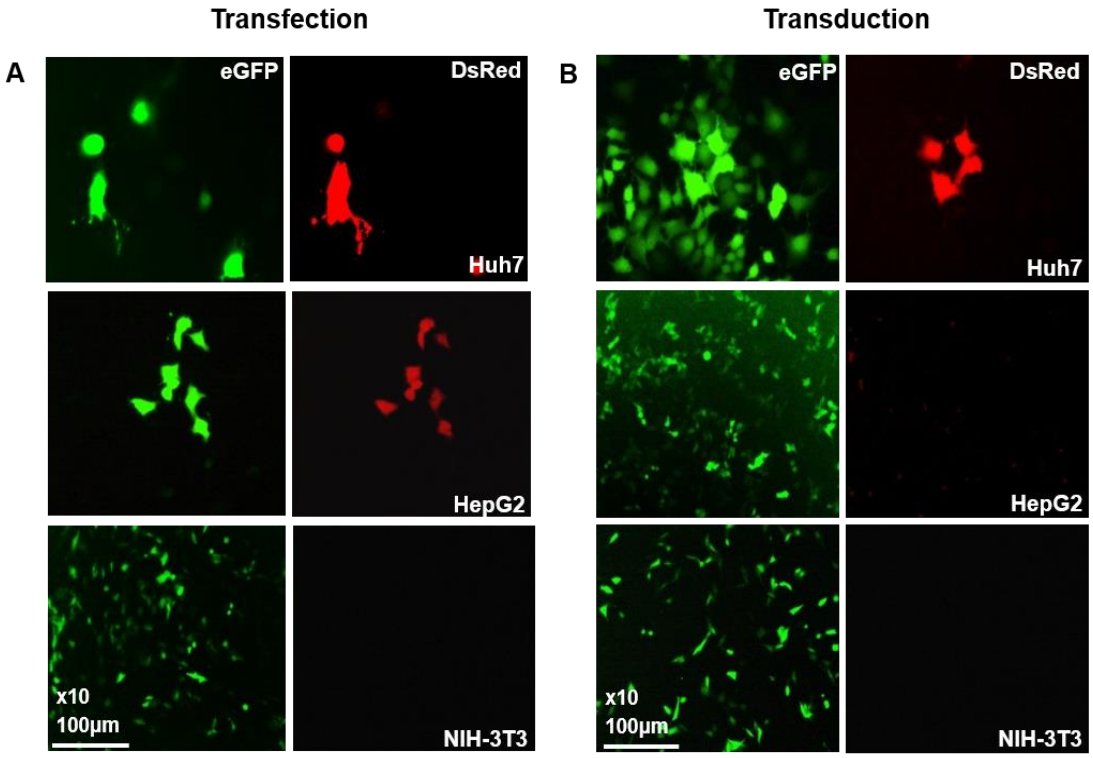

Figure 48: Validation of pLNT-SFFV-eGFP-α1AT-DsRed Reporter Construct

(A) Transfection of the pLNT-SFFV-eGFP-α1AT-DsRed hepatic reporter construct into Huh7, HepG2 and control fibroblast NIH-3T3 cell lines showing both eGFP and DsRed expression. **(B)** Lentiviral transduction of pLNT-SFFV-eGFP-α1AT-DsRed into Huh7, HepG2 and NIH-3T3 cells showing eGFP but very low levels of DsRed. Images are representative of n=3 biological repeats.

The expression of eGFP, driven by SFFV promoter, and DsRed, driven by the endogenous α1AT promoter, in transduced Huh7 cells was also assessed by flow cytometry (Figure 49). 66.8% of transduced Huh7 cells expressed eGFP (Figure 49C) whilst 0.3% were DsRed-positive. (Figure 49B). Only 0.1% of the transduced population of Huh7 cells were found to be double-positive for both eGFP and DsRed (Figure 49D). This result correlates with fluorescence microscopy results of visible levels of both eGFP and DsRed in transduced Huh7 cells.

SFFV-eGFP/α1AT-DsRed double positive cells would indicate successfully transduced cells expressing DsRed driven by the α1AT promoter in Huh7 cells.

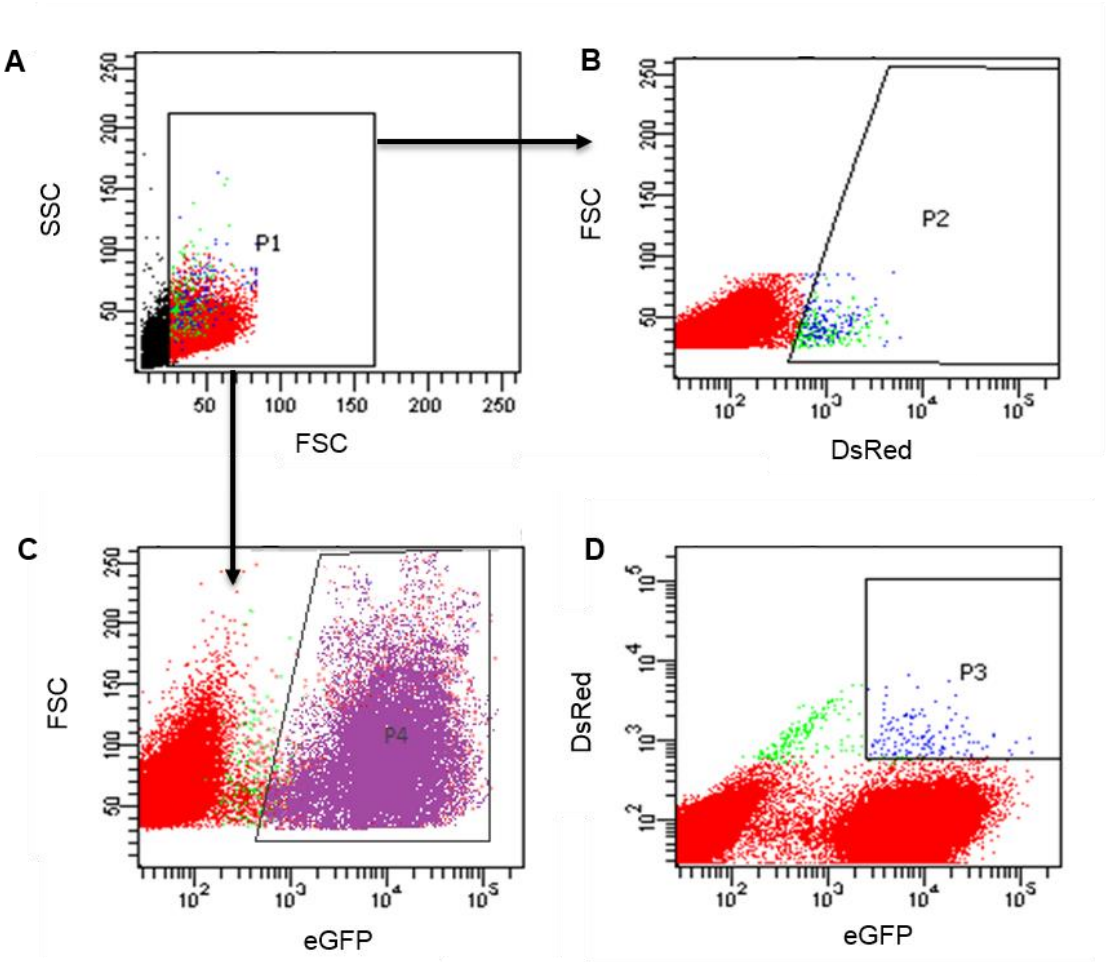

Figure 49: Flow cytometry analysis of the CombiCult® hepatic reporter

Huh7 cells were transduced with the pLNT-SFFV-eGFP-α1AT-DsRed hepatic reporter construct and fluorescence was quantified by flow cytometry. **(A)** Live cells were selected on the basis of forward scatter (FSC) and side scatter (SSC) (P1), with subsequent gating on **(B)** α1AT-DsRed+ cells (gate P2), and **(C)** SFFV-eGFP+ cells (gate P4). **(D)** Double positive α1AT-DsRed+SFFV-eGFP+ Huh7 cells are gated in P3. Note: Fluorescence gates were established to exclude background levels of fluorescence in wildtype Huh7 cells, which was subsequently removed from the analysis.

Further investigation was carried out to assess the reasons for low levels of DsRed expression of the liver-specific reporter construct into hepatic cells Huh7 and HepG2 cells upon lentiviral transduction. Methods trialled to increase the levels of DsRed expression upon lentiviral transduction included testing the hypothesis that the low levels of DsRed expression could be due to low levels of α1AT in the *in vitro* liver carcinoma Huh7 and HepG2 cell lines. This was addressed by the transient treatment of both Huh7 and HepG2 cells with DMEM-complete media containing 2% DMSO to terminally differentiate the hepatocarcinoma cell lines. It has been previously reported that transient 2% DMSO treatment for a period of three days increases the levels of liver-specific markers including α1AT in Huh7 cells [161]. This is due to DMSO being a HDAC inhibitor and forcing the unspecific differentiation of cells through the ability to disrupt the function of histone deacetylases. However, it was found that after transient 2% DMSO treatment of both Huh7 and HepG2 cells following the same previously published protocol [161], no increase in the levels of DsRed fluorescence was observed (Figure 50A). This result was further validated using an alternative HDAC inhibitor, valproic acid (VPA), which also had no effect (Figure 50B).

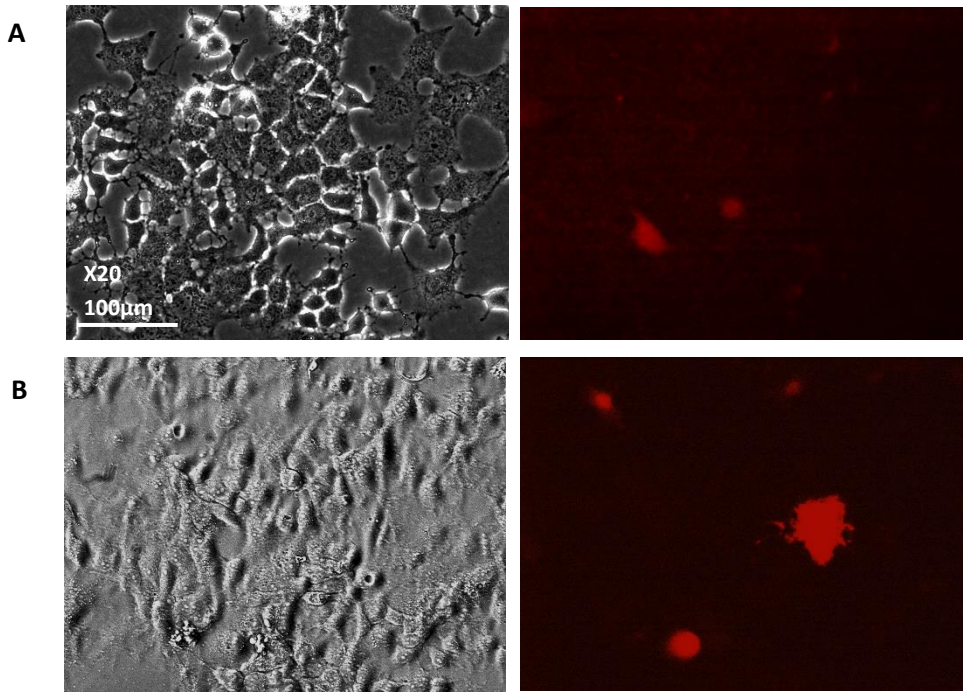

Figure 50: Effect of HDAC inhibitors on CombiCult® hepatic reporter activity

(A) Huh7 cells transduced with pLNT-SFFV-eGFP-α1AT-DsRed following three days of treatment with 2% DMSO to increase the expression of hepatic markers including α1AT. **(B)** Huh7 cells transduced with pLNT-SFFV-eGFP-α1AT-DsRed following treatment with a different HDAC inhibitor, VPA. Images are representative of three biological repeats.

6.3.1.2 pLNT- α1AT-DsRed Hepatic Reporter Construct

The next optimisation step in addressing the issue of low levels of α1AT-DsRed expression upon lentiviral transduction of the pLNT-SFFV-eGFP-α1AT-DsRed reporter construct consisted of removing the constitutive SFFV-eGFP selection element of the reporter construct. This was done to ascertain whether the strong SFFV viral promoter was interfering with the comparatively weaker truncated α1AT promoter driving DsRed expression.

To produce the optimised reporter construct after initial validation, the SFFV-eGFP element was removed from the lentiviral backbone by carrying out a *MluI* restriction digest. Vector backbone containing only the α1AT-DsRed hepatic reporter was then religated and transformed into competent *E. coli* followed by growing on ampicillin resistant plates (see Methods 2.2.3, 2.2.4 and 2.2.6). Extracted DNA was checked on a 1% agarose gel for correct clones lacking the SFFV-eGFP element. This produced a liver-specific reporter construct containing only the α1AT-DsRed hepatic reporter element with no selectable marker for transduction efficiency. Lentivirus for the pLNT-α1AT-DsRed construct was produced in 293T cells and subsequently transduced into Huh7 cells in three biological repeats (see Methods 2.1.11). It was found that there was more DsRed expression upon the removal of the SFFV-eGFP element compared to the very low expression levels seen in the previous reporter construct containing SFFV-eGFP selectable marker (Figure 51A).

DsRed expression levels driven by the α1AT promoter in pLNT-α1AT-DsRed transduced Huh7 cells were quantified through FACS analysis (see Methods 2.4.6). Fluorescence gates were established to ascertain levels of background auto-fluorescence in wildtype Huh7 cells before analysis of DsRed expression in pLNT-α1AT-DsRed transduced Huh7 cells. 29.8% of transduced Huh7 cells were positive for DsRed expression (Figure 51B). This compares to 0.3% of cells positive for sole DsRed expression and 0.1% of cells that were dual positive for eGFP and DsRed in Huh7 cells transduced with the.pLNT-SFFV-eGFP-α1AT-DsRed reporter construct (Figure 51C).

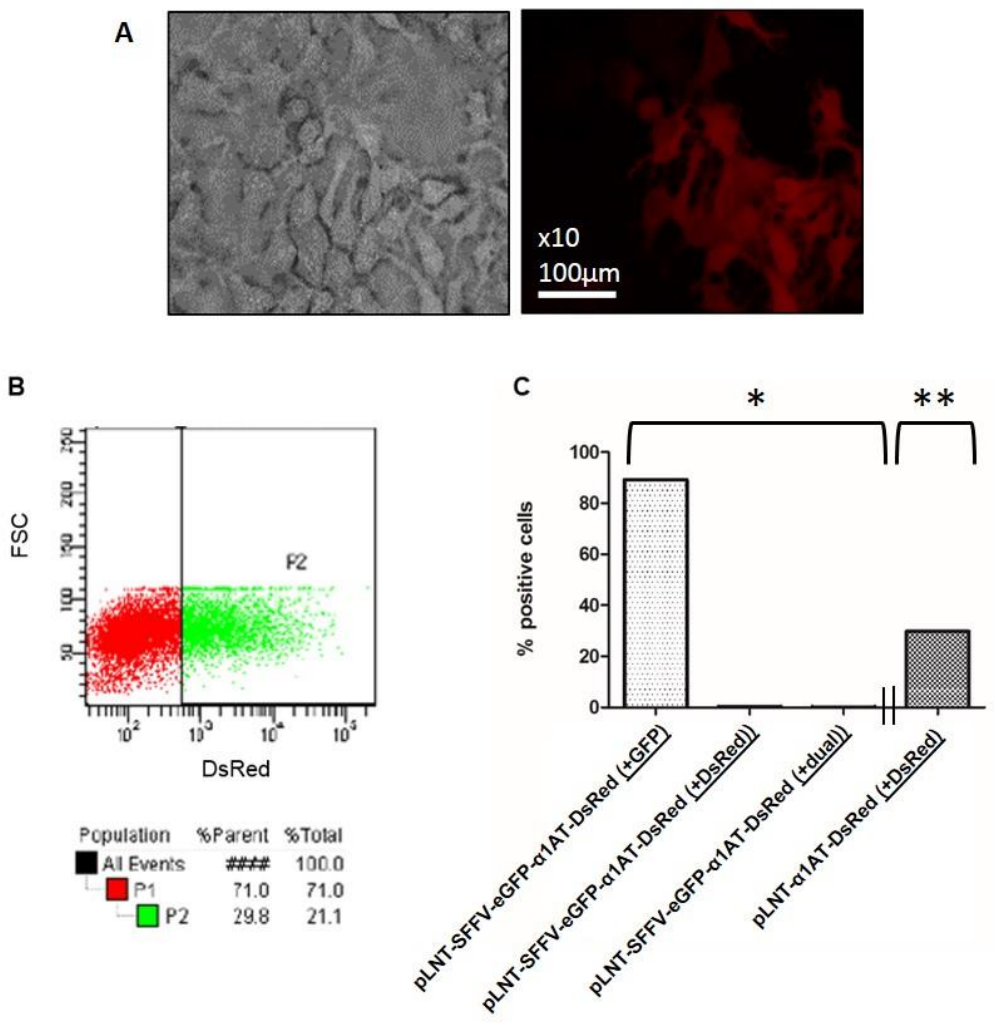

Figure 51: Validation of Optimised α1AT Liver-Specific Reporter Construct

(A) Transduction of optimised pLNT-α1AT-DsRed liver-specific construct (no SFFV-eGFP) into Huh7 showing significantly increased levels of DsRed expression. **(B)** Quantification of DsRed expression levels transduced Huh7 cells as determined by flow cytometry showing 29.8% of total cells expressing DsRed (gate P2). **(C)** Comparative quantified fluorescence in transduced Huh7 cells. ***(left)** Huh7 cells transduced with the pLNT-SFFV-eGFP- α1AT-DsRedhepatic reporter expressing sole positive eGFP (+GFP), sole positive DsRed (+DsRed) and dual positive eGFP and-DsRed (+dual). ****(right)** Huh7 cells transduced with the optimised pLNT-α1AT-DsRed reporter expressing positive DsRed (+DsRed). Presented data is from n=3 biological repeats.

6.3.1.3 pLNT-HNF4α-eGFP-Luc Hepatic Reporter Construct

HNF4α is known to be key hepatic regulator and is involved in many hepatic processes including the specification of hepatic progenitor cells from pluripotent stem cells [294] [171] [191]. The importance of HNF4α has been demonstrated by the fact that the forced expression is enough to trans-differentiate fibroblasts to HLCs with some measure of functional ability [295]. HNF4α is therefore of interest through targeting with small bioactive molecules could be employed as a strategy for producing more metabolically relevant hepatocytes. Linoleic acid has been proposed as a potential ligand for HNF4α and was therefore trialled as a potential inducer to produce more metabolically relevant HLCs. DMSO treatment is routinely used during *in vitro* culture to terminally differentiate HepaRG hepatocarcinoma cells and also used in hepatic differentiation protocols in hepatic specification stages along with other HDAC inhibitors such as sodium butyrate [133] [131] [296] [132] [297].

A lentiviral reporter construct was created to address this hypothesis which consisted of a synthetic promoter made up of eight serial HNF4α minimal binding elements driving the expression of a minimal promoter (Figure 52A). The pLNT-HNF4α-eGFP-luc lentiviral vector was created by Juliette Delhove in the McKay lab group at the WHRI, QMUL. The HNF4α promoter drives both eGFP fluorescence in pluripotent stem cell lines to monitor real-time differentiation to hepatic cells in the CombiCult® platform (Figure 52B) whilst the firefly luciferase allows for accurate quantification of HNF4α inducing factors (Figure 52C). HepaRG cells were transduced in three biological repeats with the pLNT-HNF4α-eGFP-luc lentiviral reporter at 20 MOI for two days and then media changed until the appearance of eGFP fluorescence indicating HepaRG cells expressing HNF4α (see Methods 2.1.13).

HepaRG cells were then treated for five days with assay media consisting of HBM (see Methods 2.6.1) containing either linoleic acid, 2% DMSO, linoleic acid + 2% DMSO or a control consisting of assay media. The ability of linoleic acid to increase expression of HNF4α was compared to and used in combination with 2% DMSO treatment in pLNT-HNF4α-eGFP-luc transduced HepaRG reporter cells. Following HepaRG treatment with either sole or dual inducer conditions, cells were first visualised for eGFP fluorescence driven by the from the HNF4α promoter. Levels of fluorescence from the reporter construct were assessed in comparison to control treated HepaRG cells. Subsequently, cells were lysed to carry out luciferase assays to quantitatively assess the levels of HNF4α induction (see Methods 2.5.3). After five days of treatment, it was seen that there were increased levels of eGFP fluorescence in HepaRG reporter cells treated with either linoleic acid alone or combined linoleic acid with 2% DMSO (Figure 52B). Levels of eGFP fluorescence between control cells and 2% DMSO treated reporter cells was observed to be at comparative levels. It was found through luciferase assays that sole linoleic acid treatment increased HNF4α reporter activity. An increase in reporter activation of three-fold ($p<0.001$) was observed as assessed through luciferase activity (Figure 52C). This data provides evidence for linoleic acid being a ligand for HNF4α and therefore can be used in the production of more mature HLCs upon differentiation from pluripotent hESCs. In contrast, the treatment of HepaRG cells with 2% DMSO was found to not significantly upregulate HNF4α reporter activity and was in fact shown to negatively influence the inductive potential of linoleic acid when used in combination ($p<0.01$). In addition, HepaRG cell morphology was seen to be changed upon the treatment of 2% DMSO with cells displaying a sparser, rounded morphology indicative of cell stress and apoptosis (Figure 52B).

Visualised levels of background auto-fluorescence were also found to be increased upon treatment with 2% DMSO which could also be taken as being correlated with an increase in apoptosis and cell stress.

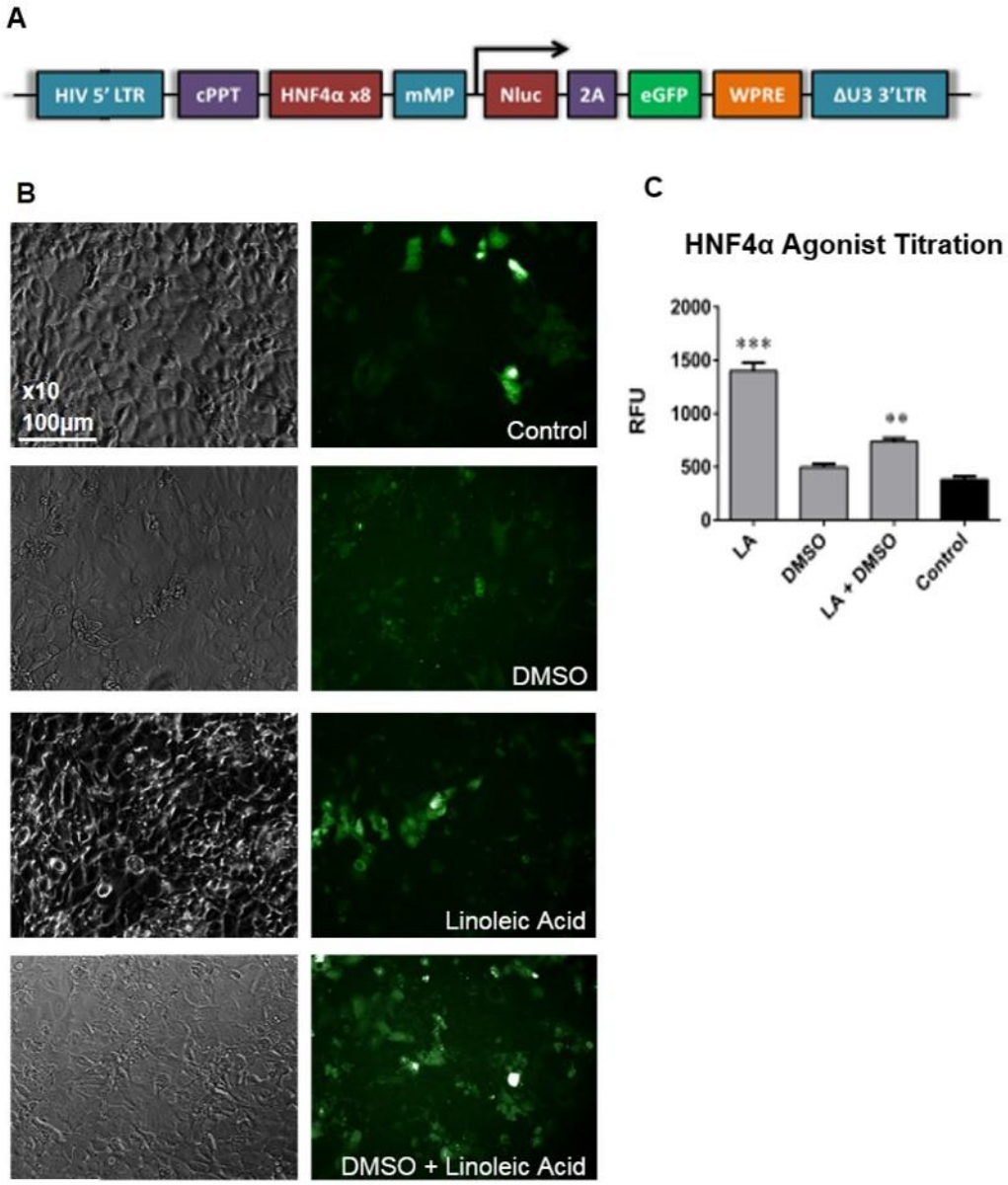

Figure 52: Linoleic Acid induction of HNF4α Reporter Construct

(A) pLNT-HNF4α-eGFP-luc lentiviral reporter construct overview demonstrating key elements. **(B)** Phase contrast and eGFP fluorescence images of lentiviral transduction of HepaRG cells with the pLNT-HNF4α-eGFP-luc reporter construct followed by either 2% DMSO, linoleic acid, combined 2% DMSO + linoleic acid or control. **(C)** Luciferase assay to measure HNF4α reporter activity upon test treatment in comparison to levels of HNF4α activity in control HepaRG cells. Data are shown as mean ± SEM of 3 repeats and differences in reporter activity versus control were determined by 1-way ANOVA with Bonferoni's post-test and significance indicated by *** ($p<0.001$) and ** ($p<0.01$). The pLNT-HNF4α-eGFP-luc lentiviral vector was created by Juliette Delhove in the McKay lab group at the WHRI, QMUL.

6.3.1.4 pLNT-LXR-eGFP-Luc Hepatic Reporter Construct

The transcription factor activated LXR reporter was constructed with a view to test the inductive ability of small bioactive molecules on NHRs with a view to upregulate CYP450 family members and produce more metabolically active HLCs. The reporter construct consisted of a synthetic promoter made up of eight serial LXR minimal binding elements driving the expression of a minimal promoter (Figure 53A). The pLNT-LXR-eGFP-luc lentiviral vector was created by Juliette Delhove in the McKay lab group at the WHRI, QMUL. Like the HNF4α reporter construct, the LXR promoter drives both eGFP fluorescence for incorporation in pluripotent stem cell lines to monitor real-time differentiation to hepatic cells in the CombiCult® platform (Figure 53B) whilst the firefly luciferase allows for accurate quantification of LXR inducing factors (Figure 53C). The targeting of NHR family members to increase the metabolic activity of HLCs differentiated from pluripotent stem cells is a key strategy in the application to drug toxicity screens. Factors involved in the upregulation of the NHRs during the CombiCult® screen included CITCO and T0901317 however their optimum concentrations during monolayer *in vitro* hepatic differentiation from pluripotent stem cells and in particular during the stages of hepatic maturation stages has not yet been determined.

To assess optimal concentrations of hepatic maturation inducing agonists, LXR reporter cells were produced using the pLNT-LXR-eGFP-luc lentiviral vector. This involved the transducing of HepaRG cells with the pLNT-LXR-eGFP-luc lentiviral vector at a 20 MOI concentration for two days and then media changed until the appearance of eGFP fluorescence indicating HepaRG cells expressing LXR. LXR reporter transduced HepaRG cells were then subjected to treatment with increasing concentrations of the T0901317 small molecule agonist to increase LXR expression.

Concentrations of 0.1µM, 1µM and 10µM was used to determine the inductive effect on the LXR reporter construct in HepaRG cells and therefore determine the optimum concentration with which to increase LXR and consequently produce the most metabolically relevant HLCs *in vitro*. T0901317 small molecule agonist containing media was refreshed day on day for a period of seven days (Figure 53B). The induction period of seven days was used to recapitulate the final stage of the CombiCult® differentiation screen which in turn was designed to improve on current *in vitro* differentiation strategies.

The small bioactive molecule T0901317 was shown to increase levels of LXR reporter activity by six-fold compared to levels of reporter activity wildtype at 1µM concentration ($p<0.001$) (Figure 53C). The 1µM concentration was seen to exhibit the highest levels of LXR reporter activation as assessed by luciferase assay in the HepaRG reporter cells. It was found that 0.1µM concentrations of T0901317 did not significantly increase levels of luciferase reporter activation in reporter HepaRG cells whilst increasing the concentration to 10µM was seen to be increase reporter activity by four-fold ($p<0.001$) compared to the control. This data demonstrates that increasing the concentration of T0901317 from 1µM to 10µM does not further increase LXR reporter activity.

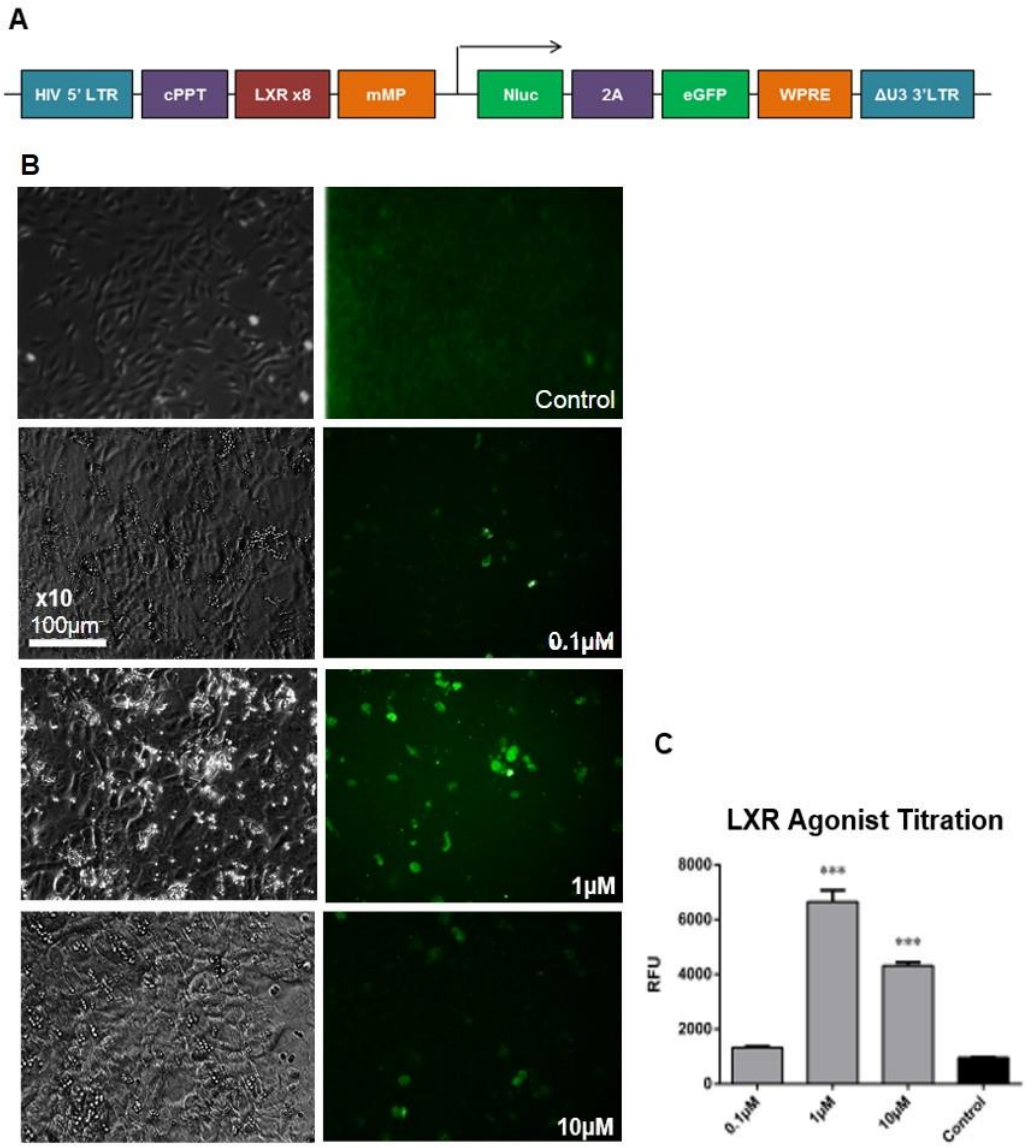

Figure 53: T0901317 Induction of LXR Reporter Construct

(A) pLNT-LXR-eGFP-luc lentiviral reporter construct overview demonstrating key elements. **(B)** Lentiviral transduction of HepaRG cells with the pLNT-LXR-eGFP-luc reporter construct followed by increasing concentrations of the small bioactive T0901317 agonist at 0.1µM, 1µM and 10µM for a period of seven days. **(C)** Luciferase assay to quantitatively measure LXR reporter activity in relative fluorescent units (RFU) upon small molecule agonist treatment for seven days. Data are shown as mean ± SEM of n repeats and differences in reporter activity versus control were determined by 1-way ANOVA with Bonferoni's post-test and significance indicated by *** ($p<0.001$). The pLNT-LXR-eGFP-luc lentiviral vector was created by Juliette Delhove in the McKay lab group at the WHRI, OMUL.

6.4 Discussion

6.4.1 Development of Liver-Specific Fluorescent Reporters

Work completed has tested liver-specific reporter constructs containing a truncated α1AT promoter driving the red fluorescent reporter gene DsRed and a second constitutive expression cassette where the green fluorescent eGFP gene is expressed from the strong constitutive SFFV gene promoter. We predicted that transduced stem cells would fluoresce green but when differentiated to hepatocytes the cells would maintain eGFP fluoresce and also DsRed due to hepatic cells expressing α1AT. It was found that this initial construct was unsuitable for use in high-throughput hepatocyte differentiation screens due to problems with SFFV-eGFP interference, resulting in very low levels of DsRed fluorescence upon viral transduction into *in vitro* liver cell lines. In initial transfection experiments, all transfected cell lines tested fluoresced green and only hepatic cell lines fluoresced red showing that the truncated α1AT promoter was specifically expressed in hepatic cell lines and not in non-hepatic control cell lines. However, lentiviral transductions of the same hepatic reporter construct showed no or very low levels of expression of the α1AT-DsRed reporter although the SFFV-eGFP reporter was fully functional. Various approaches were undertaken to resolve the anomaly between transfection and lentiviral transduction including selectively deleting each expression construct from the parental plasmid. It was found that α1AT-DsRed conditional expression could be rectified through removal of a SFFV-eGFP selectable marker. This allowed for high levels of DsRed fluorescence driven by the α1AT promoter to be obtained and quantified through FACS analysis in lentivirus transduced Huh7 cells.

Problems with co-expressing two gene cistrons in lentiviral vectors have been previously documented in which the IRES-eGFP cassette has been found to interfere with the translation of other cDNAs [298]. It has further been found that there is a much reduced expression of the second gene in these bicistronic vectors [299] [272]. The SFFV-eGFP and α1AT-DsRed are expressed in the same direction in the pLNT-SFFV-eGFP-α1AT-DsRed reporter construct and this has been shown to cause problems with the efficient expression of both gene cistrons in previously published studies. In line with this previous research, high expression from the CMV promoter driving eGFP expression was quantified whilst in contrast very low levels of DsRed expression were driven by the α1AT. An alternative strategy could be to express the eGFP and DsRed in opposite directions as this has been shown to allow for both cistrons to be successfully expressed at comparative levels [233]. The bidirectional expression approach could potentially remove the problem of promoter interference from organising the SFFV-eGFP and α1AT-DsRed cassettes in the same orientation.

Future work into producing hepatic reporter constructs could be concerned with incorporating alternative selectable marker such as a puromycin resistance gene. This can be used to select pure populations of transduced cells to be used in high-throughput differentiation screens from pluripotent stem cells to hepatocytes. However, for this to be realised the problem of promoter interference during the co-expression of two cistrons in the same direction would have to be addressed either through a bidirectional vector or through the utilisation of insulator sequences to shield from promoter interference [204] [300]. Antibiotic resistance genes rather than a fluorescence selectable marker may be more appropriate as fluorescence can only be selected through FACS.

This however could be overcome with the use of feeder-free growth conditioned pluripotent cells which can be enzymatically passaged to single cells and subsequently be recovered for replating after FACS purification through the use of ROCK inhibitor, which prevents apoptosis in single pluripotent cells [301].

If this construct proves efficacious we will compare a number of hepatic promoters replacing the truncated α1AT promoter with other relevant hepatic gene promoters. This could be done to encompass different hepatic cell markers involved in the early expansion stages and in hepatocyte maturation. Early hepatic markers such as FOXA2 and SOX17 along with mature hepatic markers such as CYP450 family members, both key to hepatocyte gene regulation and maturation, would provide real-time readout of the final and currently largely unknown steps involved in producing more functional hepatocytes. Another further direction would be concerned with the incorporation of dual reporter elements in the same lentiviral construct. This would be especially useful during the early stages of DE specification where there is a current lack of specific individual markers and current strategies therefore rely on combinations of overlapping markers to distinguish between populations of cells such as FOXA2, SOX17 and CXCR4 [77] [103]. Semb and co-workers have generated hESC lines that contain a GFP knock-in in the first intron of the FOXA2 gene which are broadly applicable to assaying DE specification in living pluripotent cells [79]; however, such analyses have been restricted to a single hESC line.

In addition to conducting targeted analysis on stage-specific regulators for hepatic differentiation, the CombiCult® hepatic differentiation screen identified a number of small molecule bioactive molecules as being important during different stages in the specification of HLCs from pluripotent hESCs.

This included the GSK3β inhibitor BIO, which was incorporated into the first stage of differentiation to mimic WNT3A signalling, typically concerned with the specification of DE from pluripotent stem cells. BIO has been used previously *in vitro* to differentiate pluripotent stem cells to DE without the exogenous addition of Activin A [121]. The activation of the WNT signalling pathway in cooperation with the activation of Nodal signalling through the exogenous addition of Activin A has been shown to more efficiently generate DE [99] [83] [263]. Other small molecules identified as being important in the CombiCult® screen included the TGFβ signalling inhibitors SB431542 and the specific SMAD3 signalling antagonist SIS3 during the hepatic specification stages of differentiation. It is known that Nodal signalling is crucial for DE specification *in vivo* however there is evidence that the downregulation of TGFβ signalling after the formation of DE and early hepatic lineage derived cells is important for further differentiation along the hepatic lineage. Previous studies have shown that Activin A/TGFβ signalling blocks the differentiation to pancreatic whilst promoting hepatic specification [82]. Spagnoli et al. (2000) implicated the downregulation of TGFβ signalling as important in the progression of bi-potent hepatic precursors to differentiate to mature hepatocytes [267]. In this way, TGFβ is important in specifying hepatic cells but the subsequent down regulation is important for maturation. The use of real-time readouts from lentiviral reporters would therefore give valuable insight into temporal signalling changes with a view to recapitulate developmental cues *in vitro*.

6.4.2 HNF4α Reporter Construct

Luciferase assays have previously been utilised an alternative means for the quantification of relative protein expression during *in vivo* studies [286]. This makes luciferase reporters a powerful tool and thus the application of luciferase as a reporter gene has been widely exploited in the study of promoter activity during *in vitro studies* [287]. The use of lentiviral constructs containing transcription factor activated binding sites which are designed and integrated upstream of a minimal promoter to drive the expression of luciferase reporters have been deployed to identify ligands for orphan receptors previously [302] [303] [304]. A parental lentivirus construct has been created by the McKay lab which allows the shuttling of consensus binding sequences through the Gateway system (Invitrogen) allowing for multiple signalling pathways to be interrogated using a common parental vector containing both eGFP and luciferase as readout assays. The use of luciferase reporters also extends to allow for the identification of temporal signalling changes over the course of cellular differentiation and serves as a powerful tool for the differentiation of pluripotent stem cells to hepatocytes. One example for the utilisation of these reporters during hepatic differentiation is in the role of TGFβ signalling firstly in the establishment of DE and then the subsequent down regulation to allow the maturation of hepatocytes. The identification of the TGFβ signalling inhibitors SB431542 and the specific SMAD3 signalling antagonist SIS3 during the hepatic specification stages of differentiation in the CombiCult® hepatocyte screen is consistent with *in vivo* knowledge [82] [267]. However, the optimal timings and dose for the administration of these small molecule inhibitors could be more precisely determined through the use of luciferase reporters which have been generated from the parental lentivirus construct through the shuffling of the TGFβ signalling consensus binding sequence upstream of a luciferase reporter cassette.

HNF4α is a key hepatic regulator and involved in many hepatic processes [171] [191]. The importance of HNF4α has been demonstrated by the fact that the forced expression is enough to trans-differentiate fibroblasts to HLCs with some measure of functional ability [295]. To investigate HNF4α during hepatic maturation, a luciferase lentiviral reporter system was used to investigate the potential of linoleic acid to upregulate the expression of the nuclear receptor HNF4α in HepaRG cells. This was investigated because of the ability of HNF4α to induce the expression of a number of the CYP450 family members and therefore presents a target to produce more metabolically relevant hepatocytes [217] [176].

It was shown that unconjugated linoleic acid was highly toxic to hESCs during the first stage of differentiation to DE and to HepaRG cultures which resulted in total cell death. This corroborates findings by Cury-Boaventura who found that linoleic acid displayed toxicity and promoted apoptosis in Raji cells; cells of hematopoietic origin [272]. In contrast, linoleic acid conjugated to BSA was found to have no discernible toxic effects when used at the same concentration on both hESCs and HepaRG cells. Five days of treatment demonstrated the ability of BSA conjugated linoleic acid to upregulate HNF4α expression three-fold in HepaRG reporter cells. It was observed that there were similar levels of GFP fluorescence between control treated HepaRG cells and sole DMSO and combined DMSO + linoleic acid treatment groups. A small increase in GFP fluorescence was seen in the sole linoleic acid treated HepaRG cells however this was quantified as a significant three-fold increase through luciferase assays ($p<0.001$). This discrepancy could be due to higher levels of autofluorescence in the HepaRG cultures that makes distinction between control and linoleic acid treatment harder to detect through fluorescence imaging but is quantifiable through more sensitive luciferase assays.

This data provides evidence that linoleic acid is indeed a ligand for HNF4α and can therefore be used with a view to produce more metabolically relevant HLCs through the ability to upregulate xenobiotic drug metabolising enzymes.

In comparison to the inductive effects of linoleic acid, 2% DMSO treatment was seen to have no effect on HNF4α expression and in fact negated the induction of linoleic acid when used in combination over five days of treatment. The HDAC inhibitors DMSO and sodium butyrate are typically used in the second stage of *in vitro* hepatic differentiation, concerned with the specification of DE to the hepatic lineage and early bi-potent hepatic progenitors [99] [133] [131] [296] [132] [297]. This is due to the ability of HDAC inhibitors to promote the activation of differentiation inducing genes through preventing removal of acetyl groups [83].

The identification of orphan receptors is important in dissecting signalling mechanisms and consequently identifying novel therapeutic targets. Sladek et al. (2002) showed that HNF4α targets and upregulates members of the CYP450 family of metabolic enzymes and therefore is an important avenue of investigation to produce more mature hepatocytes [192]. Another study by Yuan et al. (2009) used isolation/mass spectrometry (AIMS) approaches to demonstrate that HNF4α is selectively occupied by linoleic acid in mammalian cell however, the exact function of the linoleic acid ligand is yet to be fully understood [201]. Utilising agonists of hepatic master regulators at an early stage could potentially be used as a strategy to more quickly and efficiently differentiate metabolically relevant HLCs from hESCs; bypassing the traditional four-stage differentiation process *in vitro*.

A future approach could be to utilise a small bioactive molecule agonist to target HNF4α in place of linoleic acid. The identification of synthetic HNF4α agonists have been utilised previously by Lee et al. (2013) to increase levels of HNF4α with a view to increase β-cell replication [305].

In addition, phase II NHRs and transporters involved in the elimination of drug compounds are also upregulated by HNF4α [217] and the knock down of HNF4α has been shown to decrease target genes.

The next stage of analysis would be to transduce pluripotent hESCs with the HNF4α reporter construct and assess the optimal time during hepatic differentiation to administer linoleic acid by taking cell lysate samples for luciferase reporter activation using the current reporter construct. A future direction of investigation would be to incorporate the HNF4α promoter into the secreted Nanoluc lentiviral reporters. As well as holding advantages in fluorescence intensity and lower background fluorescence levels this new generation of luciferase reporter has the distinct advantage of being a naturally secreted form of luciferase allowing for conditioned media to be collected as opposed to lysing cells [306]. This would be advantageous in the context of this study and in the CombiCult® platform as it allows for the day-on-day changes in HNF4α to be assessed and give a better understanding as to key inducers of master hepatic regulators. Linoleic acid was used in the first stage of differentiation during the CombiCult® differentiation screen and therefore could be utilised in more efficiently differentiating hESCs to HLCs by the utilisation at different stages of differentiation.

6.4.3 LXR Reporter Construct

The small bioactive molecule T0901317 was used assess the optimum concentration to upregulate LXR reporter activity. This was investigated as LXR and other NHRs have a direct effect of the upregulation of members of the CYP450 family and can be used as a strategy to produce more metabolically relevant hepatocytes. It was shown that 1µM concentration T0901317 increased levels of LXR activity by six-fold compared to control treated HepaRG cells. It has previously been implicated by Mitro et al. (2007) that the small molecule agonist T0901317 also has a degree of affinity for another member of the NHR family, the PXR [307]. It was shown that T0901317 increases the activity of PXR target genes in addition to targets of LXR including CD36, which is involved in metabolism of fatty acids. In addition, transcriptomic screening by Chen et al. (2014) showed that the overexpression of LXR promoted hepatic maturation of bi-potent HepaRG cell cultures [102]. This study suggests that LXR is important in hepatic maturation through increasing markers and functions of mature hepatocytes including increased metabolic enzyme activity, urea secretion and glycogen metabolism. LXR was also been shown to increase the expression of a number of proliferation-associated factors including HNF4α. HepaRG cells are routinely used in toxicity studies and are normally required to be terminally differentiated in DMSO containing culture media for a period of four weeks. However, this same study demonstrated that through the overexpression of LXR functional differentiated HLCs could be obtained after seven days. This gives rise for the potential of the small bioactive molecule T0901317 to be utilised to target and upregulate LXR as opposed to the use of overexpression constructs.

Transferring this knowledge to the *in vitro* differentiation of HLCs from pluripotent stem cells can be used as a strategy for producing more metabolically relevant hepatocytes in future studies. Further to this, LXR is associated with the peroxisome proliferator-activated receptor (PPAR) pathway which in turn is implicated in the maturation of hepatic cells and tissue and in liver regeneration [308]. The ability of T0901317 to induce a wider range of target genes is not shared by more specific LXR agonists, such as GW3965. GW3965 was investigated as a maturation inducing factor and also identified as being important in the final stage of the CombiCult® hepatocyte screen through the ability of GW3965 to induce LXR activation [309]. However, the utilisation of T0901317 could be used with a view to increase the activity of a wider range of LXR/PXR target genes during the latter stages of hepatic differentiation to produce more metabolically functional hepatocytes.

With a view to future hepatic maturation studies, luciferase reporters allow an accurate quantification of reporter activity whilst the new generation of secreted Nluc lentiviral vectors allow day on day changes in reporter activity to be assessed. Therefore, they hold an advantage over traditional luciferase reporters which require the lysing of cells at the end of the differentiation process to assess levels of reporter induction/inhibition. In this way, day on day changes in master hepatic maturation factors can be determined with much greater accuracy and in real-time which would allow for a much more in-depth analysis of differentiation.

Chapter 7: General Discussion

7.1 Project Overview

The findings of this research project have contributed to the overall knowledge and understanding of the differentiation of pluripotent stem cells to HLCs. Insights gained have helped move towards the goal of achieving the production of metabolically relevant hepatocytes for the use in drug toxicity screens. This thesis has demonstrated the following findings:

- **CMV promoters are not highly expressed in pluripotent hESCs.**
- **Novel factors promote hepatic maturation *in vitro*.**
- **Linoleic acid is a ligand for the HNF4α receptor.**
- **Luciferase reporters can be utilised to determine optimum concentrations of maturation inducing agonists.**

There is a demand from the biotechnology industry for an inexhaustible supply of metabolically functional hepatocytes to be used in regenerative medicine to help to repair, augment or replace damaged tissues and with which to perform toxicity assay screens on early stage drugs. It has been shown in rat models that hepatocytes have the capacity to undergo high levels of proliferation following hepatectomy [164]. However, isolated primary hepatocytes quickly lose their proliferative potential when cultured *in vitro* and dedifferentiate [310]. The liver-specific functions of these primary hepatocytes have been seen to be progressively lost with extended *in vitro* culture due to gene expression changes in master hepatic regulators [310]. Phenotypic and genotypic variability is also a significant problem amongst isolated donor primary hepatocyte samples.

Current HLCs produced through the *in vitro* differentiation rely on the exogenous addition of growth factors [111] [145] [136] and so far have yet to show the proliferative potential and functional activity of *in vivo* hepatocytes.

The *in vitro* differentiation of pluripotent stem cells to hepatocytes is hampered by two major bottlenecks. Firstly, in DE specification from pluripotent stem cells where Nodal is known to be the key driver during *in vivo* mouse development [91] [109]. However, it has been shown that the addition of exogenous recombinant Nodal to monolayer cultures of pluripotent stem cells resulted in a lack of differentiation and no suppression of pluripotent markers as assessed through qPCR and undifferentiated colony morphology [245]. Consequently the related TGFβ family member Activin A is routinely used to mimic Nodal signalling and differentiate human pluripotent stem cells *in vitro* [87] [110] [111] [84] [145] [83]. However, the use of Activin A produces off target gene activation (McKay et al unpublished) in the process of DE specification. Investigation into the underlying signalling mechanisms is therefore needed with a view to efficiently differentiate pluripotent stem cells to homogenous populations of DE.

The second bottleneck is in the maturation of differentiated cells to metabolically relevant hepatocytes. Currently, only foetal-like HLCs have been produced which exhibit low levels of metabolic activity and inducibility upon drug administration [111] [145] [136]. The maturation of these pluripotent stem cell derived HLCs has so far remained elusive and the signalling cues pushing the terminal differentiation of hepatocytes *in vitro* have yet to be fully understood. The ability of pluripotent stem cells to give rise to unlimited amounts of cell types of interest makes then an extremely attractive proposition.

7.1.1 CMV promoters display low transduction and expression in hESCs

Tools with which to knock down Nodal/Cripto signalling *in vitro* were assessed using lentiviral shRNA vectors. The pGIPZ lentiviral shRNA vector system utilise the CMV viral promoter driving shRNA knock down of Nodal/Cripto. However, after extended investigation using both the huES1-OCT4-GFP and Shef3 hESC lines successful pGIPZ transgene expression could not be obtained at any lentiviral MOI concentration trialled. The failure in transgene expression from the pGIPZ lentiviral vectors into both huES1-OCT4-eGFP and Shef3 cell lines has hampered the further dissection of the role of Nodal/Cripto in DE specification through gene knockdown. Other promoters from different lentiviral vectors used in this thesis such as the SFFV viral promoter to drive expression of eGFP have been successfully transduced and expressed in pluripotent stem cell lines. Taken together, this provides evidence that there is a problem with expression of the CMV promoter in human pluripotent stem cell lines.

The use of lentiviral vectors to genetically modify a host genome through delivery of transgenes is a powerful tool to dissect signalling mechanisms or drive differentiation of stem cells [311]. Lentiviral vectors display high transduction levels in a number of cell lines tested however the expression of transgenes has been seen to be a problem; particularly in human pluripotent stem cells [110]. A mechanism of DNA methylation-mediated silencing has been proposed by Cherry et al. (2000) who showed that culture of ES cells transduced with a retroviral vector lost expression of GFP driven by a viral promoter. Subsequent treatment with a DNA demethylating agent, 5-azadeoxycytidine, was sufficient to reactivate expression of GFP. This leads suggests that the expression of transgenes in ES cells is regulated in part by methylation-dependant mechanisms [312].

A number of previous studies have found the lack of efficient expression of the CMV promoter in pluripotent stem cell lines followed by rapid silencing [251] [253] [253] [254] [110] [312] corroborating the findings in this thesis. In these studies, alternative viral promotes including human elongation factor 1α (EF1α) and phosphoglycerate kinase 1 promoter (PGK) were shown to be more highly expressed and maintain expression levels for extended periods of cell culture in comparison to CMV promoters. This makes them a better option for the use in gene knock down and overexpression experiments in human pluripotent stem cell studies.

Promoter interference has also been hypothesised as a reason for low CMV expression levels in pluripotent stem cell lines transduced with dual reporter constructs. Luo et al. (2014) proposed that interference between two promoters, CMV and EF1α, was responsible for lack of eGFP fluorescence which was driven by a CMV promoter [313]. Interestingly, the red fluorescence protein expressed through the EF1α promoter in this construct was maintained after eGFP was no longer detectable through microscopy in pluripotent cell lines. Promoter interference between the PGK promoter driving puromycin resistance in the pGIPZ construct and the CMV promoter driving shRNA knockdown could be a reason for the lack of detectable eGFP fluorescence in the Nodal/Cripto shRNA knock down lentiviral constructs. The findings in this thesis and other studies therefore highlight the problems in expression of the CMV viral promoter in hESCs [313].

7.1.2 Nodal/Cripto conditioned media specifies SOX17+ cells

Conditioned media has previously been utilised to promote the maintenance of pluripotency in a feeder-free conditioned human pluripotent cell lines. This has been achieved through the collection of conditioned media produced from supportive MEF feeder cells and application to feeder-free cells on an appropriate ECM [25] [17] [25]. The same approach was used with a view to differentiate pluripotent cells through the application of DE inducing factors as opposed to maintaining them in a pluripotent state. The approach of using conditioned media to differentiate stem cells has been applied previously to oestrogenic and chondrogenic differentiation [314], neuronal differentiation [315], cardiac differentiation [316] showing the potential of isolating differentiation factors in conditioned media to drive pluripotent stem cell differentiation.

In this thesis, “producer cells” were created to secrete Nodal and Cripto proteins into cell culture media which was collected following 24 hours of conditioning and subsequently exhibited activation of TGFβ reporter cells. Nodal/Cripto conditioned media treatment resulted in SOX17+ cells, a marker of DE, from pluripotent stem cells as assessed through ICC staining. Nodal/Cripto conditioned media as well as 100ng/ml Activin A treatment was seen to produce greater numbers of SOX17+ cells over a period of five days against differentiation in basal media with no DE inducing factors. It is of note however that even though there were very few cells following treatment with basal media containing no DE inducing factors, they were almost exclusively SOX17+. Levels of SOX17+ staining as assessed through ICC staining was seen to be comparative between sole Nodal, sole Cripto and combined Nodal/Cripto conditioned media assessed against the use of 100ng/ml Activin A.

The comparative numbers of cells staining positive for SOX17+ was surprising in the sole Cripto conditioned media treatments as Cripto is not a direct ligand for the activation of TGFβ signalling but is in fact a signalling co-factor of Nodal. This result could be evidence of the amplification of existing Nodal signalling through the presence of excess Cripto. Nodal/Cripto conditioned media treatments and the use of 100ng/ml Activin A was seen to increase the numbers of SOX17+ cells compared to cells treated with media containing additional DE inducing factors. This would be expected as the default differentiation pathway of human pluripotent stem cells is biased towards the neuroectodermal lineage [245] [19] [83].

The ability of Nodal/Cripto conditioned media to produce SOX17+ cells demonstrates the potential of using the Nodal/Cripto conditioned media approach as opposed to Activin A to differentiate pluripotent stem cells to DE *in vitro*. Further investigation is needed to properly characterise the difference in the populations of SOX17+ cells produced through conditioned media versus the use of 100ng/ml Activin A, which has been shown to activate off target gene expression (McKay et al. unpublished). Current DE specification efficiencies through the utilisation of Activin A are ~70-85% of the differentiated cell population as assessed through the staining of markers such as SOX17 and FOXA2 [148] [83]. Numbers of ICC stained SOX17+ cells obtained through Nodal/Cripto conditioned media was seen to be at comparable levels to the addition of 100ng/ml Activin A. ICC staining for the co-localisation of a battery of DE markers including FOXA2 and CXCR4 would allow better assessment of the populations of SOX17+ cells seen in this study along with qPCR analysis.

It has been shown that WNT signalling in collaboration with Activin A more efficiently specifies DE cells with higher expression of characteristic markers [99]. Further evidence of the importance of WNT signalling was demonstrated by Tahamtini et al. (2013) who used the small molecule CHIR99021, a GSK-3β inhibitor mimicking WNT signalling activation, to prime pluripotent stem cells which exhibited increased numbers of both SOX17 and FOXA2 cells upon DE differentiation using Activin A than populations observed without priming [122]. It has been hypothesised through previous studies that the targeted activation of WNT signalling through the use of small bioactive molecules upregulates the downstream expression of Nodal and this is the driver of efficient DE specification *in vitro* [121]. The use of Nodal/Cripto conditioned media with GSK-3β inhibitors is therefore an avenue of investigation to potentially amplify the homogenous differentiation of pluripotent stem cells to DE.

7.1.3 Novel factors promote hepatic maturation *in vitro*

This project set out to identify novel hepatic maturation inducting factors as well as to transfer *in vivo* knowledge of hepatic specification to *in vitro* cell culture systems to differentiate pluripotent stem cells to metabolically relevant hepatocytes. Through the completion of the CombiCult® hepatocyte screen, novel factors were identified which promoted differentiation at different stages to the most highly expressing CYP1A1/A2 and CYP3A4 HLCs (Figure 54). Following monolayer validation utilising CombiCult®-identified factors it was found that the highest levels of CYP3A4 induction was in protocols containing hepatic differentiation factors which have not previously been applied to *in vitro* protocols.

It was found that small but significant increases in the levels of CYP3A4 family induction upon drug administration could be achieved. Although further optimisation of the concentrations of small bioactive agonists need to be accurately defined which promote optimal activation whilst avoiding toxicity. CYP1A1/A2 levels were seen to be consistent across all protocols tested in this study. From observations seen in the completion of the CombiCult® hepatocyte screen, novel factors were identified including small molecule inhibitors/agonists of pathways known to be important along the process of hepatic differentiation. Key factors and conclusions from individual stages of CombiCult® differentiation are detailed in the following sections:

7.1.3.1 TGFβ signalling inhibition

Nodal signalling is critical for establishment of DE during early *in vivo* development, capable of giving rise to both DE and mesoderm [246] [87]. High levels of Nodal signalling persist until DE is specified and is subsequently down regulated [87] [88]. The down regulation of Nodal signalling is required for the progression to the hepatic lineage from specified DE [82] [246]. SB-431542, a TGFβ1/Alk7 inhibitor has been used in recent studies to promote hepatic specification and maturation and was seen in this thesis to be present in a large majority of top differentiation protocols [236]. The specific SMAD3 signal inhibitor SIS3 was also found to be present in the majority of top protocols in the second stage of differentiation and consequently associated with producing the most dual-positive CYP1A1/A2 and CYP3A4 HLCs. This provides further evidence that TGFβ signalling inhibition following the establishment of DE populations from pluripotent stem cells in the first stage of differentiation is important for the progression to the hepatic lineage during *in vitro* protocols.

7.1.3.2 Growth factors

Growth factors including TGFα were found to be highly prevalent in the protocols which produced the highest CYP1A1/A2 and CYP3A4 expressing HLCs. TGFα was utilised in the third stage of differentiation concerned with the proliferation of hepatic progenitor cells following specification from DE cells. The result that TGFα is prevalent in differentiation protocols at this stage of differentiation is in line with findings observed through *in vivo* studies. TGFα has been shown to be involved in the promotion of hepatic progenitor cell pool proliferation and expansion in cooperation with HGF upon liver injury; it's proliferative potential has further been implicated in hepatocellular carcinoma through overexpression in mice models [317] [318] [319].

7.1.3.3 NHR agonists

Small molecule agonists of PXR, CAR, LXR and PPARα in the later stages of differentiation were found to be present in a large majority of the top 23 CombiCult® differentiation protocols. The LXR agonists T0901317 and GW3965, CAR agonist CITCO, PXR agonist SR12813 and PPARα agonist GW7647 were all found to be present in the top protocols.

NHRs are known to be key factors in liver metabolism through the regulation of members of the CYP450 family. In this way, NHRs are involved in the regulation of detoxification and removal of xenobiotic compounds [320] [214]. The ability to target NHR induction for maturation and detoxification purposes through the utilisation of small bioactive molecules is therefore of interest for the use in drug toxicity screens [264] [321] [322]. As a result, current studies are increasingly focussed on the use of small molecule inhibitors/agonists of key signalling pathways through the stages of hepatic differentiation [235] [234] [236].

7.1.3.4 Fatty acids

Additional factors present in the final stage of the CombiCult® protocols included the fatty acid DHA. The effects of DHA has been studied in child patients with non-alcoholic fatty liver disease (NAFLD) and it was found to promote hepatocyte survival and hepatic progenitor cell activation as assessed through the comparison of before and after liver biopsies [323]. DHA was found in combination with small molecule agonists of NHRs in protocols producing the most highly expressing CYP1A1/A2 and CYP3A4 HLCs. Linoleic acid was also identified in a number of top CombiCult® protocols during early stages of differentiation. Linoleic acid is a proposed ligand for HNF4α [324] [212] which has been shown to be a key in the development of the liver [189] [190] [191].

7.1.3.5 Hormones

In addition to small bioactive molecules, hormones including progesterone and βestradiol, which have not previously been studied in the context of hepatic differentiation and maturation *in vitro*, were identified as potential avenues for further investigation to promote hepatic maturation. Progesterone and βestradiol were found to be present in 12 out of 23 of the top protocols identified through the CombiCult® hepatocyte screen. It is not yet clear the mechanisms by which these hormones promote hepatic maturation in the later stages of differentiation but it has been shown by Filant et al. (2012) that progesterone upregulates Hgf expression in the uterus of sheep and could be a mechanism for hepatic maturation [325].

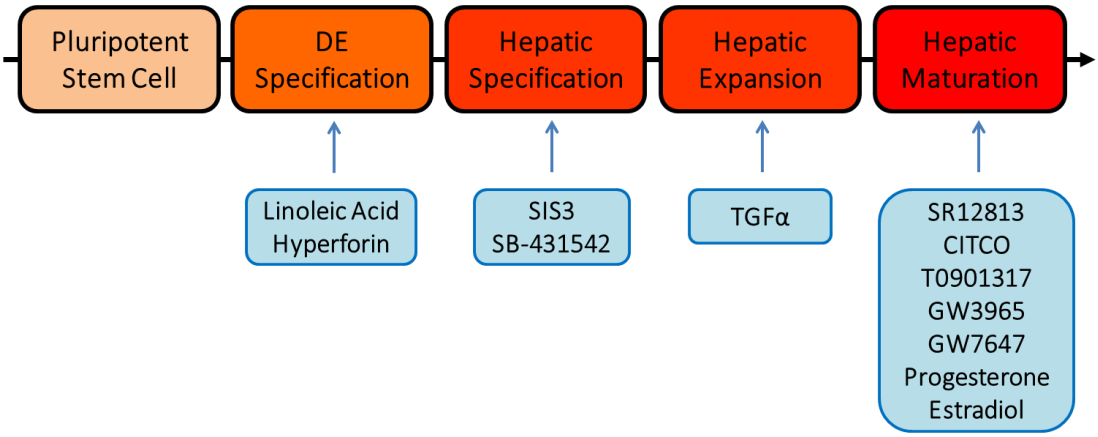

Figure 54: Novel hepatic differentiation factors identified through CombiCult®

New *in vitro* differentiation factors were identified through the four stages for hepatic specification and maturation utilising the CombiCult® platform. Novel factors are displayed below the stage of differentiation which they were found to be prevalent in producing the most highly expressing CYP1A1/A2 and CYP3A4 HLCs in the CombiCult® hepatic screen.

7.1.4 Linoleic acid is a ligand for HNF4α

The identification of orphan receptor ligands is important in dissecting signalling mechanisms and consequently identifying novel therapeutic targets with which to differentiate cell types of interest. Utilising small bioactive molecules in this thesis was aimed to induce the upregulation of key hepatic regulators at different points along the differentiation process to more efficiently differentiate metabolically relevant HLCs. In other studies it has been shown that HNF4α, a hepatic master regulator, plays a key role in the development of the liver [189] [190] [191] [212]. Jover et al. (2004) showed that HNF4α regulates a wide variety of liver specific factors including members of the CYP450 superfamily of metabolic enzymes including CYP3A4 [198].

However, the HNF4α ligand has remained largely elusive despite a number of proposed candidates including linoleic acid [324] [212]. Due to the key role played by HNF4α as a general regulator of members of the CYP450 family, the targeted activation of HNF4α can be utilised with a view to producing more metabolically active hepatocytes *in vitro* through the ability of HNF4α to upregulate xenobiotic drug metabolising enzymes.

A luciferase reporter containing a HNF4α synthetic promoter made up of eight serial HNF4α minimal binding elements driving the expression of a minimal promoter allowed the quantitative analysis of linoleic acid induction of HNF4α. This was carried out to address the hypothesis that linoleic acid is a ligand for HNF4α [324]. Using this reporter system, it was shown that treatment with BSA-conjugated linoleic acid had the ability to upregulate HNF4α activity three-fold in HepaRG cells. This outcome provides further evidence that linoleic acid is a ligand for the HNF4α receptor and is in line with previous studies suggesting the inductive potential of linoleic acid [324]. Future work would be concerned with the optimal time to administer linoleic acid. In the CombiCult® screen and subsequent monolayer validation linoleic acid was only used in the first stage of differentiation but due to the inductive potential on HNF4α activity, the use at later stages of differentiation should be investigated.

7.2 Future Work

7.2.1 DE Specification

The use of lentiviral shRNA vectors driven with different viral promoters could be a new direction with which to knock down Nodal/Cripto in hESCs before quantitative analysis of DE populations. The CMV containing pGIPZ promoters could not be expressed in the pluripotent stem cell lines in this study but the utilisation of different viral promoters shown to exhibit superior expression could be addressed. Future work concerning the use of Nodal/Cripto overexpression conditioned media would primarily concerned with the further validation of the concept through quantitative qPCR analysis for the loss of pluripotency-associated markers including OCT4, SOX2 and NANOG coupled with the induction of marker sets characteristic of DE including SOX17, FOXA2 and CXCR4. Comparisons would be made into the differences in gene expression between the use of Nodal/Cripto conditioned media and the use of Activin A. Comparative day-on-day changes concerning suppression of pluripotency-associated markers coupled with analysing the robustness of DE specific gene expression would give a better understanding of the underlying signalling mechanisms. A goal of disecting the underlying signalling mechanisms would be the replacement of growth factors with potent agonists of the Nodal signalling pathway with a view to more efficiently differentiate DE cells.

Further future DE specification approaches that could be addressed include the overexpression of DE inducing factors, including SOX17. Studies in mouse embryonal carcinoma cells, which closely mimic epiblast cells, have shown that the overexpression of LIM homeobox 1 (Lhx1) promotes differentiation to DE as assessed through the presence of the endoderm markers Sox17, FoxA2 and Gata6 [326].

Interestingly, investigation by Hasegawa and Shirayoshi (2015) showed that the overexpression of Lhx1 did not result in the induction of markers associated with extra-embryonic endoderm including Sox7 and Hnf4α [326]. Other studies carried out in mouse pluripotent stem cells demonstrated that the overexpression of Sox17 promoted the expression of endoderm-specific genes and differentiation towards DE [327]. Down regulation of Sox17 in separate studies have demonstrated the maintenance of pluripotency markers and the lack of differentiation potential whilst forced expression promotes differentiation to endoderm [328].

In addition to the role of Nodal/Cripto in DE specification, LGR5 is a source of future investigation. LGR5 is a marker which was found through transcriptomic analysis to be strongly upregulated following six days of DE specification from pluripotent stem cells utilising day-on-day addition of Activin A (McKay et al. unpublished). The role of LGR5 is therefore of interest in the specification of DE from pluripotent stem cells and is a source of future study to more efficiently differentiate DE. LGR5 was first identified as a marker of rapidly self-renewing intestinal crypt stem cells [329] and subsequently found in self-renewing multipotent stem cells in the stomach [330] and hair follicles [331] as well as marker of endodermal progenitor (EP) cells [332]. LGR5 has also been shown to be a WNT signalling target so the role of LGR5 in DE specification is an interesting prospect [323] [333]. Further to the potential role in DE specification, LRG5 has been shown to be upregulated in response to liver injury in coordination with the onset of WNT signalling to promote the self-renewal of progenitor cells to repopulate damaged tissue [334]. The targeting of LRG5 is therefore attractive as WNT signalling is important in both DE specification and in hepatic differentiation.

The role of WNT signalling during the specification of DE could be further examined through the use WNT overexpression conditioned media using lentiviral constructs that the McKay lab have already produced.

7.2.2 Hepatic Maturation

Future investigation of the CombiCult® derived HLCs would include comparisons with isolated primary hepatocytes and more in-depth comparisons with HepaRG cells. This comparative analysis would follow the optimisation of identified hepatic maturation inducing factors to better assess levels of hepatic maturity between optimised protocols and the current best models for metabolic assays.

Following the identification of certain factors at defined stages of differentiation including linoleic acid, TGFβ signalling inhibitors, TGFα, progesterone, βestradiol, small molecule agonists of the NHRs and CYP450 family members, different media permutations would be explored to identify factors that best work in synergy to promote hepatic specification and maturation. The utilisation of fluorescent lentiviral reporter cell lines produced in this thesis have given a better understanding of ligands for hepatic master regulators as well as a platform to determine optimum concentrations of small bioactive molecules with which to promote hepatic maturation.The use of lentiviral reporters could also be used in future investigations to give an accurate quantification of factors promoting the induction of critical regulatory processes during hepatic differentiation *in* vitro. These would include small molecule agonists including LXR agonists T0901317 and GW3965, CAR agonist CITCO, PXR agonist SR12813 and PPARα agonist GW7647 identified through the CombiCult® hepatocyte screen.

The use of fluorescent-luciferase reporters could be extended in future work across all stages of hepatic differentiation to give better insights into new, novel factors that are critical at key checkpoints along this process. This could include the incorporation of SOX17 and FOXA2 into a lentivrial reporter construct to better assess the effects of small molecule agonists on early *in vitro* DE specification.

With the power of the CombiCult® platform to identify new and novel factors that promote the differentiation of pluripotent stem cells, hepatic maturation screens could be carried out with a much larger scope to incorporate increased numbers of potential maturation inducing molecules. This approach could be investigated once hepatic progenitor populations are established following stage 3 of differentiation.

7.3 Conclusion

The CombiCult® technology platform developed by Plasticell has successfully been applied to commercially produce “osteoMAX-XF” defined culture media to efficiently differentiate osteogenic cells from mesenchymal stem cells (MSCs), demonstrating the power and potential of the platform being applied to obtain cell types of interest. These osteogenic cells were shown to exhibit superior characteristics than previously available protocols. This was achieved through the identification of key media components that allow for efficient differentiation in the CombiCult® platform [335]. The use of the CombiCult® platform in this project has provided new avenues of investigation with new and novel hepatic differentiation/maturation inducing factors. Traditionally differentiation protocols have been reliant on trial and error experiments utilising growth factors which is both costly and time consuming.

Significant progress in the differentiation of pluripotent stem cells to DE and subsequently hepatic specification has been made but the CombiCult® platform can fast track the isolation of efficient differentiation protocols.

The aim of this thesis was to investigate the production of metabolically relevant hepatocytes and whilst HLCs derived from this project so far haven't produced large changes in CYP450 family member activity upon drug administration, advances in the identification of small molecules to direct differentiation have been made. There however remains a lack of understanding concerned with the efficient differentiation of DE from pluripotent stem cells from which the hepatic lineage is derived. The role of Nodal signalling has been well characterised *in vivo* and future work is ongoing into the precise manipulations required to more efficiently generate DE in comparison to the use of Activin A. There remain many avenues of investigation into identification of new hepatic maturation inducing factors as well as media/matrix combinations with which to best differentiate the most metabolically relevant hepatocytes.

Thesis Bibliography

1. Kaneko, K.J., *Chapter Eight - Metabolism of Preimplantation Embryo Development: A Bystander or an Active Participant?*, in *Current Topics in Developmental Biology*, DePamphilis, M.L., Editor. 2016, Academic Press. p. 259-310.
2. De Los Angeles, A., Ferrari, F., Xi, R., Fujiwara, Y., Benvenisty, N., Deng, H., Hochedlinger, K., Jaenisch, R., Lee, S., Leitch, H.G., Lensch, M.W., Lujan, E., Pei, D., Rossant, J., Wernig, M., Park, P.J., and Daley, G.Q., *Hallmarks of Pluripotency.* Nature, 2015. **525**: p. 469.
3. Ishiuchi, T. and Torres-Padilla, M.-E., *Towards an Understanding of the Regulatory Mechanisms of Totipotency.* Current Opinion in Genetics & Development, 2013. **23**(5): p. 512-518.
4. Seydoux, G. and Braun, R.E., *Pathway to Totipotency: Lessons from Germ Cells.* Cell, 2006. **127**(5): p. 891-904.
5. Rinkenberger, J.L. and Werb, Z., *Trophoblast A2 - Brenner, Sydney*, in *Encyclopedia of Genetics*, Miller, J.H., Editor. 2001, Academic Press: New York. p. 2070-2071.
6. Vallier, L., Touboul, T., Chng, Z., Brimpari, M., Hannan, N., Millan, E., Smithers, L.E., Trotter, M., Rugg-Gunn, P., Weber, A., and Pedersen, R.A., *Early Cell Fate Decisions of Human Embryonic Stem Cells and Mouse Epiblast Stem Cells Are Controlled by the Same Signalling Pathways.* PLoS ONE, 2009. **4**(6): p. e6082.
7. Takahashi, K., Tanabe, K., Ohnuki, M., Narita, M., Ichisaka, T., Tomoda, K., and Yamanaka, S., *Induction of Pluripotent Stem Cells from Adult Human Fibroblasts by Defined Factors.* Cell, 2007. **131**(5): p. 861-872.
8. Thomson, J.A., Itskovitz-Eldor, J., Shapiro, S.S., Waknitz, M.A., Swiergiel, J.J., Marshall, V.S., and Jones, J.M., *Embryonic Stem Cell Lines Derived from Human Blastocysts.* Science, 1998. **282**(5391): p. 1145-1147.
9. Festuccia, N., Osorno, R., Wilson, V., and Chambers, I., *The Role of Pluripotency Gene Regulatory Network Components in Mediating Transitions between Pluripotent Cell States.* Current Opinion in Genetics & Development, 2013. **23**(5): p. 504-511.
10. Kim, N. and Cho, S.-G., *Clinical Applications of Mesenchymal Stem Cells.* The Korean Journal of Internal Medicine, 2013. **28**(4): p. 387-402.
11. Wang, S., Qu, X., and Zhao, R.C., *Clinical Applications of Mesenchymal Stem Cells.* Journal of Hematology & Oncology, 2012. **5**: p. 19-19.
12. Evans, M.J. and Kaufman, M.H., *Establishment in Culture of Pluripotential Cells from Mouse Embryos.* Nature, 1981. **292**: p. 154.
13. Martin, G.R., *Isolation of a Pluripotent Cell Line from Early Mouse Embryos Cultured in Medium Conditioned by Teratocarcinoma Stem Cells.* Proceedings of the National Academy of Sciences, 1981. **78**(12): p. 7634-7638.
14. Pera, M.F., Reubinoff, B., and Trounson, A., *Human Embryonic Stem Cells.* Journal of Cell Science, 2000. **113**(1): p. 5-10.
15. Xu, C., Inokuma, M.S., Denham, J., Golds, K., Kundu, P., Gold, J.D., and Carpenter, M.K., *Feeder-Free Growth of Undifferentiated Human Embryonic Stem Cells.* Nature Biotechnology, 2001. **19**: p. 971 - 974.

16. Thomson, J.A. and Marshall, V.S., *4 Primate Embryonic Stem Cells*, in *Current Topics in Developmental Biology*, Pedersen, R.A. and Schatten, G.P., Editors. 1997, Academic Press. p. 133-165.
17. McElroy, S.L. and Reijo Pera, R.A., *Preparation of Mouse Embryonic Fibroblast Feeder Cells for Human Embryonic Stem Cell Culture.* Cold Spring Harbor Protocols, 2008. **2008**(9): p. pdb.prot5041.
18. Xu, R.-H., Peck, R.M., Li, D.S., Feng, X., Ludwig, T., and Thomson, J.A., *Basic Fgf and Suppression of Bmp Signaling Sustain Undifferentiated Proliferation of Human Es Cells.* Nature Methods, 2005. **2**(3): p. 185-190.
19. Vallier, L., Alexander, M., and Pedersen, R.A., *Activin/Nodal and Fgf Pathways Cooperate to Maintain Pluripotency of Human Embryonic Stem Cells.* Journal of Cell Science, 2005. **118**(19): p. 4495-4509.
20. Matsuda, T.N., T. Nakao, K. Arai, T. Katsuki, M. Heike and T. Yokota, T., *Stat3 Activation Is Sufficient to Maintain an Undifferentiated State of Mouse Embryonic Stem Cells.* EMBO Journal, 1999. **18**: p. 4261 - 4269.
21. Dahéron, L., Opitz, S.L., Zaehres, H., Lensch, W.M., Andrews, P.W., Itskovitz-Eldor, J., and Daley, G.Q., *Lif/Stat3 Signaling Fails to Maintain Self-Renewal of Human Embryonic Stem Cells.* Stem Cells, 2004. **22**(5): p. 770-778.
22. Humphrey, R.K., Beattie, G.M., Lopez, A.D., Bucay, N., King, C.C., Firpo, M.T., Rose-John, S., and Hayek, A., *Maintenance of Pluripotency in Human Embryonic Stem Cells Is Stat3 Independent.* Stem Cells, 2004. **22**(4): p. 522-530.
23. Brown, S., Teo, A., Pauklin, S., Hannan, N., Cho, C.H.H., Lim, B., Vardy, L., Dunn, N.R., Trotter, M., Pedersen, R., and Vallier, L., *Activin/Nodal Signaling Controls Divergent Transcriptional Networks in Human Embryonic Stem Cells and in Endoderm Progenitors.* Stem Cells, 2011. **29**(8): p. 1176-1185.
24. Vallier, L., Mendjan, S., Brown, S., Chng, Z., Teo, A., Smithers, L.E., Trotter, M.W.B., Cho, C.H.-H., Martinez, A., Rugg-Gunn, P., Brons, G., and Pedersen, R.A., *Activin/Nodal Signalling Maintains Pluripotency by Controlling Nanog Expression.* Development, 2009. **136**(8): p. 1339-1349.
25. Braam, S.R., Denning, C., Matsa, E., Young, L.E., Passier, R., and Mummery, C.L., *Feeder-Free Culture of Human Embryonic Stem Cells in Conditioned Medium for Efficient Genetic Modification.* Nature Protocols, 2008. **3**(9): p. 1435-1443.
26. Stover, A.E. and Schwartz, P.H., *Adaptation of Human Pluripotent Stem Cells to Feeder-Free Conditions in Chemically Defined Medium with Enzymatic Single-Cell Passaging.* Methods in Molecular Biology, 2011. **767**: p. 137-146.
27. Sun, N., Panetta, N.J., Gupta, D.M., Wilson, K.D., Lee, A., Jia, F., Hu, S., Cherry, A.M., Robbins, R.C., Longaker, M.T., and Wu, J.C., *Feeder-Free Derivation of Induced Pluripotent Stem Cells from Adult Human Adipose Stem Cells.* Proceedings of the National Academy of Sciences of the United States of America, 2009. **106**(37): p. 15720-15725.
28. Ludwig, T.E., Bergendahl, V., Levenstein, M.E., Yu, J., Probasco, M.D., and Thomson, J.A., *Feeder-Independent Culture of Human Embryonic Stem Cells.* Nature Methods 2006. **3**: p. 637 - 646.
29. Wang, Y., Chou, B.-K., Dowey, S., He, C., Gerecht, S., and Cheng, L., *Scalable Expansion of Human Induced Pluripotent Stem Cells in the Defined Xeno-Free E8 Medium under Adherent and Suspension Culture Conditions.* Stem Cell Research, 2013. **11**(3): p. 1103-1116.
30. Villa-Diaz, L.G., Pacut, C., Slawny, N.A., Ding, J., O'Shea, K.S., and Smith, G.D., *Analysis of the Factors That Limit the Ability of Feeder Cells to*

Maintain the Undifferentiated State of Human Embryonic Stem Cells. Stem Cells and Development, 2009. **18**(4): p. 641-651.
31. Krumlauf, R., *Teratocarcinomas and Embryonic Stem Cells: A Practical Approach.* Trends in Genetics, 1987. **3**: p. 331-332.
32. Robertson, E.J., *Pluripotential Stem Cell Lines as a Route into the Mouse Germ Line.* Trends in Genetics, 1986. **2**: p. 9-13.
33. Kooreman, N.G. and Wu, J.C., *Tumorigenicity of Pluripotent Stem Cells: Biological Insights from Molecular Imaging.* Journal of the Royal Society Interface, 2010. **7**(Suppl 6): p. 753-763.
34. Gropp, M., Shilo, V., Vainer, G., Gov, M., Gil, Y., Khaner, H., Matzrafi, L., Idelson, M., Kopolovic, J., Zak, N.B., and Reubinoff, B.E., *Standardization of the Teratoma Assay for Analysis of Pluripotency of Human Es Cells and Biosafety of Their Differentiated Progeny.* PLoS ONE, 2012. **7**(9): p. e45532.
35. Martin, G.R., *Teratocarcinomas and Mammalian Embryogenesis.* Science, 1980. **209**(4458): p. 768-776.
36. Wesselschmidt, R.L., *The Teratoma Assay: An in Vivo Assessment of Pluripotency*, in *Human Pluripotent Stem Cells: Methods and Protocols*, Schwartz, P.H. and Wesselschmidt, R.L., Editors. 2011, Humana Press: Totowa, NJ. p. 231-241.
37. Hentze, H., Soong, P.L., Wang, S.T., Phillips, B.W., Putti, T.C., and Dunn, N.R., *Teratoma Formation by Human Embryonic Stem Cells: Evaluation of Essential Parameters for Future Safety Studies.* Stem Cell Research, 2009. **2**(3): p. 198-210.
38. Rungarunlert, S., Techakumphu, M., Pirity, M.K., and Dinnyes, A., *Embryoid Body Formation from Embryonic and Induced Pluripotent Stem Cells: Benefits of Bioreactors.* World Journal of Stem Cells, 2009. **1**(1): p. 11-21.
39. Pettinato, G., Wen, X., and Zhang, N., *Formation of Well-Defined Embryoid Bodies from Dissociated Human Induced Pluripotent Stem Cells Using Microfabricated Cell-Repellent Microwell Arrays.* Scientific Reports, 2014. **4**: p. 7402.
40. Kashyap, V., Rezende, N.C., Scotland, K.B., Shaffer, S.M., Persson, J.L., Gudas, L.J., and Mongan, N.P., *Regulation of Stem Cell Pluripotency and Differentiation Involves a Mutual Regulatory Circuit of the Nanog, Oct4, and Sox2 Pluripotency Transcription Factors with Polycomb Repressive Complexes and Stem Cell Micrornas.* Stem Cells and Development, 2009. **18**(7): p. 1093-1108.
41. Pan, G.J., Chang, Z.Y., Schöler, H.R., and Pei, D., *Stem Cell Pluripotency and Transcription Factor Oct4.* Cell Research, 2002. **12**(5): p. 321-329.
42. Boiani, M. and Scholer, H.R., *Regulatory Networks in Embryo-Derived Pluripotent Stem Cells.* Nature Reviews Molecular Cell Biology, 2005. **6**(11): p. 872-881.
43. Chen, L. and Daley, G.Q., *Molecular Basis of Pluripotency.* Human Molecular Genetics, 2008. **17**(R1): p. R23-R27.
44. Thompson, M., Lui, S.J., Zou, N.L., Smith, Z., Messner, A., and Ramanathan, S., *Pluripotency Factors in Embryonic Stem Cells Regulate Differentiation into Germ Layers.* Cell, 2011. **145**(6): p. 875-899.
45. Chambers, I., Colby, D., Robertson, M., Nichols, J., Lee, S., Tweedie, S., and Smith, A., *Functional Expression Cloning of Nanog, a Pluripotency Sustaining Factor in Embryonic Stem Cells.* Cell, 2003. **113**(5): p. 643-655.
46. Chambers, I., Silva, J., Colby, D., Nichols, J., Nijmeijer, B., Robertson, M., Vrana, J., Jones, K., Grotewold, L., and Smith, A., *Nanog Safeguards Pluripotency and Mediates Germline Development.* Nature, 2007. **450**: p. 1230-1234.

47. Fouse, S.D., Shen, Y., Pellegrini, M., Cole, S., Meissner, A., Van Neste, L., Jaenisch, R., and Fan, G., *Promoter Cpg Methylation Contributes to Es Cell Gene Regulation in Parallel with Oct4/Nanog, Pcg Complex, and Histone H3 K4/K27 Trimethylation.* Cell Stem Cell, 2008. **2**(2): p. 160-169.
48. Ben-Shushan, E., Thompson, J.R., Gudas, L.J., and Bergman, Y., *Rex-1, a Gene Encoding a Transcription Factor Expressed in the Early Embryo, Is Regulated Via Oct-3/4 and Oct-6 Binding to an Octamer Site and a Novel Protein, Rox-1, Binding to an Adjacent Site.* Molecular and Cellular Biology, 1998. **18**(4): p. 1866-1878.
49. Rogers, M.B., Hosler, B.A., and Gudas, L.J., *Specific Expression of a Retinoic Acid-Regulated, Zinc-Finger Gene, Rex-1, in Preimplantation Embryos, Trophoblast and Spermatocytes.* Development, 1991. **113**(3): p. 815-824.
50. Shi, W., Wang, H., Pan, G., Geng, Y., Guo, Y., and Pei, D., *Regulation of the Pluripotency Marker Rex-1 by Nanog and Sox2.* Journal of Biological Chemistry, 2006. **281**(33): p. 23319-23325.
51. Singh, A.M., Hamazaki, T., Hankowski, K.E., and Terada, N., *A Heterogeneous Expression Pattern for Nanog in Embryonic Stem Cells.* Stem Cells, 2007. **25**(10): p. 2534-2542.
52. Toyooka, Y., Shimosato, D., Murakami, K., Takahashi, K., and Niwa, H., *Identification and Characterization of Subpopulations in Undifferentiated Es Cell Culture.* Development, 2008. **135**(5): p. 909-918.
53. Draper, J.S., Pigott, C., Thomson, J.A., and Andrews, P.W., *Surface Antigens of Human Embryonic Stem Cells: Changes Upon Differentiation in Culture.* Journal of Anatomy, 2002. **200**(3): p. 249–258.
54. Shevinsky, L.H., Knowles, B.B., Damjanov, I., and Solter, D., *Monoclonal Antibody to Murine Embryos Defines a Stage-Specific Embryonic Antigen Expressed on Mouse Embryos and Human Teratocarcinoma Cells.* Cell, 1982. **30**(3): p. 697-705.
55. Watabe, T. and Miyazono, K., *Roles of Tgf-[Beta] Family Signaling in Stem Cell Renewal and Differentiation.* Cell Research, 2009. **19**(1): p. 103-115.
56. Kitisin, K., Saha, T., Blake, T., Golestaneh, N., Deng, M., Kim, C., Tang, Y., Shetty, K., Mishra, B., and Mishra, L., *Tgf-Beta Signaling in Development.* Science Signalling, 2007. **2007**(399): p. cm1.
57. Zi, Z., Chapnick, D.A., and Liu, X., *Dynamics of Tgf-B/Smad Signaling.* FEBS letters, 2012. **586**(14): p. 1921-1928.
58. Massagué, J., *Receptors for the Tgf-B Family.* Cell, 1992. **69**(7): p. 1067–1070.
59. Tremblay, K.D., Hoodless, P.A., Bikoff, E.K., and Robertson, E.J., *Formation of the Definitive Endoderm in Mouse Is a Smad2-Dependent Process.* Development, 2000. **127**(14): p. 3079-3090.
60. Heldin, C.-H., Miyazono, K., and ten Dijke, P., *Tgf-Beta Signalling from Cell Membrane to Nucleus through Smad Proteins.* Nature, 1997. **390**(6659): p. 465-471.
61. Derynck, R. and Zhang, Y.E., *Smad-Dependent and Smad-Independent Pathways in Tgf-B Family Signalling.* Nature, 2003. **425**: p. 577.
62. Massaous, J. and Hata, A., *Tgf-B; Signalling through the Smad Pathway.* Trends in Cell Biology, 1997. **7**(5): p. 187-192.
63. Massagué. J, S.J., and Wotton. D, *Smad Transcription Factors.* Genes & Development, 2005. **19**: p. 2783-2810.
64. Whitman, M., *Smads and Early Developmental Signaling by the Tgfβ Superfamily.* Genes & Development, 1998. **12**(16): p. 2445-2462.

65. Schmierer, B. and Hill, C.S., *Tgf-Beta-Smad Signal Transduction: Molecular Specificity and Functional Flexibility.* Nature Reviews Molecular Cell Biology, 2007. **8**(12): p. 970-982.
66. Mullen, Alan C., Orlando, David A., Newman, Jamie J., Lovén, J., Kumar, Roshan M., Bilodeau, S., Reddy, J., Guenther, Matthew G., DeKoter, R.P., and Young, Richard A., *Master Transcription Factors Determine Cell-Type-Specific Responses to Tgf-B Signaling.* Cell, 2011. **147**(3): p. 565-576.
67. Watanabe, M., Masuyama, N., Fukuda, M., and Nishida, E., *Regulation of Intracellular Dynamics of Smad4 by Its Leucine-Rich Nuclear Export Signal.* EMBO Reports, 2000. **1**(2): p. 176-182.
68. Xiao, Z., Watson, N., Rodriguez, C., and Lodish, H.F., *Nucleocytoplasmic Shuttling of Smad1 Conferred by Its Nuclear Localization and Nuclear Export Signals.* Journal of Biological Chemistry, 2001. **276**(42): p. 39404-39410.
69. Xiao, Z., Latek, R., and Lodish, H.F., *An Extended Bipartite Nuclear Localization Signal in Smad4 Is Required for Its Nuclear Import and Transcriptional Activity.* Oncogene, 2003. **22**: p. 1057-1069.
70. Jonk, L.J.C., Itoh, S., Heldin, C.-H., ten Dijke, P., and Kruijer, W., *Identification and Functional Characterization of a Smad Binding Element (Sbe) in the Junb Promoter That Acts as a Transforming Growth Factor-B, Activin, and Bone Morphogenetic Protein-Inducible Enhancer.* Journal of Biological Chemistry, 1998. **273**(33): p. 21145-21152.
71. Attisano, L. and Tuen Lee-Hoeflich, S., *The Smads.* Genome Biology, 2001. **2**(8): p. 3010.1-3010.8.
72. Nakayama, T., Berg, L.K., and Christian, J.L., *Dissection of Inhibitory Smad Proteins: Both N- and C-Terminal Domains Are Necessary for Full Activities of Xenopus Smad6 and Smad7.* Mechanisms of Development, 2001. **100**(2): p. 251-262.
73. Wrighton, K.H., Willis, D., Long, J., Liu, F., Lin, X., and Feng, X.-H., *Small C-Terminal Domain Phosphatases Dephosphorylate the Regulatory Linker Regions of Smad2 and Smad3 to Enhance Transforming Growth Factor-B Signaling.* Journal of Biological Chemistry, 2006. **281**(50): p. 38365-38375.
74. Izzi, L. and Attisano, L., *Regulation of the Tgf[Beta] Signalling Pathway by Ubiquitin-Mediated Degradation.* Oncogene, 2004. **23**(11): p. 2071-2078.
75. Xu, P., Liu, J., and Derynck, R., *Post-Translational Regulation of Tgf-B Receptor and Smad Signaling.* FEBS letters, 2012. **586**(14): p. 1871-1884.
76. Schiffer, M., Von Gersdorff, G., Bitzer, M., Susztak, K., and Böttinger, E.P., *Smad Proteins and Transforming Growth Factor-B Signaling.* Kidney International, 2000. **58**: p. 45-52.
77. Morrison, G.M., Oikonomopoulou, I., Migueles, R.P., Soneji, S., Livigni, A., Enver, T., and Brickman, J.M., *Anterior Definitive Endoderm from Escs Reveals a Role for Fgf Signaling.* Cell Stem Cell, 2008. **3**(4): p. 402-415.
78. Lanner, F. and Rossant, J., *The Role of Fgf/Erk Signaling in Pluripotent Cells.* Development, 2010. **137**(20): p. 3351-3360.
79. Ameri, J., Ståhlberg, A., Pedersen, J., Johansson, J.K., Johannesson, M.M., Artner, I., and Semb, H., *Fgf2 Specifies Hesc-Derived Definitive Endoderm into Foregut/Midgut Cell Lineages in a Concentration-Dependent Manner.* Stem Cells, 2010. **28**(1): p. 45-56.
80. Greber, B., Wu, G., Bernemann, C., Joo, J.Y., Han, D.W., Ko, K., Tapia, N., Sabour, D., Sterneckert, J., Tesar, P., and Schöler, H.R., *Conserved and Divergent Roles of Fgf Signaling in Mouse Epiblast Stem Cells and Human Embryonic Stem Cells.* Cell Stem Cell, 2010. **6**(3): p. 215-226.
81. LaVaute, T.M., Yoo, Y.D., Pankratz, M.T., Weick, J.P., Gerstner, J.R., and Zhang, S.-C., *Regulation of Neural Specification from Human Embryonic Stem Cells by Bmp and Fgf.* Stem Cells 2009. **27**(8): p. 1741-1749.

82. Cho, C.H.H., Hannan, N.R.F., Docherty, F.M., Docherty, H.M., Joåo Lima, M., Trotter, M.W.B., Docherty, K., and Vallier, L., *Inhibition of Activin/Nodal Signalling Is Necessary for Pancreatic Differentiation of Human Pluripotent Stem Cells.* Diabetologia, 2012. **55**(12): p. 3284-3295.
83. McLean, A.B., D'Amour, K.A., Jones, K.L., Krishnamoorthy, M., Kulik, M.J., Reynolds, D.M., Sheppard, A.M., Liu, H., Xu, Y., Baetge, E.E., and Dalton, S., *Activin a Efficiently Specifies Definitive Endoderm from Human Embryonic Stem Cells Only When Phosphatidylinositol 3-Kinase Signaling Is Suppressed.* Stem Cells, 2007. **25**(1): p. 29-38.
84. Roelandt, P., Pauwelyn, K.A., Sancho-Bru, P., Subramanian, K., Bose, B., Ordovas, L., Vanuytsel, K., Geraerts, M., Firpo, M., De Vos, R., Fevery, J., Nevens, F., Hu, W.-S., and Verfaillie, C.M., *Human Embryonic and Rat Adult Stem Cells with Primitive Endoderm-Like Phenotype Can Be Fated to Definitive Endoderm, and Finally Hepatocyte-Like Cells.* PLoS ONE, 2010. **5**(8): p. e12101.
85. Alev, C., Wu, Y., Kasukawa, T., Jakt, L.M., Ueda, H.R., and Sheng, G., *Transcriptomic Landscape of the Primitive Streak.* Development, 2010. **137**(17): p. 2863-2874.
86. Arnold, S.J. and Robertson, E.J., *Making a Commitment: Cell Lineage Allocation and Axis Patterning in the Early Mouse Embryo.* Nature Reviews Molecular Cell Biology, 2009. **10**(2): p. 91-103.
87. Tada, S., Era, T., Furusawa, C., Sakurai, H., Nishikawa, S., Kinoshita, M., Nakao, K., and Chiba, T., *Characterization of Mesendoderm: A Diverging Point of the Definitive Endoderm and Mesoderm in Embryonic Stem Cell Differentiation Culture.* Development, 2005. **132**(19): p. 4363-74.
88. Kimelman, D. and Griffin, K.J., *Vertebrate Mesendoderm Induction and Patterning.* Current Opinions in Genetic Development, 2000. **10**(4): p. 350-6.
89. Smith, J.C., *Mesoderm-Inducing Factors in Early Vertebrate Development.* EMBO Journal, 1993. **12**(12): p. 4463-70.
90. Hogan, B.L., *Bone Morphogenetic Proteins: Multifunctional Regulators of Vertebrate Development.* Genes and Development, 1996. **10**(13): p. 1580-94.
91. Schier, A.F. and Shen, M.M., *Nodal Signalling in Vertebrate Development.* Nature, 2000. **403**(6768): p. 385-9.
92. Lowe, L.A., Yamada, S., and Kuehn, M.R., *Genetic Dissection of Nodal Function in Patterning the Mouse Embryo.* Development, 2001. **128**(10): p. 1831-1843.
93. Tavares, A.T., Andrade, S., Silva, A.C., and Belo, J.A., *Cerberus Is a Feedback Inhibitor of Nodal Asymmetric Signaling in the Chick Embryo.* Development, 2007. **134**(11): p. 2051-2060.
94. Aykul, S., Ni, W., Mutatu, W., and Martinez-Hackert, E., *Human Cerberus Prevents Nodal-Receptor Binding, Inhibits Nodal Signaling, and Suppresses Nodal-Mediated Phenotypes.* PLoS ONE, 2015. **10**(1): p. e0114954.
95. Chiu, W.T., Charney Le, R., Blitz, I.L., Fish, M.B., Li, Y., Biesinger, J., Xie, X., and Cho, K.W.Y., *Genome-Wide View of Tgfβ/Foxh1 Regulation of the Early Mesendoderm Program.* Development, 2014. **141**(23): p. 4537-4547.
96. Slagle, C.E., Aoki, T., and Burdine, R.D., *Nodal-Dependent Mesendoderm Specification Requires the Combinatorial Activities of Foxh1 and Eomesodermin.* PLoS Genetics, 2011. **7**(5): p. e1002072.
97. Roessler, E., Ouspenskaia, M.V., Karkera, J.D., Vélez, J.I., Kantipong, A., Lacbawan, F., Bowers, P., Belmont, J.W., Towbin, J.A., Goldmuntz, E., Feldman, B., and Muenke, M., *Reduced Nodal Signaling Strength Via Mutation of Several Pathway Members Including Foxh1 Is Linked to Human*

Heart Defects and Holoprosencephaly. The American Journal of Human Genetics, 2008. **83**(1): p. 18-29.
98. Shim, J., Kim, S., Woo, D., Oh, C., McKay, R., and Kim, J., *Directed Differentiation of Human Embryonic Stem Cells Towards a Pancreatic Cell Fate.* Diabetologia, 2007. **50**(6): p. 1228-1238.
99. Hay, D.C., Fletcher, J., Payne, C., Terrace, J.D., Gallagher, R.C.J., Snoeys, J., Black, J.R., Wojtacha, D., Samuel, K., Hannoun, Z., Pryde, A., Filippi, C., Currie, I.S., Forbes, S.J., Ross, J.A., Newsome, P.N., and Iredale, J.P., *Highly Efficient Differentiation of Hescs to Functional Hepatic Endoderm Requires Activina and Wnt3a Signaling.* Proceedings of the National Academy of Sciences, 2008. **105**(34): p. 12301-12306.
100. Holtzinger, A., Streeter, P.R., Sarangi, F., Hillborn, S., Niapour, M., Ogawa, S., and Keller, G., *New Markers for Tracking Endoderm Induction and Hepatocyte Differentiation from Human Pluripotent Stem Cells.* Development 2015. **142**(24): p. 4253-4265.
101. Wang, P., McKnight, K.D., Wong, D.J., Rodriguez, R.T., Sugiyama, T., Gu, X., Ghodasara, A., Qu, K., Chang, H.Y., and Kim, S.K., *A Molecular Signature for Purified Definitive Endoderm Guides Differentiation and Isolation of Endoderm from Mouse and Human Embryonic Stem Cells.* Stem Cells and Development, 2012. **21**(12): p. 2273-2287.
102. Borowiak, M., Maehr, R., Chen, S., Chen, A.E., Tang, W., Fox, J.O., Schreiber, S.L., and Melton, D.A., *Small Molecules Efficiently Direct Endodermal Differentiation of Mouse and Human Embryonic Stem Cells.* Cell Stem Cell, 2009. **4**(4): p. 348-358.
103. Yasunaga, M., Tada, S., Torikai-Nishikawa, S., Nakano, Y., Okada, M., Jakt, L.M., Nishikawa, S., Chiba, T., Era, T., and Nishikawa, S.-I., *Induction and Monitoring of Definitive and Visceral Endoderm Differentiation of Mouse Es Cells.* Nature Biotechnology, 2005. **23**(12): p. 1542-1550.
104. Kanai-Azuma, M., Kanai, Y., Gad, J.M., Tajima, Y., Taya, C., Kurohmaru, M., Sanai, Y., Yonekawa, H., Yazaki, K., Tam, P.P.L., and Hayashi, Y., *Depletion of Definitive Gut Endoderm in Sox17-Null Mutant Mice.* Development, 2002. **129**(10): p. 2367-2379.
105. Viotti, M., Nowotschin, S., and Hadjantonakis, A.-K., *Sox17 Links Gut Endoderm Morphogenesis with Germ Layer Segregation.* Nature Cell Biology, 2014. **16**(12): p. 1146-1156.
106. Si-Tayeb, K., Noto, F.K., Nagaoka, M., Li, J., Battle, M.A., Duris, C., North, P.E., Dalton, S., and Duncan, S.A., *Highly Efficient Generation of Human Hepatocyte–Like Cells from Induced Pluripotent Stem Cells.* Hepatology, 2010. **51**(1): p. 297-305.
107. Song, Z., Cai, J., Liu, Y., Zhao, D., Yong, J., Duo, S., Song, X., Guo, Y., Zhao, Y., Qin, H., Yin, X., Wu, C., Che, J., Lu, S., Ding, M., and Deng, H., *Efficient Generation of Hepatocyte-Like Cells from Human Induced Pluripotent Stem Cells.* Cell Research, 2009. **19**(11): p. 1233-1242.
108. Wang, P., Rodriguez, R.T., Wang, J., Ghodasara, A., and Kim, S.K., *Targeting Sox17 in Human Embryonic Stem Cells Creates Unique Strategies for Isolating and Analyzing Developing Endoderm.* Cell Stem Cell, 2011. **8**(3): p. 335-346.
109. Vincent, S.D., Dunn, N.R., Hayashi, S., Norris, D.P., and Robertson, E.J., *Cell Fate Decisions within the Mouse Organizer Are Governed by Graded Nodal Signals.* Genes & Development, 2003. **17**(13): p. 1646-1662.
110. Cai, J., Zhao, Y., Liu, Y., Ye, F., Song, Z., Qin, H., Meng, S., Chen, Y., Zhou, R., Song, X., Guo, Y., Ding, M., and Deng, H., *Directed Differentiation of Human Embryonic Stem Cells into Functional Hepatic Cells.* Hepatology, 2007. **45**(5): p. 1229-1239.

111. Hay, D.C., Zhao, D., Ross, A., Mandalam, R., Lebkowski, J., and W, C., *Direct Differentiation of Human Embryonic Stem Cells to Hepatocyte-Like Cells Exhibiting Functional Activities.* Cloning Stem Cells, 2007. **9**(1): p. 209.
112. Sullivan, G.J., Hay, D.C., Park, I.-H., Fletcher, J., Hannoun, Z., Payne, C.M., Dalgetty, D., Black, J.R., Ross, J.A., Samuel, K., Wang, G., Daley, G.Q., Lee, J.-H., Church, G.M., Forbes, S.J., Iredale, J.P., and Wilmut, I., *Generation of Functional Human Hepatic Endoderm from Human Induced Pluripotent Stem Cells.* Hepatology, 2010. **51**(1): p. 329-335.
113. Liu, P., Wakamiya, M., Shea, M.J., Albrecht, U., Behringer, R.R., and Bradley, A., *Requirement for Wnt3 in Vertebrate Axis Formation.* Nature Genetics, 1999. **22**: p. 361-365.
114. Komiya, Y. and Habas, R., *Wnt Signal Transduction Pathways.* Organogenesis, 2008. **4**(2): p. 68-75.
115. Zhan, T., Rindtorff, N., and Boutros, M., *Wnt Signaling in Cancer.* Oncogene, 2016. **36**: p. 1461-1473.
116. Hoppler, S. and Kavanagh, C.L., *Wnt Signalling: Variety at the Core.* Journal of Cell Science, 2007. **120**(3): p. 385-393.
117. Huelsken, J. and Behrens, J., *The Wnt Signalling Pathway.* Journal of Cell Science, 2002. **115**(21): p. 3977-3978.
118. Grumolato, L., Liu, G., Mong, P., Mudbhary, R., Biswas, R., Arroyave, R., Vijayakumar, S., Economides, A.N., and Aaronson, S.A., *Canonical and Noncanonical Wnts Use a Common Mechanism to Activate Completely Unrelated Coreceptors.* Genes & Development, 2010. **24**(22): p. 2517-2530.
119. MacDonald, B.T., Tamai, K., and He, X., *Wnt/B-Catenin Signaling: Components, Mechanisms, and Diseases.* Developmental Cell, 2009. **17**(1): p. 9-26.
120. Clevers, H., *Wnt/B-Catenin Signaling in Development and Disease.* Cell, 2006. **127**(3): p. 469-480.
121. Bone, H.K., Nelson, A.S., Goldring, C.E., Tosh, D., and Welham, M.J., *A Novel Chemically Directed Route for the Generation of Definitive Endoderm from Human Embryonic Stem Cells Based on Inhibition of Gsk-3.* Journal of Cell Science, 2011. **124**(12): p. 1992-2000.
122. Tahamtani, Y., Azarnia, M., Farrokhi, A., Zarchi, A.S., Aghdami, N., and Baharvand, H., *Treatment of Human Embryonic Stem Cells with Different Combinations of Priming and Inducing Factors toward Definitive Endoderm.* Stem Cells and Development, 2013. **22**(9): p. 1419-1432.
123. Ciruna, B.G., Schwartz, L., Harpal, K., Yamaguchi, T.P., and Rossant, J., *Chimeric Analysis of Fibroblast Growth Factor Receptor-1 (Fgfr1) Function: A Role for Fgfr1 in Morphogenetic Movement through the Primitive Streak.* Development, 1997. **124**(14): p. 2829-2841.
124. Gerets. H, T.K., Gerin. B, Chanteux. H, Depelchin. B, Dhalluin. S, Atienzar. F, *Characterization of Primary Human Hepatocytes, Hepg2 Cells, and Heparg Cells at the Mrna Level and Cyp Activity in Response to Inducers and Their Predictivity for the Detection of Human Hepatotoxins.* Cell Biology and Toxicology, 2012. **2**: p. 69-87.
125. Soto-Gutiérrez, A., Kobayashi, N., Rivas-Carrillo, J.D., Navarro-Álvarez, N., Zhao, D., Okitsu, T., Noguchi, H., Basma, H., Tabata, Y., Chen, Y., Tanaka, K., Narushima, M., Miki, A., Ueda, T., Jun, H.-S., Yoon, J.-W., Lebkowski, J., Tanaka, N., and Fox, I.J., *Reversal of Mouse Hepatic Failure Using an Implanted Liver-Assist Device Containing Es Cell–Derived Hepatocytes.* Nature Biotechnology, 2006. **24**: p. 1412-1419.
126. Block, G.D., Locker, J., Bowen, W. C., Petersen, B. E., Katyal, S., and Strom, S.C., Riley, T., Howard, T. A. and Michalopoulos, G. K., *Population Expansion, Clonal Growth, and Specific Differentiation Patterns in Primary*

Cultures of Hepatocytes Induced by Hgf/Sf, Egf and Tgf Alpha in a Chemically Defined (Hgm) Medium. The Journal of Cell Biology, 1996. **132**(6): p. 1133-1149.
127. Yin, L., Sun, M., Ilic, Z., Leffert, H.L., and Sell, S., *Derivation, Characterization, and Phenotypic Variation of Hepatic Progenitor Cell Lines Isolated from Adult Rats.* Hepatology, 2002. **35**(2): p. 315-324.
128. Marion, M.-J., Hantz, O., and Durantel, D., *The Heparg Cell Line: Biological Properties and Relevance as a Tool for Cell Biology, Drug Metabolism, and Virology Studies*, in *Hepatocytes: Methods and Protocols*, Maurel, P., Editor. 2010, Humana Press: Totowa, NJ. p. 261-272.
129. Guillouzo, A., Corlu, A., Aninat, C., Glaise, D., Morel, F., and Guguen-Guillouzo, C., *The Human Hepatoma Heparg Cells: A Highly Differentiated Model for Studies of Liver Metabolism and Toxicity of Xenobiotics.* Chemico-Biological Interactions, 2007. **168**(1): p. 66-73.
130. Kanebratt, K.P. and Andersson, T.B., *Heparg Cells as an in Vitro Model for Evaluation of Cytochrome P450 Induction in Humans.* Drug Metabolism and Disposition, 2008. **36**(1): p. 137-145.
131. Cerec, V., Glaise, D., Garnier, D., Morosan, S., Turlin, B., Drenou, B., Gripon, P., Kremsdorf, D., Guguen-Guillouzo, C., and Corlu, A., *Transdifferentiation of Hepatocyte-Like Cells from the Human Hepatoma Heparg Cell Line through Bipotent Progenitor.* Hepatology, 2007. **45**(4): p. 957-967.
132. Dianat, N., Dubois-Pot-Schneider, H., Steichen, C., Desterke, C., Leclerc, P., Raveux, A., Combettes, L., Weber, A., Corlu, A., and Dubart-Kupperschmitt, A., *Generation of Functional Cholangiocyte-Like Cells from Human Pluripotent Stem Cells and Heparg Cells.* Hepatology, 2014. **60**(2): p. 700-714.
133. Kanebratt, K.P. and Andersson, T.B., *Evaluation of Heparg Cells as an in Vitro Model for Human Drug Metabolism Studies.* Drug Metabolism and Disposition, 2008. **36**(7): p. 1444-1452.
134. Touboul, T., Hannan, N.R.F., Corbineau, S., Martinez, A., Martinet, C., Branchereau, S., Mainot, S., Strick-Marchand, H., Pedersen, R., Di Santo, J., Weber, A., and Vallier, L., *Generation of Functional Hepatocytes from Human Embryonic Stem Cells under Chemically Defined Conditions That Recapitulate Liver Development.* Hepatology, 2010. **51**(5): p. 1754-1765.
135. Funakoshi, N., Duret, C., Jean-Marc Pascussi, J., Blanc, P., Maurel, P., Chavanieu, M., and Chaloin, S., *Comparison of Hepatic-Like Cell Production from Human Embryonic Stem Cells and Adult Liver Progenitor Cells: Car Transduction Activates a Battery of Detoxification Genes.* Stem Cell Reviews and Reports, 2011. **7**(5): p. 518-531.
136. Woo, D.H., Kim, S.K., Lim, H.J., Heo, J., Park, H.S., Kang, G.Y., Kim, S.E., You, H.J., Hoeppner, D.J., Kim, Y., Kwon, H., Choi, T.H., Lee, J.H., Hong, S.H., Song, K.W., Ahn, E.K., Chenoweth, J.G., Tesar, P.J., McKay, R.D.G., and Kim, J.H., *Direct and Indirect Contribution of Human Embryonic Stem Cell–Derived Hepatocyte-Like Cells to Liver Repair in Mice.* Gastroenterology, 2012. **142**(3): p. 602-611.
137. Baxter, M., Withey, S., Harrison, S., Segeritz, C.P., Zhang, F., Atkinson-Dell, R., Rowe, C., Gerrard, D.T., Sison-Young, R., Jenkins, R., Henry, J., Berry, A.A., Mohamet, L., Best, M., Fenwick, S.W., Malik, H., Kitteringham, N.R., Goldring, C.E., Piper Hanley, K., Vallier, L., and Hanley, N.A., *Phenotypic and Functional Analyses Show Stem Cell-Derived Hepatocyte-Like Cells Better Mimic Fetal Rather Than Adult Hepatocytes.* Journal of Hepatology, 2015. **62**(3): p. 581-589.

138. Schwartz, R.E., Fleming, H.E., Khetani, S.R., and Bhatia, S.N., *Pluripotent Stem Cell-Derived Hepatocyte-Like Cells.* Biotechnology Advances, 2014. **32**(2): p. 504-513.
139. Meng, Q., *Three-Dimensional Culture of Hepatocytes for Prediction of Drug-Induced Hepatotoxicity.* Expert Opinion on Drug Metabolism & Toxicology, 2010. **6**(6): p. 733-746.
140. Schuetz, J.D., Beach, D.L., and Guzelian, P.S., *Selective Expression of Cytochrome P450 Cyp3a Mrnas in Embryonic and Adult Human Liver.* Pharmacogenetics, 1994. **4**(1): p. 11-20.
141. Nebert, D.W., Wikvall, K., and Miller, W.L., *Human Cytochromes P450 in Health and Disease.* Philosophical Transactions of the Royal Society B: Biological Sciences, 2013. **368**(1612): p. 20120431.
142. Peter Guengerich, F., Waterman, M.R., and Egli, M., *Recent Structural Insights into Cytochrome P450 Function.* Trends in pharmacological sciences, 2016. **37**(8): p. 625-640.
143. Guengerich, F.P., *Human Cytochrome P450 Enzymes*, in *Cytochrome P450: Structure, Mechanism, and Biochemistry*, Ortiz de Montellano, P.R., Editor. 2005, Springer US. p. 377-530.
144. Liu, H., Kim, Y., Sharkis, S., Marchionni, L., and Jang, Y.-Y., *In Vivo Liver Regeneration Potential of Human Induced Pluripotent Stem Cells from Diverse Origins.* Science Translational Medicine, 2011. **3**(82): p. 82ra39.
145. Si-Tayeb, K., Lemaigre, F.P., and Duncan, S.A., *Organogenesis and Development of the Liver.* Developmental Cell, 2010. **18**(2): p. 175-189.
146. Kinoshita, T. and Miyajima, A., *Cytokine Regulation of Liver Development.* Biochimica et Biophysica Acta (BBA) - Molecular Cell Research, 2002. **1592**(3): p. 303-312.
147. Gordillo, M., Evans, T., and Gouon-Evans, V., *Orchestrating Liver Development.* Development, 2015. **142**(12): p. 2094-2108.
148. D'Amour, K.A., Agulnick, A.D., Eliazer, S., Kelly, O.G., Kroon, E., and Baetge, E.E., *Efficient Differentiation of Human Embryonic Stem Cells to Definitive Endoderm.* Nature Biotechnology, 2005. **23**(12): p. 1534-1541.
149. Zhang, L., Theise, N., Chua, M., and Reid, L., *The Stem Cell Niche of Human Livers: Symmetry between Development and Regeneration.* Hepatology, 2008. **48**(5): p. 1598 - 1607.
150. Tanaka, M., Itoh, T., Tanimizu, N., and Miyajima, A., *Liver Stem/Progenitor Cells: Their Characteristics and Regulatory Mechanisms.* The Journal of Biochemistry, 2011. **149**(3): p. 231-239.
151. Inamura, M., Kawabata, K., Takayama, K., Tashiro, K., Sakurai, F., Katayama, K., Toyoda, M., Akutsu, H., Miyagawa, Y., Okita, H., Kiyokawa, N., Umezawa, A., Hayakawa, T., Furue, M.K., and Mizuguchi, H., *Efficient Generation of Hepatoblasts from Human Es Cells and Ips Cells by Transient Overexpression of Homeobox Gene Hex.* Molecular Therapy, 2011. **19**(2): p. 400-407.
152. Kuhlmann, W.D. and Peschke, P., *Hepatic Progenitor Cells, Stem Cells, and Afp Expression in Models of Liver Injury.* International Journal of Experimental Pathology, 2006. **87**(5): p. 343-359.
153. Takayama, K., Nagamoto, Y., Mimura, N., Tashiro, K., Sakurai, F., Tachibana, M., Hayakawa, T., Kawabata, K., and Mizuguchi, H., *Long-Term Self-Renewal of Human Es/Ips-Derived Hepatoblast-Like Cells on Human Laminin 111-Coated Dishes.* Stem Cell Reports, 2013. **1**(4): p. 322-335.
154. Jung, J., Zheng, M., Goldfarb, M., and Zaret, K.S., *Initiation of Mammalian Liver Development from Endoderm by Fibroblast Growth Factors.* Science, 1999. **284**(5422): p. 1998-2003.

155. Rossi, J.M., Dunn, N.R., Hogan, B.L., and Zaret, K.S., *Distinct Mesodermal Signals, Including Bmps from the Septum Transversum Mesenchyme, Are Required in Combination for Hepatogenesis from the Endoderm.* Genes and Development, 2001. **1**(15): p. 1998-2009.
156. Utley, S., James, D., Mavila, N., Nguyen, M.V., Vendryes, C., Salisbury, S.M., Phan, J., and Wang, K.S., *Fibroblast Growth Factor Signaling Regulates the Expansion of A6-Expressing Hepatocytes in Association with Akt-Dependent B-Catenin Activation.* Journal of Hepatology, 2014. **60**(5): p. 1002-1009.
157. Padrissa-Altés, S., Bachofner, M., Bogorad, R.L., Pohlmeier, L., Rossolini, T., Böhm, F., Liebisch, G., Hellerbrand, C., Koteliansky, V., Speicher, T., and Werner, S., *Control of Hepatocyte Proliferation and Survival by Fgf Receptors Is Essential for Liver Regeneration in Mice.* Gut, 2015. **64**(9): p. 1444-1453.
158. Yuzugullu. H, B.K., Ozturk. N, Senturk. S, Celik. E, Toylu. A, Tasdemir. N, Yilmaz. M, Erdal. E, Akcali K. C, Atabey. N and Ozturk. M, *Canonical Wnt Signaling Is Antagonized by Noncanonical Wnt5a in Hepatocellular Carcinoma Cells.* Molecular Cancer, 2009. **8**(90): p. 1-20.
159. Yang J, C.A., Monga J. K, Preziosi M. E, Pullara F, Calero G, Lang R, Yamaguchi T. P, Nejak-Bowen K. N and Monga S. P, *Wnt5a Inhibits Hepatocyte Proliferation and Concludes B-Catenin Signaling in Liver Regeneration.* The American Journal of Pathology, 2015. **185**(8): p. 2194–2205.
160. Iwatani, M., Ikegami, K., Kremenska, Y., Hattori, N., Tanaka, S., Yagi, S., and Shiota, K., *Dimethyl Sulfoxide Has an Impact on Epigenetic Profile in Mouse Embryoid Body.* Stem Cells, 2006. **24**(11): p. 2549-2556.
161. Choi, S., Sainz, B., Corcoran, P., Uprichard, S., and Jeong, H., *Characterization of Increased Drug Metabolism Activity in Dimethyl Sulfoxide (Dmso)-Treated Huh7 Hepatoma Cells.* Xenobiotica, 2009. **39**(3): p. 205-217.
162. Rambhatla, L., Chiu, C.P., Kundu, P., Peng, Y., and Carpenter, M.K., *Generation of Hepatocyte-Like Cells from Human Embryonic Stem Cells.* Cell Transplantation, 2003. **12**(1): p. 1-11.
163. Masson, S., Daveau, M.Y., Françlois, A., Bodenant, C., Hiron, M., Ténière, P., Salier, J.P., and Scotté, M., *Up-Regulated Expression of Hgf in Rat Liver Cells after Experimental Endotoxemia: A Potential Pathway for Enhancement of Liver Regeneration.* Growth Factors, 2001. **18**(4): p. 237-250.
164. Hasuke S, I.A., Uto H,Moriuchi A, Tahara Y, Numata M, Nagata K, Hori T, Hayashi K and Tsubouchi H, *Hepatocyte Growth Factor Accelerates the Proliferation of Hepatic Oval Cells and Possibly Promotes the Differentiation in a 2-Acetylaminofluorene/Partial Hepatectomy Model in Rats.* Journal of Gastroenterology and Hepatology, 2005. **20**(11): p. 1753–1761.
165. Dailey, L., Ambrosetti, D., Mansukhani, A., and Basilico, C., *Mechanisms Underlying Differential Responses to Fgf Signaling.* Cytokine & Growth Factor Reviews, 2005. **16**(2): p. 233-247.
166. Fujimori, H., Asahina, K., Shimizu-Saito, K., Ikeda, R., Tanaka, Y., Teramoto, K., Morita, I., and Teraoka, H., *Vascular Endothelial Growth Factor Promotes Proliferation and Function of Hepatocyte-Like Cells in Embryoid Bodies Formed from Mouse Embryonic Stem Cells.* Journal of Hepatology, 2008. **48**(6): p. 962-973.
167. Oe, H., Kaido, T., Mori, A., Onodera, H., and Imamura, M., *Hepatocyte Growth Factor as Well as Vascular Endothelial Growth Factor Gene*

Induction Effectively Promotes Liver Regeneration after Hepatectomy in Solt-Farber Rats. Hepatogastroenterology, 2005. **52**(65): p. 1393-1397.
168. Hsiao, E.C., Koniaris, L.G., Zimmers-Koniaris, T., Sebald, S.M., Huynh, T.V., and Lee, S.-J., *Characterization of Growth-Differentiation Factor 15, a Transforming Growth Factor B Superfamily Member Induced Following Liver Injury.* Molecular and Cellular Biology, 2000. **20**(10): p. 3742-3751.
169. Si. Y, L.X., Cheng. M, Wang. M, Gong. Q,Yang. Y, Wang. T, Yang. W, *Growth Differentiation Factor 15 Is Induced by Hepatitis C Virus Infection and Regulates Hepatocellular Carcinoma-Related Genes.* PLoS ONE, 2011. **6**(5): p. e19967.
170. Nejak-Bowen, K. and Monga, S.P.S., *Wnt/B-Catenin Signaling in Hepatic Organogenesis.* Organogenesis, 2008. **4**(2): p. 92-99.
171. Zhong, Z., Tsukada, S., Rehman, H., Parsons, C.J., Theruvath, T.P., Rippe, R.A., Brenner, D.A., and Lemasters, J.J., *Inhibition of Transforming Growth Factor-B/Smad Signaling Improves Regeneration of Small-for-Size Rat Liver Grafts.* Liver Transplantation, 2010. **16**(2): p. 181-190.
172. Yoshida, K. and Matsuzaki, K., *Differential Regulation of Tgf-ß/Smad Signaling in Hepatic Stallate Cells between Acute and Chronic Liver Injuries.* Frontiers in Physiology, 2012. **3**: p. 1-7.
173. Jinnin. M, I.H., and Tamaki. K, *Characterization of Sis3, a Novel Specific Inhibitor of Smad3, and Its Effect on Transforming Growth Factor-1-Induced Extracellular Matrix Expression.* Molecular Pharmacology, 2006. **69**(2): p. 597–607.
174. Cantoni, L., Rozio, M., Mangolini, A., Hauri, L., and Caccia, S., *Hyperforin Contributes to the Hepatic Cyp3a-Inducing Effect of Hypericum Perforatum Extract in the Mouse.* Toxicological Sciences, 2003. **75**(1): p. 25-30.
175. Komoroski, B.J., Zhang, S., Cai, H., Hutzler, J.M., Frye, R., Tracy, T.S., Strom, S.C., Lehmann, T., Ang, C.Y.W., Cui, Y.Y., and Venkataramanan, R., *Induction and Inhibition of Cytochromes P450 by the St. John's Wort Constituent Hyperforin in Human Hepatocyte Cultures.* Drug Metabolism and Disposition, 2004. **32**(5): p. 512-518.
176. Thomas M, B.O., Klumpp B, Kandel B. A, Damm G, Weiss T. S, Klein K, Schwab M, and Zanger U. M, *Direct Transcriptional Regulation of Human Hepatic Cytochrome P450 3a4 (Cyp3a4) by Peroxisome Proliferator–Activated Receptor Alpha (Ppara).* Molecular Pharmagology, 2013. **83**: p. 709–718.
177. Melet, A., Assrir, N., Jean, P., Pilar Lopez-Garcia, M., Marques-Soares, C., Jaouen, M., Dansette, P.M., Sari, M.-A., and Mansuy, D., *Substrate Selectivity of Human Cytochrome P450 2c9: Importance of Residues 476, 365, and 114 in Recognition of Diclofenac and Sulfaphenazole and in Mechanism-Based Inactivation by Tienilic Acid.* Archives of Biochemistry and Biophysics, 2003. **409**(1): p. 80-91.
178. Frye, R.F., Zgheib, N.K., Matzke, G.R., Chaves-Gnecco, D., Rabinovitz, M., Shaikh, O.S., and Branch, R.A., *Liver Disease Selectively Modulates Cytochrome P450–Mediated Metabolism.* Clinical Pharmacology & Therapeutics, 2006. **80**(3): p. 235-245.
179. Wrighton, S.A., Schuetz, E.G., Thummel, K.E., Shen, D.D., Korzekwa, K.R., and Watkins, P.B., *The Human Cyp3a Subfamily: Practical Considerations.* Drug Metabolism Reviews, 2000. **32**: p. 339-361.
180. Denison, M.S. and Whitlock, J.P., *Xenobiotic-Inducible Transcription of Cytochrome P450 Genes.* Journal of Biological Chemistry, 1995. **270**(31): p. 18175-18178.

181. Mahatthanatrakul, W., Nontaput, T., Ridtitid, W., Wongnawa, M., and Sunbhanich, M., *Rifampin, a Cytochrome P450 3a Inducer, Decreases Plasma Concentrations of Antipsychotic Risperidone in Healthy Volunteers.* Journal of Clinical Pharmacy and Therapeutics, 2007. **32**(2): p. 161-167.
182. Walsh, A.A., Szklarz, G.D., and Scott, E.E., *Human Cytochrome P450 1a1 Structure and Utility in Understanding Drug and Xenobiotic Metabolism.* Journal of Biological Chemistry, 2013. **288**(18): p. 12932-12943.
183. Yoshinari, K., Ueda, R., Kusano, K., Yoshimura, T., Nagata, K., and Yamazoe, Y., *Omeprazole Transactivates Human Cyp1a1 and Cyp1a2 Expression through the Common Regulatory Region Containing Multiple Xenobiotic-Responsive Elements.* Biochemical Pharmacology, 2008. **76**(1): p. 139-145.
184. Michalopoulos, G.K., Bowen, W.C., Mul, Egrave, K, and Luo, J., *Hgf, Egf and Dexamethasone-Induced Gene Expression Patterns During Formation of Tissue in Hepatic Organoid Cultures.* Gene Expression, 2003. **11**(2): p. 55-75.
185. Agarwal, S., Holton, K.L., and Lanza, R., *Efficient Differentiation of Functional Hepatocytes from Human Embryonic Stem Cells.* Stem Cells, 2008. **26**(5): p. 1117-1127.
186. Baharvand, H., Hashemi, S.M., and Shahsavani, M., *Differentiation of Human Embryonic Stem Cells into Functional Hepatocyte-Like Cells in a Serum-Free Adherent Culture Condition.* Differentiation, 2008. **76**(5): p. 465-477.
187. Bailly-Maitre, B., de Sousa, G., Boulukos, K., Gugenheim, J., and Rahmani, R., *Dexamethasone Inhibits Spontaneous Apoptosis in Primary Cultures of Human and Rat Hepatocytes Via Bcl-2 and Bcl-Xl Induction.* Cell Death and Differentiation, 2001. **8**: p. 279 - 288.
188. Al-Adsani, A., Burke, Z.D., Eberhard, D., Lawrence, K.L., Shen, C.-N., Rustgi, A.K., Sakaue, H., Farrant, J.M., and Tosh, D., *Dexamethasone Treatment Induces the Reprogramming of Pancreatic Acinar Cells to Hepatocytes and Ductal Cells.* PLoS ONE, 2010. **5**(10): p. e13650.
189. Zhong, W., Sladek, F.M., and Darnell Jr, J.E., *The Expression Pattern of a Drosophila Homolog to the Mouse Transcription Factor Hnf-4 Suggests a Determinative Role in Gut Formation.* EMBO Journal, 1993. **12**(2): p. 537-544.
190. Fereshteh Parviz, C.M., Wendy D Garrison, Laura Savatski, John W Adamson, Gang Ning, Klaus H Kaestner, Jennifer M Rossi, Kenneth S Zaret & Stephen A Duncan, *Hepatocyte Nuclear Factor 4 Controls the Development of a Hepatic Epithelium and Liver Morphogenesis.* Nature Genetics, 2003. **34**: p. 292 - 296.
191. Watt, A.J., Garrison, W.D., and Duncan, S.A., *Hnf4: A Central Regulator of Hepatocyte Differentiation and Function.* Hepatology, 2003. **37**(6): p. 1249-1253.
192. Sladek, F.M., *Desperately Seeking... Something.* Molecular Cell, 2002. **10**(2): p. 219-221.
193. Sladek, F.M., Zhong, W.M., Lai, E., and Darnell, J.E., *Liver-Enriched Transcription Factor Hnf-4 Is a Novel Member of the Steroid Hormone Receptor Superfamily.* Genes & Development, 1990. **4**(12b): p. 2353-2365.
194. Vallim, T. and Salter, A.M., *Regulation of Hepatic Gene Expression by Saturated Fatty Acids.* Prostaglandins, Leukotrienes and Essential Fatty Acids (PLEFA), 2010. **82**(4): p. 211-218.
195. Jump, D.B., Botolin, D., Wang, Y., Xu, J., Christian, B., and Demeure, O., *Fatty Acid Regulation of Hepatic Gene Transcription.* The Journal of Nutrition, 2005. **135**(11): p. 2503-2506.

196. Bonzo, J.A., Ferry, C.H., Matsubara, T., Kim, J.-H., and Gonzalez, F.J., *Suppression of Hepatocyte Proliferation by Hepatocyte Nuclear Factor 4α in Adult Mice.* The Journal of Biological Chemistry, 2012. **287**(10): p. 7345-7356.
197. Jover, R., Bort, R., Gómez-Lechón, M.J., and Castell, J.V., *Cytochrome P450 Regulation by Hepatocyte Nuclear Factor 4 in Human Hepatocytes: A Study Using Adenovirus-Mediated Antisense Targeting.* Hepatology, 2001. **33**(3): p. 668-675.
198. Jover, R., Bort, R., Gómez-Lechón, M.J., and Castell, J.V., *Cytochrome P450 Regulation by Hepatocyte Nuclear Factor 4 in Human Hepatocytes: A Study Using Adenovirus-Mediated Antisense Targeting.* Hepatology, 2001. **33**(3): p. 668-675.
199. Tegude, H., Schnabel, A., Zanger, U.M., Klein, K., Eichelbaum, M., and Burk, O., *Molecular Mechanism of Basal Cyp3a4 Regulation by Hepatocyte Nuclear Factor 4α: Evidence for Direct Regulation in the Intestine.* Drug Metabolism and Disposition, 2007. **35**(6): p. 946-954.
200. Lu, H., Gonzalez, F.J., and Klaassen, C., *Alterations in Hepatic Mrna Expression of Phase Ii Enzymes and Xenobiotic Transporters after Targeted Disruption of Hepatocyte Nuclear Factor 4 Alpha.* Toxicological Sciences, 2010. **118**(2): p. 380-390.
201. Yuan, X., Ta, T.C., Lin, M., Evans, J.R., Dong, Y., Bolotin, E., Sherman, M.A., Forman, B.M., and Sladek, F.M., *Identification of an Endogenous Ligand Bound to a Native Orphan Nuclear Receptor.* PLoS ONE, 2009. **4**(5): p. e5609.
202. Dhe-Paganon, S., Duda, K., Iwamoto, M., Chi, Y.-I., and Shoelson, S.E., *Crystal Structure of the Hnf4α Ligand Binding Domain in Complex with Endogenous Fatty Acid Ligand.* Journal of Biological Chemistry, 2002. **277**(41): p. 37973-37976.
203. Torchia, J., Rose, D.W., Inostroza, J., Kamei, Y., Westin, S., Glass, C.K., and Rosenfeld, M.G., *The Transcriptional Co-Activator P/Cip Binds Cbp and Mediates Nuclear-Receptor Function.* Nature, 1997. **387**: p. 677.
204. Rhee, J., Inoue, Y., Yoon, J.C., Puigserver, P., Fan, M., Gonzalez, F.J., and Spiegelman, B.M., *Regulation of Hepatic Fasting Response by Pparγ Coactivator-1α (Pgc-1): Requirement for Hepatocyte Nuclear Factor 4α in Gluconeogenesis.* Proceedings of the National Academy of Sciences, 2003. **100**(7): p. 4012-4017.
205. Renaud, J.P. and Moras*, D., *Structural Studies on Nuclear Receptors.* Cellular and Molecular Life Sciences CMLS, 2000. **57**(12): p. 1748-1769.
206. Egea, P.F., Mitschler, A., Rochel, N., Ruff, M., Chambon, P., and Moras, D., *Crystal Structure of the Human Rxrα Ligand-Binding Domain Bound to Its Natural Ligand: Retinoic Acid.* The EMBO Journal, 2000. **19**(11): p. 2592-2601.
207. Wisely, G.B., Miller, A.B., Davis, R.G., Thornquest, A.D., Jr., Johnson, R., Spitzer, T., Sefler, A., Shearer, B., Moore, J.T., Miller, A.B., Willson, T.M., and Williams, S.P., *Hepatocyte Nuclear Factor 4 Is a Transcription Factor That Constitutively Binds Fatty Acids.* Structure, 2002. **10**(9): p. 1225-1234.
208. Duda, K., Chi, Y.-I., and Shoelson, S.E., *Structural Basis for Hnf-4α Activation by Ligand and Coactivator Binding.* Journal of Biological Chemistry, 2004. **279**(22): p. 23311-23316.
209. Fang, B., Mane-Padros, D., Bolotin, E., Jiang, T., and Sladek, F.M., *Identification of a Binding Motif Specific to Hnf4 by Comparative Analysis of Multiple Nuclear Receptors.* Nucleic Acids Research, 2012. **40**(12): p. 5343-5356.

210. Sladek, F.M., *What Are Nuclear Receptor Ligands?* Molecular and Cellular Endocrinology, 2011. **334**(1-2): p. 3-13.
211. Chang, T.T. and Hughes-Fulford, M., *Molecular Mechanisms Underlying the Enhanced Functions of Three-Dimensional Hepatocyte Aggregates.* Biomaterials, 2014. **35**(7): p. 2162-2171.
212. Hwang-Verslues, W.W. and Sladek, F.M., *Hnf4α — Role in Drug Metabolism and Potential Drug Target?* Current Opinion in Pharmacology, 2010. **10**(6): p. 698-705.
213. Yue, H.-Y., Yin, C., Hou, J.-L., Zeng, X., Chen, Y.-X., Zhong, W., Hu, P.-F., Deng, X., Tan, Y.-X., Zhang, J.-P., Ning, B.-F., Shi, J., Zhang, X., Wang, H.-Y., Lin, Y., and Xie, W.-F., *Hepatocyte Nuclear Factor 4α Attenuates Hepatic Fibrosis in Rats.* Gut, 2010. **59**(2): p. 236-246.
214. Bookout, A.L., Jeong, Y., Downes, M., Yu, R.T., Evans, R.M., and Mangelsdorf, D.J., *Anatomical Profiling of Nuclear Receptor Expression Reveals a Hierarchical Transcriptional Network.* Cell, 2006. **126**(4): p. 789-799.
215. Xie, W., Radominska-Pandya, A., Shi, Y., Simon, C.M., Nelson, M.C., Ong, E.S., Waxman, D.J., and Evans, R.M., *An Essential Role for Nuclear Receptors Sxr/Pxr in Detoxification of Cholestatic Bile Acids.* Proceedings of the National Academy of Sciences, 2001. **98**(6): p. 3375-3380.
216. Schulman, I.G. and Heyman, R.A., *The Flip Side: Identifying Small Molecule Regulators of Nuclear Receptors.* Chemistry & Biology, 2004. **11**(5): p. 639-646.
217. Tirona, R.G., Lee, W., Leake, B.F., Lan, L.B., Cline, C.B., Lamba, V., Parviz, F., Duncan, S.A., Inoue, Y., Gonzalez, F.J., Schuetz, E.G., and Kim, R.B., *The Orphan Nuclear Receptor Hnf4α Determines Pxr- and Car-Mediated Xenobiotic Induction of Cyp3a4.* Nature Medicine, 2003. **9**: p. 220-224.
218. Kandel, B.A., Ekins, S., Leuner, K., Thasler, W.E., Harteneck, C., and Zanger, U.M., *No Activation of Human Pregnane X Receptor by Hyperforin-Related Phloroglucinols.* Journal of Pharmacology and Experimental Therapeutics, 2014. **348**(3): p. 393-400.
219. Watkins, R.E., Maglich, J.M., Moore, L.B., Wisely, G.B., Noble, S.M., Davis-Searles, P.R., Lambert, M.H., Kliewer, S.A., and Redinbo, M.R., *A Crystal Structure of Human Pxr in Complex with the St. John's Wort Compound Hyperforin.* Biochemistry, 2003. **42**(6): p. 1430-1438.
220. Kliewer, S.A., Goodwin, B., and Willson, T.M., *The Nuclear Pregnane X Receptor: A Key Regulator of Xenobiotic Metabolism.* Endocrine Reviews, 2002. **23**(5): p. 687-702.
221. Tolson, A.H. and Wang, H., *Regulation of Drug-Metabolizing Enzymes by Xenobiotic Receptors: Pxr and Car.* Advanced Drug Delivery Reviews, 2010. **62**(13): p. 1238-1249.
222. Kliewer, S.A., Moore, J.T., Wade, L., Staudinger, J.L., Watson, M.A., Jones, S.A., McKee, D.D., Oliver, B.B., Willson, T.M., Zetterström, R.H., Perlmann, T., and Lehmann, J.M., *An Orphan Nuclear Receptor Activated by Pregnanes Defines a Novel Steroid Signaling Pathway.* Cell, 1998. **92**(1): p. 73-82.
223. Lehmann, J.M., McKee, D.D., Watson, M.A., Willson, T.M., Moore, J.T., and Kliewer, S.A., *The Human Orphan Nuclear Receptor Pxr Is Activated by Compounds That Regulate Cyp3a4 Gene Expression and Cause Drug Interactions.* The Journal of Clinical Investigation, 1998. **102**(5): p. 1016-1023.
224. Staudinger, J.L., Goodwin, B., Jones, S.A., Hawkins-Brown, D., MacKenzie, K.I., LaTour, A., Liu, Y., Klaassen, C.D., Brown, K.K., Reinhard, J., Willson, T.M., Koller, B.H., and Kliewer, S.A., *The Nuclear Receptor Pxr Is a*

Lithocholic Acid Sensor That Protects against Liver Toxicity. Proceedings of the National Academy of Sciences, 2001. **98**(6): p. 3369-3374.
225. Xie W, B.J.L., Downes M, Blumberg B, Simon C. M, Nelson M. C, Neuschwander B. A, Brunt E. M, Guzelian P. S and Evans R. M., *Humanized Xenobiotic Response in Mice Expressing Nuclear Receptor Sxr.* Nature, 2000. **406**: p. 435-439.
226. Wada, T., Gao, J., and Xie, W., *Pxr and Car in Energy Metabolism.* Trends in Endocrinology and Metabolism, 2009. **20**(6): p. 273-279.
227. di Masi, A., Marinis, E.D., Ascenzi, P., and Marino, M., *Nuclear Receptors Car and Pxr: Molecular, Functional, and Biomedical Aspects.* Molecular Aspects of Medicine, 2009. **30**(5): p. 297-343.
228. Maglich, J.M., Parks, D.J., Moore, L.B., Collins, J.L., Goodwin, B., Billin, A.N., Stoltz, C.A., Kliewer, S.A., Lambert, M.H., Willson, T.M., and Moore, J.T., *Identification of a Novel Human Constitutive Androstane Receptor (Car) Agonist and Its Use in the Identification of Car Target Genes.* Journal of Biological Chemistry, 2003. **278**(19): p. 17277-17283.
229. Perrot, N., ChesnÉ, C., De Waziers, I., Conner, J., Beaune, P.H., and Guillouzo, A., *Effects of Ethanol and Clofibrate on Expression of Cytochrome P-450 Enzymes and Epoxide Hydrolase in Cultures and Cocultures of Rat Hepatocytes.* European Journal of Biochemistry, 1991. **200**(1): p. 255-261.
230. Zhao, C. and Dahlman-Wright, K., *Liver X Receptor in Cholesterol Metabolism.* Journal of Endocrinology, 2010. **204**(3): p. 233-240.
231. Shenoy, S.D., Spencer, T.A., Mercer-Haines, N.A., Alipour, M., Gargano, M.D., Runge-Morris, M., and Kocarek, T.A., *Cyp3a Induction by Liver X Receptor Ligands in Primary Cultured Rat and Mouse Hepatocytes Is Mediated by the Pregnane X Receptor.* Drug Metabolism and Disposition, 2004. **32**(1): p. 66-71.
232. T, S.G.a.L., *Structure, Function and Regulation of the Abc1 Gene Product.* Current Opinion in Lipidology, 2001. **12**(2): p. 129-140.
233. Chen, K.-T., Pernelle, K., Tsai, Y.-H., Wu, Y.-H., Hsieh, J.-Y., Liao, K.-H., Guguen-Guillouzo, C., and Wang, H.-W., *Liver X Receptor A (Lxrα/Nr1h3) Regulates Differentiation of Hepatocyte-Like Cells Via Reciprocal Regulation of Hnf4α.* Journal of Hepatology, 2014. **61**(6): p. 1276-1286.
234. Shan, J., Schwartz, R.E., Ross, N.T., Logan, D.J., Thomas, D., Duncan, S.A., North, T.E., Goessling, W., Carpenter, A.E., and Bhatia, S.N., *Identification of Small Molecules for Human Hepatocyte Expansion and Ips Differentiation.* Nature Chemical Biology, 2013. **9**(8): p. 514-520.
235. Siller, R., Greenhough, S., Naumovska, E., and Sullivan, Gareth J., *Small-Molecule-Driven Hepatocyte Differentiation of Human Pluripotent Stem Cells.* Stem Cell Reports, 2015. **4**(5): p. 939-952.
236. Tasnim, F., Phan, D., Toh, Y.-C., and Yu, H., *Cost-Effective Differentiation of Hepatocyte-Like Cells from Human Pluripotent Stem Cells Using Small Molecules.* Biomaterials, 2015. **70**: p. 115-125.
237. Hernandez, D., *Massively Parallel Combinatorial Screening.* Genetic Engineering and Biotechnology News, 2015. **35**: p. 28-29.
238. Abai, A., Li, M., Jeyakumar, J., Hook, L., Asbrock, N., and Chu, V., *A Xeno-Free, Serum-Free Defined Medium to Rapidly Differentiate Human Mesenchymal Stem Cells to Osteoblasts.* ISSCR Poster Presentations, 2013.
239. Tarunina, M., Hernandez, D., Kronsteiner-Dobramysl, B., Pratt, P., Watson, T., Hua, P., Gullo, F., van der Garde, M., Zhang, Y., Hook, L., Choo, Y., and Watt, S.M., *A Novel High-Throughput Screening Platform Reveals an Optimized Cytokine Formulation for Human Hematopoietic Progenitor Cell Expansion.* Stem Cells and Development, 2016. **25**(22): p. 1709-1720.

240. Kusuda Furue, M., Tateyama, D., Kinehara, M., Na, J., Okamoto, T., and Sato, J.D., *Advantages and Difficulties in Culturing Human Pluripotent Stem Cells in Growth Factor-Defined Serum-Free Medium.* In Vitro Cellular & Developmental Biology. Animal, 2010. **46**(7): p. 573-576.
241. Mehta, A., Mathew, S., Viswanathan, C., and Majumdar, A.A., *Intrinsic Properties and External Factors Determine the Differentiation Bias of Human Embryonic Stem Cell Lines.* Cell Biology International, 2010. **34**(10): p. 1021-1031.
242. Wu, H., Xu, J., Pang, Z.P., Ge, W., Kim, K.J., Blanchi, B., Chen, C., Südhof, T.C., and Sun, Y.E., *Integrative Genomic and Functional Analyses Reveal Neuronal Subtype Differentiation Bias in Human Embryonic Stem Cell Lines.* Proceedings of the National Academy of Sciences of the United States of America, 2007. **104**(34): p. 13821-13826.
243. Graf, T. and Stadtfeld, M., *Heterogeneity of Embryonic and Adult Stem Cells.* Cell Stem Cell, 2008. **3**(5): p. 480-483.
244. Bradford, M.M., *A Rapid and Sensitive Method for the Quantitation of Microgram Quantities of Protein Utilizing the Principle of Protein-Dye Binding.* Analytical Biochemistry, 1976. **7**(72): p. 248-254.
245. Vallier, L., Reynolds, D., and Pedersen, R.A., *Nodal Inhibits Differentiation of Human Embryonic Stem Cells Along the Neuroectodermal Default Pathway.* Developmental Biology, 2004. **275**(2): p. 403-421.
246. Takenaga, M., Fukumoto, M., and Hori, Y., *Regulated Nodal Signaling Promotes Differentiation of the Definitive Endoderm and Mesoderm from Es Cells.* Journal of Cell Science, 2007. **120**(12): p. 2078-2090.
247. Toivonen, S., Lundin, K., Balboa, D., Ustinov, J., Tamminen, K., Palgi, J., Trokovic, R., Tuuri, T., and Otonkoski, T., *Activin a and Wnt-Dependent Specification of Human Definitive Endoderm Cells.* Experimental Cell Research, 2013. **319**(17): p. 2535-2544.
248. Nostro, M.C., Sarangi, F., Ogawa, S., Holtzinger, A., Corneo, B., Li, X., Micallef, S.J., Park, I.-H., Basford, C., Wheeler, M.B., Daley, G.Q., Elefanty, A.G., Stanley, E.G., and Keller, G., *Stage-Specific Signaling through Tgfβ Family Members and Wnt Regulates Patterning and Pancreatic Specification of Human Pluripotent Stem Cells.* Development, 2011. **138**(5): p. 861-871.
249. Brons, I.G.M., Smithers, L.E., Trotter, M.W.B., Rugg-Gunn, P., Sun, B., Chuva de Sousa Lopes, S.M., Howlett, S.K., Clarkson, A., Ahrlund-Richter, L., Pedersen, R.A., and Vallier, L., *Derivation of Pluripotent Epiblast Stem Cells from Mammalian Embryos.* Nature, 2007. **448**(7150): p. 191-195.
250. Chen, A.E., Borowiak, M., Sherwood, R.I., Kweudjeu, A., and Melton, D.A., *Functional Evaluation of Es Cell-Derived Endodermal Populations Reveals Differences between Nodal and Activin a-Guided Differentiation.* Development, 2013. **140**(3): p. 675-686.
251. Norrman, K., Fischer, Y., Bonnamy, B., Wolfhagen Sand, F., Ravassard, P., and Semb, H., *Quantitative Comparison of Constitutive Promoters in Human Es Cells.* PLoS ONE, 2010. **5**(8): p. e12413.
252. Wang R, L.J., Jiang H, Qin L. J, and Yang H. T, *Promoter-Dependent Egfp Expression During Embryonic Stem Cell Propagation and Differentiation.* Stem Cells and Development, 2008. **17**(2): p. 279-290.
253. Mao, G., Marotta, F., Yu, J., Zhou, L., Yu, Y., Wang, L., and Chui, D., *DNA Context and Promoter Activity Affect Gene Expression in Lentiviral Vectors.* Acta Bio Medica Atenei Parmensis, 2008. **79**(3): p. 192-196.
254. Liew, C.-G., Draper, J.S., Walsh, J., Moore, H., and Andrews, P.W., *Transient and Stable Transgene Expression in Human Embryonic Stem Cells.* Stem Cells, 2007. **25**(6): p. 1521-1528.

255. Alves da Silva, M.L., Costa-Pinto, A.R., Martins, A., Correlo, V.M., Sol, P., Bhattacharya, M., Faria, S., Reis, R.L., and Neves, N.M., *Conditioned Medium as a Strategy for Human Stem Cells Chondrogenic Differentiation.* Journal of Tissue Engineering and Regenerative Medicine, 2015. **9**(6): p. 714-723.
256. Jin, L.T., Jiho, J., Jeokyung, K., Ho, B.S., Jae, J.G., Heungsoo, S., Wook, K.D., and Soo, K.B., *Mesenchymal Stem Cell-Conditioned Medium Enhances Osteogenic and Chondrogenic Differentiation of Human Embryonic Stem Cells and Human Induced Pluripotent Stem Cells by Mesodermal Lineage Induction.* Tissue Engineering, 2014. **20**(7): p. 1306-1313.
257. Llames, S., García-Pérez, E., Meana, Á., Larcher, F., and del Río, M., *Feeder Layer Cell Actions and Applications.* Tissue Engineering Reviews, 2015. **21**(4): p. 345-353.
258. Richards, M., Fong, C.-Y., Chan, W.-K., Wong, P.-C., and Bongso, A., *Human Feeders Support Prolonged Undifferentiated Growth of Human Inner Cell Masses and Embryonic Stem Cells.* Nature Biotechnology, 2002. **20**: p. 933.
259. Doetschman, T.C., Eistetter, H., Katz, M., Schmidt, W., and Kemler, R., *The in Vitro Development of Blastocyst-Derived Embryonic Stem Cell Lines: Formation of Visceral Yolk Sac, Blood Islands and Myocardium.* Journal of Embryology and Experimental Morphology, 1985. **87**(1): p. 27-45.
260. Richards, M., Tan, S., Fong, C.Y., Biswas, A., Chan, W.K., and Bongso, A., *Comparative Evaluation of Various Human Feeders for Prolonged Undifferentiated Growth of Human Embryonic Stem Cells.* Stem Cells, 2003. **21**(5): p. 546-556.
261. Ma, H., Zhang, Y., Wang, H., Han, C., Lei, R., Zhang, L., Yang, Z., Rao, L., Qing, H., Xiang, J., and Deng, Y., *Effect and Mechanism of Mitomycin C Combined with Recombinant Adeno-Associated Virus Type Ii against Glioma.* International Journal of Molecular Sciences, 2014. **15**(1): p. 1-14.
262. Parent, R., Marion, M.-J., Furio, L., Trépo, C., and Petit, M.-A., *Origin and Characterization of a Human Bipotent Liver Progenitor Cell Line.* Gastroenterology, 2004. **126**(4): p. 1147-1156.
263. Sumi, T., Tsuneyoshi, N., Nakatsuji, N., and Suemori, H., *Defining Early Lineage Specification of Human Embryonic Stem Cells by the Orchestrated Balance of Canonical Wnt/Beta-Catenin, Activin/Nodal and Bmp Signaling.* Development, 2008. **135**(17): p. 2969-2979.
264. Moore, L.B., Goodwin, B., Jones, S.A., Wisely, G.B., Serabjit-Singh, C.J., Willson, T.M., Collins, J.L., and Kliewer, S.A., *St. John's Wort Induces Hepatic Drug Metabolism through Activation of the Pregnane X Receptor.* Proceedings of the National Academy of Sciences of the United States of America, 2000. **97**(13): p. 7500-7502.
265. Nguyen Lananh, N., Furuya Momoko, H., Wolfraim Lawrence, A., Nguyen Anthony, P., Holdren Matthew, S., Campbell Jean, S., Knight, B., Yeoh George, C.T., Fausto, N., and Parks, W.T., *Transforming Growth Factor-Beta Differentially Regulates Oval Cell and Hepatocyte Proliferation.* Hepatology, 2006. **45**(1): p. 31-41.
266. Yuji, N., Meifang, W., and I., C.B., *Changes in Tgf-B Receptors of Rat Hepatocytes During Primary Culture and Liver Regeneration: Increased Expression of Tgf-B Receptors Associated with Increased Sensitivity to Tgf-B-Mediated Growth Inhibition.* Journal of Cellular Physiology, 1998. **176**(3): p. 612-623.

267. Spagnoli, F.M., Cicchini, C., Tripodi, M., and Weiss, M.C., *Inhibition of Mmh (Met Murine Hepatocyte) Cell Differentiation by Tgf(Beta) Is Abrogated by Pre-Treatment with the Heritable Differentiation Effector Fgf1.* Journal of Cell Science, 2000. **113**(20): p. 3639.
268. Gage, B.K., Webber, T.D., and Kieffer, T.J., *Initial Cell Seeding Density Influences Pancreatic Endocrine Development During in Vitro Differentiation of Human Embryonic Stem Cells.* PLoS ONE, 2013. **8**(12): p. e82076.
269. Nair, G.G. and Odorico, J.S., *Ptf1a Activity in Enriched Posterior Foregut Endoderm, but Not Definitive Endoderm, Leads to Enhanced Pancreatic Differentiation in an in Vitro Mouse Esc-Based Model.* Stem Cells International, 2016. **2016**: p. 1-15.
270. Fang, Y. and Eglen, R.M., *Three-Dimensional Cell Cultures in Drug Discovery and Development.* SLAS DISCOVERY: Advancing Life Sciences R&D, 2017. **22**(5): p. 456-472.
271. Engert, S., Burtscher, I., Liao, W.P., Dulev, S., Schotta, G., and Lickert, H., *Wnt/B-Catenin Signalling Regulates Sox17 Expression and Is Essential for Organizer and Endoderm Formation in the Mouse.* Development, 2013. **140**(15): p. 3128-3138.
272. Cury-Boaventura, M.F., Gorjão, R., de Lima, T.M., Newsholme, P., and Curi, R., *Comparative Toxicity of Oleic and Linoleic Acid on Human Lymphocytes.* Life Sciences, 2006. **78**(13): p. 1448-1456.
273. Taniguchi, F., Harada, T., Deura, I., Iwabe, T., Tsukihara, S., and Terakawa, N., *Hepatocyte Growth Factor Promotes Cell Proliferation and Inhibits Progesterone Secretion Via Pka and Mapk Pathways in a Human Granulosa Cell Line.* Molecular Reproduction and Development, 2004. **68**(3): p. 335-344.
274. Huang, P., Zhang, L., Gao, Y., He, Z., Yao, D., Wu, Z., Cen, J., Chen, X., Liu, C., Hu, Y., Lai, D., Hu, Z., Chen, L., Zhang, Y., Cheng, X., Ma, X., Pan, G., Wang, X., and Hui, L., *Direct Reprogramming of Human Fibroblasts to Functional and Expandable Hepatocytes.* Cell Stem Cell, 2014. **14**(3): p. 370-384.
275. Huh, C.-G., Factor, V.M., Sánchez, A., Uchida, K., Conner, E.A., and Thorgeirsson, S.S., *Hepatocyte Growth Factor/C-Met Signaling Pathway Is Required for Efficient Liver Regeneration and Repair.* Proceedings of the National Academy of Sciences of the United States of America, 2004. **101**(13): p. 4477-4482.
276. Braeuning, A., *Liver Cell Proliferation and Tumor Promotion by Phenobarbital: Relevance for Humans?* Archives of Toxicology, 2014. **88**(10): p. 1771-1772.
277. Cameron, K., Tan, R., Schmidt-Heck, W., Campos, G., Lyall, Marcus J., Wang, Y., Lucendo-Villarin, B., Szkolnicka, D., Bates, N., Kimber, Susan J., Hengstler, Jan G., Godoy, P., Forbes, Stuart J., and Hay, David C., *Recombinant Laminins Drive the Differentiation and Self-Organization of Hesc-Derived Hepatocytes.* Stem Cell Reports, 2015. **5**(6): p. 1250-1262.
278. Murayama, N., Usui, T., Slawny, N., Chesne, C., and Yamazaki, H., *Human Heparg Cells Can Be Cultured in Hanging-Drop Plates for Cytochrome P450 Induction and Function Assays.* Drug Metabolism Letters, 2015. **9**(1): p. 3-7.
279. Vermet, H., Raoust, N., Ngo, R., Esserméant, L., Klieber, S., Fabre, G., and Boulenc, X., *Evaluation of Normalization Methods to Predict Cyp3a4 Induction in Six Fully Characterized Cryopreserved Human Hepatocyte Preparations and Heparg Cells.* Drug Metabolism and Disposition, 2016. **44**(1): p. 50-60.
280. Tohru, I., Tomokazu, M., Haruka, M., Ken, S., Masaya, S., Masakiyo, H., Kan, C., Takahiro, M., Hideki, A., Kiyoshi, O., and Tetsuro, S., *Cyp3a4*

Inducible Model for in Vitro Analysis of Human Drug Metabolism Using a Bioartificial Liver. Hepatology, 2003. **37**(3): p. 665-673.
281. Liu, Y., Flynn, T.J., Xia, M., Wiesenfeld, P.L., and Ferguson, M.S., *Evaluation of Cyp3a4 Inhibition and Hepatotoxicity Using Dmso-Treated Human Hepatoma Huh-7 Cells.* Cell biology and toxicology, 2015. **31**(4-5): p. 221-230.
282. Hart, S.N., Cui, Y., Klaassen, C.D., and Zhong, X.-b., *Three Patterns of Cytochrome P450 Gene Expression During Liver Maturation in Mice.* Drug Metabolism and Disposition, 2009. **37**(1): p. 116-121.
283. Szabo, M., Veres, Z., Baranyai, Z., Jakab, F., and Jemnitz, K., *Comparison of Human Hepatoma Heparg Cells with Human and Rat Hepatocytes in Uptake Transport Assays in Order to Predict a Risk of Drug Induced Hepatotoxicity.* PLoS ONE, 2013. **8**(3): p. e59432.
284. Garcia-Canton, C., Minet, E., Anadon, A., and Meredith, C., *Metabolic Characterization of Cell Systems Used in in Vitro Toxicology Testing: Lung Cell System Beas-2b as a Working Example.* Toxicology in Vitro, 2013. **27**(6): p. 1719-1727.
285. Hay, D.C., Zhao, D., Fletcher, J., Hewitt, Z.A., McLean, D., Urruticoechea, U.A., Black, J.R., Elcombe, C., Ross, J.A., Wolf, R., and Cui, W., *Efficient Differentiation of Hepatocytes from Human Embryonic Stem Cells Exhibiting Markers Recapitulating Liver Development in Vivo.* Stem Cells, 2008. **26**(4): p. 894-902.
286. Buckley, S.M.K., Delhove, J.M.K.M., Perocheau, D.P., Karda, R., Rahim, A.A., Howe, S.J., Ward, N.J., Birrell, M.A., Belvisi, M.G., Arbuthnot, P., Johnson, M.R., Waddington, S.N., and McKay, T.R., *In Vivo Bioimaging with Tissue-Specific Transcription Factor Activated Luciferase Reporters.* Scientific Reports, 2015. **5**: p. 11842.
287. Liang, Q., Dmitriev, I., Kashentseva, E., Curiel, D.T., and Herschman, H.R., *Noninvasive of Adenovirus Tumor Retargeting in Living Subjects by a Soluble Adenovirus Receptor-Epidermal Growth Factor (Scar-Egf) Fusion Protein.* Molecular Imaging and Biology 2004. **6**(6): p. 385-394.
288. Tardiff, J. and Krauter, K.S., *Divergent Expression of Alpha1-Protease Inhibitor Genes in Mouse and Human.* Nucleic Acids Research, 1998. **26**(16): p. 3794-3799.
289. Hafenrichter, D., Wu, X., Rettinger, S., Kennedy, S., Flye, M., and Ponder, K., *Quantitative Evaluation of Liver-Specific Promoters from Retroviral Vectors after in Vivo Transduction of Hepatocytes.* Blood, 1994. **84**(10): p. 3394-3404.
290. Kramer, M.G., Barajas, M., Razquin, N., Berraondo, P., Rodrigo, M., Wu, C., Qian, C., Fortes, P., and Prieto, J., *In Vitro and in Vivo Comparative Study of Chimeric Liver-Specific Promoters.* Molecular Therapy, 2003. **7**(3): p. 375-385.
291. Ciliberto, G., Dente, L., and Cortese, R., *Cell-Specific Expression of a Transfected Human Antitrypsin Gene.* Cell, 1985. **41**(2): p. 531-540.
292. De Simone, V., Ciliberto, G., Hardon, E., Paonessa, G., Palla, F., Lundberg, L., and Cortese, R., *Cis- and Trans-Acting Elements Responsible for the Cell-Specific Expression of the Human Alpha 1-Antitrypsin Gene.* The EMBO Journal, 1987. **6**(9): p. 2759-2766.
293. Hardon, E.M., Frain, M., Paonessa, G., and Cortese, R., *Two Distinct Factors Interact with the Promoter Regions of Several Liver-Specific Genes.* The EMBO Journal, 1988. **7**(6): p. 1711-1719.
294. DeLaForest, A., Nagaoka, M., Si-Tayeb, K., Noto, F.K., Konopka, G., Battle, M.A., and Duncan, S.A., *Hnf4a Is Essential for Specification of Hepatic*

Progenitors from Human Pluripotent Stem Cells. Development 2011. **138**(19): p. 4143-4153.
295. Tao, L., Shichang, Z., Dedong, X., and Yingjie, W., *Induction of Hepatocyte-Like Cells from Mouse Embryonic Stem Cells by Lentivirus-Mediated Constitutive Expression of Foxa2/Hnf4a.* Journal of Cellular Biochemistry, 2013. **114**(11): p. 2531-2541.
296. Malinen, M.M., Kanninen, L.K., Corlu, A., Isoniemi, H.M., Lou, Y.-R., Yliperttula, M.L., and Urtti, A.O., *Differentiation of Liver Progenitor Cell Line to Functional Organotypic Cultures in 3d Nanofibrillar Cellulose and Hyaluronan-Gelatin Hydrogels.* Biomaterials, 2014. **35**(19): p. 5110-5121.
297. Baxter, M.A., Rowe, C., Alder, J., Harrison, S., Hanley, K.P., Park, B.K., Kitteringham, N.R., Goldring, C.E., and Hanley, N.A., *Generating Hepatic Cell Lineages from Pluripotent Stem Cells for Drug Toxicity Screening.* Stem cell research, 2010. **5**(1): p. 4-22.
298. Mansha, M., Wasim, M., Ploner, C., Hussain, A., Latif, A.A., Tariq, M., and Kofler, A., *Problems Encountered in Bicistronic Ires-Gfp Expression Vectors Employed in Functional Analyses of Gc-Induced Genes.* Molecular Biology Reports, 2012. **39**(12): p. 10227-10234.
299. Kim, K.-J., Kim, H.-E., Lee, K.-H., Han, W., Yi, M.-J., Jeong, J., and Oh, B.-H., *Two-Promoter Vector Is Highly Efficient for Overproduction of Protein Complexes.* Protein Science, 2004. **13**(6): p. 1698-1703.
300. Bell, A.C., West, A.G., and Felsenfeld, G., *Insulators and Boundaries: Versatile Regulatory Elements in the Eukaryotic Genome.* Science, 2001. **291**(5503): p. 447-450.
301. Watanabe, K., Ueno, M., Kamiya, D., Nishiyama, A., Matsumura, M., Wataya, T., Takahashi, J.B., Nishikawa, S., Nishikawa, S.-i., Muguruma, K., and Sasai, Y., *A Rock Inhibitor Permits Survival of Dissociated Human Embryonic Stem Cells.* Nature Biotechnology, 2007. **25**: p. 681-686.
302. Ramsay, D., Bevan, N., Rees, S., and Milligan, G., *Detection of Receptor Ligands by Monitoring Selective Stabilization of a Renilla Luciferase-Tagged, Constitutively Active Mutant, G-Protein-Coupled Receptor.* British Journal of Pharmacology, 2001. **133**(2): p. 315-323.
303. Mazerbourg, S., Sangkuhl, K., Luo, C.-W., Sudo, S., Klein, C., and Hsueh, A.J.W., *Identification of Receptors and Signaling Pathways for Orphan Bone Morphogenetic Protein/Growth Differentiation Factor Ligands Based on Genomic Analyses.* Journal of Biological Chemistry, 2005. **280**(37): p. 32122-32132.
304. Raghuram, S., Stayrook, K.R., Huang, P., Rogers, P.M., Nosie, A.K., McClure, D.B., Burris, L.L., Khorasanizadeh, S., Burris, T.P., and Rastinejad, F., *Identification of Heme as the Ligand for the Orphan Nuclear Receptors Rev-Erbα and Rev-Erbβ.* Nature Structural and Molecular Biology, 2007. **14**(12): p. 1207-1213.
305. Lee, S.-H., Athavankar, S., Cohen, T., Kiselyuk, A., and Levine, F., *Reversal of Lipotoxic Effects on the Insulin Promoter by Alverine and Benfluorex: Identification as Hnf4α Activators.* ACS Chemical Biology, 2013. **8**(8): p. 1730-1736.
306. Tannous, B.A., Kim, D.-E., Fernandez, J.L., Weissleder, R., and Breakefield, X.O., *Codon-Optimized Gaussia Luciferase Cdna for Mammalian Gene Expression in Culture and in Vivo.* Molecular Therapy, 2005. **11**(3): p. 435-443.
307. Nico, M., Leo, V., Russell, R., Alan, K., and Enrique, S., *T0901317 Is a Potent Pxr Ligand: Implications for the Biology Ascribed to Lxr.* FEBS Letters, 2007. **581**(9): p. 1721-1726.

308. Gazit, V., Huang, J., Weymann, A., and Rudnick, D.A., *Analysis of the Role of Hepatic Pparγ Expression During Mouse Liver Regeneration.* Hepatology 2012. **56**(4): p. 1489-1498.
309. Joseph, S.B., McKilligin, E., Pei, L., Watson, M.A., Collins, A.R., Laffitte, B.A., Chen, M., Noh, G., Goodman, J., Hagger, G.N., Tran, J., Tippin, T.K., Wang, X., Lusis, A.J., Hsueh, W.A., Law, R.E., Collins, J.L., Willson, T.M., and Tontonoz, P., *Synthetic Lxr Ligand Inhibits the Development of Atherosclerosis in Mice.* Proceedings of the National Academy of Sciences, 2002. **99**(11): p. 7604-7609.
310. Greetje, E., Tom, H., Peggy, P., Sarah, S., Mathieu, V., Tamara, V., and Vera, R., *Molecular Mechanisms Underlying the Dedifferentiation Process of Isolated Hepatocytes and Their Cultures.* Current Drug Metabolism, 2006. **7**(6): p. 629-660.
311. Bréjot, T., Blanchard, S., Hocquemiller, M., Haase, G., Liu, S., Nosjean, A., Heard, J.M., and Bohl, D., *Forced Expression of the Motor Neuron Determinant Hb9 in Neural Stem Cells Affects Neurogenesis.* Experimental Neurology, 2006. **198**(1): p. 167-182.
312. Brooks, A.R., Harkins, R.N., Wang, P., Sheng, Q.H., Pengxuan, L., and Rubanyi, G.M., *Transcriptional Silencing Is Associated with Extensive Methylation of the Cmv Promoter Following Adenoviral Gene Delivery to Muscle.* The Journal of Gene Medicine, 2004. **6**(4): p. 395-404.
313. Luo, X.-H., Chang, Y.-J., and Huang, X.-J., *Improving Cytomegalovirus-Specific T Cell Reconstitution after Haploidentical Stem Cell Transplantation.* Journal of Immunology Research, 2014. **2014**: p. 631951.
314. Lee, J.K., Responte, D.J., Cissell, D.D., Hu, J.C., Nolta, J.A., and Athanasiou, K.A., *Clinical Translation of Stem Cells: Insight for Cartilage Therapies.* Critical reviews in biotechnology, 2014. **34**(1): p. 89-100.
315. Zhang, J.Q., Yu, B.X., Ma, B.F., Yu, W.H., Zhang, A.X., Huang, G., Mao, F.F., Zhang, X.M., Wang, Z.C., Li, S.N., Lahn, B.T., and Xiang, A.P., *Neural Differentiation of Embryonic Stem Cells Induced by Conditioned Medium from Neural Stem Cell.* NeuroReport, 2006. **17**(10): p. 981-986.
316. Timmers, L., Lim, S.K., Hoefer, I.E., Arslan, F., Lai, R.C., van Oorschot, A.A.M., Goumans, M.J., Strijder, C., Sze, S.K., Choo, A., Piek, J.J., Doevendans, P.A., Pasterkamp, G., and de Kleijn, D.P.V., *Human Mesenchymal Stem Cell-Conditioned Medium Improves Cardiac Function Following Myocardial Infarction.* Stem Cell Research, 2011. **6**(3): p. 206-214.
317. Webber, E.M., Wu, J.C., Wang, L., Merlino, G., and Fausto, N., *Overexpression of Transforming Growth Factor-Alpha Causes Liver Enlargement and Increased Hepatocyte Proliferation in Transgenic Mice.* The American Journal of Pathology, 1994. **145**(2): p. 398-408.
318. Tomiya, T., Ogata, I., and Fujiwara, K., *Transforming Growth Factor A Levels in Liver and Blood Correlate Better Than Hepatocyte Growth Factor with Hepatocyte Proliferation During Liver Regeneration.* The American Journal of Pathology, 1998. **153**(3): p. 955-961.
319. Tamano, S., Merlino, G.T., and Ward, J.M., *Rapid Development of Hepatic Tumors in Transforming Growth Factor Alpha Transgenic Mice Associated with Increased Cell Proliferation in Precancerous Hepatocellular Lesions Initiated by N-Nitrosodiethylamine and Promoted by Phenobarbital.* Carcinogenesis, 1994. **15**(9): p. 1791-1798.
320. Honkakoski, P. and Negishi, M., *Regulation of Cytochrome P450 (Cyp) Genes by Nuclear Receptors.* Biochemical Journal, 2000. **347**(2): p. 321-337.
321. Tzameli, I., Pissios, P., Schuetz, E.G., and Moore, D.D., *The Xenobiotic Compound 1,4-Bis[2-(3,5-Dichloropyridyloxy)]Benzene Is an Agonist Ligand*

for the Nuclear Receptor Car. Molecular and Cellular Biology, 2000. **20**(9): p. 2951-2958.
322. Kumar, N., Lyda, B., Chang, M.R., Lauer, J.L., Solt, L.A., Burris, T.P., Kamenecka, T.M., and Griffin, P.R., *Identification of Sr2211: A Potent Synthetic RorγSelective Modulator.* ACS Chemical Biology, 2012. **7**(4): p. 672-677.
323. Alterio, A., Alisi, A., Liccardo, D., and Nobili, V., *Non-Alcoholic Fatty Liver and Metabolic Syndrome in Children: A Vicious Circle.* Hormone Research in Paediatrics, 2014. **82**(5): p. 283-289.
324. Zhu, D.Y., Wu, J.Y., Li, H., Yan, J.P., Guo, M.Y., Wo, Y.B., and Lou, Y.J., *Ppar-B Facilitating Maturation of Hepatic-Like Tissue Derived from Mouse Embryonic Stem Cells Accompanied by Mitochondriogenesis and Membrane Potential Retention.* Journal of Cellular Biochemistry, 2010. **109**(3): p. 498-508.
325. Filant, J., Zhou, H., and Spencer, T.E., *Progesterone Inhibits Uterine Gland Development in the Neonatal Mouse Uterus.* Biology of Reproduction, 2012. **86**(5): p. 146.
326. Hasegawa, A. and Shirayoshi, Y., *P19 Cells Overexpressing Lhx1 Differentiate into the Definitive Endoderm by Recapitulating an Embryonic Developmental Pathway.* Yonago Acta Medica, 2015. **58**(1): p. 15-22.
327. Xue-Bin, Q., Jie, P., Cong, Z., and Shu-Yang, H., *Sox17 Facilitates the Differentiation of Mouse Embryonic Stem Cells into Primitive and Definitive Endoderm in Vitro.* Development, Growth & Differentiation, 2008. **50**(7): p. 585-593.
328. Niakan, K.K., Ji, H., Maehr, R., Vokes, S.A., Rodolfa, K.T., Sherwood, R.I., Yamaki, M., Dimos, J.T., Chen, A.E., Melton, D.A., McMahon, A.P., and Eggan, K., *Sox17 Promotes Differentiation in Mouse Embryonic Stem Cells by Directly Regulating Extraembryonic Gene Expression and Indirectly Antagonizing Self-Renewal.* Genes & Development, 2010. **24**(3): p. 312-326.
329. Barker, N., van Es, J.H., Kuipers, J., Kujala, P., van den Born, M., Cozijnsen, M., Haegebarth, A., Korving, J., Begthel, H., Peters, P.J., and Clevers, H., *Identification of Stem Cells in Small Intestine and Colon by Marker Gene Lgr5.* Nature, 2007. **449**: p. 1003-1007.
330. Barker, N., Huch, M., Kujala, P., van de Wetering, M., Snippert, H.J., van Es, J.H., Sato, T., Stange, D.E., Begthel, H., van den Born, M., Danenberg, E., van den Brink, S., Korving, J., Abo, A., Peters, P.J., Wright, N., Poulsom, R., and Clevers, H., *Lgr5 Positive Stem Cells Drive Self-Renewal in the Stomach and Build Long-Lived Gastric Units in Vitro.* Cell Stem Cell, 2010. **6**(1): p. 25-36.
331. Jaks, V., Barker, N., Kasper, M., van Es, J.H., Snippert, H.J., Clevers, H., and Toftgård, R., *Lgr5 Marks Cycling, yet Long-Lived, Hair Follicle Stem Cells.* Nature Genetics, 2008. **40**: p. 1291-1299.
332. Cheng, X., Ying, L., Lu, L., Galvão, A.M., Mills, J.A., Lin, H.C., Kotton, D.N., Shen, S.S., Nostro, M.C., Choi, J.K., Weiss, M.J., French, D.L., and Gadue, P., *Self-Renewing Endodermal Progenitor Lines Generated from Human Pluripotent Stem Cells.* Cell stem cell, 2012. **10**(4): p. 371-384.
333. Garcia, M.I., Ghiani, M., Lefort, A., Libert, F., Strollo, S., and Vassart, G., *Lgr5 Deficiency Deregulates Wnt Signaling and Leads to Precocious Paneth Cell Differentiation in the Fetal Intestine.* Developmental Biology, 2009. **331**(1): p. 58-67.
334. Huch, M., Dorrell, C., Boj, S.F., van Es, J.H., van de Wetering, M., Li, V.S.W., Hamer, K., Sasaki, N., Finegold, M.J., Haft, A., Grompe, M., and

Clevers, H., *In Vitro Expansion of Single Lgr5+ Liver Stem Cells Induced by Wnt-Driven Regeneration.* Nature, 2013. **494**(7436): p. 247-250.
335. Tarunina, M., Hernandez, D., Johnson, C.J., Rybtsov, S., Ramathas, V., Jeyakumar, M., Watson, T., Hook, L., Medvinsky, A., Mason, C., and Choo, Y., *Directed Differentiation of Embryonic Stem Cells Using a Bead-Based Combinatorial Screening Method.* PLoS ONE, 2014. **9**(9): p. e104301.